THE SYNTHESES, STRUCTURES AND DYNAMIC BEHAVIOUR OF STERICALLY CROWDED ORGANIC AND ORGANOMETALLIC COMPLEXES

By

LAURA E. HARRINGTON, B. Sc.

A Thesis

Submitted to the School of Graduate Studies

in Partial Fulfillment of the Requirements

for the Degree

Doctor of Philosophy

McMaster University

STERICALLY CROWDED ORGANIC AND ORGANOMETALLIC COMPLEXES

DOCTOR OF PHILOSOPHY (2004)
(Chemistry)

McMaster University
Hamilton, Ontario

TITLE: The Syntheses, Structures and Dynamic Behaviour of Sterically Crowded Organic and Organometallic Complexes

AUTHOR: Laura E. Harrington

SUPERVISOR: Dr. Michael J. McGlinchey

NUMBER OF PAGES: xvii, 398

ABSTRACT

The chemistry of crowded organic and organometallic complexes has been explored by the incorporation of bulky substituents into cyclopentadienone and benzene architectures, with the ultimate goal of creating a system that exhibits correlated rotation of peripheral groups.

The inclusion of naphthyl groups into η^4-(2,3,4,5-tetraaryl)cyclopentadienone rhodium acetylacetonate derivatives increases the steric hindrance of the propeller blades, as observed by the generation of numerous rotamers at low-temperature. By using the ^{31}P NMR signal of the triphenylphosphine moiety, the barrier to rotation of the naphthyl substituents was determined to be 8.2 kcal mol^{-1}. In hexa-β-naphthylbenzene, the barrier to rotation is approximately 17 kcal mol^{-1}, which is comparable to that of a *meta*-substituted phenyl group. The presence of numerous proximal/distal naphthyl rotational isomers is evident in the structure of penta-β-naphthylferrocenylbenzene, in which the substituents experience significant steric interplay and offer the potential for the observation of correlated rotation.

The influence of an organometallic unit on the stabilization of positive charge in a sterically crowded cyclopentadienyl cation has also been explored. In the absence of the metal moiety, the cation formed by the protonation of 2,3,4,5-tetraphenylcyclopentadienone (**1.26**) undergoes extensive rearrangement to give 5-*H* benzo[*a*]fluorene-5-one (**4.38**), whereas 3-ferrocenyl-2,4,5-

triphenylcyclopentadienone (**1.27**) is stabilized by metal participation, as evidenced by the barrier to rotation of the resulting hydroxy-fulvalene cation; these results have been rationalized using DFT calculations.

Furthermore, the potential for control over the barrier to rotation has been investigated for the first time by the examination of indenyl and fluorenyl groups as peripheral substituents. The synthesis and dynamic behaviour of an indenyl-triptycene complex revealed the severe degree of interaction between the blades of the triptycene and the indenyl unit. The attempted incorporation of a metal fragment onto the indene yields instead addition to one of the triptycene blades, thus preventing the possibility of utilizing haptotropic shifts to alter the barrier to triptycene rotation.

Finally, the attempted synthesis of pentaphenylfluorenyl benzene was thwarted by the formation and reaction of fluorenyl radicals. The result was the unanticipated preparation of a Gomberg dimer, as well as substituted naphthacene molecules.

ACKNOWLEDGEMENTS

I would first like to express my gratitude to my supervisor, Dr. Michael J. McGlinchey. Dr. McGlinchey has an unwavering enthusiasm for chemistry, and a passion for all things scientific. He has given me the opportunity to independently explore chemistry, and has been the source of innumerable "crazy ideas" that have become interesting stories. He has also nurtured my love for science, and has become not only a respected mentor, but a good friend. I thank him for his never-ending support and encouragement, for offering me the incredible opportunity to visit him in Ireland, and for allowing me to grow both as a scientist and as a professional. Slainte!

I would also like to acknowledge the other members of my Ph.D. committee – Dr. Ignacio Vargas-Baca and Dr. John F. Valliant – for all their support and encouragement. They have both opened their labs and offices to me, and have offered valuable advice – both chemically and professionally – numerous times. I admire both of them immensely, I appreciate all their comments and suggestions, and I have learned so much by their example.

There are many others in the Department of Chemistry that I would like to thank for their help during my time at McMaster – many of them have gone out of their way for me, and I appreciate it. I would like to acknowledge the Office staff – Josie Petrie, Tammy Feher and Barbra DeJean, as well as Carol Dada, who has been an incredible listener and has helped in so many ways through the years. Also, Brian Sayer, Kirk Green, George Timmins and Mike Malott, who work so hard to keep all our equipment running smoothly, and are always available to help. Thank you also to Tadek Olech, who worked so hard to give me good mass spectrometry data so many times, I appreciate your efforts. I would especially like to thank Jim Britten – I have learned so much about X-ray crystallography from Jim, and have pushed him and the X-ray machines to the limits for some of my molecules. I thank him for fighting for so many important

results, for his teaching and training, and for becoming a great friend and mentor. Another special acknowledgement belongs to Don Hughes – I have spent much time with Don and have learned from him a great deal. He has gone out of his way for me many times, and has taught me so much about NMR, and the "behind the scenes" workings of the lab. I thank him for his support of my chemistry, as well as my future goals, and for his friendship and guidance throughout. I have always enjoyed catching up with Don, and discussing other important life issues – especially tennis!!

There have also been many co-workers and colleagues in the lab that have become great friends. I would like to thank Dr. Hari Gupta for his help getting me started in the lab, and for always making me laugh. Pippa Lock has always been a wonderful ear, and a great example of an admired teacher. I thank Francis Ogini for his help in the lab – I learned a lot from Frank, and always enjoyed his singing and dancing. John Kaldis has always looked after "his girls", and I thank him for his help so many times in the lab and with X-ray crystallography. I loved working beside John, and I appreciate his continued friendship and support. Stacey Brydges has been a wonderful mentor and friend, I have learned a great deal from Stacey, and I admire so much about her. I enjoyed our many long discussions, and knowing that she would always be there if I needed her – I thank her for her friendship. Finally, I would like to acknowledge Nada Reginato, a great comrade. I really enjoyed working with Nada, she made life in the lab so much fun, and she has always been – and always will be – a truly great friend. I also thank another good friend, Paul Zelisko. I have enjoyed working with Paul on various projects in the Department, and I thank him for his wonderful listening, support and friendship.

I would also like to acknowledge financial support from NSERC Canada and McMaster University through graduate school.

For their never-ending encouragement and love, I would like to thank all of my family and friends - I have had wonderful support throughout my time at

McMaster. I especially thank my parents Noel and Pauline, my sister Sheila, and my brother-in-law Rob, as well as the Harrington's – Bob, Gay, Greg, Luma, Katy and Bradley. I thank them all for always being interested in my work and my future, for trying to understand my chemistry, and for always cheering me on. I love you all so much, thank you for being there for me.

Finally, I would like to thank my husband, Cam. It's hard to put into words how much his support has meant over the years, and how wonderful it has been to have a "partner-in-crime" to share in all my adventures. Thank you so much for lifting me up when I was down, and for cheering me on during good times. Thank you also for showing me so much of the world, I have learned a lot from you, and I admire you in so many ways. I love you.

TABLE OF CONTENTS

LIST OF TABLES

LIST OF FIGURES

LIST OF COMMONLY USED SYMBOLS AND ABBREVIATIONS

acac	acetylacetonate
Ar	Aryl substituent
COSY	Correlated Spectroscopy
Cp	Cyclopentadienyl group
CSA	Chemical Shift Anisotropy
DFT	Density Functional Theory
EHMO	Extended Hückel Molecular Orbital
ESR	Electron Spin Resonance
$\Delta G^{\neq}$	Gibbs Free Energy of Activation
h	hour(s)
HMBC	Heteronuclear Multiple Bond Correlation
HOMO	Highest Occupied Molecular Orbital
HSQC	Heteronuclear Single Quantum Coherence
IR	Infrared
LUMO	Lowest Unoccupied Molecular Orbital
NMR	Nuclear Magnetic Resonance
T	Temperature
VT-NMR	Variable-Temperature Nuclear Magnetic Resonance

CHAPTER ONE

Introduction

1.1 Fundamental Concepts

1.1.1 Aromaticity

Since Michael Faraday discovered benzene, or "bicarburet of hydrogen," in 1825,[1] the idea of aromaticity and the properties of aromatic molecules have been the subject of considerable research interest and debate. To date, a universally accepted definition of aromaticity does not exist, and the criteria used to describe aromatic systems are continually evolving. The need for such a description first arose in order to characterize thermally stable organic molecules that easily underwent substitution, but not addition reactions.[2]

The historical development of this qualitative concept continued with Kekulé's description of benzene as a 6-membered ring in 1865 (**1.1**);[3] this was followed closely by Erlenmeyer's suggestion that molecules reacting in a manner analogous to benzene were aromatic.[4] The expansion of these ideas to include alternating single and double bonds,[5] and later resonance structures,[6] were revolutionized in the 1930's with the introduction of the Hückel rule.[7] This concept states that cyclic, conjugated, planar molecules with [4*n*+2] π-electrons are more stable than those with only 4*n* π-electrons (e.g. cyclobutadiene, **1.2**), and are considered aromatic. The Hückel rule is based on molecular orbital theory,[8] which reveals that molecules with [4*n*+2] π-electrons have a relatively

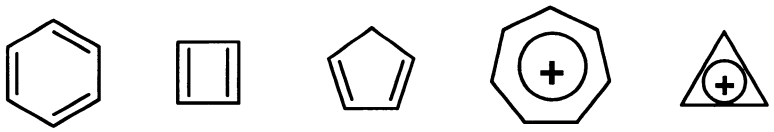

1.1 **1.2** **1.3** **1.4** **1.5**

*Chart 1.1: Aromatic molecules **1.1**, **1.4** and **1.5**, antiaromatic molecule **1.2** and the relatively acidic cyclopentadiene, **1.3**.*

large energy gap between the HOMO (Highest Occupied Molecular Orbital) and LUMO (Lowest Unoccupied Molecular Orbital), whereas the corresponding HOMO's for systems with $4n$ π-electrons are non-bonding and half filled (Figure 1.1). The result is increased stability for the former systems, and relative instability for the latter, as the higher energy π-electrons are only weakly bound.[9] Evidence for this rule was observed in the unusual acidity of cyclopentadiene (**1.3**) and the unexpected stability of the cycloheptatrienyl and cyclopropenyl cations (**1.4** and **1.5**, Chart 1.1).[10,11]

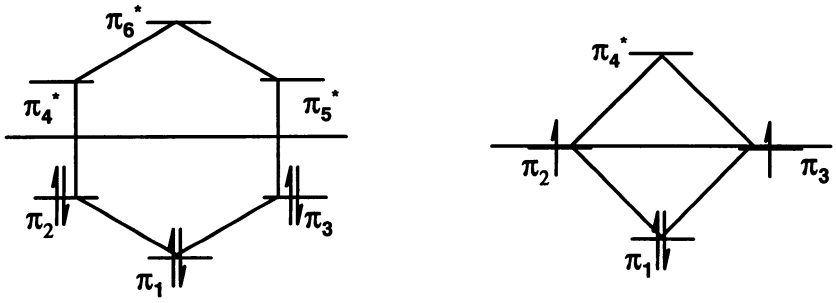

*Figure 1.1: Energy level diagrams for benzene (**1.1**) and cyclobutadiene (**1.2**); the dotted line represents the non-bonding energy level.*

Throughout the evolution of the criteria for an aromatic system, attention has focused alternately on chemical definitions, which emphasize the energetic properties of the excited state, and on physical qualities, which concentrate on

the ground state characteristics.[2] Attempts to modify a "universal definition" to accommodate both fundamental aspects has led to a variety of approaches, including pseudo-aromaticity (non-benzenoid aromatic compounds), quasi-aromaticity (acyclic conjugated π-electron systems) and others.[2] In general, aromatic systems exhibit the following characteristics:[9,12] i) low tendency to undergo addition reactions but experience facile electrophilic substitution; ii) possess resonance energy (that is, a lower than expected heat of hydrogenation); iii) nearly equal C-C bond lengths (intermediate between C-C and C=C distances), and iv) the presence of a diamagnetic ring current.

Though a generally applicable definition of aromaticity has yet to be accepted, a widely used criterion is the magnetic behaviour associated with the ring currents induced by the cyclic electron delocalization of aromatic species. The advent of nuclear magnetic resonance (NMR) spectroscopy[13,14] allowed for the experimental determination of the presence of a "closed ring of electrons," thus referring to the "aromatic sextet" introduced by Armit and Robinson in 1925, which was an empirical generalization used to describe aromatic compounds.[2,15] Accordingly, a compound that can sustain an induced ring current is called *diatropic*, and is considered aromatic.[16] The application of an external magnetic field to an aromatic system results in the circulation of the loop of electrons in a diamagnetic ring current, which possesses a field of its own (Figure 1.2). The protons directly attached to the aromatic ring feel the additive effect of the external and induced fields, and consequently exhibit chemical shifts with larger δ

values than in the absence of the diamagnetic ring current. In contrast, protons directly above or inside the ring experience a decreased magnetic field, and display chemical shifts of smaller δ values than expected.[16] As a result, the magnetic properties of a system are now widely used as an indicator of aromatic behaviour.

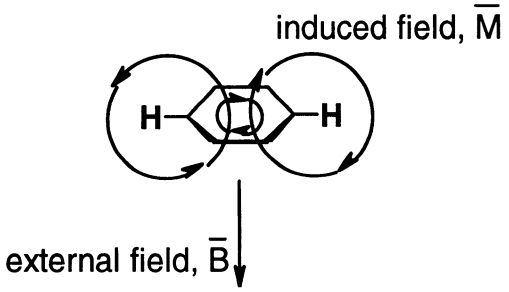

Figure 1.2: Induced ring current in aromatic systems exposed to an external magnetic field.

Research into the properties, reactivity and other characteristics of aromatic systems continues to be the subject of much discussion in the literature, and has been extended to non-carbon based systems. The lack of a widely applicable and accepted definition of aromaticity will continue to be the foundation of exploration and investigation for many years to come.

1.1.2 Organometallic Chemistry

Organometallic chemistry is a subject area with a rich history of discovery, a wide base of exploration that touches many other aspects of chemistry and biology, and a range of application that has revolutionized chemical research.[17-19]

Strictly defined, an organometallic compound contains a bond between a metal and a carbon atom. Research in this area began in 1827 when Zeise prepared the platinum ethene complex $[PtCl_3(C_2H_4)]^-$ (**1.6**),[17,18,19] and continued in 1848 when Frankland characterized diethylzinc (**1.7**), formed by the treatment of ethyl iodide with metallic zinc.[19] The rich chemistry of metal-carbonyl compounds began in 1890, with the synthesis of tetracarbonyl nickel, $[Ni(CO)_4]$ (**1.8**), by Mond, Langer and Quinke, and many other metal carbonyl compounds were prepared by Hieber in the 1930's.[18] The early 1900's also saw the development of Grignard's organomagnesium halides (eg. **1.9**), which broadened the utility of organometallic reagents by offering new applications.[19]

The true advent of the current wealth of organometallic chemistry began with the discovery of ferrocene (**1.10**) in 1951.[20] The interest generated by this

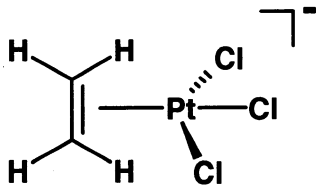

1.6

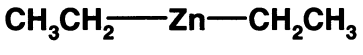

1.7

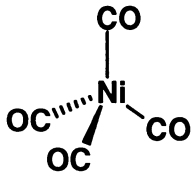

1.8

1.9

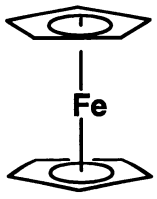

1.10

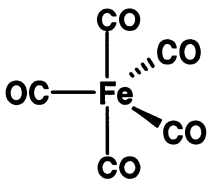

1.11

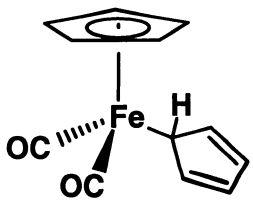

1.13

*Chart 1.2: Organometallic complexes **1.6** – **1.11**, **1.13**.*

report was recently expressed by F. A. Cotton,[21] who described first the frustration of chemists in the research area attempting to create such unstable and unlikely complexes, and then the excitement and enthusiasm as the revolutionary discovery of Kealy and Pauson was repeated and confirmed.

The rules governing the formation of organometallic complexes begin with the "18-electron rule", introduced by Sidgwick in the 1920's. Sidgwick noticed that the metal atom in a carbonyl complex had the same electron count (18) as the noble gas at the end of that period in the Periodic Table.[18] The rationale for this rule arises from the orbitals possessed by the metal; eighteen electrons are required to fill the one *s*, three *p* and five *d* orbitals. Stable complexes are formed by the combination of metal and ligand electrons to give an 18-electron count; all of the valence electrons from the metal atom and all electrons donated by the ligands, as well as the overall charge of the complex, are taken into consideration. For example, $Fe(CO)_5$ (**1.11**) is an 18-electron complex since iron (0) contains 8 *d*-electrons, and each CO group contributes 2 electrons to the electron count.

There are many exceptions to the 18-electron rule, most notably complexes of the heavier d^8 metals [Rh(I), Ir(I), Ni(II), Pd(II) and Pt(II)], which have a preference for square planar, 16-electron complexes.[18] As atomic number increases, the *d*-shell becomes increasingly stabilized so that the higher energy d_{x2-y2} orbital does not participate in bonding, and as a result, square planar geometries are favoured. In addition, steric and electronic factors are

often in competition for the smaller Group 3, 4 and 5 metals, and 16- or 17-electron complexes frequently result.

Another important term in the description of organometallic complexes is hapticity. When unsaturated ligands are bonded to a metal, it is necessary to identify how many of the carbon atoms are actually involved in the interaction. This feature is specified by the prefix η^n (pronounced "eta"); the superscript *n* represents the number of atoms bonded to the metal. For instance, in ferrocene, each of the five carbons in each cyclopentadienyl ring are bonded to the metal, this would be represented by the formula $(\eta^5\text{-}C_5H_5)_2Fe$.

Organometallic complexes have found numerous applications in modern chemistry; from catalysis to the activation of small molecules, from uses in organic synthesis to crucial roles in biochemistry.[17-19] Metal complexes have also played a pivotal role in the development of the chemistry of sterically crowded aromatic molecules, as will be discussed.

1.1.3 Fluxionality

Since the development of organometallic chemistry and the first studies on metal carbonyl complexes, the concept of fluxionality has been explored. As described by Faller,[22] the term *stereochemically nonrigid molecules* describes species that perform intramolecular rearrangements at rates that affect NMR lineshapes at accessible temperatures. Interconverting molecules that are chemically and structurally equivalent are termed *fluxional*.

Scheme 1.1

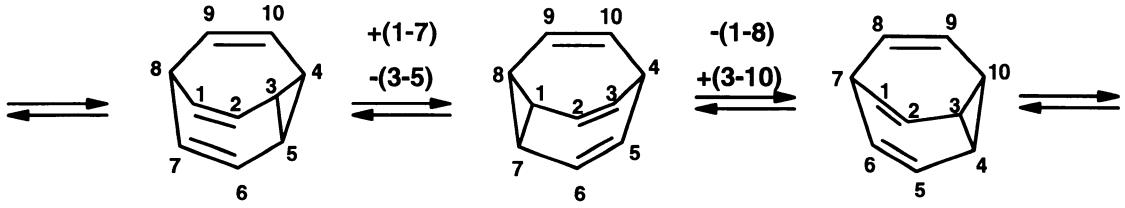

1.12

The first suggestion of the rapid, intramolecular rearrangement of molecules involved descriptions of bullvalene (**1.12**), which can undergo an immense number of degenerate rearrangements, resulting in the same molecule,[21,23] and is described as a substance with no permanent carbon-carbon bonds (Scheme 1.1).[23] Reports of this chemistry were closely followed by the introduction of the Berry pseudorotation,[24] and the development of the idea of polytopal rearrangements. Polytopes are described as different shapes for the same AB_n molecule, which is defined by the arrangement of B atoms around an A core.[21] This idea came under investigation when the ^{13}C NMR spectrum of $Fe(CO)_5$ showed only one signal instead of the anticipated two peaks (one for the equatorial carbon atoms, one for the axial carbons), suggesting that the carbonyl ligands were undergoing rapid rearrangement, resulting in the equivalence of the carbon atoms on the NMR timescale.[21] The Berry-pseudorotation rapidly interconverts the axial CO groups with two of the equatorial ligands, thus only one type of CO is present (Scheme 1.2).

Scheme 1.2

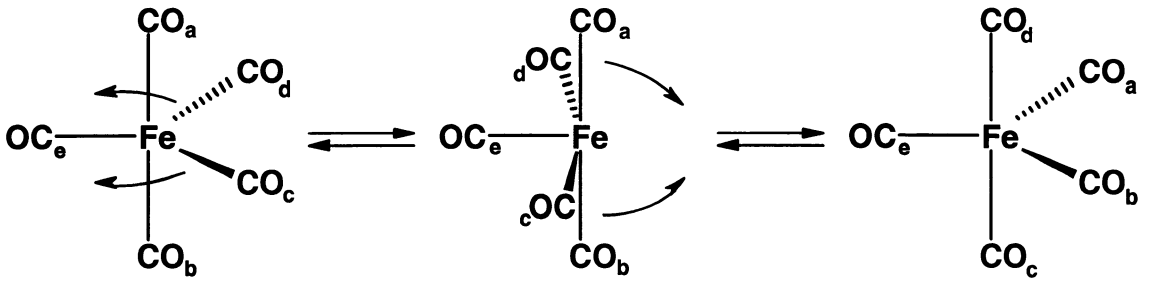

A crucial development in the history of fluxional organometallic complexes involved studies on $(\eta^5\text{-}C_5H_5)Fe(CO)_2(\eta^1\text{-}C_5H_5)$ (**1.13**, Chart 1.2, page 5),[25] which exhibited two singlets of equal intensity in the ^1H NMR spectrum rather than the expected singlet for the $\pi\text{-}C_5H_5$ protons and multiplet attributable to the inequivalent protons in the η^1-coordinated ring. This led to the suggestion that the molecule was performing a 1,2-rearrangement faster than could be resolved using NMR spectroscopy, thus the $\sigma\text{-}C_5H_5$ ring was said to be rotating, resulting in the equivalence of the protons. Cotton and Davison[26] later examined this complex using variable-temperature NMR and were able to confirm its fluxionality, as the anticipated multiplet was resolved at low temperatures. This development was significant because the appearance of the spectra allowed Cotton and Davison to propose a rearrangement pathway; the coalescence of the peaks occurred at different rates and temperatures. A random rearrangement could therefore be discounted, and 1,2- or 1,3-shifts became the only acceptable explanations. Thus, this iron complex was the first organometallic system to be subjected to a complete variable-temperature NMR

study and line-shape analysis, leading to the mechanistic determination of the pathway of the rearrangement.[26] From the point of view of the subsequently developed Woodward-Hoffmann rules,[27] these 1,2-shifts can actually be recategorized as 1,5-suprafacial sigmatropic shifts.

Fluxionality has since become a concept of immense importance, as has the interpretation of fluxional behaviour, as determined by the barrier to rotation or rearrangement by means of variable-temperature NMR spectroscopy.

1.1.4 Determination of Barriers to Rotation

Dynamic NMR spectroscopy has been an invaluable tool for the determination of barriers to rotation for fragments of a molecule. The analysis of line broadening and coalescence of resonances is the primary technique for measuring kinetic data by NMR spectroscopy.[22] The examination of lineshapes and relative broadenings has led to the elucidation of activation energy parameters for rearrangements, as well as the corresponding mechanisms.

A simple description involves the simulation of spectral lineshapes using computational programs[28] with two-site exchange formulas. For two singlet resonances with equal populations, the NMR signals are separated when there is no exchange phenomenon. As the temperature is increased and the sites begin to exchange, the signals broaden and finally coalesce when the exchange rate is comparable to the frequency difference between the two sites. The broad, coalesced peak begins to sharpen again until it becomes a single, well-resolved

peak in the limit of fast exchange. The difficulty in considering coupling behaviour, intermolecularly exchanging systems, and multi-site exchange has necessitated the use of computer simulations in order to extract and report the most reliable data possible. There are numerous possible treatments and approaches to determining barriers to rotation and activation energy parameters, and the simplest is the consideration of exchange between two equal sites.

At a given temperature (T), the rate constant (k) for exchange is given by:[29]

$$k = \frac{\pi \delta \upsilon}{\sqrt{2}} \qquad 1.1$$

where δv is the frequency difference in Hz between the signals for the sites of the exchanging system. This expression is satisfactory if approximate free energies of activation are required. The activation energy is related to the rate constant according to the Eyring equation:

$$k = \frac{k_B T}{h} e^{-\Delta G^{\ddagger}/RT} \qquad 1.2$$

where k_B, h and R are constants, $\Delta G^{\ddagger}$ is the free energy of activation and T is the temperature (in Kelvin). This may be combined with Equation 1.1 to give:[29]

$$\Delta G_c^{\ddagger} = RT_c [22.96 + \ln (T_c / \delta \upsilon)] \qquad 1.3$$

where R is the ideal gas constant (in cal mol^{-1} deg^{-1}).

Thus, Equation 1.3 may be used to determine the free energy of activation at the coalescence temperature for the exchange of an equally populated two-site system. The accuracy of the resulting values depends on the accuracy with which the coalescence temperature and chemical shift difference are measured. Typical errors are estimated to be ± 0.5 kcal mol^{-1}.[29]

The development of this technique for the determination of barriers to rotation has revolutionized the study of sterically hindered organic and organometallic complexes. Methods to compare the influence of different substituents and molecular architectures are crucial to the development of novel organic and organometallic systems.

1.2 Sterically Hindered Organic and Organometallic Complexes

1.2.1 Steric Hindrance and Restricted Rotation

The ground-breaking ideas of van't Hoff, published in 1875,[30] revolutionized chemical research in his time, and continue to be the basis for our modern understanding of many chemical postulates (though some also acknowledge Le Bel as a co-founder of modern stereochemistry[31,32]). Van't Hoff is credited with establishing the foundation for stereochemistry with his proposal that a saturated carbon atom forms a tetrahedral arrangement of bonds, and that single bonds experience free rotation. While his ideas about the tetrahedral carbon have formed the "cornerstone of chemistry", van't Hoff's concept of free

rotation was found to be slightly flawed.[33] The basis of the theory was the *non-existence* of rotational isomers; rotation was not considered to be continuous, and the possible rotamers were not deemed equivalent. As a consequence, it was not possible to have two rotational isomers of equal energy such that rapid interconversion occurred.

The first intimation of restricted rotation was by Bischoff in 1891 while investigating multiply substituted ethanes, and this work led to the introduction of the term *dynamic isomerism*, used to describe the rotation process.[34] The isolation of the rotamers of 2,2'-dinitrophenyl-6,6'-dicarboxylic acid (**1.14**) by Christie and Kenner in 1922[35] constituted the first experimental evidence for restricted rotation about single bonds, and was considered an exception to the rule developed by van't Hoff (Chart 1.3).[33] The bulky *ortho* groups present on each ring prevented the rapid rotation about the central C-C bond, thus restricting its rotation and yielding separable enantiomers. Thus, van't Hoff's ideas were still valid, except in the extreme case of such "gross steric factors".[33]

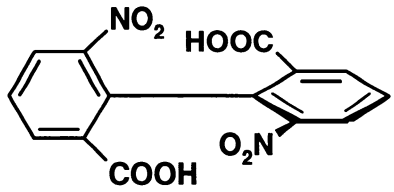

1.14

*Chart 1.3: One rotamer of molecule **1.14**, which exhibits restricted rotation about the central C-C bond.*

In 1932, Eyring carried out potential energy calculations and determined that the barrier to rotation about the C-C bond in ethane was between 0.18 and 0.36 kcal mol^{-1}.[36,37] Such small barriers clearly concurred with experimental observations, since there had been no other reports of isomerism related to restricted rotation about single bonds. However, basing criteria for internal rotation on the lack of evidence for separable rotamers is clearly flawed when the barrier to interconversion is so insignificant.

The revolution of this concept occurred in the 1930's with the development of physical methods of investigating structural properties.[33] Measurements of the heat of hydrogenation of ethene and the calorimetric determination of the entropy of ethane were found to be in disagreement with computational models based on unrestricted free rotation about the central single bond. Pitzer and Kemp resolved these differences by proposing a small barrier to methyl rotation, thus achieving agreement between model and experiment.[33,38-40] Following this work, restricted rotation was observed in many species, however, chemical isolation of rotamers was not possible unless the barrier to rotation exceeded 15 kcal mol^{-1}.[33]

1.2.2 Molecular Propellers and Gears

A particular application of restricted rotation is the formation of molecular propellers and gears. Stimulated by the work of Gust and Mislow in the 1970's, this area of research has become the subject of widespread interest. Since the influential work of these pioneers, the understanding of the complex

stereochemical phenomena that may result from propeller interconversion has led to decades of discussion and debate in the literature; progress in this area has recently been reviewed.[41]

Gust and Mislow recognized that compounds exhibiting isomerism as a result of restricted internal rotation are well represented by a system that contains two or more aromatic rings bonded to a central atom (Z).[42-44] In the case of triaryl systems (Ar_3ZX), all four substituents are arranged tetrahedrally about the central atom, Z, represented by C, P, or B, and X represents a ligand or atom with local conical symmetry (H, CH_3, halogen), or an electron pair. In these instances, the aryl groups, considered as "blades", radiate from a central propeller axis (Z), and may be arranged parallel or perpendicular to the plane containing the three *ipso* carbons, or may assume an intermediate conformation, thus forming a propeller. The most energetically favourable arrangement involves the propeller conformation, in which the aromatic rings are twisted in the same sense, imparting a helical conformation to the molecule, as determined by X-ray crystallographic[45] and NMR investigations.[45-47]

If each of the aryl groups in Ar_3ZX bears a different substituent, then several possible isomers may result. Specifically, isomerism results from the distribution of the substituents on the two sides of the plane containing the *ipso* carbon atoms, and there are 2^3 possible arrangements. The propeller may exhibit two helicities, and when X is CH, each of these assemblies is chiral, and may therefore exist as two enantiomers, resulting in $2^3(4) = 32$ possible isomers

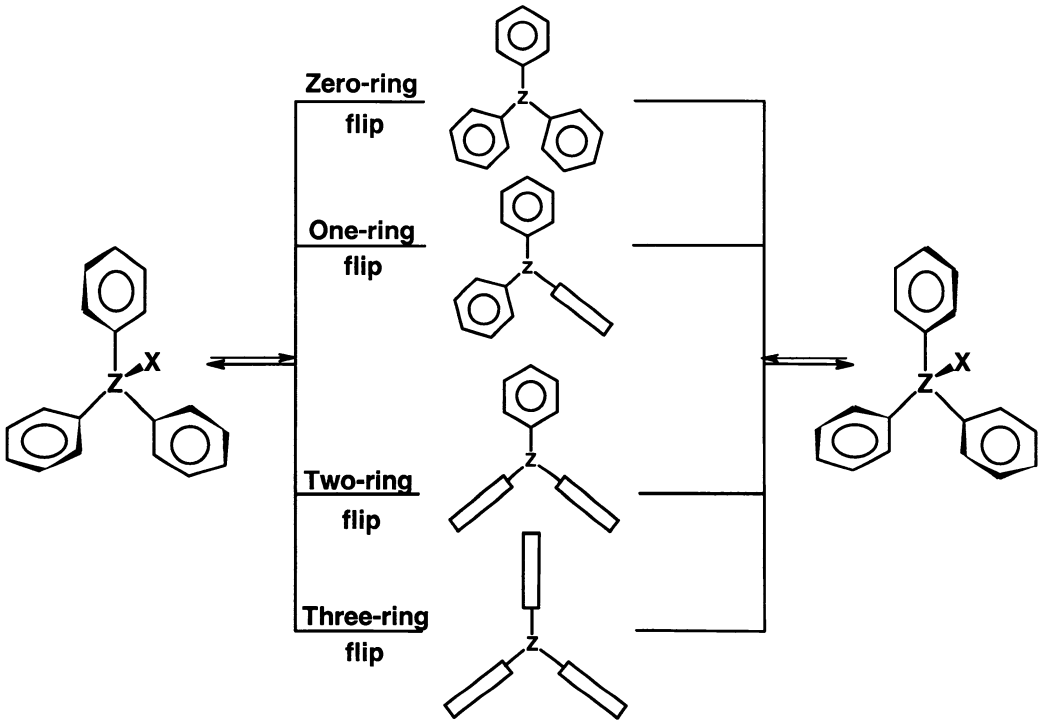

Figure 1.3: Rotational (flip) mechanisms for Ar_3ZX systems; the structures in the centre represent approximate transition state geometries.

(for X = CH). Such species, in which each ring is different and the maximum number of isomers is possible are referred to as *maximally labeled*.[43] Building on Kurland's description of the interconversion of the rotational isomers of triarylcarbonium ions,[48] Gust and Mislow have outlined four potential *flip mechanisms* which reverse the helicity of the structure.[42] As depicted in Figure 1.3, the torsional motion of the rings along the path of helicity reversal may occur through the central reference plane (which interchanges the edges of the ring) or through a plane perpendicular to the central reference plane (resulting in no edge exchange – referred to as a *flip*).[43] The authors were then able to review related cases in the literature and describe the isomeric interconversion according to the

proposed mechanisms, thus establishing the generality of the concept.[42] These examinations also led to the determination of the *threshold mechanism*, or stereoisomerization mechanism of lowest energy, to be the *two-ring flip*, in which only one ring actually passes through the central reference plane, resulting in edge interchange.[43,49] This result is also supported by entropy arguments, in which the level of organization required to perform *only* the three-ring flip mechanism (which is the most favourable in terms of avoiding steric interactions) renders this situation unfavourable.

1.2.3 Correlated Rotation and Residual Stereoisomerism

Further studies on these systems led to the proposal of another seminal concept by Mislow.[43] In a system containing two or more aryl rings bonded to a central atomic center (Z), rotation of one of the aryl substituents about the C-Z bond is *sensed* by the other rings such that no ring moves independently of the others. This idea resulted in the introduction of the concept of *correlated rotation*, which refers to the sympathetic motion resulting from the strong coupling of the rotational motion of the bulky substituents. In many instances, the interaction between the substituents is so intense that correlated rotation is energetically more favourable than the independent motion of each propeller blade.

Moreover, the establishment of the two-ring flip isomerization mechanism as the preferred pathway for propeller interconversion also necessitates the development of the idea of *residual stereoisomerism*.[43,50] This concept refers to

the generation of a closed subset of interconverting isomers from the full set at a particular time-scale of observation. In other words, there is a set of rearrangement pathways that interconverts all isomers of a system. However, not all isomers are possible on a specific time-scale, thus closed subsets are generated. In this case, the zero-, one- and three-ring flip mechanisms are possible, though not energetically preferred, and there is a limit to the number of possible isomers that may be created by successive application of the two-ring flip mechanism alone. At the time, there were no cases of residual stereoisomerism in maximally labeled Ar_3X systems since the energetic requirements of the 3 alternative flip mechanisms were still accessible in the systems studied.[43]

In 1980, Mislow and co-workers reported the first study of the separation and identification (by X-ray crystallography) of the residual stereoisomers of the maximally labeled system, **1.15** (Chart 1.4).[51] The barrier for isomer interconversion by a one- or three-ring flip was determined to be 17.8 kcal mol^{-1}, whereas the two-ring flip to interconvert the propeller helicity exhibited a barrier of 11-12 kcal mol^{-1}. Several other triaryl propellers have since been investigated, and a wide range of barriers to rotation have been determined.[52]

1.2.4 Six-Membered Ring Systems

The investigation of propeller interconversion has also been extended to studies on C_6Ar_6 systems, in which the peripheral substituents are rotating about a central ring rather than a central atom. X-ray crystallographic investigations of hexaphenylbenzene (**1.16**)[53,54] revealed a propeller conformation of aryl substituents with interplanar angles of 65(75)° relative to the central ring, and electron diffraction studies reveal that, in the gas phase, the peripheral groups are perpendicular to the central ring, with oscillations of ±10°.[55] Gust extended these studies to include hexaarylbenzenes with substituents in the *ortho* or *meta* positions (**1.17** – **1.19**, Chart 1.4).[56] Variable-temperature NMR studies revealed barriers to rotation of ~38 kcal mol^{-1} for the *ortho*–methoxy (**1.17**) or –methyl (**1.18**) substituted derivatives, whereas *meta*–substitution (**1.19**) resulted in barriers of ~16 kcal mol^{-1}. In this initial investigation, Gust realized that these systems were extremely stereochemically complex and suggested the presence

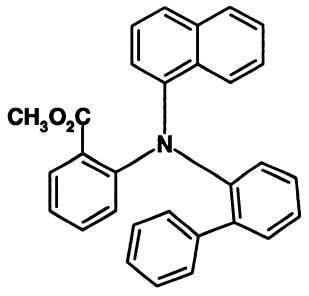

1.15

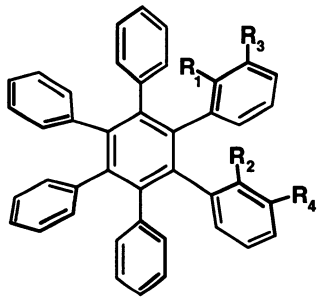

1.16: R_1, R_2, R_3, R_4 = H
1.17: R_1 = OCH_3; R_2 = CH_3; R_3, R_4 = H
1.18: R_1, R_2 = CH_3; R_3, R_4 = H
1.19: R_1, R_2 = H; R_3, R_4 = CH_3

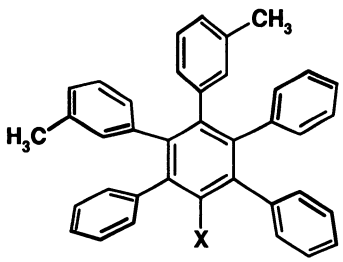

1.20: X = H, Me, Et, Ph, $CH(OH)CH_3$, $CH(CH_3)_2$, $C(CH_3)_3$

*Chart 1.4: Maximally labelled triarylamine (**1.15**) and substituted hexaphenylbenzene derivatives **1.16** – **1.19**.*

of subtle isomerization behaviour that would complicate future research.[56]

Gust's prediction proved to be accurate, and he later published a mathematical study on the stereoisomerization of hexaarylbenzenes, which revealed 13 possible rearrangement modes and 64 rotational isomers for a maximally labeled system.[57] Subsequent variable-temperature NMR investigations revealed that the threshold mechanism was one in which a single aryl group rotated at a time, thus the motion of the substituents was not correlated.[57] However, the replacement of one aryl group with a hydrogen atom (**1.20**) only decreased the barrier to rotation for a *meta*–methyl substituted system by 2 kcal mol^{-1}.[58] Incorporating a variety of increasingly bulky substituents into the central ring revealed the transmission of steric effects around the circumference from sites that were remote from the rotating ring. Gust used his results to elegantly describe the rationale behind the relatively high barriers to rotation in hexaarylbenzenes:[58] steric strain cannot be relieved by "splaying motions" of the rings in the plane of the central ring. The structure of benzene derivatives is such that any increase in the in-plane angle between two adjacent groups results in a decrease in the analogous angle between all other substituents, which increases the strain in those regions of the molecule. As a result, the barriers to rotation in these systems are reflective of the buttressing effects of the *ortho*-hydrogens, and the steric interactions are transmitted throughout the molecule, not just adjacent to the rotating peripheral ring.

1.2.5 Five-Membered Ring Systems

In an extension of the concept of transmission of steric effects through a ring system, attention then focused on 5-membered ring derivatives in which the barrier to rotation was expected to be reduced, since the substituents are farther apart on the ring. Haywood-Farmer and Battiste previously determined the barrier to rotation in 2,5-diphenyl-3,4-di-*o*-tolyl cyclopentadienone (**1.21**, Chart 1.5) as 21.8 kcal mol^{-1} for the *o*-tolyl groups.[59] Moreover, investigations of tetra-*o*-tolyl cyclopentadienone (**1.22**) revealed two rotational processes: one for the α-rings, and one for the β-substituents.[60,61] The former occurred rapidly on the NMR time-scale, and decoalescence was observed at low-temperature. The more hindered β-rings did not rotate at room temperature, and coalescence was observed only at high temperatures. No barriers were reported for either process, but the assumption was made that the aryl groups were oriented perpendicular to the central ring in solution, and the rotational processes were uncorrelated.

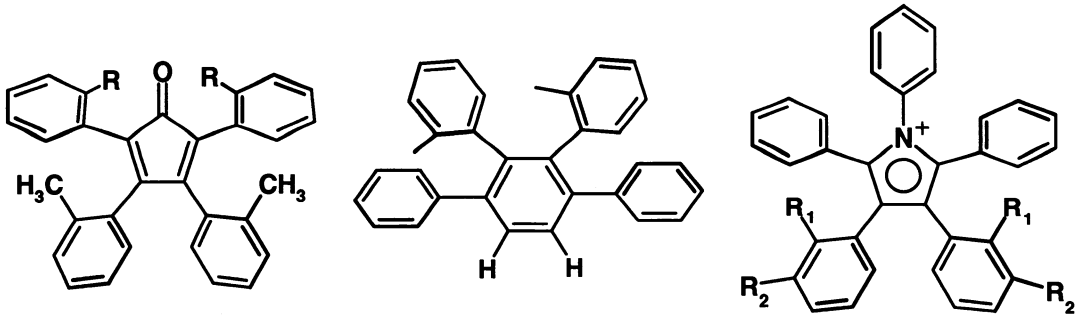

1.21: R = H
1.22: R = CH_3

1.23

1.24: R_1 = H; R_2 = CH_3
1.25: R_1 = CH_3; R_2 = H

Chart 1.5: Five- and six-membered ring systems containing crowded substituents.

In comparison with the Haywood-Farmer and Battiste study,[59] Gust reported the analogous barrier to rotation in 1,4-diphenyl-2,3-di-*o*-tolylbenzene (**1.23**) to be > 25.6 kcal mol^{-1}.[62] The small difference in energy (~3.8 kcal mol^{-1}) did not form a good basis for the determination of the effect of ring size, and it was noted that in each case there were other substituents on the central ring besides aryl groups, thus the influence of buttressing effects could not be discounted. Instead, Gust suggested comparing barriers to rotation in 1,2-di-*m*-tolyl-3,4,5,6-tetraphenylbenzene (**1.19**, 17.0 kcal mol^{-1}) and 3,4-di-*m*-tolyl-1,2,5-triphenylpyrrole (**1.24**).[62] Unfortunately, variable-temperature studies of **1.24** revealed only a single methyl resonance down to –85 °C, suggesting that rotation was still rapid at low temperatures and the barrier was too small to determine by means of NMR spectroscopy. The extension of these investigations to the *ortho*-methyl substituted derivatives (**1.18**, Chart 1.4 and **1.25**, Chart 1.5) allowed for the determination of the barrier to rotation of pyrrole **1.25** to be 19.9 kcal mol^{-1}, whereas the analogous process in **1.18** was ~38 kcal mol^{-1}, revealing a difference of 18 kcal mol^{-1}. This difference was attributed to the decrease in steric repulsions in the transition state of **1.25** relative to **1.18** because of the decreased ring size and larger angle between adjacent rings,[62] thus supporting Gust's hypothesis. Other 5-membered ring systems that have been examined include the products of the treatment of tetraphenylcyclopentadienone (tetracyclone, **1.26**) or 3-ferrocenyl-2,4,5-triphenylcyclopentadienone (**1.27**) with

C_6F_5Li (**1.28**, **1.29**, Scheme 1.3), which yielded barriers to rotation of 19 – 20 kcal mol^{-1} by simulation of the ^{19}F NMR spectra.[63]

Scheme 1.3

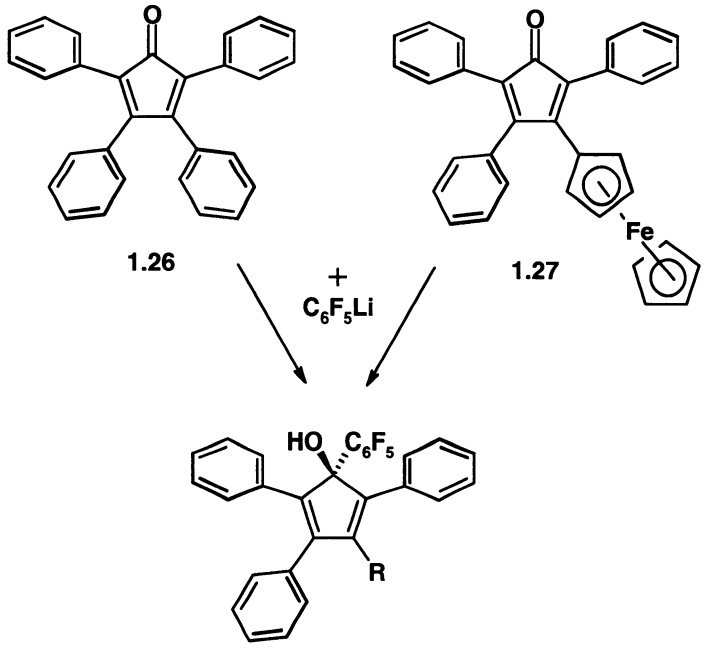

1.28: R = Ph
1.29: R = Fc

Furthermore, Brydges and McGlinchey have performed an exhaustive investigation of the torsional angles of the peripheral substituents and threshold rotational mechanisms in C_5Ar_5 and C_5Ar_4X systems.[64] By examining the solid-state data available for these propeller molecules, and performing structure correlation studies, the internal oscillations of nearest (1,2) and next-nearest (1,3) aryl groups were found to be only partially correlated. The study revealed that the threshold mechanism of helicity interconversion is the *delayed n-ring-flip*, in which the rotation of the rings is nonsynchronous, and that the highly organized

transition states required for a correlated mechanism are much less likely. Brydges also invoked the Parity Rule for dynamic gearing, which disallows correlated rotation in a closed cyclic array comprised of an odd number of meshed gears.[44] Thus, C_5Ar_5 systems do not possess the "tongue-and-groove" arrangement necessary for interdependent rotation, and prefer consecutive localized rotations over correlated ring flips.[64]

1.2.6 The "Cogwheel Effect" and Peralkyl-Substituted Derivatives

An alternative approach to extending the chemistry of molecular rotors is to alter the identity of the substituents on the central ring. The introduction of the concept of *cogwheeling*,[65,66] which describes the coupled disrotation of two aryl groups attached to a common atomic center, led to the requirement of greater intermeshing of the peripheral substituents. The visualization of a cogwheel (spur-gear or bevel gear) required the interaction of a "tooth" and a "notch" (Figure 1.4); aryl groups may serve as a tooth, however, the model lacked the

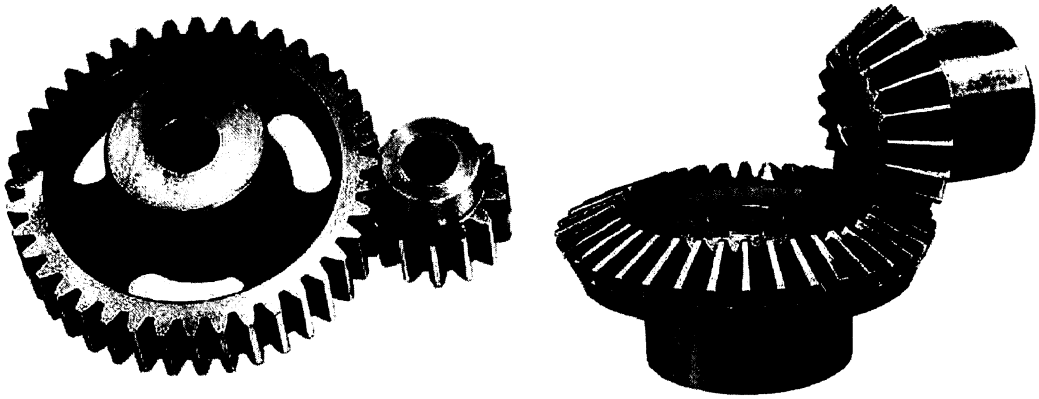

Figure 1.4: A cogwheel (spur-gear) and bevel gear.

notch necessary for sufficient intermeshing.[44] The search for a more accurate mimic of the macromechanical system led to the investigation of alkyl groups as peripheral substituents; alkyl groups can serve as three-fold rotors, and provide the necessary "notches" to model a cogwheel. It also became crucial during the development of molecular analogues of common machinery to distinguish between an *iconic* model, in which the model resembled the object in form alone, and an *analogic* model, in which the function or behaviour of the object was also mimicked.[44]

The prototypical model for these systems was hexamethylbenzene (**1.30**), which exhibited a structure of D_{3d} symmetry in the solid state,[67] with a barrier to geared methyl group rotation of 1 kcal mol^{-1}.[68] In the homosubstituted hexaethylbenzene (**1.31**)[69,70] and hexacyclopropylbenzene (**1.32**),[71] the alkyl

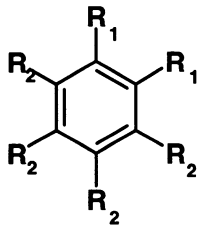

1.30: R_1, $R_2 = CH_3$
1.31: R_1, $R_2 = CH_2CH_3$
1.32: R_1, $R_2 = C(CH_3)_3$
1.34: $R_1 = CH_2CH_3$; $R_2 = CH(CH_3)_2$
1.35: $R_1 = C(CH_3)_3$; $R_2 = CH(CH_3)_2$
1.36: $R_1 = CH(CH_3)_2$; $R_2 = C(CH_3)_3$

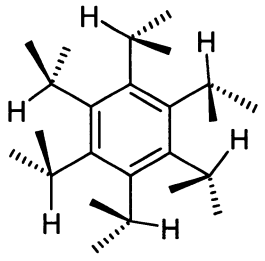

1.33

Chart 1.6: Hexaalkyl-substituted benzenes, and the statically gear-meshed rotor hexaisopropylbenzene, ***1.33****.*

groups were arranged alternately above and below the plane of the central ring. The barrier to uncorrelated[72] ethyl rotation in **1.31** was determined to be 11.5 kcal mol^{-1},[69] and **1.32** did not exhibit restricted rotation down to –30 °C. The X-ray crystal structure of C_6Et_6[69] confirmed the alternating proximal/distal arrangement of substituents, resulting from cooperative nonbonded interactions.[73] In contrast, hexaisopropylbenzene (**1.33**) exhibited an interlocking "tongue-and-groove" arrangement, providing a gear-meshed conformation with a barrier to uncorrelated isopropyl group rotation of > 22 kcal mol^{-1}.[41,74,75]

Mislow and co-workers[76] have examined the rotational processes of **1.34**, **1.35** and **1.36** (Chart 1.6), representing hetero-alkylsubstituted benzenes. The alkyl groups were found to maintain the conformation they adopted in the homosubstituted analogues, and the barriers to rotation remained reflective of this arrangement. In particular, there was a high-energy process (12.7 kcal mol^{-1}) resulting from the "unfreezing" of the intermeshed isopropyl groups, and a low-energy process (9.9 kcal mol^{-1}) representing the rapid rotation of all other alkyl groups in the complex. Clearly the presence of all six isopropyl groups was necessary for sufficient interaction between the substituents, and substitution resulted in a dramatic decrease of the barrier to isopropyl rotation.

Mislow has proposed the collective term *static gear effect* to represent this meshing of alkyl groups in the *ground state*.[77] This must be distinguished from the *dynamic gear effect* that results from the influence of intermeshing a chemical rotor with a neighbouring group on the rate or mechanism of a process, which is

applied to the dynamics of conformational interconversions (the *transition state* of a dynamic process).[77] In this discussion of the analogy between chemical and mechanical gears, it is also essential to consider the weighty contrast that exists between these systems; mechanical gears move with uniform angular velocity, whereas rotation in chemical gears involves coupling between torsional and vibrational motions and the resultant variation in interatomic distances and angles. Thus the fundamental flaw in the design of such systems is that the net disrotatory motion of the gear blades does not necessarily involve movement along a pathway resembling the uniform rotation of a mechanical gear. Nevertheless, the analogy provides a foundation for the design of potential systems, as long as the fundamental basis for the chemical behaviour does not become obscured by the simplicity of the model.[77] Thus, it remains that the coupling of torsional motions is a necessary result of the change in geometry of one of the rotors in a multi-rotor system.

1.2.7 Organometallic Derivatives of Peralkyl-Substituted Benzenes

During the investigation of the rotational behaviour of such species, it became evident that the symmetry of the system must be lowered in order to observe the internal rotation using VT-NMR. In C_6Ar_6 systems, this was accomplished by labelling the edges of the aryl groups, as in **1.17 – 1.19**. An alternative approach was to label the faces of the molecule by coordinating the central ring to an organometallic moiety. This method, of course, also introduced

the possibility of correlated rotation between a bulky organic ligand and the organometallic moiety, if the system was designed to foster significant steric interplay. However, the limit of the method lay in the degree to which the stereodynamics of the molecule were perturbed by the presence of the metal.[78] The observation of dynamic behaviour in both the free and complexed system could be used to determine the magnitude of this disturbance, and provided information on the "steric complementarity" between the two fragments.[78]

Studies on tricarbonyl chromium (**1.37**) and molybdenum (**1.38**) complexes of hexaethylbenzene revealed a barrier to ethyl rotation of 11.5 kcal mol^{-1}, [69,70] and the ethyl groups maintained an alternating up/down arrangement (Chart 1.7). However, substitution of one carbonyl group in $(C_6Et_6)Cr(CO)_3$ with a triphenylphosphine (**1.39**)[70] or triethylphosphine (**1.40**)[79] ligand increased the steric interaction of the ethyl groups with the organometallic moiety, and all of the methyl groups were located above the plane of the central ring. In each instance, the ethyl group rotations were found to be uncorrelated. Moreover, in $(C_6Et_6)Cr(CO)_2(PMe_3)$ (**1.41**),[80] the ethyl groups were found to adopt a 1,2,3,5-distal-4,6-proximal arrangement in the solid state, and multiple isomers formed by ethyl group rotation coexisted in solution.

The potential for steric interactions between the peripheral substituents and the organometallic moiety became an issue of debate following the report of McGlinchey and co-workers of the dynamic behaviour of $(C_6Et_6)Cr(CO)_2(CS)$ (**1.42**).[81] In the X-ray crystal structure the ethyl groups adopted the favoured

alternating distal/proximal arrangement, and variable-temperature ^{13}C NMR studies revealed a 2:1:2:1 pattern for each of the aromatic ring carbons, as well as the methylene and methyl environments, which was consistent with a C_s geometry. Slowed tripodal rotation was invoked as the explanation for this low-temperature behaviour, though restricted ethyl group rotation and the formation of a different 1,2,3,5-distal-4,6-proximal isomer in solution (which would also be consistent with C_s symmetry) could not be ruled out; this was a favoured explanation by Mislow and Hunter since there was no previous evidence for

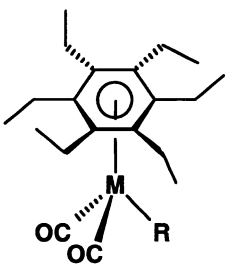

1.37: M = Cr; R = CO
1.38: M = Mo; R = CO
1.42: M = Cr; R = CS

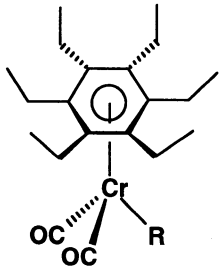

1.39: R = PPh_3
1.40: R = PEt_3

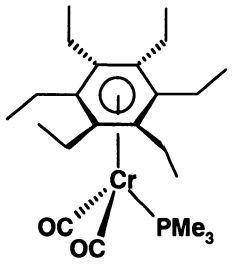

1.41

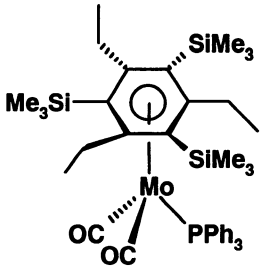

1.43

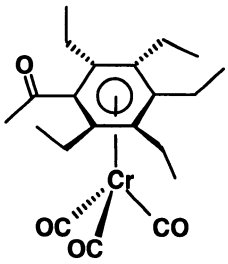

1.44

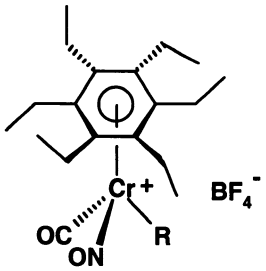

1.45: R = CO
1.46: R = CS

Chart 1.7: Organometallic derivatives of hexaalkylbenzene; the identity of the other metal substituents determines the distal/proximal arrangement of the alkyl groups.

restricted tripodal rotation.[82] Further reports by these authors on several C_6Et_6 complexes concurred; variable-temperature NMR spectra could be explained by considering restricted ethyl rotation. Barriers to ethyl group rotation in such complexes were determined, with a range of 8.3 to 11.7 kcal mol^{-1}, and the issue was considered "unsettled".[83,84]

The breakthrough came in 1989, when Hunter and Weissensteiner reported the crystal structure and dynamic behaviour of dicarbonyltriphenylphosphine (η^6-1,3,5-triethyl-2,4,6-tris(trimethylsilyl)benzene) molybdenum (0) (**1.43**).[85] In the solid state **1.43** adopted a conformation in which one ethyl group and all trimethylsilyl groups were oriented distal to the organometallic moiety, and the other two ethyl groups were oriented proximally. Several decoalescence phenomena were observed, and the resolution of two carbonyl resonances at 145 K were consistent only with restricted tropodal rotation. This report was closely followed by McGlinchey and co-workers' study of pentaethylacetophenone chromium tricarbonyl (**1.44**).[86] The substituents adopted a 1-proximal acetyl-2,4,6-distal-3,5-proximal ethyl conformation both in the solid state and in solution, as observed by ^{13}C NMR spectroscopy. The carbonyl resonances were split into a 2:1 pattern in solution at –100 °C and in the solid-state NMR spectrum at room temperature, thus providing unequivocal evidence for restricted tripodal rotation.[86] This work established the possibility of interactions between the sufficiently bulky peripheral substituents and the organometallic moiety. The subsequent challenge was to determine if their motions were correlated.

In order to achieve this goal, McGlinchey and co-workers systematically designed molecules that would contain the C_6Et_6 ligand, but reduced the symmetry of the tripod. They avoided the use of sterically demanding substituents such as triphenylphosphine since these complicated the analysis by generating mixtures of isomers. Instead, they chose to investigate small, cylindrical ligands possessing similar steric requirements as the carbonyl group.[87] Treatment of $(C_6Et_6)Cr(CO)_3$ (**1.37**) or $(C_6Et_6)Cr(CO)_2(CS)$ (**1.42**) with $NO^+BF_4^-$ resulted in the formation of $(C_6Et_6)Cr(CO)_2(NO)^+BF_4^-$ (**1.45**) or $(C_6Et_6)Cr(CO)(CS)(NO)^+BF_4^-$ (**1.46**), respectively. Both complexes were characterized by X-ray crystallography, and in each case, the hexaethylbenzene ligand adopted the 1,3,5-proximal-2,4,6-distal arrangement. Variable-temperature NMR studies revealed two independent fluxional processes: uncorrelated rotation of the ethyl groups (11.5 kcal mol^{-1}) and restricted tripodal rotation (9.5 kcal mol^{-1}). This suggested that the motion of the tripod and the rotation of the peripheral substituents were not correlated and these systems did not behave analogously to a molecular bevel gear.

In each of these instances, it was clear that the presence of the metal significantly perturbed the stereodynamics of the arene system, likely by raising the ground state energy of the complex, and thereby reducing the barrier to alkyl-aryl rotation; this was indicative of poor complementarity between the arene and the metal moiety.[78] In an elegant study, Kilway and Siegel reported evidence that quantified this effect on the dynamic behaviour of related derivatives of

C_6Et_6.[78] Variable-temperature NMR investigations of molecules **1.47** – **1.49**, and their chromium carbonyl complexes **1.47(Cr)** – **1.49(Cr)** (Chart 1.8) were conducted with the assumption that the distal/proximal arrangement of the peripheral substituents would be maintained. In each instance the barrier to rotation did not change significantly with metal complexation; 7.7 kcal mol^{-1} (**1.47**), 6.6 kcal mol^{-1} (**1.47(Cr)**), 9.4 kcal mol^{-1} (**1.48**), 8.9 kcal mol^{-1} (**1.48(Cr)**), 11.2 kcal mol^{-1} (**1.49**), 11.8 kcal mol^{-1} (**1.49(Cr)**) (each ± 0.3 kcal mol^{-1}).[78] This result confirmed that these systems are good models for the dynamics of the parent compound, and that transition metals are valuable tools for desymmetrization. The authors invoked a "lock and key" complementarity between the arene and metal tripod as an explanation, and proposed that there may be dynamic correlation between their rotational behaviours.[78] Increasing the ring-center metal distance in substituting Mo for Cr drastically decreased the barrier to tripodal rotation, and removed the steric interplay between the metal moiety and the arene system.[88]

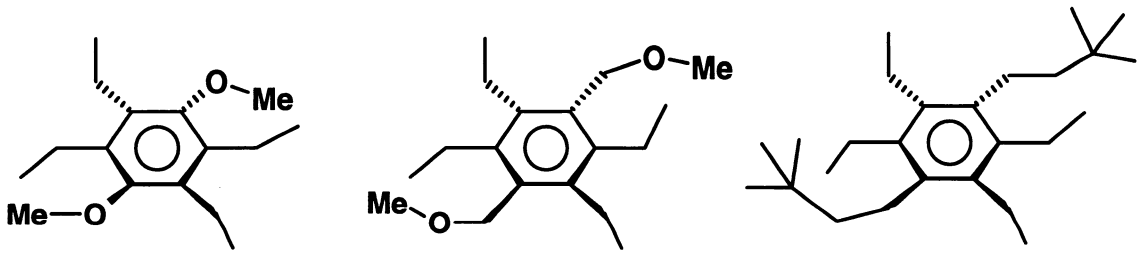

1.47 **1.48** **1.49**

Chart 1.8: Persubstituted arenes that serve as models for steric complementarity between the metal and the arene.

1.2.8 Organometallic Complexes of Peraryl-Substituted Derivatives

The conformational variability of hexaethylbenzene prompted the investigation of peripheral aryl substituents that could not merely rotate away from potential steric hindrance; thus, organometallic derivatives of aryl-substituted benzenes have also been investigated. Treatment of 1,3,5-triphenylbenzene with chromium carbonyl yielded products in which the metal moiety was coordinated to the central ring or one, two or all three of the peripheral phenyl rings (Scheme 1.4). However, these complexes did not exhibit restricted rotation down to –90 °C.[89] The analogous reaction involving hexaphenylbenzene afforded **1.54**, in which the metal was coordinated to a peripheral ring. In the variable-temperature NMR, each of the *ortho*, *meta* and *para* carbon atoms of the peripheral groups exhibited two sets of coalescing

Scheme 1.4

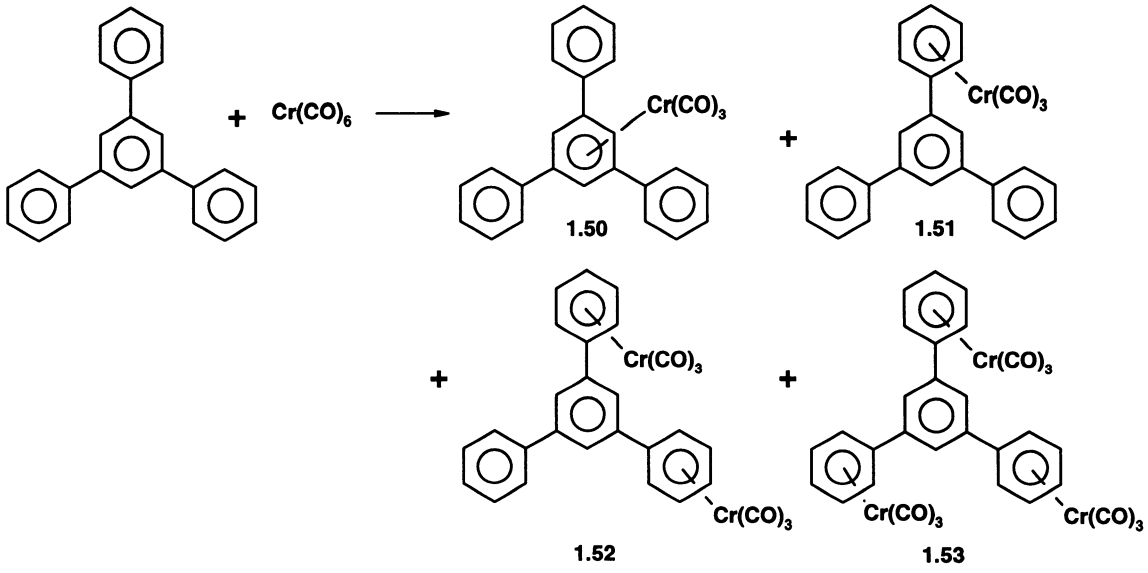

peaks, leading to six independent determinations of $\Delta G^{\ddagger}$, each in the range of 12.2 ± 0.2 kcal mol^{-1}.[90] The near equivalence of these barriers suggested that the isomerizations belonged to the same fluxional process, in particular, the rotation of the chromium carbonyl-complexed ring relative to the central ring. If the other rings were perpendicular to the central ring on the NMR time-scale, then this rotation created a system of C_{2v} symmetry (at room temperature), rendering the *ortho* and *meta* carbon sets of the symmetry related rings equivalent, resulting in the observed coalescence behaviour. Since the *ortho* and *meta* carbons in the uncoordinated peripheral rings were equivalent, neither restricted nor rapid rotation was evident in those rings. At low temperature, the system exhibited C_s symmetry, as depicted in Chart 1.9.

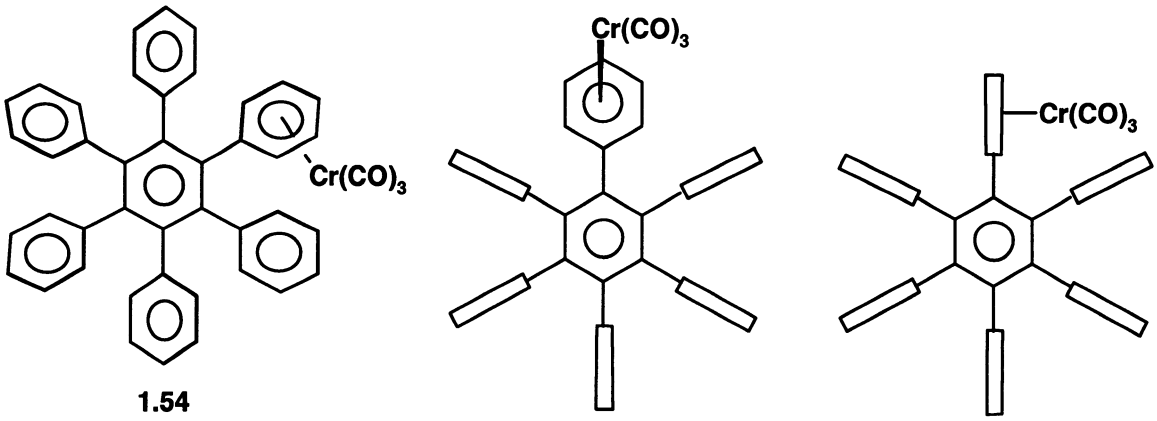

1.54

Chart 1.9: Hexaphenylbenzene chromium tricarbonyl, ***1.54****, and the two rotamers possessing C_s symmetry.*

An alternative approach was to incorporate the metal moiety as a peripheral substituent. In 1978, Rausch and Siegel prepared C_6Ph_5Fc (**1.55**) by Diels-Alder treatment of tetracyclone (**1.26**) with phenyl-ferrocenyl acetylene, however, no structural or dynamic data were reported (Scheme 1.5).[91] Gupta *et al.* previously prepared 2,4,5-triphenyl-3-ferrocenylcyclopentadienone (**1.27**), and various metal derivatives,[92] and this ligand was later treated with diphenylacetylene to yield **1.55** using a complementary approach.[93] The X-ray crystal structure of **1.55** revealed a curious phenomenon: the dihedral angles of

Scheme 1.5

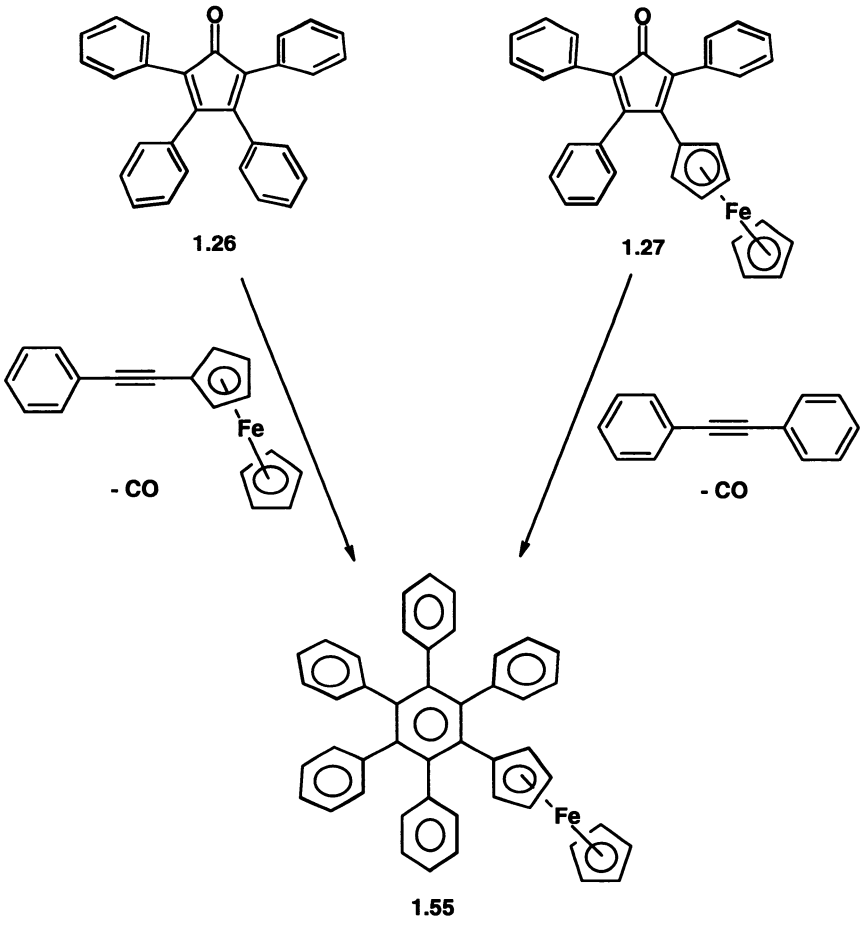

the peripheral substituents showed an incremental progression of 51°, 64°, 70°, 81°, 89° and 120°. The postulation that the rotation of the ferrocenyl moiety would induce a "domino effect" such that the remaining aryl groups rotated in a correlated fashion was difficult to overlook. Unfortunately, variable-temperature NMR studies revealed that all fluxional processes were rapid to accessible temperatures on the NMR time-scale.[92]

Derivatives of 5-membered ring systems have also been investigated, and in many cases, the barriers to rotation were small or unobservable (C_5Ar_5,[94-104] C_5Ar_4X[92,102,105-115]). The peripheral rings adopt a propeller conformation, with dihedral angles of approximately 50°. This represents a compromise between the fully coplanar arrangement (which would maximize both orbital overlap and steric repulsion) and the perpendicular array of groups (which minimizes steric repulsion but prevents orbital overlap and conjugation).[116,117] In the crowded complex $(C_5Ph_5)Fe(CO)(PPhMe_2)(COEt)$ (**1.56**, Chart 1.10), two fluxional processes were evident in the low-temperature NMR spectra.[117] As the rotation of the chiral tripod was slowed, the five cyclopentadienyl carbon atoms became inequivalent, allowing the barrier to tripodal rotation of 8.7 ± 0.3 kcal mol^{-1} to be determined. Moreover, the restricted rotation of either the peripheral aryl groups or the phosphine ligand resulted in the formation of many rotamers, yielding a barrier to rotation of 11.7 ± 0.3 kcal mol^{-1}.[117] The significant difference between these barriers indicated that the motions of the substituents were uncorrelated.

Thus, the steric interplay between substituents in the 5-membered ring systems studied thus far does not appear to be sufficient to induce correlated rotation.

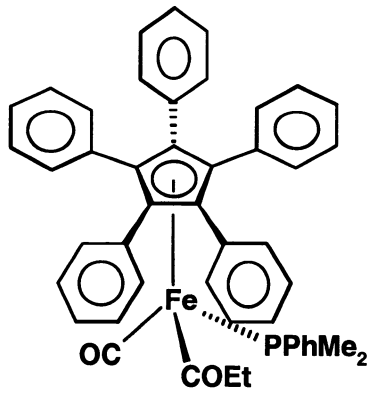

1.56

*Chart 1.10: Pentaphenylcyclopentadienyl iron complex **1.56**.*

1.2.9 Seven-Membered Ring Systems

By analogy to the contraction of 6-membered ring systems and the examination of crowded 5-membered rings, the expansion to 7-membered rings was expected to decrease the distance between the substituents and result in greater interaction. Diels-Alder treatment of tetracyclone (**1.26**) with triphenylcyclopropene yielded the desired C_7Ph_7H (**1.58**).[118] An X-ray crystallographic analysis of the system revealed the formation of the anticipated boat-shape, in which the initially formed **1.58a** underwent a conformational flip to give **1.58b**, such that the unique phenyl ring was axial and straddled the pseudo mirror plane (Scheme 1.6). The other phenyl rings were extremely sterically hindered, and barriers to rotation of ~ 9 kcal mol^{-1} (rings A and C) and 11 kcal mol^{-1} (rings B) were estimated, thereby revealing that their rotation was not correlated.

Scheme 1.6

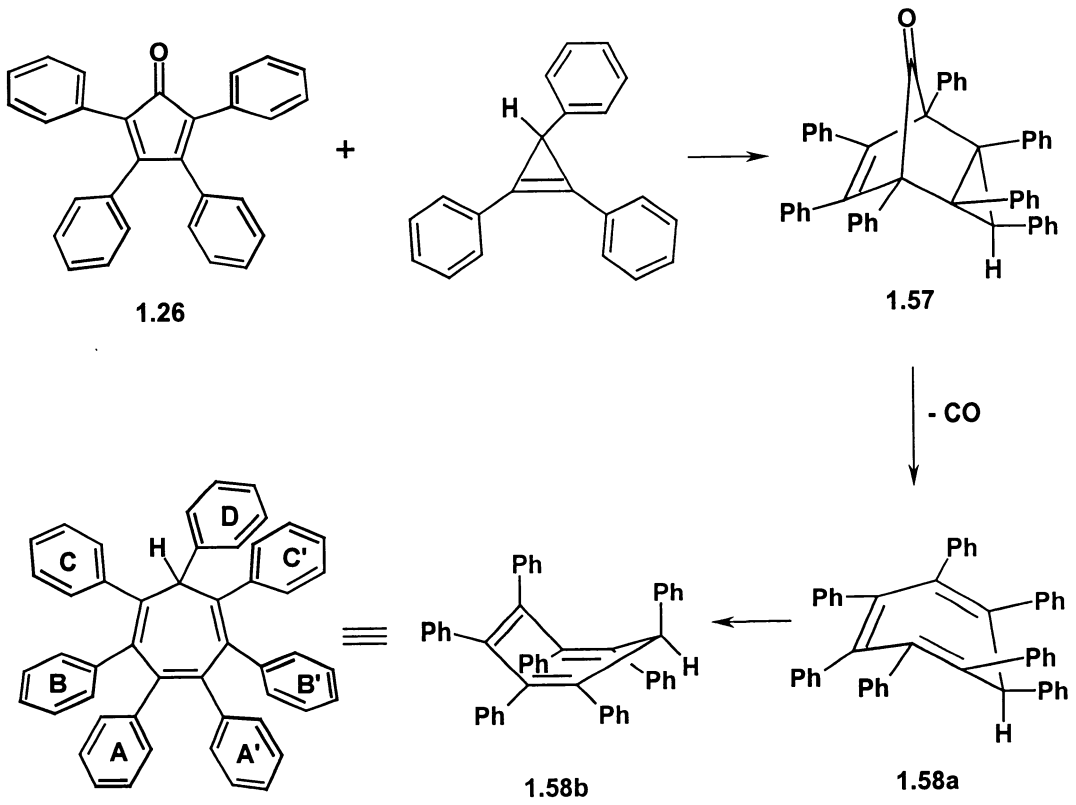

1.26 1.57 1.58b 1.58a

Treatment of C_7Ph_7H with bromine resulted in the formation of the aromatic cation $C_7Ph_7^+Br^-$ (**1.59**, Scheme 1.7); crystals of the cation were obtained upon slow evaporation from trifluoroacetic acid.[119] The tropylium cation adopted a shallow boat conformation, and the phenyl groups possessed average dihedral

Scheme 1.7

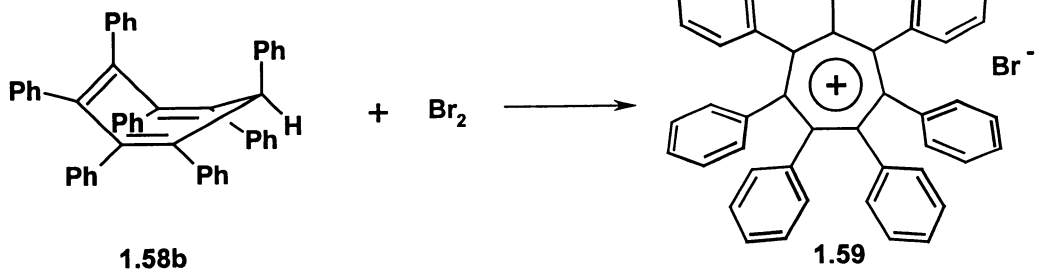

1.58b 1.59

angles of 80° relative to the central ring. Attempts to coordinate an organometallic moiety to the central ring were not successful, and yielded instead products **1.60** and **1.61** (Chart 1.11).[118]

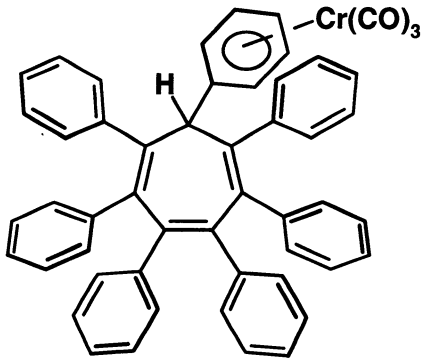

1.60

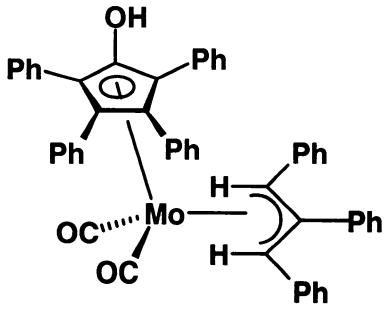

1.61

*Chart 1.11: Organometallic complexes resulting from the treatment of **1.58b** with $Cr(CO)_6$ (**1.60**), or **1.57** with $Mo(CO)_6$ (**1.61**).*

Analogous to the 6-membered ring systems, the incorporation of a ferrocenyl substituent into a 7-membered ring has also been also investigated.[93] An X-ray crystal structure of the boat-shaped complex C_7Ph_6FcH revealed that the ferrocene was located on the carbon adjacent to the sp^3 hybridized carbon, whereby the initially formed **1.62** underwent a [1,5]-hydrogen shift after decarbonylation but before the cycloheptatriene ring inversion to yield **1.63** (Scheme 1.8). As with C_7Ph_7H, different barriers to rotation were determined for different peripheral aryl groups, thus their rotation was again uncorrelated. Numerous attempts at preparing the cation $C_7Ph_6Fc^+$ were unsuccessful, the complex instead formed the related ferricinium salt $C_7Ph_6FcH^+SbF_6^-$.

Scheme 1.8

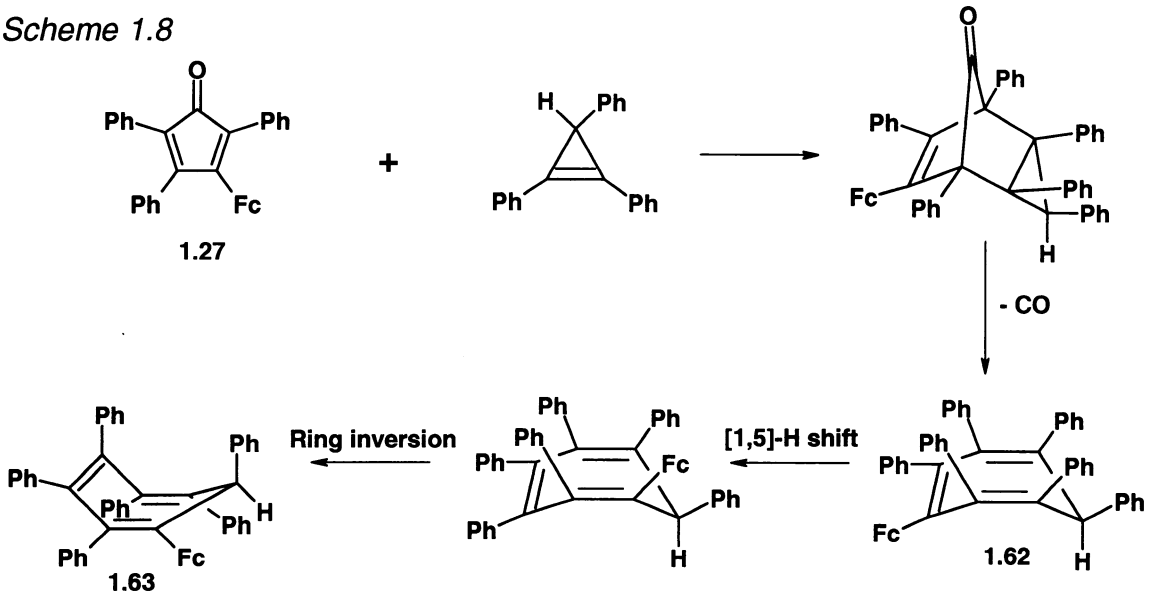

Through the historical development of molecular propeller systems and crowded molecules, numerous ground-breaking accounts have outlined the necessary design parameters and steric requirements. Clearly, the substituents must be bulky enough to induce significant interactions, however, they must be small enough to allow the synthesis of the desired derivative, and to prevent locking the molecule into one conformation. The molecule must also be suitably labelled, so that restricted rotation may be observed and barriers may be determined using variable-temperature NMR. These key features must be maintained in the development of future derivatives.

1.3 Alternative Gearing Systems

1.3.1 Triptycene Derivatives

A further attractive structure that has been examined as a prototype for a molecular gear is the triptycene molecule (**1.64**). Triptycene models a three-bladed gear, and offers multiple sites for functionalization, as well as the potential for significant intermeshing of other substituents between the blades. The molecule is synthesized by the action of benzyne (generated from isoamyl nitrite and anthranilic acid) on anthracene (Scheme 1.9); suitable substitution on the anthracene or the anthranilic acid yields the desired derivative, and numerous examples have been synthesized. [77,120-126] Oki and co-workers have examined the rotational barriers in a variety of substituted triptycenes, and have established a significant dependence of the barrier to rotation on the identity of the 1-(peri-) substituent; barriers ranging from < 8 kcal mol^{-1} to 31 kcal mol^{-1} have been determined.[127,128] Later studies confirmed this observation,[129,130] and similar results have been achieved for 9-benzyl–[131-135] or phenoxy–[133,135-137] substituted

Scheme 1.9

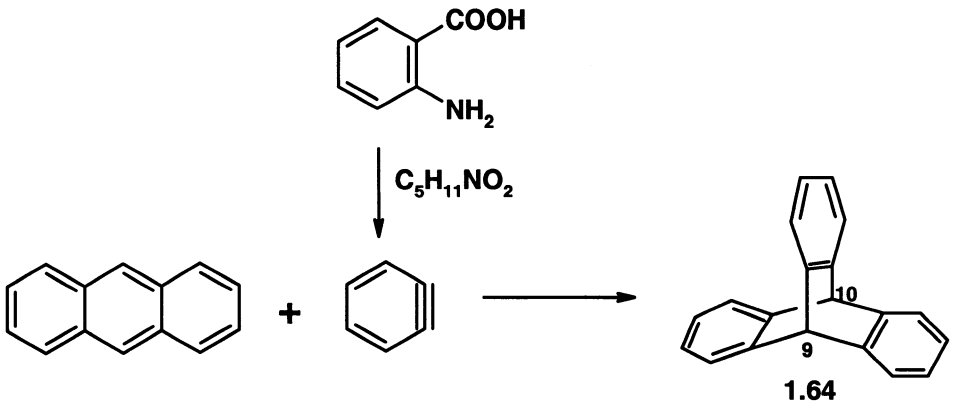

1.64

derivatives. Remarkably, atropisomerism has also been realized in these systems, in which restricted rotation about a single C-C bond allowed stable, rotational isomers to be isolated. Two rotamers of 8-bromo-1,4-dimethyl-9-(2-methylbenzyl)triptycene (**1.65**) were separated and characterized, with a barrier to interconversion of 27.2 kcal mol^{-1}.[138] The origin of this behaviour was attributed to the multi-step process necessary to interconvert the isomers, which involved the high energy step of the passage of an aryl group over a peri-substituent. Other related atropisomers have since been isolated.[139-144]

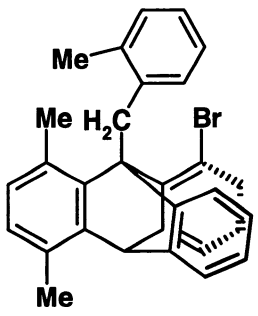

1.65

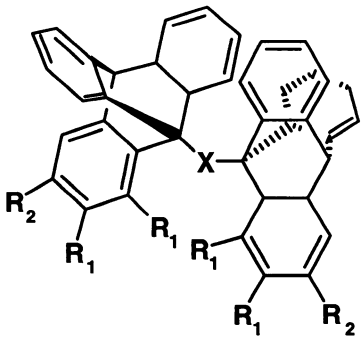

1.66: X = O; R_1, R_2 = H
1.67: X = CH_2; R_1, R_2 = H
1.68: X = CH_2; R_1 = CH_3; R_2 = H
1.69: X = O; R_1 = H; R_2 = Cl

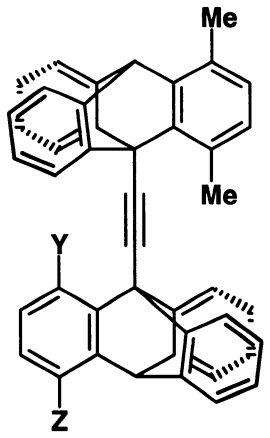

1.70: Y = F, Cl, Br, I; Z = H
1.71: Y = Me; Z = Me
1.72: Y = Ph, Mes; Z = H

*Chart 1.12: Substituted triptycene derivatives **1.65 – 1.72**.*

Also of particular relevance to this discussion is the formation of bis(triptycyl) complexes, in which the blades of two triptycene units may be intermeshed. In both bis(1-triptycyl)–ether (**1.66**) and –methane (**1.67**), the barrier to rotation was found to be less than 8 kcal mol^{-1},[145] revealing that these

systems were extremely conformationally flexible and could remain mobile in crowded environments. However, computational analysis of the conformations of bis(1-triptycyl)methane revealed that the triptycene units were securely meshed[146] and that the molecule underwent coupled disrotation of the triptycene groups (dynamic gearing).[147] This prediction was realized by the synthesis and characterization of bis(2,3-dimethyl-9-triptycyl)methane (**1.68**),[148] and bis(4-chloro-1-triptycyl)ether (**1.69**),[149] in which two isomers were isolated at ambient temperature and interconversion was observed only at elevated temperatures ($\Delta G^{\neq}$ = ~34 kcal mol^{-1} (**1.68**) and > 24 kcal mol^{-1} (**1.69**), Chart 1.12). As above, several related derivatives have been examined with comparable results,[150] and the X-ray crystal structure of bis(9-triptycyl)ether has confirmed the bevel-gear geometry of this molecule in the solid state.[151] Several other atoms have been examined as central points in Tp_2X systems, with barriers ranging from 20.4 kcal mol^{-1} (X = Si) to 41.0 kcal mol^{-1} (X = O).[152,153]

A further extension of these ideas was the examination of bis(triptycyl)ethynes, such that a two-carbon bridge separated the gears, rather than one atom.[152] As before, the identity of the peri-substituent was crucial for the observation of correlated rotation, and barriers of 11.6 kcal mol^{-1} (F) to 17.3 kcal mol^{-1} (I) have been determined for complexes **1.70**, whereas a barrier of 15.5 kcal mol^{-1} was calculated for the tetramethyl complex **1.71**.[154,155] Moreover, the C≡C bond was found to deviate significantly from linearity in the crystal structure of the tetramethyl derivative, offering evidence for the severe steric

interactions in this complex.[155] Similar deformations were also observed in derivatives containing a peri-aryl substituent (**1.72**), and barriers to rotation varied from 15.8 kcal mol^{-1} (Ph) to 18.8 kcal mol^{-1} (Mes).[156]

1.3.2 Organometallic Derivatives of Triptycene

Various organometallic derivatives of triptycene have also been created.[157-164] Pohl and Willeford first synthesized the chromium tricarbonyl triptycene complex (**1.73**), in which the metal moiety was coordinated to one of the blades. They calculated the closest distance between the carbonyl oxygen atoms and the center of the next blade to be ~ 2 Å, and postulated that the triptycene unit would distort to allow the tripod to rotate freely.[157] This hypothesis was later realized with the determination of the X-ray crystal structure of the

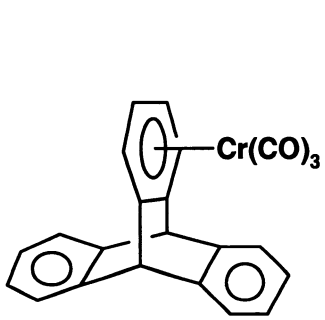

1.73

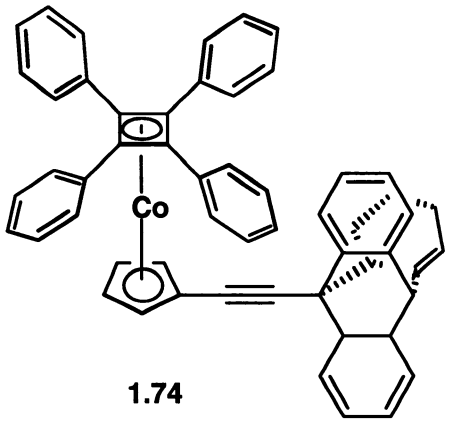

1.74

*Chart 1.13: The chromium carbonyl complex of triptycene (**1.73**) and Richards' metallocene molecular gear (**1.74**).*

chromium carbonyl complex[160] in which the dihedral angle between the planes of the blades containing the metal was increased, resulting in a decrease of the other two dihedral angles from the expected 120° in uncomplexed triptycene.

A particularly influential study, reported by Stevens and Richards in 1997, was the first to result in the formation of a "metallocene molecular gear" (**1.74**, Chart 1.13).[165] The objective of intermeshing the four-toothed tetraphenylcyclobutadiene with the three-toothed triptycene was inspirational, although the variable-temperature NMR of the complex revealed the rapid rotation of the phenyl groups and triptycene unit to low temperatures, and no crystal structure was obtained. Nonetheless, the concept of correlating the rotation of a triptycene gear with another metal substituent was pioneered, and this would become a model for future systems.

1.3.3 A Triptycene Molecular Brake and Ratchet

The direct application of triptycene towards the creation of a "molecular brake" was first realized by Kelly and co-workers. As an initial attempt, the authors synthesized **1.75** with the expectation that coordinating a metal atom to the bipyridine moiety would activate the brake and stop the rotation of the triptycene.[166] Instead, free rotation was observed down to –120 °C, and the system was compared to a playing card fastened to a wheel of a bicycle, whereby it was dislodged with each successive rotation. The initial goal was finally achieved by removing one of the "linker" atoms and synthesizing the

Scheme 1.10

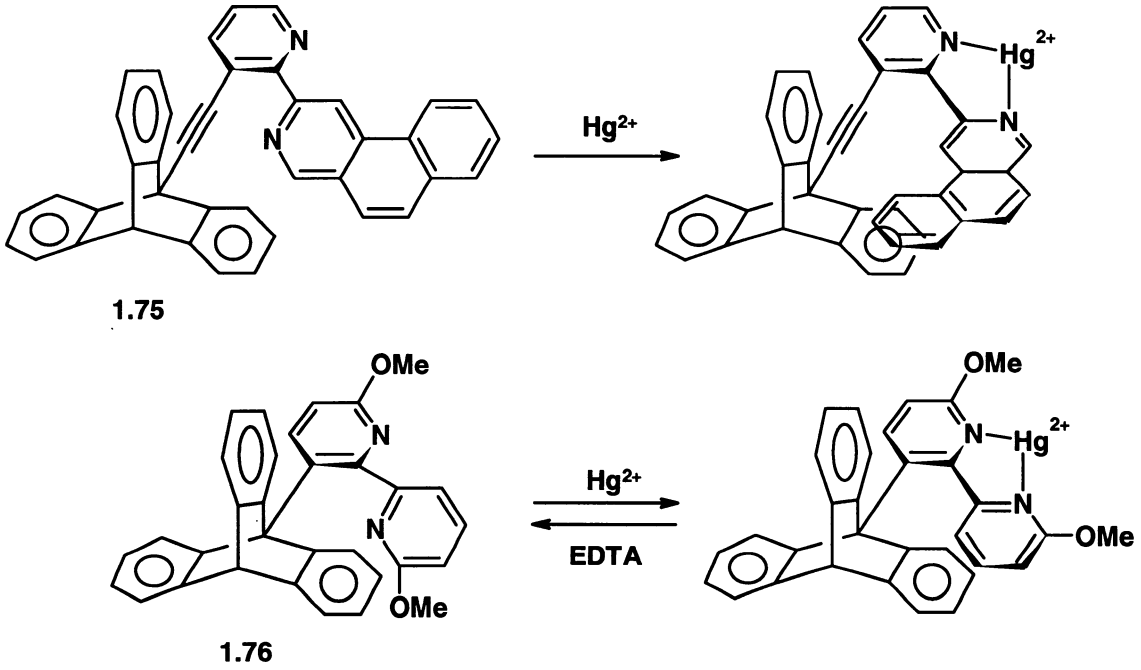

related derivative **1.76**. Coordinating a mercury ion to the bipyridine moiety resulted in the cessation of triptycene rotation at –30 °C; warming the sample allowed the brake to "slip" (Scheme 1.10). The addition of EDTA to the solution removed the mercury ion, and free rotation returned.[166]

In another elegant study, Kelly attempted to create a molecular ratchet, in which a triptycene moiety served as the ratchet wheel and a helicene as the pawl and spring (**1.77**, **1.78**, Chart 1.14). Variable-temperature NMR investigations revealed the restricted rotation of the complexes, however, unidirectional motion could not be enforced.[167,168] Instead, the helicenes were described as "friction brake[s]" that could inhibit ($\Delta G^{\neq}$ = ~25 kcal mol^{-1}), but not prevent, the rotation of the triptycene unit. As an extension to this investigation, unidirectional motion

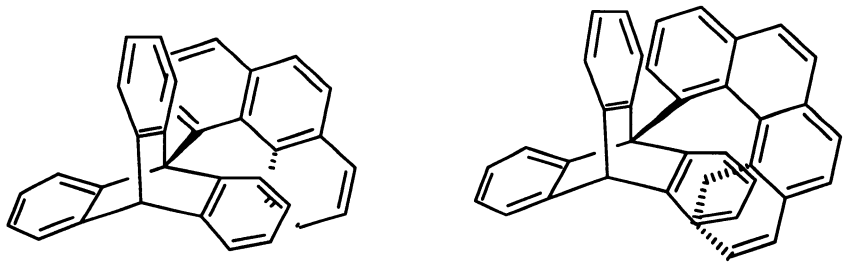

1.77 **1.78**

*Chart 1.14: Kelly's molecular ratchets **1.77** and **1.78**.*

was induced by lowering the energy barrier to clockwise rotation (Scheme 1.11).[169] The phosgene served to activate molecule **1.79**, which then reacted with the hydroxypropyl tether on the helicene to form the urethane; rotation could then occur. Addition of $NaBH(OEt)_3$ cleaved the urethane, and the rotation had been achieved. The entire process was slow (~3h), however, the goal had been

Scheme 1.11

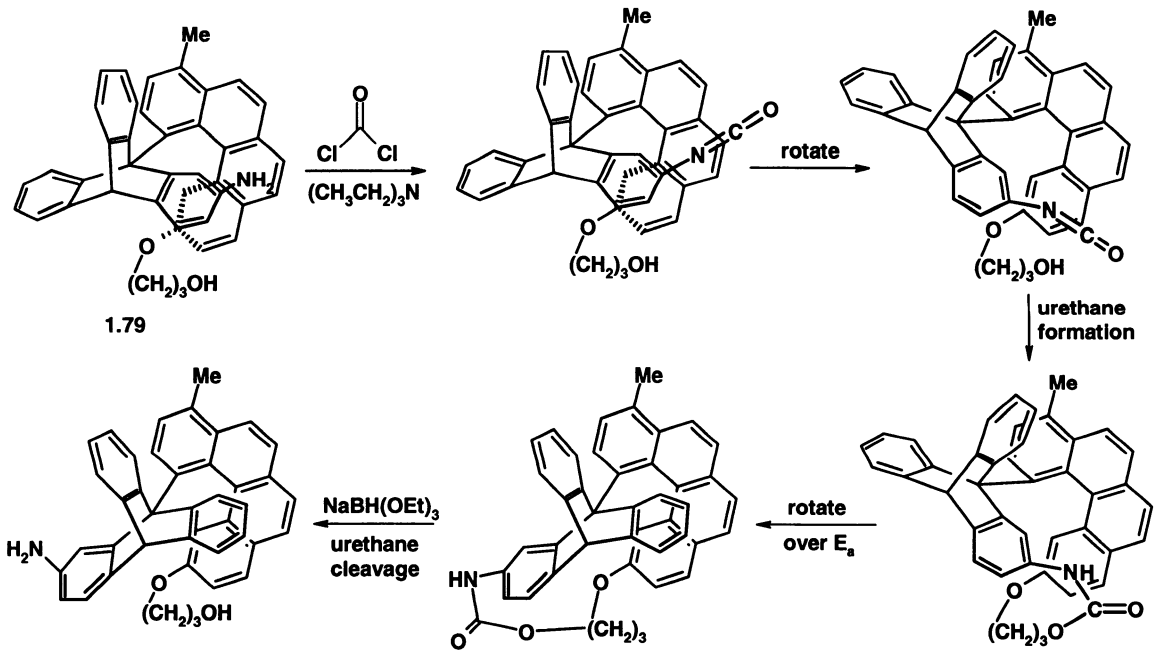

achieved, and Kelly succeeded in describing the first chemically driven molecular motor.

1.4 Molecular Machinery and Nanotechnology

A molecular machine may be defined as an assembly of discrete components designed to perform work resulting from an appropriate external stimulus.[170] There is currently widespread interest in the design and application of such systems, resulting in the development of nanotechnology and nanoscience as rapidly growing fields of research. As physicists and engineers attempt to construct miniature analogues of useful devices, chemists approach this area from the bottom and attempt to create nanoscale machines[170-173] (nanoscale dimensions range from 1 to 100 billionths of a meter; a nanometer). As elegantly outlined by Balzani *et al*,[170] the characteristics of molecular machines include (i) the kind of energy necessary to induce useful function, (ii) the type of movement enacted by the components of the system, (iii) the ability to control and monitor this movement, (iv) the potential for repeating the action at will, (v) the time-scale in which the movement is enacted, and (vi) the actual function performed. In reality, the movements can be rotation about bonds, or the formation and destruction of noncovalent interactions. Temperature may be utilized for control, and changes in spectroscopic properties allow for monitoring the actions of the system; this also limits the time-scale of observation. The operation of the structure must also be reversible in order to repeat the

function.[170] The crucial factor that remains to be defined is the predictable function of the system. There is also extensive discussion on the energy requirements and methods of supply for such machines; chemical reactions can provide energy, but the necessity for a constant supply of reactants, and a method to remove waste products complicate the application of this concept.[170] As a result, the current focus is on the use of photochemistry and electrochemistry in the modeling of future systems, and progress in this area is continually under review. [44,170,173,174]

Certainly, the models for artificial molecular machines are their analogues that occur frequently in nature.[173] Examples include the rotary motor F_1-ATPase[175,176] and the linear motor myosin (Figure 1.5).[173] The complexity of such systems is unlikely to be matched synthetically, and as elegantly stated by Balzani and Stoddart, "living organisms represent the synergistic integration of

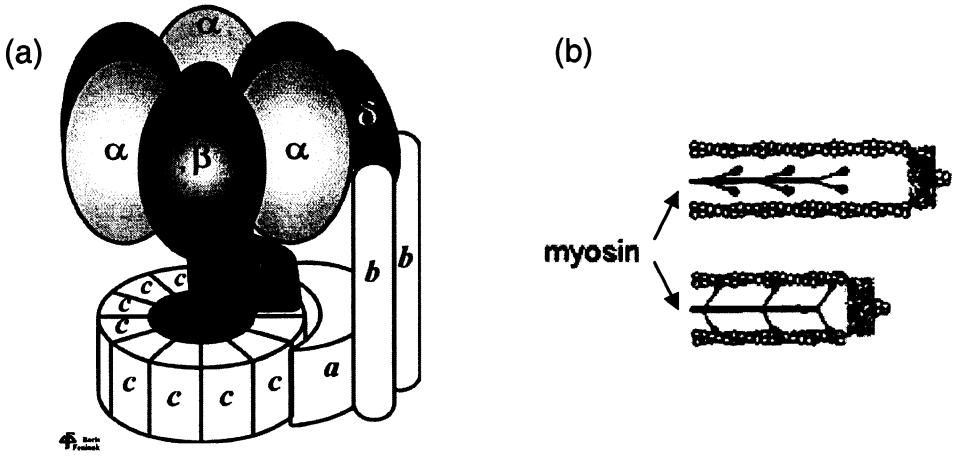

Figure 1.5: The rotary motor ATP-synthase (a) and the linear motor myosin (b).

functionally diverse molecular machines."[173] Nonetheless, the challenge of designing even simple microscopic analogues of macroscopic devices has occupied the minds of innumerable researchers worldwide. Several molecular-scale models of common equipment, objects and machines have been reported, including a C_{60} soccer ball,[177] artificial muscles,[178] compasses and gyroscopes,[179] a ring-containing dumbbell,[180] a single-molecule rotor,[181] a molecular pinwheel,[182] a screw-propeller,[183] a turnstile,[184] a wheelbarrow,[185,186] and an abacus,[187] as well as Kelly's brake, ratchet, and motor described above.[188] Moreover, some of the most widely investigated and well-developed molecular machines are the switches and motors based on rotaxane archetectures[189-192] or other crowded molecules.[193,194] For instance, the switchable rotaxane, **1.80**, in which the electron acceptor (ring) interacts preferentially with the benzidine unit. Upon oxidation of the benzidine, the ring is reversibly shifted to the biphenol group (Scheme 1.12), behaving analogously to a translating wheel on an axle.[190,195]

Specific applications of the molecular propellers and gears described involve the transmission of information along a molecular chain. A macromolecule composed of adequately arranged rotors may undergo correlated rotation so that information may be transferred from one end of the molecule to the other.[44,196] Biali and co-workers first investigated the possibility of this proposed application by computationally studying propeller chains composed of n rings ($n > 2$) pairwise linked by ($n - 1$) methylene units (**1.81**).[196] The goal was to

Scheme 1.12

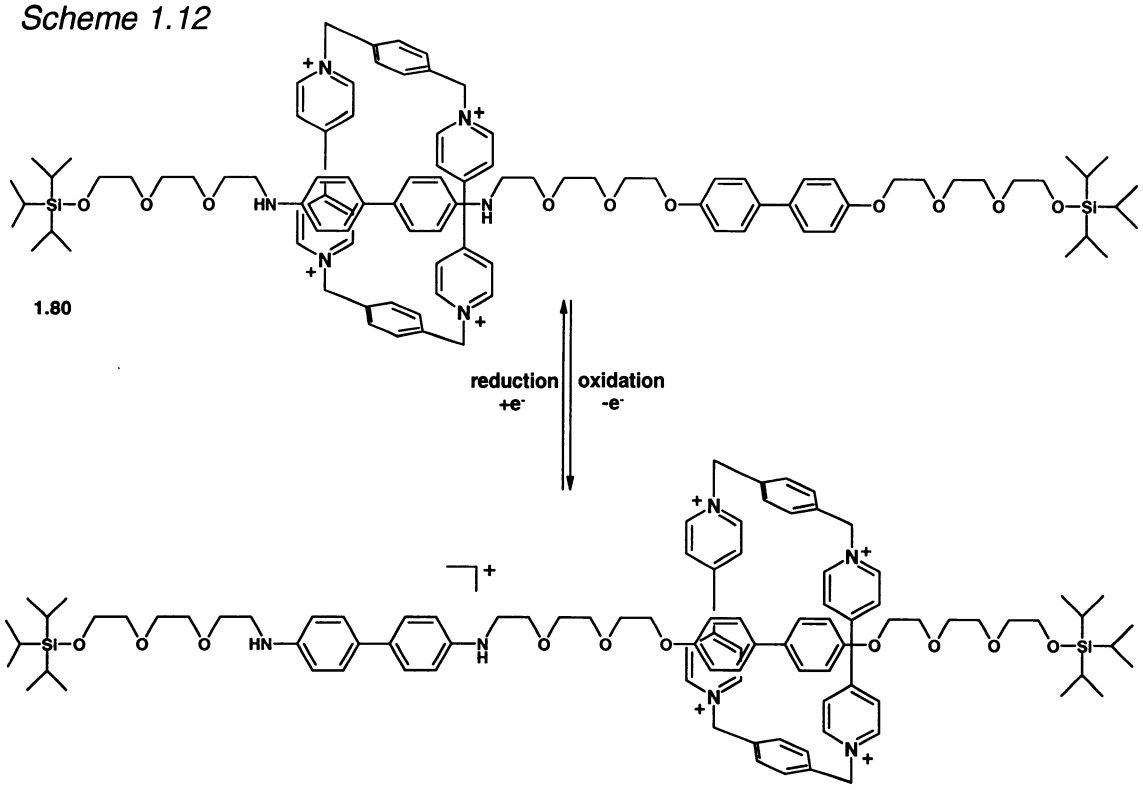

determine the feasibility of transmission of information by correlated rotation of all the rings along the chain, and the model systems chosen were **1.82**–**1.84** (Chart 1.15), involving permethylated aryl groups attached through methylene linkers.

Executing a complicated computational analysis, the authors determined that the threshold barriers to propeller interconversion were different in the parent molecule (**1.82**) than the systems containing longer chains (**1.83** and **1.84**). The barrier for uncorrelated ring rotation should be independent of chain length, however, the barrier for correlated rotation should increase with the length of the chain, since increasing the number of rings involved also intensifies the repulsive interactions. Thus, the longer the chain, the smaller the energetic preference is

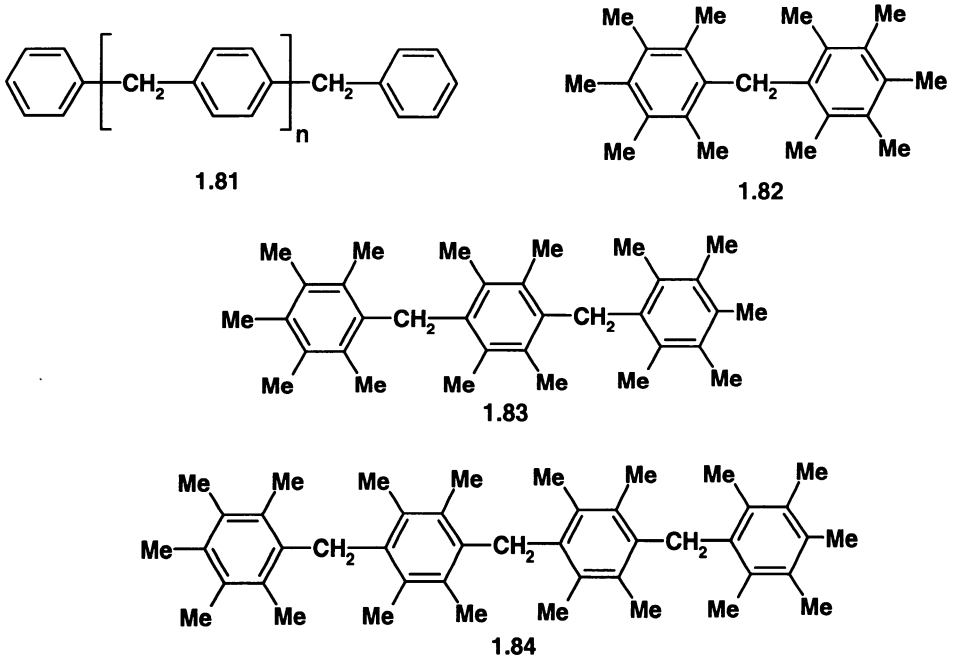

Chart 1.15: Molecular chains investigated for potential transmission of information.

for correlated rotations, and uncorrelated motions become more feasible. In the systems under investigation, the lowest energy interconversion process involved the correlated disrotation of only two rings at one time; performing localized disrotations in succession minimized the steric interactions. Overall, it was clear that the desired application required the thoughtful design of a system with securely intermeshed substituents and with a significant energy gap between correlated and uncorrelated rotation mechanisms.[196]

An alternative approach to this investigation is the examination of triptycene-based gear trains. Iwamura et al. first studied the phase relationship between the remote substituents in 9,10-bis(3-chloro-9-triptycyloxy)triptycene (**1.85**, Chart 1.16), and found that the separation of two gears by an additional

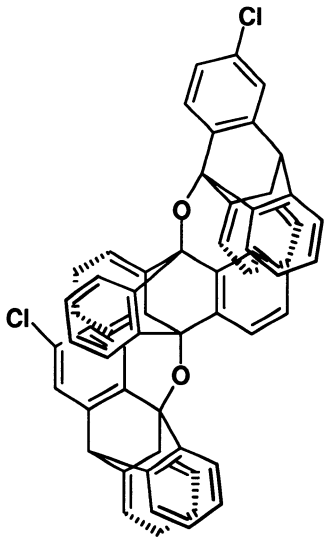

1.85

*Chart 1.16: Doubly-geared molecular gear-train **1.85**.*

triptycene unit allowed for the formation of doubly geared molecules.[197] Two isomers were isolated at ambient temperature, and the interconversion occurred at elevated temperatures by a gear-slip mechanism, with a barrier of 43.2 kcal mol^{-1}.[197,198] Consequently, the concept of molecular gear-trains was successfully introduced, and research in the area continues.[44] Of course, suitably substituted and intermeshed monomeric structures must first be constructed in order to continue progress in this area.

1.5 Objectives of the Research

Upon review of the progress and development of the chemistry of sterically crowded organic and organometallic molecules, it is clear that the many advances made towards understanding the features required for a structure to exhibit correlated rotation have not been successfully applied to the creation of

such a system. The molecule must contain substituents with extreme steric constraints to induce coupled behaviour, as well as a suitable NMR probe to allow for the observation of rotation dynamics. The primary goal of this thesis is to create a system that exhibits correlated rotation. This will be accomplished by: (i) increasing the steric hindrance of the peripheral aryl substituents by incorporating β-naphthyl groups and fluorenyl substituents into 5- and 6-membered organic and organometallic molecules, and (ii) attempting to apply the attractive features of triptycene architectures to the synthesis of an organometallic molecular brake, controlled by the hapticity of the metal fragment.

The chemistry of peraryl-substituted molecules has been developed by investigating *ortho*- or *meta*-substituted derivatives, however, larger groups that maintain planarity have not been investigated. The extension of this chemistry by the inclusion of the bulkier naphthyl groups that serve as phenyl substituents with a "labeled edge", thus allowing for the distinction between distal and proximal isomers, is described in Chapter 2. Naphthyl substituents have been incorporated into the central ring in tetraarylcyclopentadienone molecules and their rhodium acetylacetonate derivatives, and the consequent dynamic behaviour is discussed. Further advancing on this approach, the sterically-crowded hexanaphthylbenzene and pentanaphthylferrocenylbenzene have been synthesized and their dynamic behaviour is described in Chapter 3.

As well as creating crowded systems in an attempt to induce correlated rotation, the steric crowding in these molecules may also be used to stabilize

reactive species. The protonation of crowded cyclopentadienones, which may result in the formation of an antiaromatic cation, is an area of research that remains to be explored. Chapter 4 describes the treatment of tetraphenylcyclopentadienone and 3-ferrocenyl-2,4,5-triphenylcyclopentadienone with a strong acid, and the characterization of the resulting products. There is an interesting contrast between the reactivity of the organic and organometallic molecules, and dramatically different products are the result.

An interesting approach to the extension of the chemistry of triptycenes is the substitution of an indenyl group onto one of the bridgehead carbon atoms. The coordination of a metal to the 6-membered ring of the indene, followed by migration to the 5-membered ring induced by deprotonation, provides the opportunity to control the steric contribution of the metal moiety, and the rate of rotation experienced by the triptycene unit. Chapter 5 recounts the attemped synthesis of an organometallic molecular brake in which the hapticity of the metal controls the rotation of the triptycene.

The application of this concept to a sterically crowded benzene molecule was also explored by the attempted synthesis of pentaphenylfluorenylbenzene, in which the metal could again migrate from the 6- to the 5-membered ring of the fluorene and increase the steric hindrance of the peripheral substituent. Chapter 6 describes the proposed synthetic route to this complex, and the unexpected radical reactivity of the fluorenyl ligand that results instead in the formation of numerous interesting molecules.

CHAPTER TWO

Rhodium Acetylacetonate Complexes of β-Naphthyl-Substituted Cyclopentadienones

2.1 Introduction

In an attempt to extend the chemistry of sterically crowded cyclopentadienones, derivatives incorporating naphthyl substituents have been synthesized.[199] The general chemistry of cyclopentadienones (**2.1**) has been reviewed,[200,201] and some barriers to rotation have been reported. In 1971, Haywood-Farmer and Battiste published a study on the synthesis and dynamic behaviour of 3,4-di-*o*-tolyl-2,5-diphenylcyclopentadienone (**1.21**), and reported the observation of two signals for the *o*-methyl groups in the ^{1}H NMR spectrum at ambient temperatures.[59] This occurrence was attributed to the presence of two isomers in which the *o*-tolyl groups were oriented in a *cis* or *trans* arrangement (Chart 2.1), and the interconversion of these rotamers was prevented by the restricted rotation of the peripheral substituents. The coalescence of the two signals at 137 °C allowed for the determination of the barrier to *o*-tolyl rotation as 21.8 ± 0.4 kcal mol^{-1}.

Building on this initial communication, Willem and Pepermans investigated the dynamic behaviour of tetra-*o*-tolylcyclopentadienone (**1.22**).[60,61] The NMR spectra of tetraphenylcyclopentadienone (**1.26**, page 23) revealed rapid rotation and an average perpendicular arrangement of peripheral substituents.[60,201] This arrangement formed the basis for the authors' discussion of the results, although

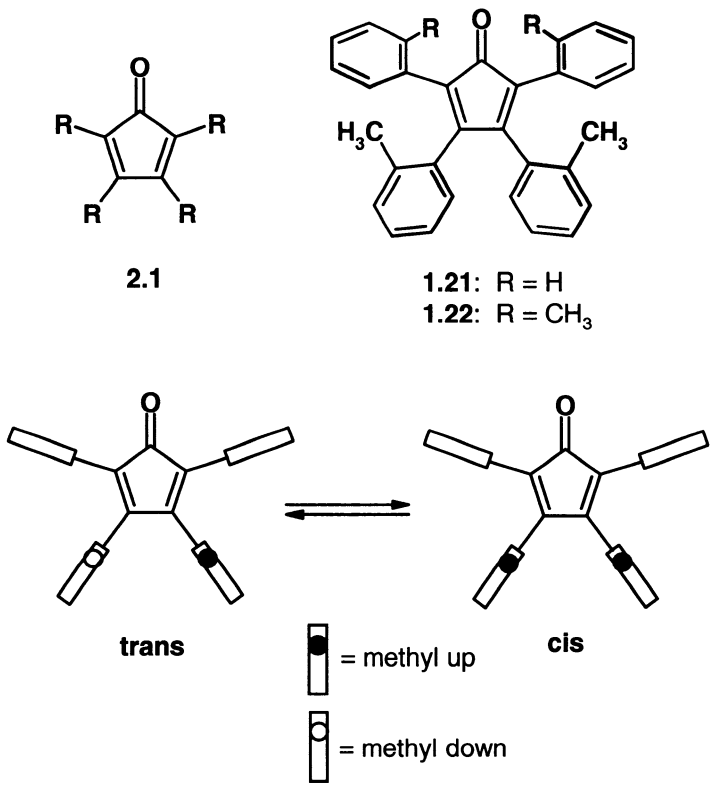

*Chart 2.1: Cyclopentadienone (**2.1**) and o-tolyl substituted derivatives (**1.21**, **1.22**).*

the contribution of a propeller structure was not entirely discounted. The low-temperature ^{1}H NMR spectrum revealed several signals in the region of the methyl groups, and the ^{13}C NMR spectrum displayed several methyl and carbonyl carbon environments; warming the sample resulted in complex coalescence behaviour. This behaviour was interpreted according to the presence of two independent coalescence phenomena: the rotation of the α-substituents and the β-aryl groups, with barriers to rotation of approximately 15 (α) and 20 (β) kcal mol^{-1}. An analysis of the possible modes of rotational isomerization led to the conclusion that the motions of the substituents were uncorrelated, and the authors (perhaps prematurely) extrapolated this to

represent the generality of this phenomenon in molecules containing peripheral groups attached to a central ring.[60]

Numerous organometallic derivatives of cyclopentadienones have been identified as minor products resulting from the treatment of substituted alkynes with metal carbonyls; deliberate syntheses are less common.[110,202] For instance, Rausch and Clearfield observed the formation of the cobalt complexes **2.2** and **2.3** in very low yields (~ 8% and 2%, respectively) upon treatment of (η^5-C_5H_5)$Co(CO)_2$ with phenyl-1-naphthyl acetylene and phenyl-2-naphthyl acetylene (Chart 2.2).[202] The complexes were not crystallographically characterized, and no dynamic behaviour was discussed. In a related investigation, Rausch has also reported the synthesis and X-ray crystallographic characterization of the dimesityl derivative, **2.4**.[203] Restricted rotation of the mesityl groups was observed at ambient temperatures, and the barrier to rotation was reported to be appreciably greater than in the analogous cyclobutadiene complex (**2.5**), although no numerical value was provided.

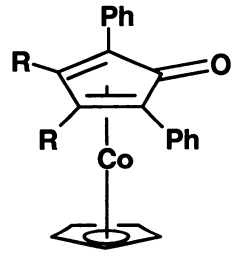

2.2: R = 1-naphthyl
2.3: R = 2-naphthyl

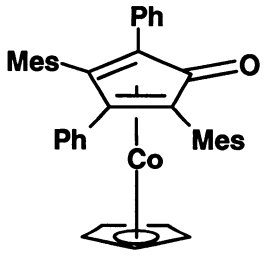

2.4

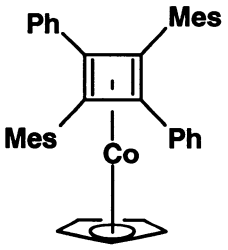

2.5

*Chart 2.2: Rausch's cobalt complexes **2.2** – **2.5**.*

Morris and co-workers have described the deliberate formation of the molybdenum complexes **2.6** and **2.7** upon treatment of 1 or 2 equivalents of tetracyclone (**1.26**) with $Mo(CO)_6$, respectively (Chart 2.3).[110] The authors did not determine barriers to phenyl rotation, although some fluxional behaviour was observed (for **2.6**) and attributed to the rotation of the cyclopentadienone unit about the metal-C_5 bond.

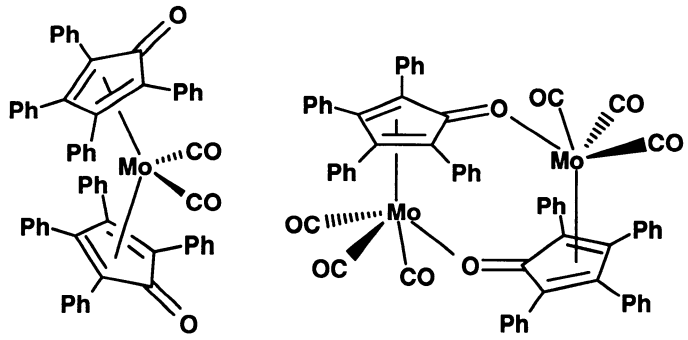

2.6 **2.7**

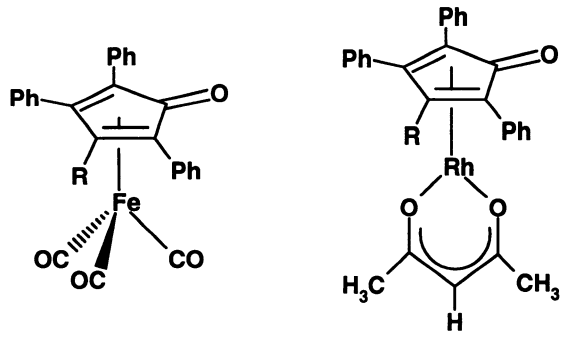

2.8: R = Ph
2.10: R = Fc

2.9: R = Ph
2.11: R = Fc

*Chart 2.3: Molybdenum and iron carbonyl complexes of tetracyclone (**2.6** – **2.8**, **2.10**) and rhodium acetylacetonate derivatives (**2.9**, **2.11**).*

Similarly, tetracyclone (**1.26**) reacted with $Fe_2(CO)_9$ and $(acac)Rh(C_2H_4)_2$ (acac = acetylacetonate) to give complexes **2.8** and **2.9**, respectively (Chart

2.3).[92] Both complexes have been characterized by X-ray crystallography, and **2.9** formed a head-to-tail dimer in the solid state. There was no evidence for fluxional behaviour in solution to accessible temperatures on the NMR time-scale for either complex. Moreover, treatment of 3-ferrocenyl-2,4,5-triphenylcyclopentadienone (**1.27**) with both metallic starting materials resulted in the formation of two monomeric species, **2.10** and **2.11**. Both species were again characterized by X-ray crystallography, and likewise exhibited fluxional behaviour in solution. The iron complex **2.10** showed evidence for restricted tripodal rotation, however, this was likely the result of steric intervention by the ferrocenyl group. The rhodium derivative **2.11** exhibited NMR spectra consistent with restricted rotation of the Rh(acac) moiety, and a barrier of 12 kcal mol^{-1} was determined.[92]

In an attempt to extend this research and to increase the steric demand of the peripheral rings, the incorporation of naphthyl substituents has been investigated, and this work has recently been published.[199] These groups effectively serve as phenyl groups with a "labeled edge", allowing for the distinction between syn (distal) and anti (proximal) isomers. A few studies have been aimed towards the development of naphthyl substituents for use as controls over structure and reactivity, as well as peripheral substituents in propeller structures.[51,204-207] A notable application of the steric hindrance offered by a naphthyl group is the chiral cyclopentadienyl ligand (**2.12**) proposed by Baker, *et al.*[208] in which the constrained motion of an α-naphthyl substituent would restrict

the site of metal coordination and generate a chiral cyclopentadienyl metal complex with the potential for use in asymmetric synthesis (Chart 2.4). Naphthyl analogues of complexes **2.8** and **2.9** are attractive first targets in this study in order to determine the influence of naphthyl groups on the barrier to rotation.

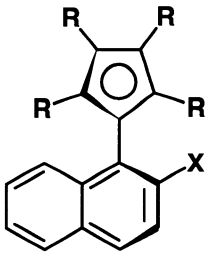

2.12

Chart 2.4: Baker's proposed chiral cyclopentadienyl ligand containing a naphthyl moiety.

2.2 Results and Discussion

2.2.1 Synthetic methodology

As depicted in Scheme 2.1, the cyanide-catalyzed dimerization of β-naphthaldehyde to the corresponding naphthoin (**2.13**, 96%), subsequent oxidation with $CuSO_4$ in pyridine to yield β-naphthil (**2.14**, 93%), and reaction with 1,3-diphenylpropanone or 1,3-bis(*m*-xylyl)propanone[209] gave the required 3,4-di-(β-naphthyl)-2,5-diarylcyclopentadienones (**2.15a**, 61% and **2.15b**, 82%). The identities of these products were verified using mass spectrometry, NMR spectroscopy and IR spectroscopy, and pure products were obtained by column chromatography.

Scheme 2.1

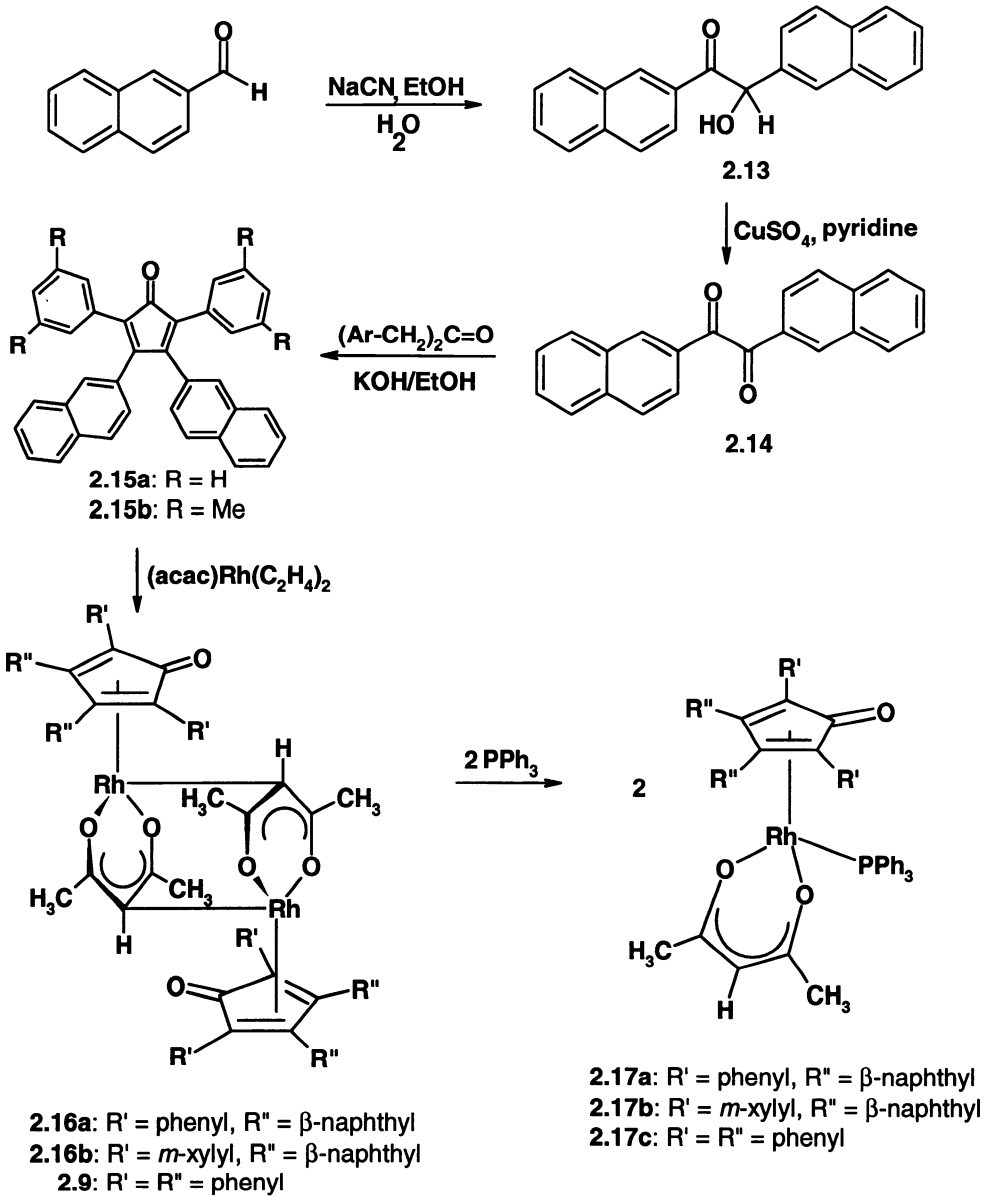

2.2.2 X-Ray Crystallographic Results

Treatment of **2.15a** and **2.15b** with (acetylacetonato)bis(ethylene)-rhodium(I) gave the desired complexes (**2.16a**, 78% and **2.16b**, 90%), identified by mass spectrometry, NMR and IR spectroscopy, and X-ray crystallography; the

structures are shown in Figure 2.1 (fully labelled thermal ellipsoid plots for all crystal structures can be found in Appendix I). Both molecules adopted a head-to-tail dimeric arrangement in which the rhodium was bonded to the γ-carbon of the acetylacetonate ligand, as previously found for the analogous (C_4Ph_4C=O)Rh(acac) complex (**2.9**) and similar compounds.[92,210-215] The bond distance from the rhodium in one monomer to the γ-carbon of the acetylacetonate ligand of the other monomer was 2.353(9) Å in **2.16a** and 2.389(6) Å in **2.16b**, values comparable to the 2.39(1) Å found in the tetracyclone analogue **2.9**.[92] These bond lengths may also be compared with the increased distance of

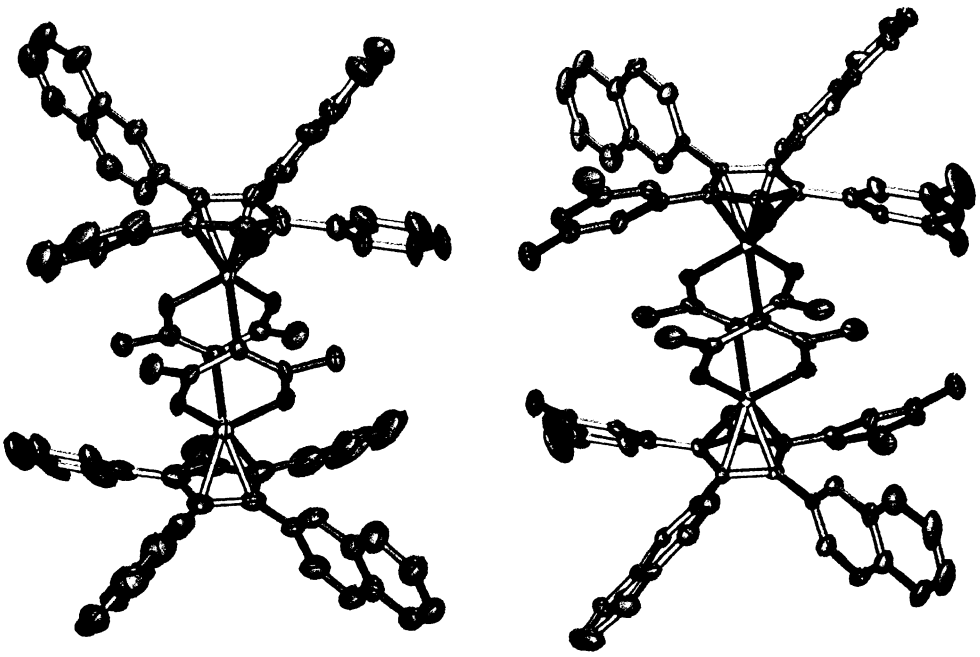

*Figure 2.1: Molecular structures of the dimers [(C_4Ar_2(β-naphthyl)$_2$C=O) Rh(acac)]$_2$, Ar = phenyl, m-xylyl, (**2.16a, 2.16b**), with hydrogen atoms omitted for clarity.*

2.408 Å displayed in the [Cp*Ru(acac)] dimer **2.18**,[210,212] and the decreased 2.287(6) Å found in the dication $[\{Cp^*Rh(acac)\}_2]^{2+}$ **(2.19)** synthesized by Maitlis and co-workers (Chart 2.5).[215] The aryl substituents in the α-positions of the cyclopentadienone rings of **2.16a** and **2.16b** were arranged in a "cup-shaped" geometry around the metal, the latter being in a square pyramidal environment in which the centers of the two cyclopentadienone double bonds and the acetylacetonate oxygen atoms formed a square plane capped by the γ-carbon of the other monomer.

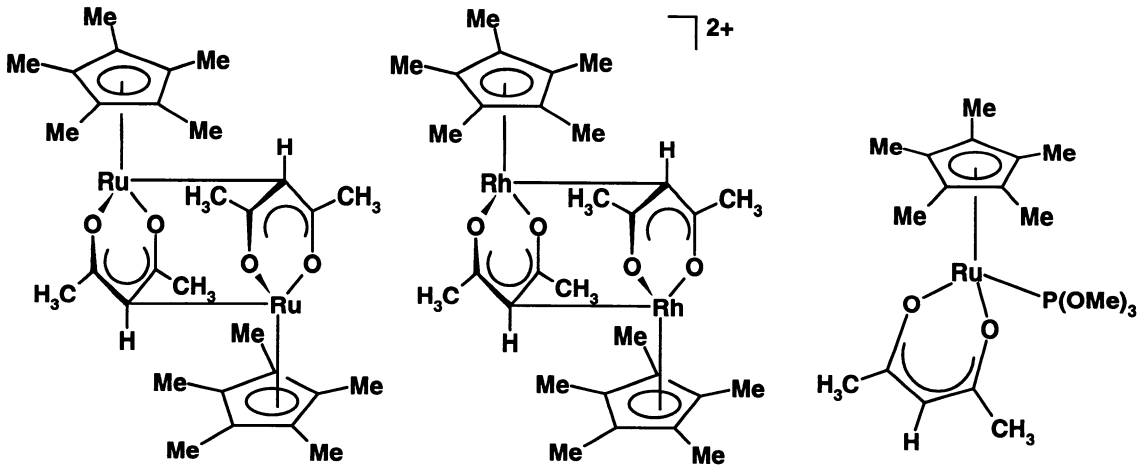

*Chart 2.5: Molecules **2.18 – 2.20**.*

The Rh-C bond distances to the cyclopentadienone carbons C(2)-C(5) ranged from 2.116(10) Å to 2.155(6) Å in the dimers. However, the Rh(1)-C(1) distance was much longer, 2.412(12) Å [2.412(7) Å] for **2.16a** [**2.16b**], which is in agreement with previous studies.[92] The carbonyl carbon was bent away from the

plane of the cyclopentadienone ring by 19.5(1)° [16.0(3)°], similar to that found for the tetracyclone analogue (17°).[92] The Rh-acac ring formed an angle of 68.9(4)° [69.8(3)°] with the plane of the cyclopentadienone ring carbons, closely approximating the 65° found in the tetracyclone derivative (**2.9**), but significantly deviating from the near orthogonal arrangement found in the 3-ferrocenyl-2,4,5-triphenylcyclopentadienone analogue (88°, **2.11**).[92] The corresponding inter-planar angle between the plane of the pentamethylcyclopentadienyl ring and that containing O(1)-Ru-O(2) in the $[Cp^*Ru(acac)]_2$ system (**2.18**) was 58°.[210,212]

Interestingly, in **2.16a**, the two naphthyl ligands on the cyclopentadienone ring of one monomer were arranged distally with respect to the dimeric core, whereas the naphthyl rings in the other half of the molecule adopted proximal orientations, which precluded the presence of a C_2 axis in the dimer. In addition, **2.16a** contained open channels between the dimeric units, which were partially occupied by dichloromethane solvent molecules. The solvent was essential to the structural integrity of the sample, as the crystals rapidly collapsed to powder if the solvent was allowed to evaporate. In **2.16b**, there was one naphthyl group distal and one proximal in each monomer, and the molecule possessed an inversion center. Crystals of **2.16b** did not have the same structural dependence on the presence of solvent; however, disordered, partially occupied solvent molecules were present in the structure.

In continuation of our investigation of the chemistry of these electrophilic species, **2.16a** and **2.16b** were allowed to react with two equivalents of

triphenylphosphine at room temperature to yield **2.17a** (98%) and **2.17b** (84%), respectively, in which the dimers were cleaved upon addition of the phosphine ligand. As before, the aryl groups exhibited a "cup-shaped" orientation in the α-positions of the cyclopentadienone rings (Figure 2.2).

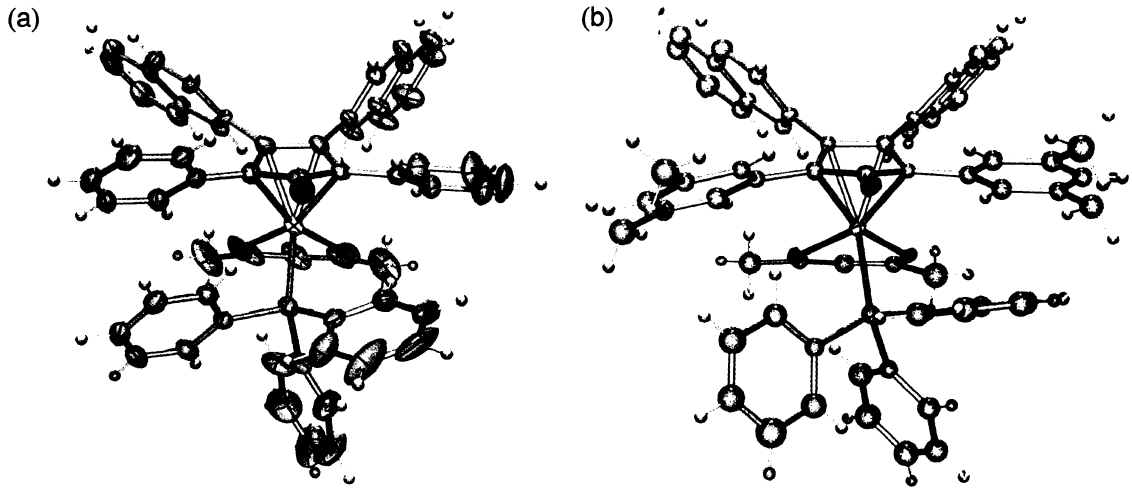

*Figure 2.2: Molecular structures of (C_4Ar_2(β-naphthyl)$_2$C=O) Rh(acac)(PPh_3), (a) Ar = phenyl, (b) Ar = m-xylyl, (**2.17a, 2.17b**).*

The rhodium was once again situated in a square-based pyramidal environment, and the distances from the rhodium to atoms C(2) through C(5) in the cyclopentadienone ring ranged from 2.141(11) Å to 2.177(3) Å; the Rh-C(1) distance was 2.450(3) Å [2.448(13) Å] in **2.17a**[**2.17b**]. The carbonyl group was bent away from the rest of the molecule by 21.0(3)° [22(1)°], slightly greater than in the dimer. The Rh-P distance was 2.3861(10) Å [2.402(4) Å], somewhat longer than the conventional range of literature values (2.201 Å – 2.303 Å),[216] and significantly longer than the Ru-P distance (2.245 Å) found in Koelle's Cp*Ru(acac)($P(OMe)_3$) system (**2.20**),[210] presumably as a result of the increased

steric hindrance provided by the naphthyl substituents. In contrast to **2.16a**, **2.16b** and other dimeric structures, the plane of the acac ring in **2.17a**[**2.17b**] made a much smaller angle of 37.3(2)° [37.8(6)°] with the C(2)-C(5) plane of the cyclopentadienone ring, likely as a result of the steric bulk of the added phosphine. This observation paralleled the behaviour of Cp*Ru(acac)($P(OMe)_3$) (**2.20**) which also formed a corresponding interplanar angle of 37°.[210]

A particularly interesting feature of the crystal structure of **2.17a** (Figure 2.3) was that one of the naphthyl rings was disordered and exhibited both distal and proximal orientations in a 55:45 ratio, respectively. Similar behaviour was reported in a molybdenum complex containing the 1-(2,5-dimethoxyphenyl)-

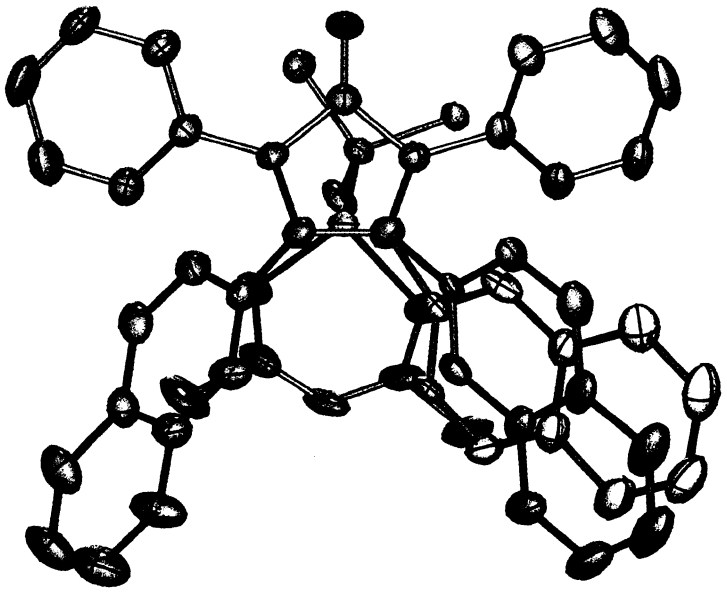

*Figure 2.3: Top down view of **2.17a**, showing one disordered β-naphthyl substituent.*

2,3,4,5-tetraphenylcyclopentadienyl ligand (Chart 2.6).[113,217] In the dimeric species **2.21**, the dimethoxyphenyl groups were apparently rigid, and no barrier to rotation was determined, while in complex **2.22**, this aryl rotation barrier was reported to be 16.3 kcal mol^{-1}. The solid state structure of **2.22** revealed a disorder in which the dimethoxyphenyl group was found in two conformations with occupancies of 0.24 and 0.76. In contrast, **2.17b** contained two distal naphthyl groups.

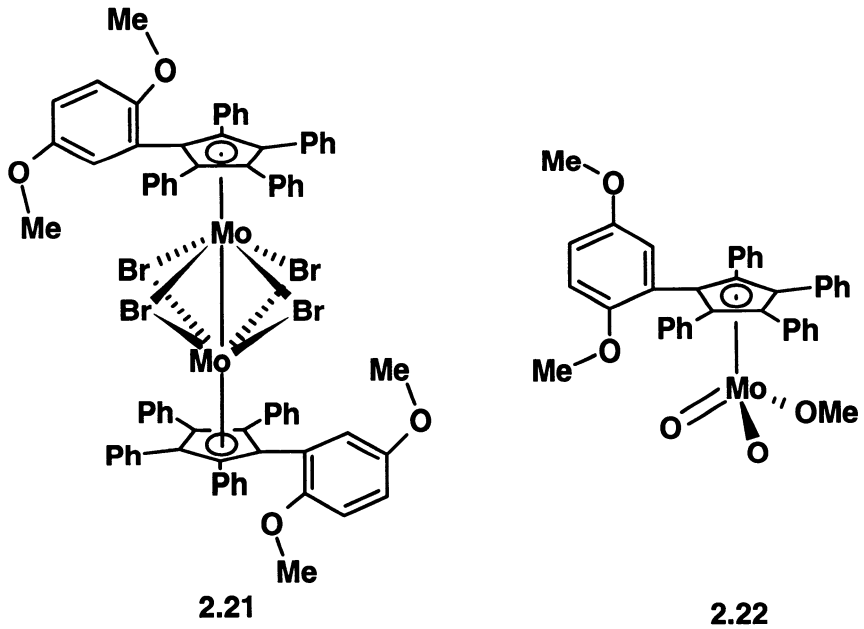

2.21 **2.22**

*Chart 2.6: Molecules **2.21** and **2.22**.*

It is interesting to note the presence of several combinations of naphthyl orientations in the four crystal structures: in **2.16a**, one monomer had both naphthyls distal, the other monomer had both proximal; in **2.16b**, both monomers contained one distal and one proximal naphthyl. In the monomer **2.17a**, one naphthyl was distal and one was disordered proximal/distal, while **2.17b**

contained two distal naphthyl groups. The various naphthyl conformations observed in the solid state illustrate the ability of these complexes to accommodate the bulk of the naphthyl groups, and support the contention that many of these rotamers are present in solution at low temperature, at the limits of restricted naphthyl rotation, in the absence of crystal packing forces.

2.2.3 Variable Temperature NMR Results

Prior to a discussion on the spectra of the rhodium complexes, an unexpected result was obtained for ligand **2.15b**. The 500 MHz ^{1}H NMR spectra obtained at room temperature revealed the presence of two types of naphthyl group environments (Figure 2.4). The only behaviour that would result in this observation is the formation of two rotamers (C_s and C_i) that do not interconvert

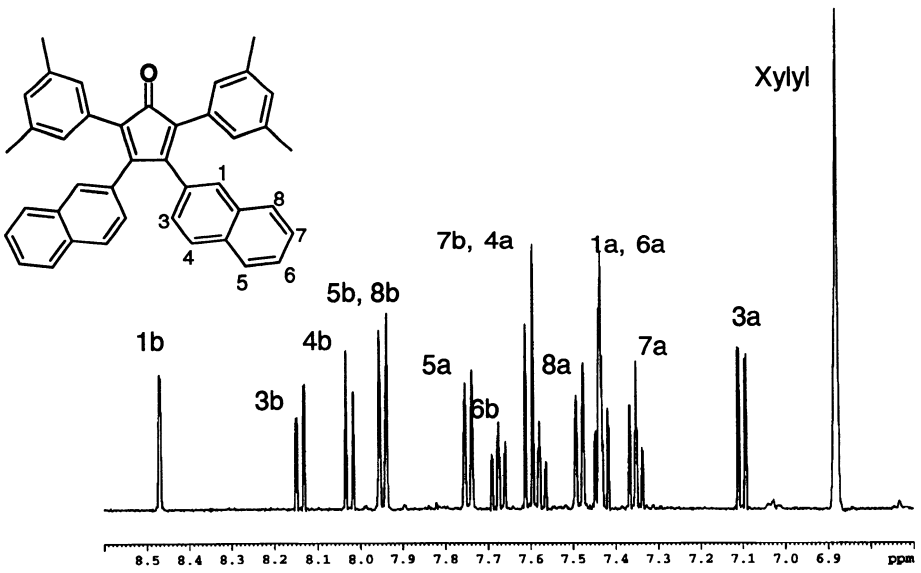

*Figure 2.4: ^{1}H NMR of **2.15b** at room temperature in the aromatic region.*

at ambient temperatures. Thus the naphthyl groups and *m*-xylyl substituents experienced significant steric interactions and exhibited restricted rotation at room temperature.

The ^{1}H and ^{13}C NMR spectra of **2.16a** and **2.16b** at room temperature each showed a single methyl signal for the acac ligand, and the expected, well-resolved resonances readily assignable to the β-naphthyl and phenyl, or *m*-xylyl, substituents. However, in both systems, cooling the sample from 303 K to 263 K resulted in the broadening and dispersion of the ^{1}H and ^{13}C aromatic resonances. Moreover, as the temperature was reduced, the initially sharp ^{1}H peaks at 2.13 ppm and 2.16 ppm for the acac-methyl protons in **2.16a** and **2.16b**

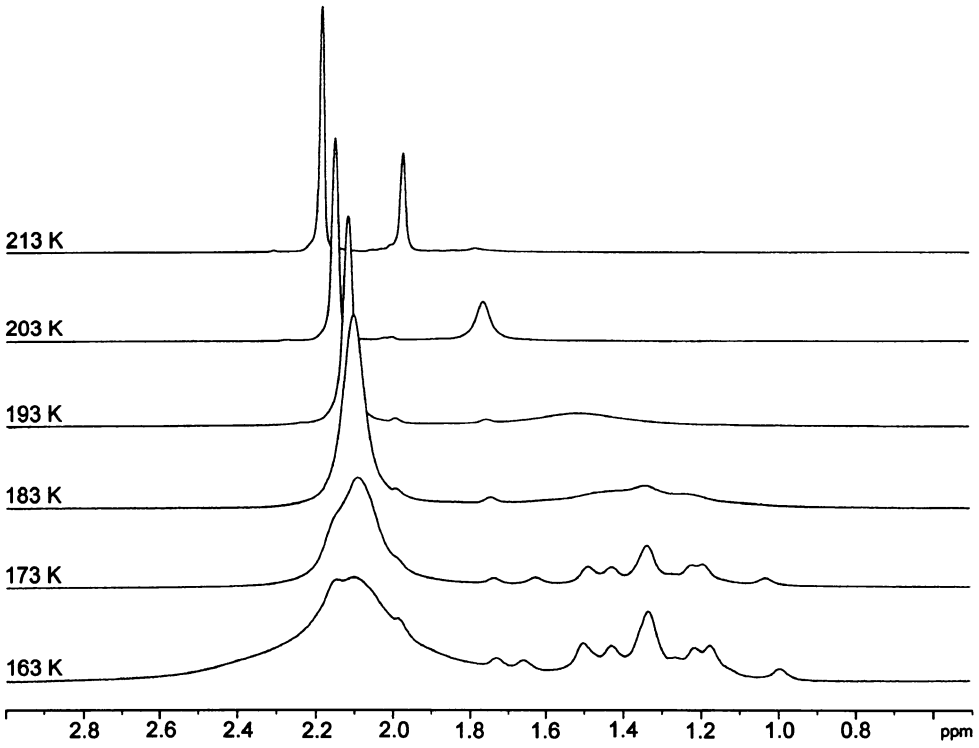

Figure 2.5a: Variable-temperature 500 MHz ^{1}H NMR spectrum of ***2.16b*** *in the region of the m-xylyl-methyl and acac-methyl protons.*

respectively, broadened and gradually moved to markedly lower frequencies.

Furthermore, in both molecules, further cooling induced the splitting of the broad peak for the acac methyl protons and, at 173 K, several peaks centered around 1.35 ppm began to emerge (Figure 2.5a for **2.16b**). Similar splitting behaviour was also observed in the ^{13}C regime, whereby the resonance of the acac methyl carbon at 27.7 ppm (for **2.16b**) clearly split into several peaks (Figure 2.5b).

It is apparent that the methyl groups of the acetylacetonate ligand serve as probes for the observation of the fluxional behaviour of the naphthyl groups.

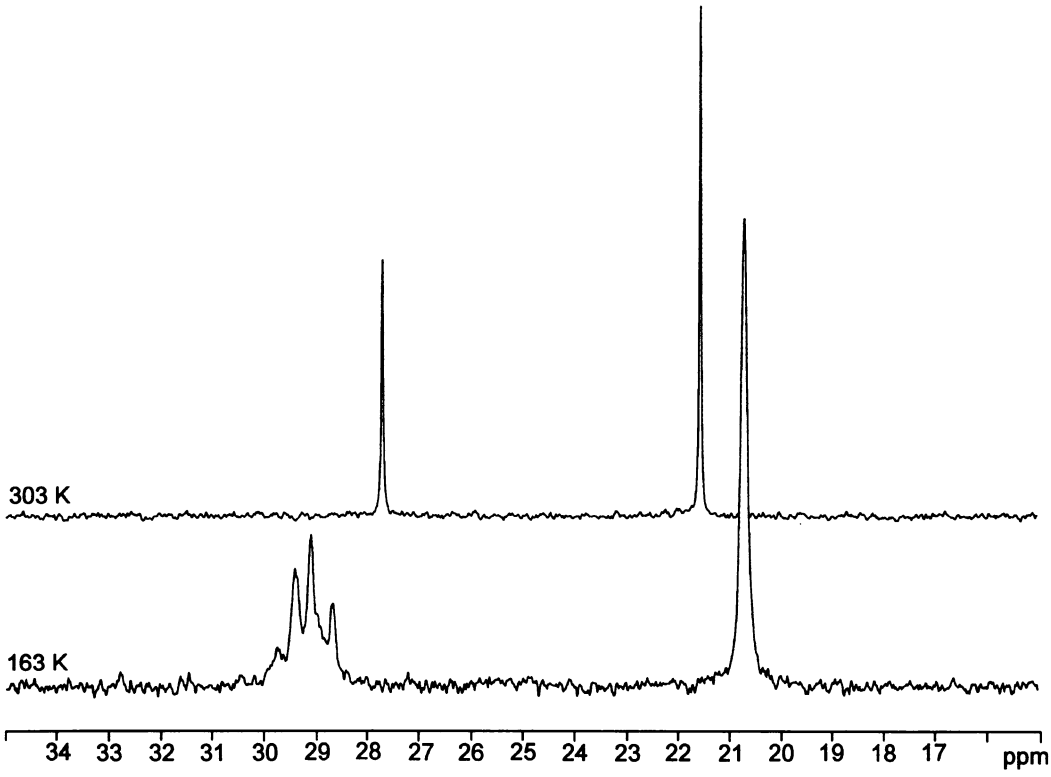

*Figure 2.5b: Variable-temperature 125 MHz ^{13}C NMR spectrum of **2.16b** in the region of the m-xylyl-methyl and acac-methyl carbons.*

In order for the protons and carbons of the acac methyl groups to split, they must have been in different chemical and magnetic environments at low temperature. Thus, if **2.16a** and **2.16b** exhibited rapid monomer-dimer equilibria at room temperature (analogous to the behaviour of Koelle's Cp*Ru(acac) system, **2.18**),[211] then time-averaged NMR spectra would be expected in which there would be only one peak for the acac-methyl protons and carbons, and all of the naphthyl environments should also be equivalent. However, at lower temperatures, as the dimer concentration increased, restricted rotation of the naphthyl groups was evident. One obvious effect on the ^{1}H NMR spectra was the gradual shift to lower frequency of the acac-methyl resonances as the temperature was reduced. This phenomenon is readily explained in terms of the increasing fraction of dimer in the sample, whereby the methyl protons lie in the aromatic shielding region of the aryl substituents in the other half of the molecule.

Although a barrier to Rh(acac) rotation relative to a tetra-substituted cyclopentadienone ring has been reported,[92] this involved the replacement of a peripheral phenyl group in tetracyclone by a bulky ferrocenyl substituent (**2.11**). This not only prevented dimer formation, but also provided the asymmetrical substitution required for the examination of the fluxional behaviour of the acetylacetonate group. In that case, two methyl signals were observed at low temperature in the ^{1}H and ^{13}C NMR spectra, yielding a barrier to acac rotation of 12.5 kcal mol^{-1}, and isoenergetic rotamers were interconverting. In both **2.16a** and **2.16b**, and for the tetracyclone analogue, **2.9**, the solid state structures were

such that the ketonic unit eclipsed the Rh(1)-C(7A) bond. EHMO (Extended Hückel Molecular Orbital) calculations revealed that this rotamer was favoured because of better overlap between the frontier orbitals of the Rh(acac) and the π system of the cyclopentadienone. As a result of this, the presence of detectable quantities of other rotamers would not be expected, since the "pseudo-tripod" cannot adopt conformers of comparable energy. This leaves restricted naphthyl rotation as the only viable explanation for the plethora of acac-methyl resonances.

If the dimer of **2.16b** shown in Figure 2.1 was the only isomer present in solution, then two methyl signals would be anticipated, as the molecule would have effective C_i symmetry. The observation of multiple methyl resonances indicated that the rotation of the naphthyls was hindered and that several conformations could co-exist at low temperature. Table 2.1 and Chart 2.7 list the seven possible isomers of the dimers (each of which bears four acac-methyl groups) that may be present as a result of restricted naphthyl rotation. If all rotamers were equally probable, there would be sixteen equally intense methyl

Table 2.1: Possible Isomers of 2.16a and 2.16b

Isomer	Point Group	Naphthyl orientation	Number of identical isomers	Number of methyl resonances	Predicted intensities of methyl peaks
A	C_{2h}	All distal	1	1	4
B	C_{2h}	All proximal	1	1	4
C	C_s	Upper half, both distal; lower half, both proximal	2	2	4,4
D	C_1	3 distal, 1 proximal	4	4	4,4,4,4
E	C_1	3 proximal, 1 distal	4	4	4,4,4,4
F	C_2	1 distal, 1 proximal on each ring	2	2	4,4
G	C_i	1 distal, 1 proximal on each ring, with an inversion center	2	2	4,4

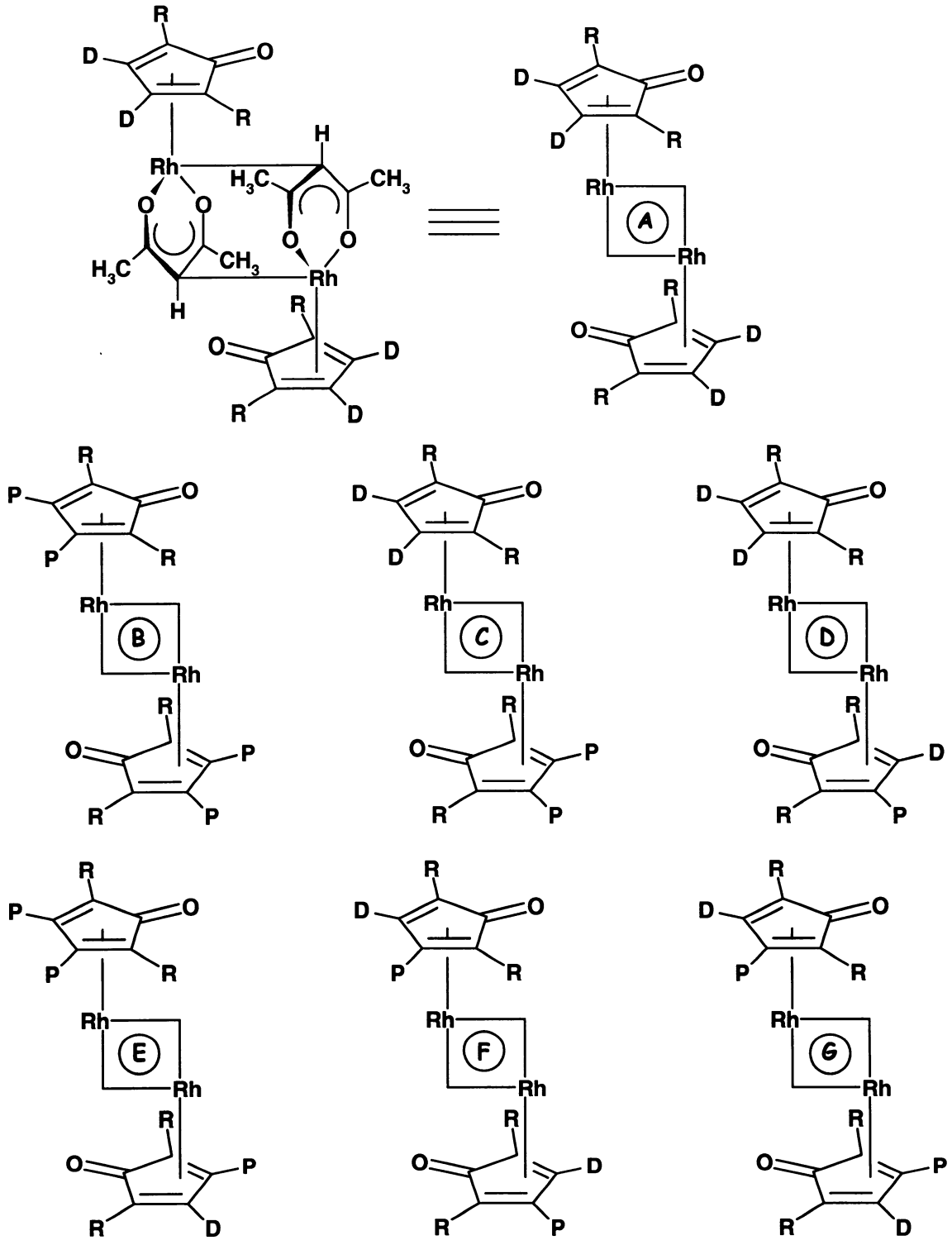

*Chart 2.7: Possible isomers of **2.16**; P and D represent Proximal and Distal β-naphthyl substituents, respectively, R is a phenyl or m-xylyl substituent. Only one enantiomer of the chiral compounds is shown.*

singlets. At 173 K, the ^{1}H and ^{13}C NMR spectra of **2.16a** and **2.16b** exhibited several acac-methyl environments, and the numerous peaks originated from the presence of the more energetically favourable rotamers, with intensities governed by the relative fraction of each isomer present. This interpretation was supported by the variable-temperature ^{1}H NMR spectroscopic behaviour of (tetracyclone)Rh(acac), **2.9**, whose acac-methyl signal likewise exhibited a gradual shielding upon cooling (δ 2.09 ppm at 303 K, δ 1.12 at 163 K) *but which never lost its singlet character.* The complexity of the spectra of **2.16a** and **2.16b** precluded the determination of activation parameters, since the assignment of each line to its respective rotamer and the determination of the relative population of the isomers was not viable.[60]

With the goal of determining a barrier for naphthyl rotation, variable-temperature NMR data were also acquired for **2.17a** and **2.17b**. In the spectra of both complexes, the peaks for the acac-methyl protons and carbons did not split, even at 163 K. However, as illustrated in Figure 2.6, the ^{31}P NMR spectrum of **2.17a**[**2.17b**] yielded a doublet with J_{Rh-P} of 165.6 Hz [167.3 Hz] at room temperature, which split into two doublets at 163 K.

There are several possible explanations for the origin of the ^{31}P splitting at low temperature, (a consequence of the use of an indirect method of observation): (i) hindered rotation of the metal tripod, (ii) restricted rotation about the P-C_{ipso} bonds of the triphenylphosphine propeller, and (iii) restricted naphthyl rotation. Molecular modeling studies suggested that there was no significant

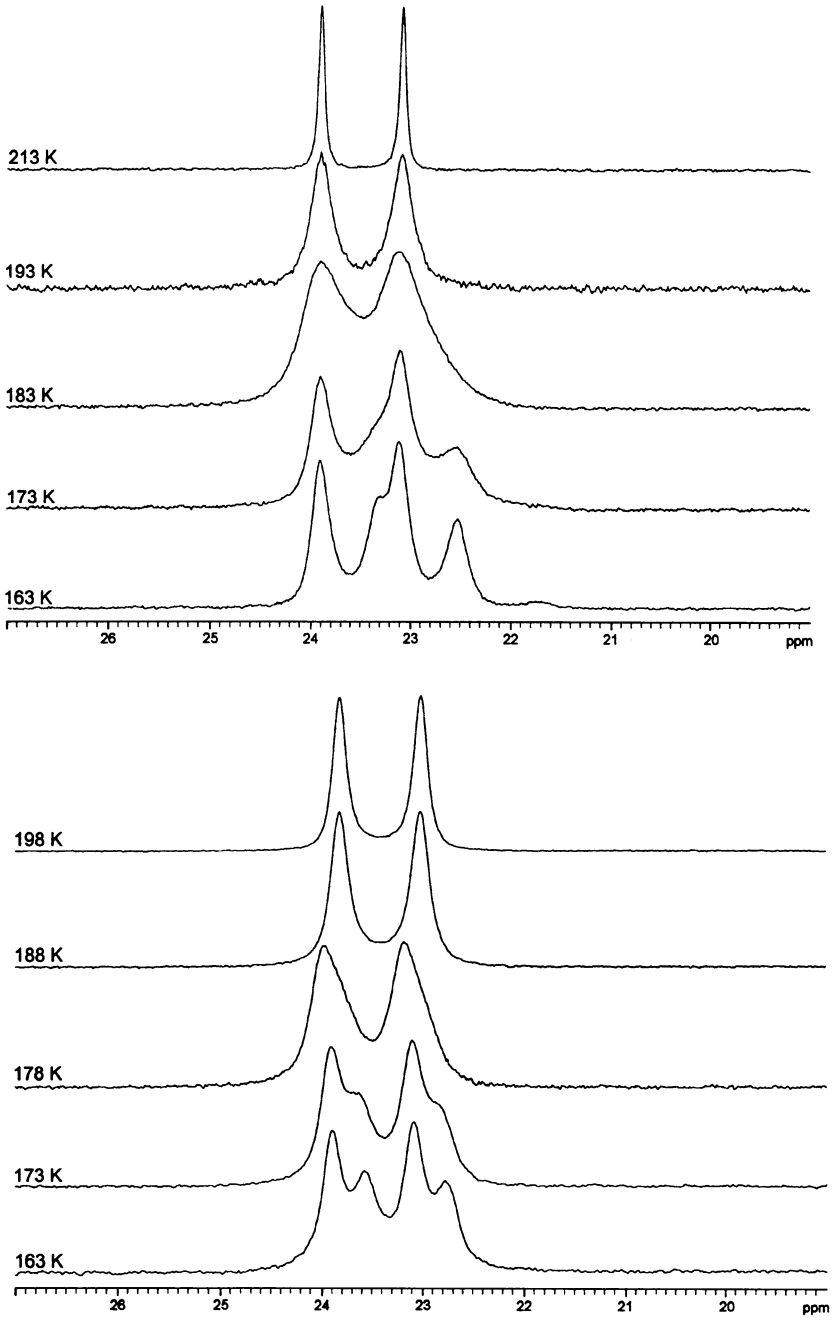

Figure 2.6: Variable-temperature 202 MHz ^{31}P NMR spectra of ***2.17a*** *and* ***2.17b****, respectively.*

steric barrier to tripodal rotation attributable to the presence of the naphthyl groups, which might have been expected to interfere with the bulky

triphenylphosphine ligand during rotation. Moreover, a variable-temperature study of the (tetracyclone)Rh(acac)(PPh_3) analogue, **2.17c**, showed no splitting in either the proton or phosphorus NMR spectra at low temperatures. This observation supported the view that the fluxional behaviour was attributable to restricted rotation of the naphthyl groups, rather than the slowed rotation of the Rh(acac)(PPh_3) unit with respect to the cyclopentadienone ring. The substitution of two phenyl groups by two naphthyl substituents (which effectively acted as *meta*-substituted phenyl rings) was not likely to create enough steric strain to drastically increase the barrier to tripodal rotation, especially if the naphthyl groups could rotate and move to accommodate the bulk of the triphenylphosphine. However, EHMO calculations suggested that there was a significant *electronic* barrier to tripodal rotation in the PPh_3 systems. This was a consequence of the less favourable overlap of the frontier orbitals on the cyclopentadienone ring with those of the Rh(acac)(PPh_3) unit when the tripod was rotated through 180° from that observed crystallographically. Slowed tripodal rotation would merely result in the formation of a single rotamer, with essentially no detectable concentration of any other, and only one peak would be expected in the ^{31}P NMR spectrum. Thus, restricted tripodal rotation was not the origin of the fluxional behaviour in these systems.

There is precedence in the literature for the observation of restricted rotation about the P-C_{ipso} bonds of the triphenylphosphine ligand.[43,48,49,52,79,84,97,218-226] In the solid state[218] and in solution,[49] PPh_3 adopted a

chiral, propeller conformation in which the helix could be oriented in a clockwise or anti-clockwise orientation, resulting in a pair of enantiomers. Conformational analyses of the dynamic behaviour of triphenylphosphine have been performed by Mislow[43,52,219] and Kurland,[48] and the interconversion of enantiomers or full rotation about P-C_{ipso} bonds have been determined to involve cooperative motion of the phenyl substituents.[218,220] The use of PR_3 as a probe to monitor dynamic behaviour in other regions of a molecule has also been established[79,84,97,117,222-226] and it has previously been suggested that the ligand may not serve as an innocent probe, but may also give rise to different conformers at low-temperature.[117] Barriers to rotation of tri-substituted phosphines in many organometallic derivatives have been established,[220-222,224] and several studies have shown that steric, rather than electronic, factors are dominant in determining their magnitude.[223] Examples include an upper barrier of 7.6 kcal mol^{-1} for P-C_{ipso} rotation in $(C_5H_5)Fe(CO)(CN)(PPh_3)$ (**2.23**) estimated by Faller, *et al.*[224] and 10.3 kcal mol^{-1} determined by Davies, *et al.*[220] for $(C_5H_5)Fe(CO)(COCH_3)(PPh_3)$ (**2.24**, Chart 2.8).

In **2.17a** and **2.17b**, cessation of P-C_{ipso} rotation would result in the formation of enantiomers, as expected, however, these would not be differentiable by NMR spectroscopy without the presence of another source of chirality in the molecule, that is, the creation of diastereomers. As described by Willem,[60] the "fundamental inability of NMR spectroscopy to distinguish enantiomers or enantiotopic sites in an achiral environment" prevents the

observation of this behaviour without another chiral center in the molecule. This

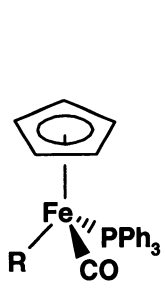

2.23: R = CN
2.24: R = $COCH_3$

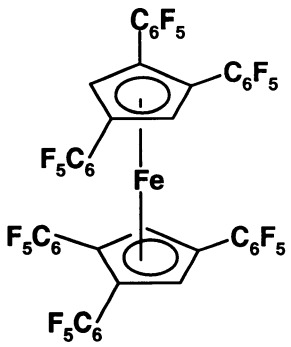

2.25

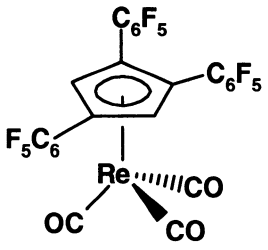

2.26

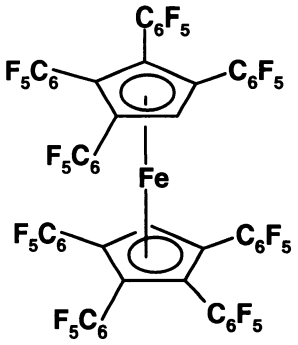

2.27

*Chart 2.8: Molecules **2.23 – 2.27**.*

involves the restricted rotation of the naphthyl substituents, which would result in the formation of diastereomers and allow for the differentiation of phosphorus environments by NMR spectroscopy. Thus, even if P-C_{ipso} rotation was slowed, the naphthyl groups must also exhibit restricted rotation in order for the different environments of the phosphorus atoms to be distinguishable. Similarly, restricted Rh-P rotation alone would not result in decoalescence of the phosphorus spectrum.

Consequently, it is possible to assert that the observation of the second ^{31}P NMR doublet is consistent only with the slowed interconversion of the naphthyl groups between their two favoured conformations (distal/distal and distal/proximal). The presence of the two rotamers would place the phosphorus nuclei in different environments, thus influencing the appearance of the ^{31}P NMR spectrum. Activation enthalpies for the naphthyl rotation processes in **2.17a** and

2.17b were derived from Eyring plots prepared by lineshape analysis of the ^{31}P spectra, yielding barriers of 8.2 ± 0.5 kcal mol^{-1} (Figure 2.7).

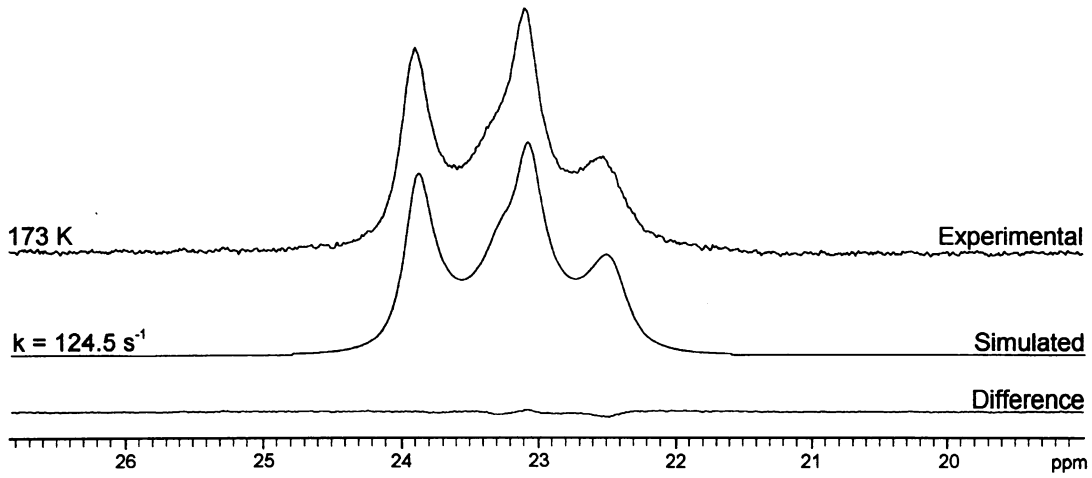

*Figure 2.7: Example of simulated lineshape spectra using the MEXICO program for **2.17a**.*

This may be compared with the reported barriers of 8-10 kcal mol^{-1} for pentafluorophenyl rotation in $[1,2,4\text{-}(C_6F_5)_3C_5H_2]_2Fe$ (**2.25**) and $[1,2,4\text{-}(C_6F_5)_3C_5H_2]Re(CO)_3$[115] (**2.26**) and 9 ± 1 kcal mol^{-1} for hindered phenyl rotation in $[C_5(C_6H_5)_4H]_2Fe$ (**2.27**, Chart 2.8).[108] However, the barrier is smaller than those observed by Haywood-Farmer and Battiste,[59] as well as Willem, for the *o*-methyl substituted cyclopentadienones (**1.21**, **1.22**).[60,61] It has been established that substitution in the *ortho* position of the peripheral groups in these sterically encumbered molecules dramatically increases barriers to rotation, and that *meta*-substitution merely reflects the buttressing effects of the *ortho*-protons.[41,56,58] A β-naphthyl group acts effectively as a *meta*-substituted phenyl group, thus the

barrier to rotation would be expected to be much lower than in these *ortho*-substituted cyclopentadienones.

Finally, there is another interesting feature of the ^{31}P NMR spectra of **2.17a-c** that merits comment; the spectral lineshapes exhibited a significant temperature and magnetic field dependence (Figure 2.8). At room temperature, the 202 MHz ^{31}P spectra exhibited low intensity, broad, asymmetrical peaks, however, as the temperature was decreased, the peaks became sharper and more symmetrical. The ^{31}P spectra were also run on a lower field instrument (81 MHz), and the peaks were noticeably sharper.

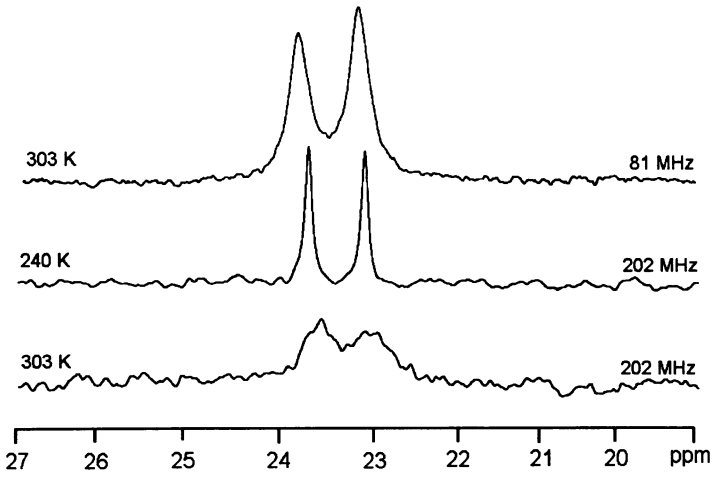

*Figure 2.8: Field strength and temperature dependence of the ^{31}P NMR lineshape for **2.17a**.*

The exact cause of this behaviour has not been established, but the data suggest that it is the result of the influence of the chemical shift anisotropy (CSA) relaxation mechanism. The shape of the ^{31}P lines improved at lower field, which could be attributable either to the decreased spin-spin (T_2) relaxation as a result

of the CSA of the phosphorus, or to reduced scalar relaxation from the CSA-induced T_1 of the rhodium. CSA relaxation is also implied by the asymmetry of the doublet, which is characteristic of a relaxation cross-term between dipolar coupling and CSA. This is a well-established effect[227,228] that has recently become important as the basis for the TROSY experiment in the structure determination of large biological macromolecules.[229] This outcome is not present at low temperature, and thus does not impede the observation of splitting behaviour.

2.3 Conclusions

The incorporation of naphthyl substituents into cyclopentadienone-rhodium complexes resulted in the formation of mixtures of rotamers in which the naphthyls could adopt either proximal or distal orientations. In the dimers **2.16a** and **2.16b**, slowed naphthyl rotation could be detected by observation of the acetylacetonate ^{1}H NMR methyl resonances. In the phosphine complexes **2.17a** and **2.17b**, the variable-temperature ^{31}P NMR spectra yielded enthalpies of activation for naphthyl rotation of 8.2 $\pm$ 0.5 kcal mol^{-1}. It is clear that naphthyl substitution has an appreciable affect on the steric hindrance of cyclopentadienone systems, and that there is potential for interactions with other bulky substituents on the organometallic moiety.

CHAPTER THREE

Hindered Benzene Derivatives Containing β-Naphthyl Substituents

3.1 Introduction

3.1.1 Sterically Crowded Benzenes

The pioneering work by Gust and Mislow[42,43] on sterically hindered organic molecules, especially hexa-substituted arenes, prompted a number of subsequent studies on molecular paddle-wheels and propellers.[41] Recognition of the novelty and utility of a system that could exhibit correlated rotation of crowded substituents about a central ring[50,230] stimulated a variety of investigations directed towards their potential application as molecular machines.[44,147,231]

On the NMR time scale, the pendant groups in hexaarylbenzenes are perpendicular to the central ring, and substitution is required to invoke observable barriers to rotation. *Ortho*-substituted derivatives exhibit significantly higher barriers to peripheral ring rotation (~ 33 kcal mol^{-1}), than do their *meta*-substituted analogues. In the latter cases, the barriers (~ 17 kcal mol^{-1}) are more reflective of the buttressing effects of the *ortho*-hydrogens.[232] These activation energy values have been ascribed to diastereomeric interconversions via the independent rotation of one ring at a time through approximately π radians.[56,232] Ultimately, these successive rotations provide the most favourable pathway for inversion of the propeller helicity; enantiomerization requires the rotation of *all*

substituted peripheral rings, and the synchronous, correlated rotation of six rings is energetically disfavoured.

3.1.2 Naphthyl-Substituted Derivatives

The necessity for increased steric bulk and the presence of a probe to detect restricted rotation has led to the proposal of derivatives containing naphthyl substituents, which act as phenyl groups with a labelled edge and a greater "wingspan". The progress achieved with the development of cyclopentadienone complexes[199] has been extended to benzene derivatives, with the goal of achieving correlated rotation of the peripheral substituents.

Several naphthyl-substituted benzene complexes have been synthesized and characterized, and some barriers to rotation have been determined. Magill and co-workers have investigated the melting and viscosity behaviour of 1,3,5-tri-α-naphthylbenzene (**3.1**), and described the molecule as "propeller-like" with a marked inability to change its orientation in the melt as a result of the interlocking between molecules and the restricted rotation of the substituents.[233,234] Moreover, Alfimov et al. described the unusual fluorescence properties of liquid solutions of 1,4-di-β-naphthylbenzene (**3.2**), and attributed the behaviour to the presence of conformers that differ by rotation of the aryl fragments about the single bonds joining them to the central ring.[235,236] These studies were later disputed by McMahon and Whitaker. An independent synthesis and ^{13}C NMR spectroscopic investigation of **3.1** revealed a barrier to rotation of ~ 12 kcal mol^{-1}, which did not allow for the observation of rotamers at room temperature, as

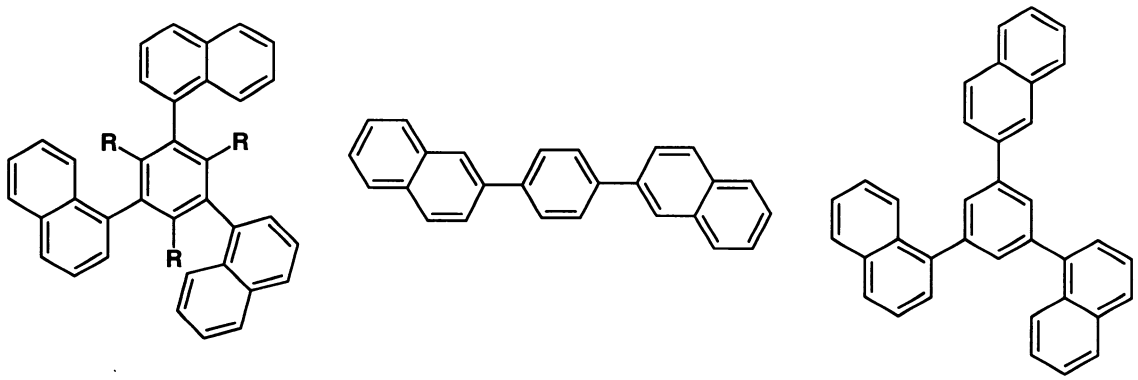

3.1: R = H
3.4: R = CH_3

3.2

3.3

*Chart 3.1: Naphthyl-substituted benzenes **3.1** – **3.4**.*

reported by Magill.[237] Complementary studies on 1,3-di-α-naphthyl-5-β-naphthylbenzene (**3.3**) established barriers to rotation of 12 kcal mol^{-1} and < 9 kcal mol^{-1} for rotation of the α- and β-naphthyl substituents, respectively.[237] Thus, the steric hindrance offered by naphthyl substituents was established, and barriers were determined for 1,3,5-trisubstituted derivatives (Chart 3.1).

Focusing on fully-substituted compounds, Katz has reported studies on 1,3,5-tri-α-naphthyl-2,4,6-trimethylbenzene (**3.4**), a molecule which exhibits significant steric interactions.[238] The NMR spectrum of the complex revealed the presence of more than one rotamer, and a barrier to interconversion of 30 kcal mol^{-1} was estimated. The syntheses of several other naphthyl-substituted benzenes have been described, however, no further dynamic behaviour has been reported.[239]

3.1.3 Organometallic Complexes

As previously established, the use of organometallic moieties may provide alternative options for increasing steric hindrance and supplying probes for NMR spectroscopic experiments. This idea was further developed by McGlinchey et al.: the replacement of a peripheral phenyl ring in C_6Ph_6 by a ferrocenyl group led to intriguing results, including the possibility of correlated rotation.[93] In the solid state, C_6Ph_5Fc (**1.55**) did not adopt a propeller conformation, but rather exhibited an incremental progression of dihedral angles, (51° to 120°), as discussed in more detail below. It was tempting to invoke a "domino effect" such that rotation of the ferrocenyl group would proceed with correlated rotation of the phenyl rings.[64] However, since variable-temperature ^1H and ^{13}C NMR studies on **1.55** gave no indication of restricted ferrocenyl or phenyl ring rotation on the NMR time-scale, no definitive conclusions could be drawn.[93]

Prior to this work, there was only one report of analogous organometallic derivatives containing naphthyl substituents. Treatment of $(\eta^5\text{-}C_5H_5)Co(CO)_2$ with phenyl-α-naphthylacetylene or phenyl-β-naphthylacetylene yielded several cyclobutadiene- and cyclopentadienone-cobalt complexes (**2.2**, **2.3**, **3.5 – 3.8**),[202] however, no dynamic behaviour was discussed. This work describes investigations of the syntheses, structures and dynamic behaviour of hexa-β-naphthylbenzene and ferrocenyl-penta-β-naphthylbenzene.

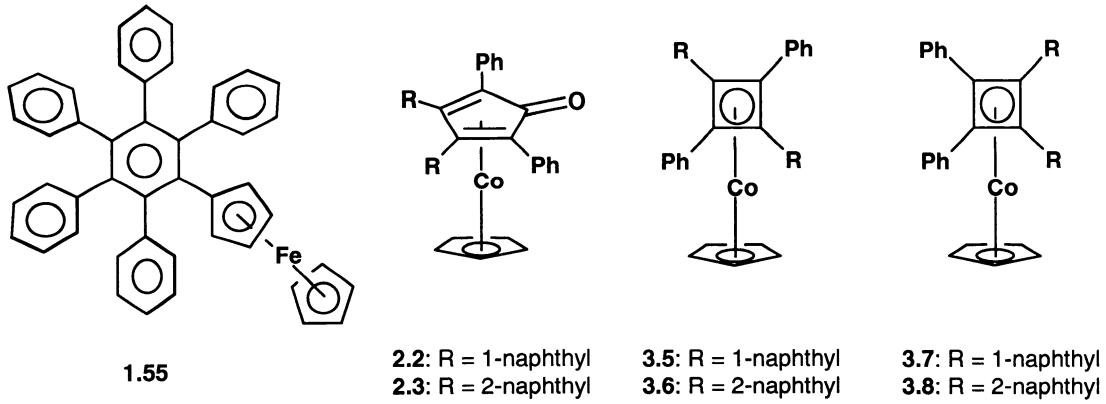

1.55

2.2: R = 1-naphthyl
2.3: R = 2-naphthyl

3.5: R = 1-naphthyl
3.6: R = 2-naphthyl

3.7: R = 1-naphthyl
3.8: R = 2-naphthyl

*Chart 3.2: Organometallic complex **1.55** and naphthyl-containing derivatives **2.2**, **2.3** and **3.5** – **3.8**.*

3.2 Results and Discussion

3.2.1 Hexa-β-naphthylbenzene

3.2.1.1 Synthesis

The most straightforward route to a fully substituted ring was the Diels-Alder reaction of di-β-naphthyl acetylene with tetra-β-naphthylcyclopentadienone. The synthesis of the former precursor was adapted from a published synthesis of

Scheme 3.1

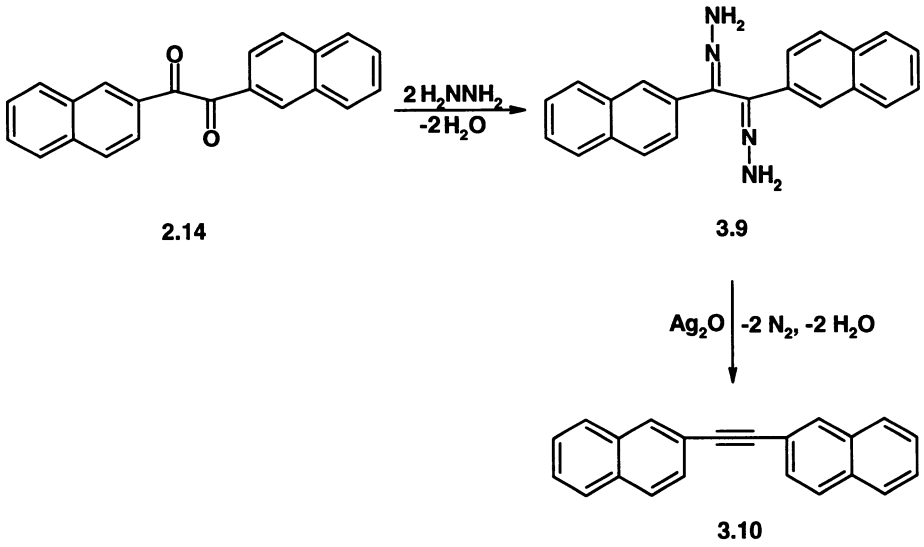

2.14

3.9

3.10

diphenylacetylene.[237,238] The method used involved the reaction of naphthil (**2.14**) with hydrazine hydrate to form naphthil dihydrazone (**3.9**, 43%), which was then treated with silver oxide, yielding the desired acetylene (**3.10**, 95%), (Scheme 3.1).

The other precursor necessary for the synthesis of hexanaphthylbenzene was tetranaphthylcyclopentadienone. The ligand was produced by first performing a phase transfer reaction to form the substituted ketone **3.11** (79%), which could then be treated with naphthil (**2.14**) to afford the desired product (**3.12**, 61%, Scheme 3.2). As before, all products were purified by column

Scheme 3.2

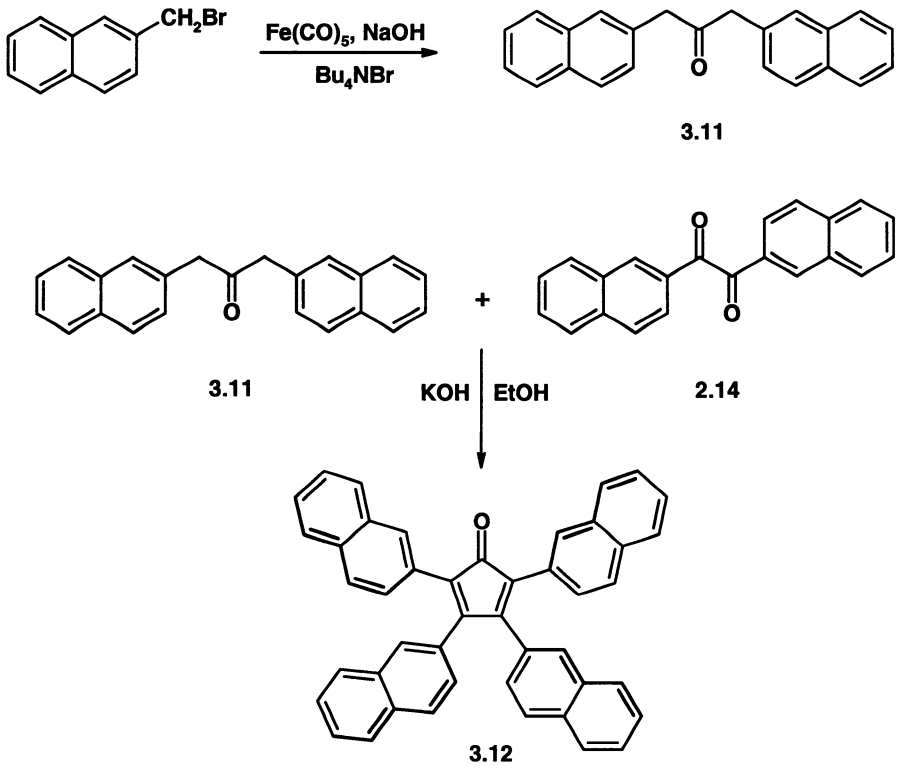

chromatography, and their identities were confirmed primarily by mass spectrometry and NMR spectroscopy.

Finally, the Diels-Alder reaction of **3.10** and **3.12** yielded the desired hexa-β-naphthylbenzene (**3.13**, 60%, Scheme 3.3).

Scheme 3.3

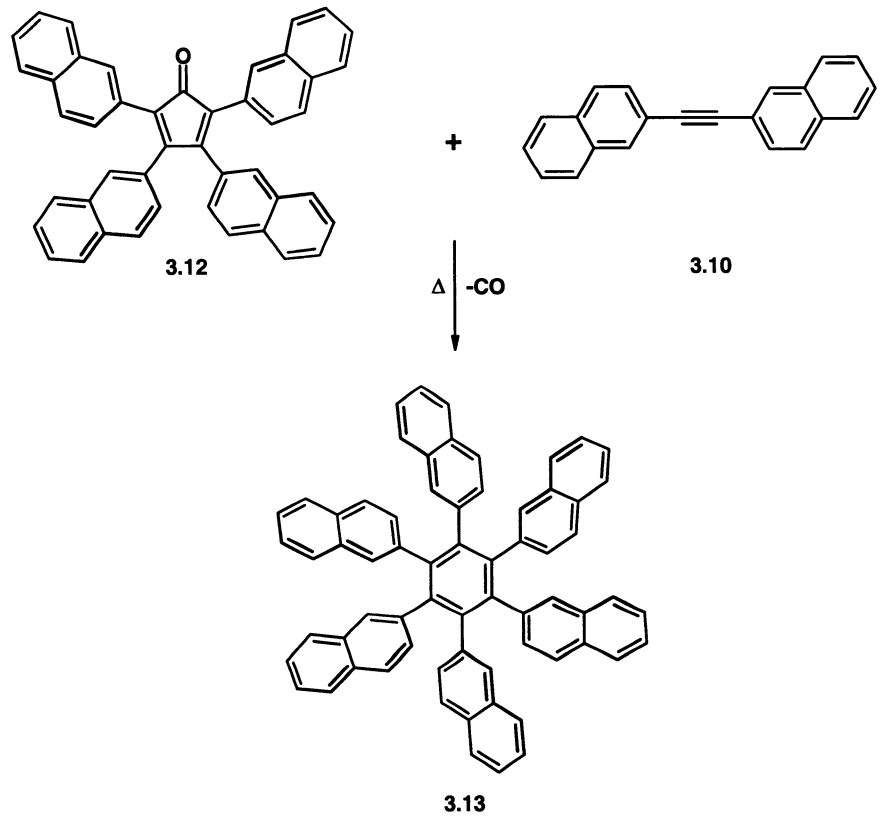

3.2.1.2 X-Ray Crystallographic Results

Each of the precursors along the synthetic route to hexanaphthylbenzene has been crystallographically characterized in order to establish the relative positions of the naphthyl substituents. To begin with, molecule **3.9** crystallized in

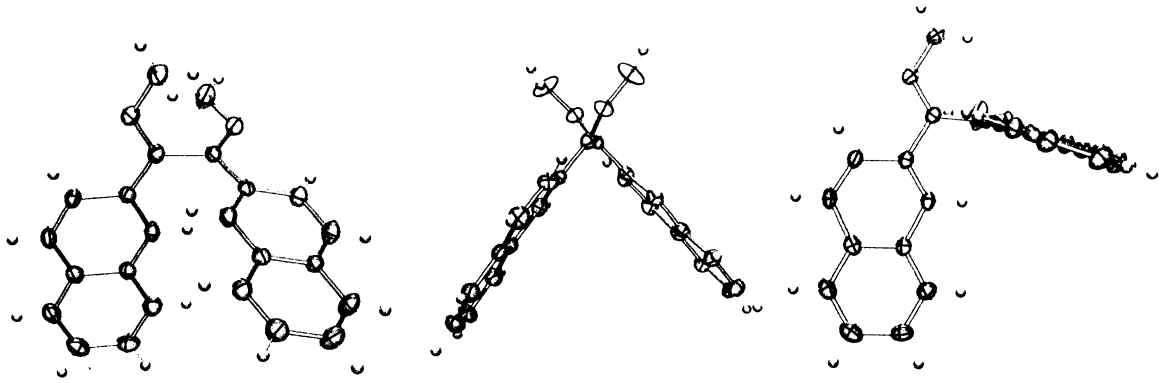

*Figure 3.1: Views of the X-ray crystal structure of **3.9**.*

space group $P2_1/c$ (Figure 3.1). The C=N and N-N bond lengths were 1.297(3) and 1.352(3) Å, respectively, and the N-N=C bond angle was 118.3(2)°. The two naphthyl substituents as well as the C-C=N-N moieties were almost perpendicular to each other, with interplanar angles of 83.6(2)° and 76.9(1)°, respectively. Moreover, the naphthyl group and hydrazone attached to the same carbon were nearly coplanar, with a slight twist of 5.4(5)° (C(1)) and 10.9(5)° (C(2)).

Dinaphthylacetylene (**3.10**) has also been characterized by X-ray crystallography. The molecule crystallized in space group Cc with a C-C triple bond length of 1.187(6) Å (Figure 3.2). The naphthyl substituents were oriented exactly parallel to each other, and formed an anti arrangement. A particularly interesting feature of the crystal structure was the packing of the molecules, as illustrated in Figure 3.3. Observing the packing from the top illustrates the curious "criss-cross" orientation of the naphthyl groups.

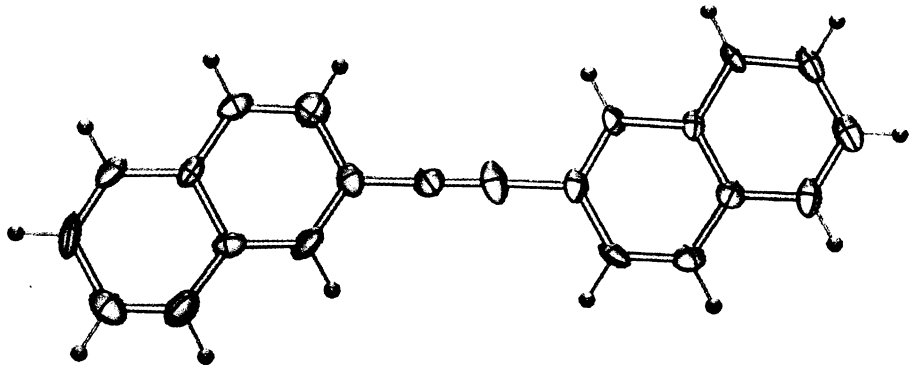

Figure 3.2: X-ray crystal structure of di-β-naphthyl acetylene.

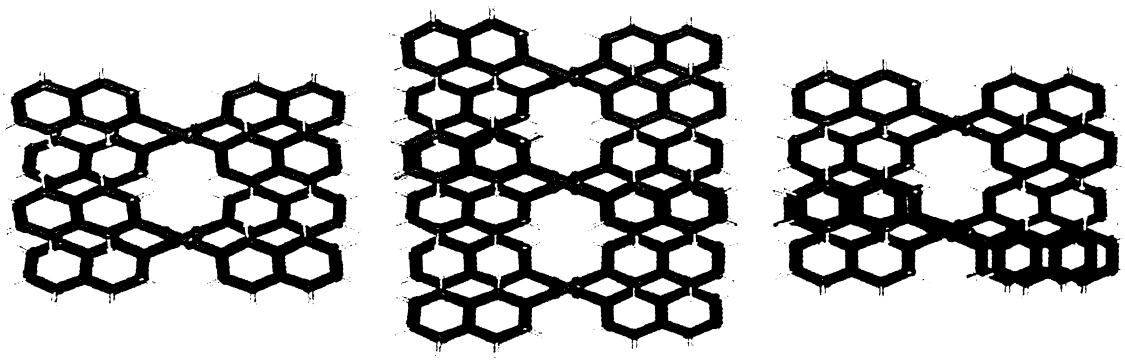

*Figure 3.3: Crystal packing of **3.10** illustrating the criss-cross arrangement of molecules.*

Finally, from the crystal structure of the cyclopentadienone **3.12** (Figure 3.4), it was clear that the two naphthyl groups in the α-position were in a less sterically encumbered environment than those in the β-position, and as a result, were able to bend more prominently. The α-positioned naphthyl groups exhibited a dihedral angle of 25.1(5)° with respect to the central ring, whereas the β-

naphthyl groups adopted angles of 55.7(4)°. The C=O bond length was 1.231(8) Å, and the C-C single and double bonds in the ring were 1.503(6) Å and 1.352(6) Å, respectively. The naphthyl groups were arranged in a propeller conformation, and were oriented in an alternating up (proximal)/down (distal) fashion to minimize steric interactions.

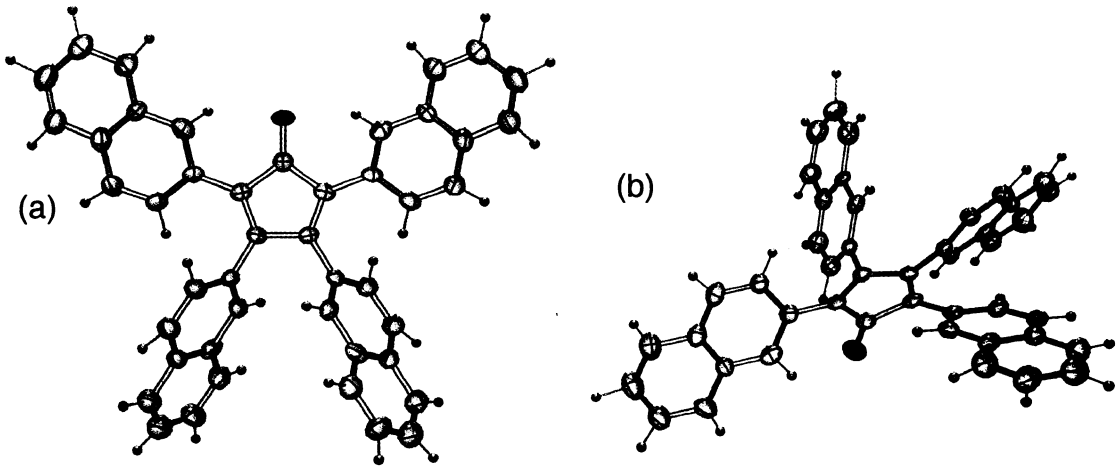

Figure 3.4: Top (a) and front (b) views of the X-ray crystal structure of tetra-β-naphthylcyclopentadienone, ***3.12****.*

Several attempts have been made to crystallize hexanaphthylbenzene, **3.13**. The molecule crystallized in very small, thin needles, and many attempts to acquire data were thwarted by weak diffraction. Moreover, larger crystals have been obtained and data has been acquired using both Mo and Cu radiation. The resulting diffraction patterns were of very low resolution and revealed complex disorder behaviour in which the ordered stacks of molecules were disordered relative to one another. This disorder has also been confirmed by powder diffraction studies, and a complete, resolved structure has not been obtained.

Attempts at co-crystallization with other species have also proven unsuccessful in yielding single crystals acceptable for analysis. The use of synchrotron radiation is currently being explored in an attempt to acquire improved data, however, it is unclear whether the inherent disorder can be overcome. Analysis of the powder diffraction data using the modeling program "Materials Studio"[240] has allowed for the development of a plausible model, in which the naphthyl groups are perpendicular to the central ring, and each molecule is rotated 30° relative to its neighbours in the stacking pattern (Figure 3.5). The distal/proximal orientation of the naphthyl substituents cannot be resolved, however, this calculated packing pattern fits the powder diffraction data with an agreement of 14 %.

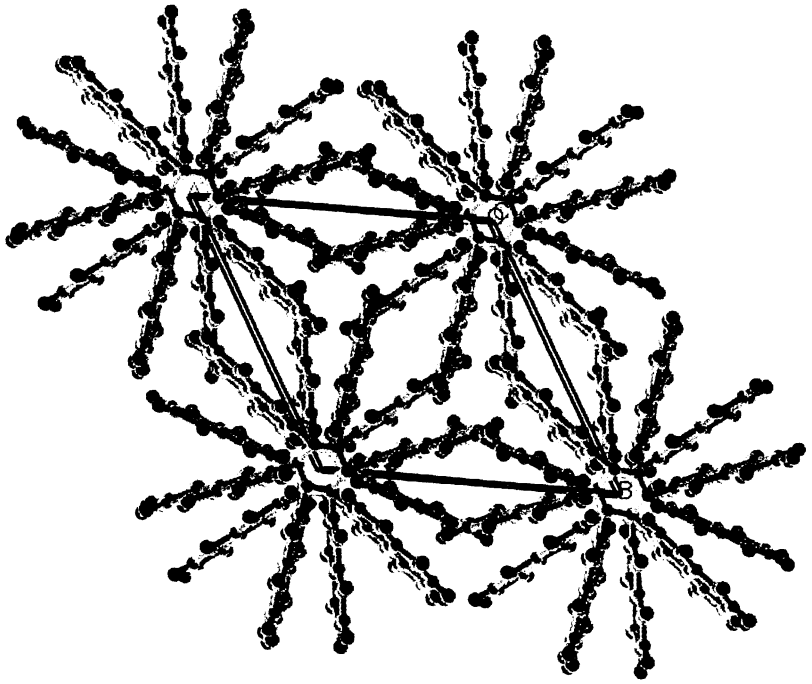

*Figure 3.5: Proposed packing pattern for **3.13**, illustrating the 30° rotation of successive molecules.*

3.2.1.3 NMR Spectroscopic Results

Variable-temperature NMR spectra of hexanaphthylbenzene have revealed restricted rotation of the β-naphthyl substituents even at ambient temperatures. Low-temperature studies did not yield clean, well-resolved decoalescences, thus the number of isomers and barrier to rotation could not be determined (Figure 3.6). However, high-temperature spectra revealed the formation of one type of naphthyl environment at 363 K (Figure 3.7), suggesting that rapid rotation was occurring at this temperature. The complexity of the

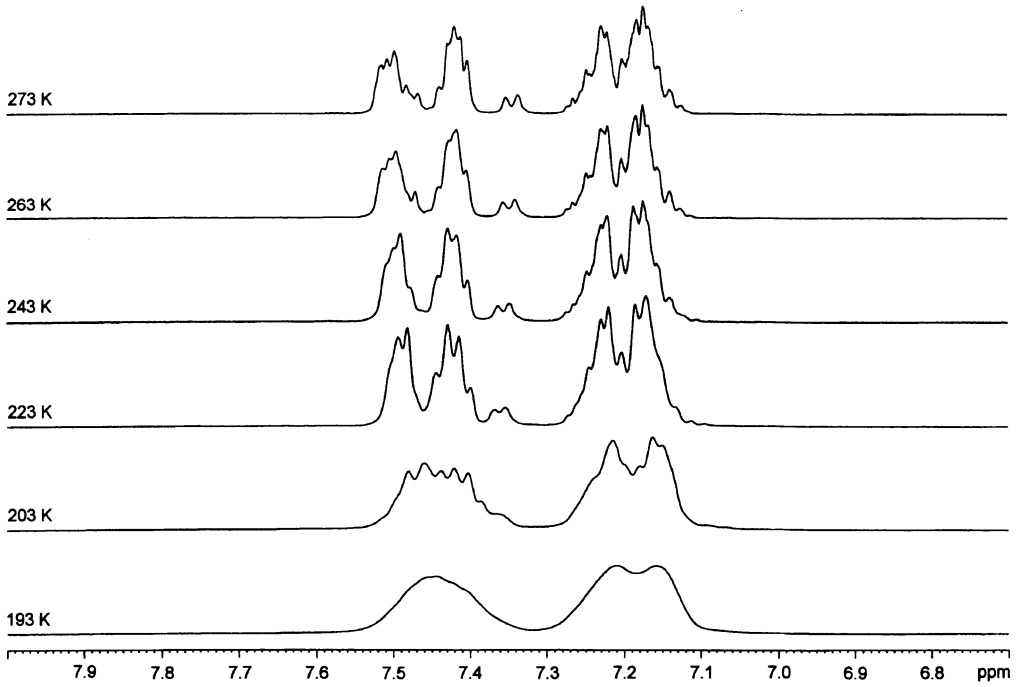

Figure 3.6: Low-temperature 500 MHz ^1H NMR spectra of hexa-β-naphthylbenzene in CD_2Cl_2.

spectra as the temperature was reduced complicated the analysis, and it was not possible to determine the mechanism of interconversion, or whether or not the process was correlated. Moreover, as previous studies have shown,[93] several isomers may be present at low temperature, with intensities governed by the relative energy of each fraction; this also made spectral analysis a non-trivial task.

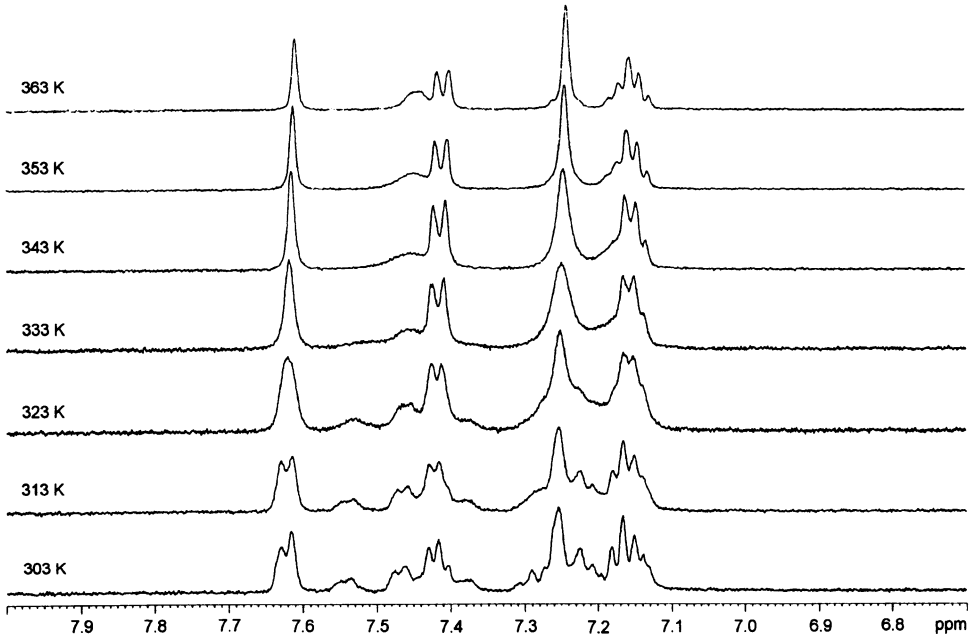

Figure 3.7: High-temperature 500 MHz ^{1}H NMR spectra of hexa-β-naphthylbenzene in DMSO.

The coalescence of the peaks at 7.47 and 7.54 ppm at 343 K resulted in the determination of the barrier to naphthyl rotation as 17 ± 1 kcal mol^{-1}; the same outcome was obtained by considering the coalescence of the signals at

7.61 and 7.63 ppm at 323 K. This value can be compared with the analogous barrier of 8.2 ± 0.5 kcal mol^{-1} in the rhodium acetylacetonate derivatives **2.17a** and **2.17b**. As anticipated, the incorporation of a greater number of naphthyl groups significantly increased the rotational barrier; progressing to a six-membered ring also brought the substituents into closer contact. This result was also consistent with Mislow's *meta*-methyl substituted benzenes, in which the indirect influence of the bulky *meta*-substituent on the sterically crowded hydrogen was reflected in the barrier to rotation, and a comparable value was reported.[232] From these data it can be concluded that naphthyl substituents do serve as models of *meta*-substituted phenyl groups, and impart significant steric effects on neighbouring atoms.

Numerous attempts to coordinate a metal atom to one of the rings in the system have been unsuccessful. As established in previous studies,[116] this would label the "faces" of the molecule and allow for a more thorough analysis of the dynamic behaviour, and perhaps allow for a crystallographic determination of the structure of this highly crowded system. As an alternative approach, derivatives containing a ferrocenyl substituent have also been examined in order to provide a more useful NMR spectroscopic label to the system and maintain the steric crowding necessary for restricted or correlated rotation.

3.2.2 Penta-β-naphthylferrocenylbenzene

3.2.2.1 Synthesis

The preparation, structure and dynamic behaviour of **3.16** has recently been reported.[241] The synthesis of **3.16** was achieved by a method similar to that previously reported for C_6Ph_5Fc (**1.55**),[93] and is summarized in Scheme 3.4. The sodium cyanide catalyzed reaction of ferrocene carboxaldehyde with β-naphthaldehyde, followed by manganese dioxide oxidation yielded the diketone **3.14** in 88% yield. The selectivity of this reaction was the result of the

Scheme 3.4

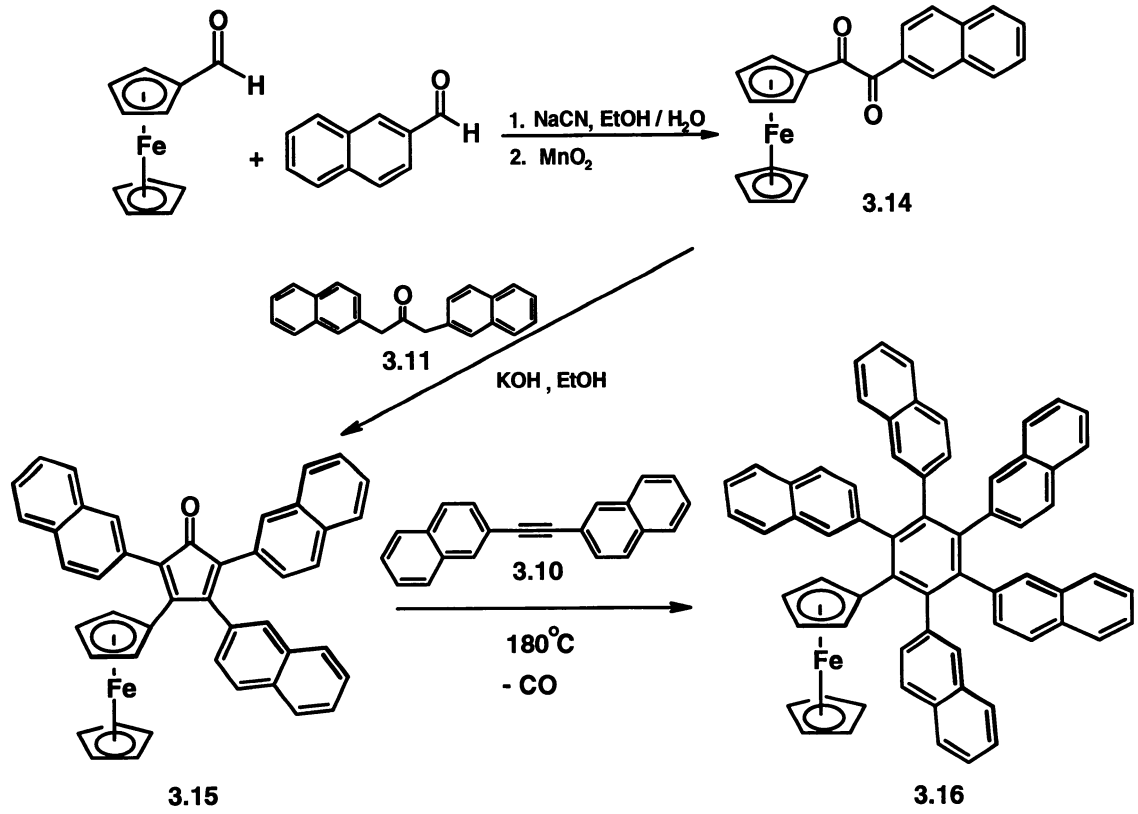

destabilization of negative charge by the ferrocenyl substituent; the formation of the intermediate ferrocenyl cyanohydrin anion is disfavoured. An aldol condensation of **3.14** with 1,3-di-(β-naphthyl)propanone (**3.11**) then furnished 3-ferrocenyl-2,4,5-tri-(β-naphthyl)cyclopentadienone (**3.15**, 49%). This compound then underwent a Diels-Alder addition to di-(β-naphthyl)acetylene (**3.10**) at 180 °C and, after loss of carbon monoxide, afforded the desired product, **3.16** with a yield of 22%.

3.2.2.2 X-Ray Crystallographic Results

Numerous attempts to grow single crystals of **3.16** suitable for an X-ray crystallographic study were thwarted, either by the slow decomposition of the sample or by efflorescence. Finally, slow evaporation of a CH_2Cl_2 solution furnished crystals that were uniformly small and thin, and by no means ideal candidates for a crystallographic investigation. Nevertheless, it was possible to acquire a data set from which the atom connectivity could be established and the molecule could be unequivocally characterized, though the bond lengths and angles could not be measured accurately.

The molecule exhibited several interesting features (Figure 3.8), most notably the up/down orientations of the naphthyl substituents. The possibility of two orientations for each naphthyl group often leads to disorder in crystal structures,[199] and in this instance, three of the naphthyl groups exhibited a disorder in which both orientations were represented. In particular, this

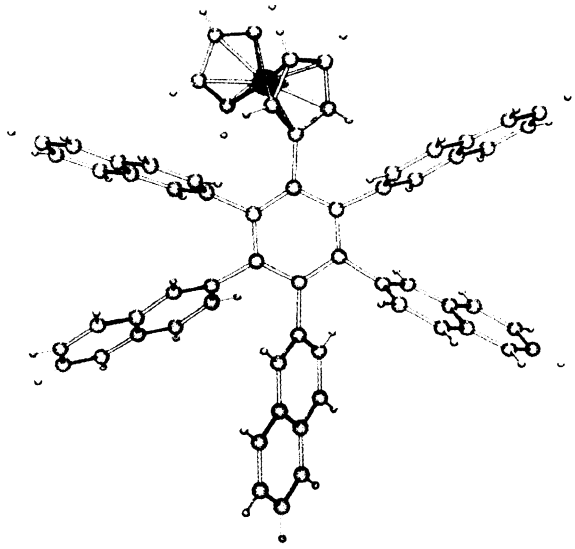

*Figure 3.8: X-ray crystal structure of **3.16**.*

phenomenon was observed for the naphthyl substituents at the central ring carbons C(2) and C(6) (i.e. those adjacent to the ferrocenyl substituent), as well as for the naphthyl ring bonded to C(3). It is tempting to draw a parallel between the solid state structure, in which these diastereomers are clearly similar in energy, and the solution state dynamic behaviour, in which several naphthyl groups apparently exhibit restricted rotation, and give rise to more than one conformer. This phenomenon will be described in greater detail.

It is also informative to examine the dihedral angles of the peripheral substituents with respect to the central ring. As noted previously, in the crystal structure of **1.55** (see Figure 3.9a) there was an incremental progression of angles from 51° to 120°, thus suggesting a "domino effect" that may offer insight into the mechanism for propeller interconversion. This may be contrasted with

the propeller conformation in hexaphenylbenzene, in which all of the phenyl groups adopted interplanar angles of 65° with respect to the central ring.[53,54] In **3.16** (see Figure 3.9b), there was a progression of angles similar to that expressed by **1.55** (error ~1°): 134° for the ferrocenyl substituent, followed by 106°, 81°, 62°, 65° and 73° for the naphthyls bonded to central ring carbons C(6) through C(2). The interesting contrast to **1.55** was that the naphthyl groups bonded to carbons C(2) through C(4) exhibited a decrease in dihedral angle rather than an increase; thus, the angles did not display a clear incremental

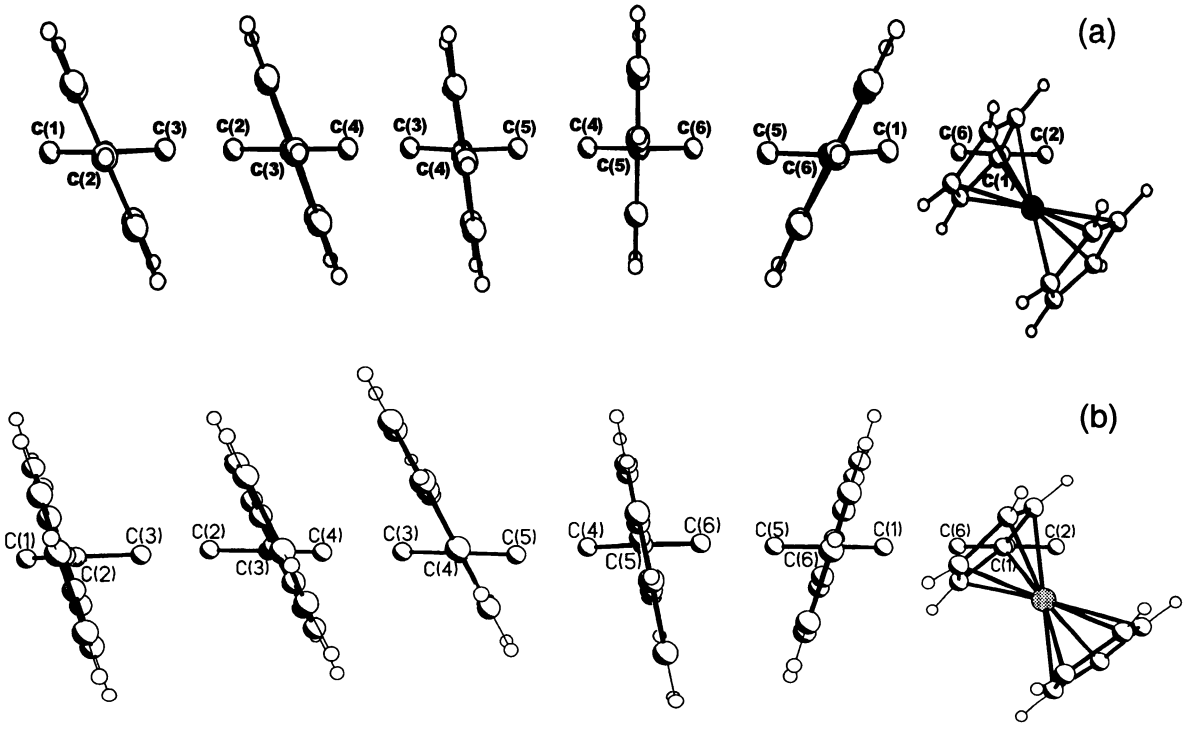

*Figure 3.9: Progression of dihedral angles in (a) pentaphenylferrocenyl-benzene, **1.55**, and in (b) penta-β-naphthylferrocenylbenzene **3.16**.*

progression leading to propeller interconversion. This phenomenon was not limited to the groups adjacent to the bulky ferrocenyl group; there was evidently significant interaction between the naphthyl substituents themselves, leading to the expression of more dramatic dihedral angles than in the phenyl analogue. The interplanar angles displayed were not influenced by the disorder in the up/down orientation of the naphthyl groups since these conformations were coplanar.

Although the quality of the X-ray crystal structure did not permit the evaluation of bond lengths and angles with precision, it did allow for a realistic assessment of the relative orientations of the peripheral substituents. In particular, viable comparisons could be made with the dihedral angles formed by the peripheral substituents relative to the central ring in pentaphenylferrocenylbenzene, **1.55**, penta-β-naphthylferrocenylbenzene, **3.16**, and hexaphenylbenzene.

3.2.2.3 NMR Spectroscopic Results

As indicated above, the 500 MHz ^{1}H and 125 MHz ^{13}C NMR spectra of pentaphenylferrocenylbenzene, **1.55**, remained essentially unchanged to temperatures as low as 188 K, thus offering no evidence for the restricted rotation of the ferrocenyl group or peripheral phenyl substituents. In contrast, although at room temperature the 500 MHz ^{1}H NMR spectrum of the naphthyl analogue, **3.16**, exhibited the expected well-resolved aromatic signals

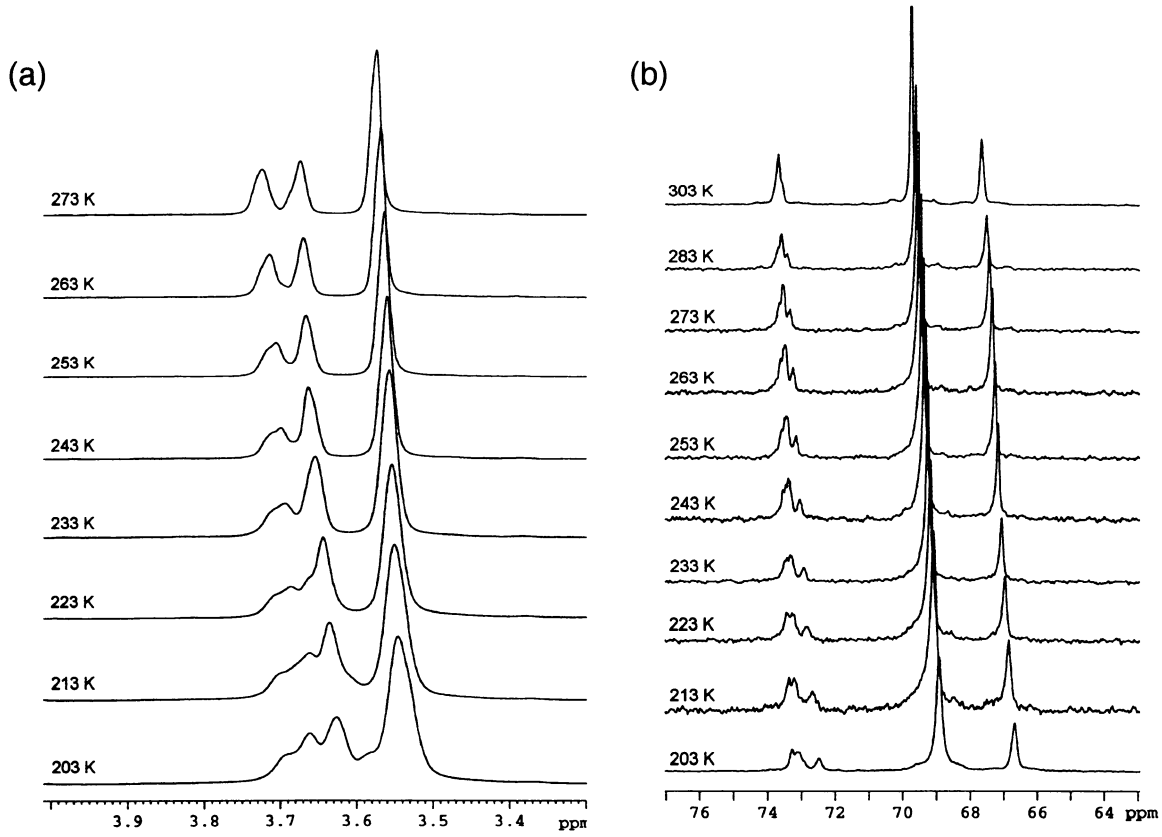

*Figure 3.10: Variable-temperature NMR spectra of **3.16**, showing the decoalescence behaviour of (a) the ferrocenyl ^{1}H environments at 500 MHz, and (b) the corresponding ^{13}C resonances at 125 MHz.*

attributable to the naphthyl and ferrocenyl protons, as the temperature was decreased, there was a marked broadening of all of the signals in the ferrocenyl region. Moreover, the singlet at 3.73 ppm, assigned to the α-CH protons in the C_5H_4 ring, split into at least 3 peaks (3.58, 3.66 and 3.69 ppm at 203 K; Figure 3.10a). These findings were mirrored in the 125 MHz ^{13}C spectra, in which the corresponding peak for the ferrocenyl α-carbon gradually split into three peaks as the temperature was reduced (72.5, 73.1 and 73.3 ppm at 203 K; Figure 3.10b). The peaks for the other ferrocenyl carbon and hydrogen atoms appeared to

broaden, but did not cleanly split at low temperature. There was similar broadening and splitting behaviour in the aromatic region, but severe overlap of the naphthyl signals in both the proton and carbon regimes at low temperature rendered these peak assignments ambiguous, even at 11.74 T.

If the ferrocenyl and naphthyl ring rotations were slowed on the NMR time-scale, and the molecule adopted a single favoured conformation, four equal intensity ^{1}H and ^{13}C resonances attributable to the C_5H_4 moiety would be expected. However, since decoalescence gave rise to three signals of unequal intensity for the ferrocenyl α-carbon, it is unlikely that restricted ferrocenyl rotation is the single explanation for the observed behaviour. An alternative rationale is that restricted rotation of the naphthyl groups resulted in the formation of a number of diastereomers and, as a result, each ferrocenyl environment gave rise to distinct peaks, the intensities of which corresponded to the relative stability of each of the rotamers.

It is also instructive to consider the possibility that the system exhibits residual stereoisomerism, in which restricted rotation results in the generation of closed subsets of rotational isomers that are separated by substantial barriers. This behaviour has been established in maximally labelled Ar_3Z and Ar_3ZX moieties,[43,50] such that the correlated motion of the aryl rings imposes a constraint on the relationship between torsional angles, restricting the possible interconversion pathways between the full set of conformers. The extension of this concept to molecule **3.16** implies correlated rotation between the ferrocenyl

group and the naphthyl rings, thus achieving the goal of enforcing interdependent motion of all the peripheral substituents on a central benzene ring. This possibility requires that the naphthyl rings can be oriented in various proximal/distal arrangements, thus generating several diastereomers that interconvert slowly on the NMR time-scale at low temperatures; a phenomenon that has been clearly illustrated by the X-ray crystal structure of **3.16**.

3.3 Conclusions

The integration of β-naphthyl substituents into novel benzene architectures has clearly established the utility of this bulky fragment. The choice of β-naphthyl instead of the even more crowded α-naphthyl group allowed for the relatively facile synthesis and characterization of the various synthetic templates. The ability of the substituent to adopt proximal and distal orientations complicated the X-ray crystallographic and NMR spectroscopic analysis of the hexanaphthylbenzene, however, a barrier to β-naphthyl rotation of 17 ± 1 kcal mol^{-1} has been determined.

Moreover, the combination of one ferrocenyl and five β-naphthyl substituents within a benzene ring resulted in the generation of at least three diastereomers arising from different up/down combinations of the naphthyl substituents. Evidence of this was present in the solid state, in which three of the naphthyl rings exhibited disorder, and in solution, as the variable-temperature NMR spectra revealed the presence of several rotamers. Increasing the steric

bulk from a phenyl group to a naphthyl substituent clearly enhanced the interaction between the peripheral substituents and generated the potential for observing correlated rotation in a six-bladed propeller.

CHAPTER FOUR

Investigation of the Protonation of Tetracyclone and Ferrocenyl-Substituted Tetracyclone

4.1 Introduction

4.1.1 Steric Protection

As attempts are made to create a system that exhibits correlated rotation, molecules containing increasingly crowded substituents have been created. Outside of the objective of achieving the initial goal, these species may be of broader interest as a result of the steric protection they offer. This chapter explores the use of sterically crowded molecules in the attempted creation and observation of unstable cationic species.

4.1.2 Cyclopentadienyl Cations

Cyclopentadienones, **2.1**, have been used extensively as synthetic intermediates, most notably in Diels-Alder reactions.[200,201] The localized nature of the bonding in these valuable synthons has been well established. Evidence

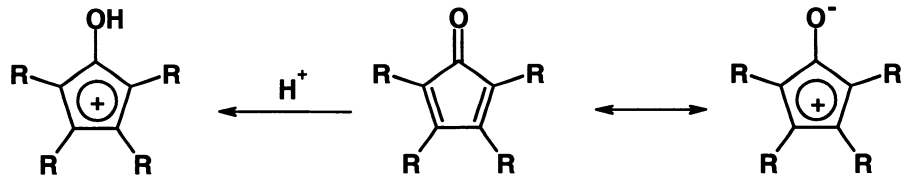

4.2 **2.1** **4.1**

1.26: R = Ph

*Chart 4.1: Cyclopentadienones **1.26** and **2.1**, charge separated form **4.1** and the cyclopentadienyl cation, **4.2**.*

of this includes the X-ray crystal structure[242] and the characteristic infrared frequency of the carbonyl group (~1710 cm^{-1}) in tetracyclone (**1.26**, page 23), which reflects the presence of a "true" C=O double bond. Thus, the ionic resonance form (**4.1**) does not contribute appreciably to the overall structure of the molecule. An area of research that remains incomplete is the protonation of cyclopentadienones, which requires the formation of unstable, 4π anti-aromatic cations, **4.2** (Chart 4.1).

The qualitative description of antiaromaticity has proven to be as controversial as that of aromaticity (Section 1.1.1). In general, antiaromatic species are expected to exhibit the following criteria:[9,12] (i) contain $4n\,\pi$ electrons in a cyclic, conjugated system; (ii) decreased delocalization as well as destabilization from cyclic conjugation; (iii) alternation of bond lengths; and (iv) a small diamagnetic anisotropy. Many of these conditions do not apply to all related systems, and geometric effects are often overlooked in qualitative discussions. In many instances, antiaromatic species exhibit degenerate structural isomerism and can adopt a variety of equivalent non-symmetrical structures. In 4π and 8π systems, distortion can occur such that unequal population of degenerate orbitals is avoided, resulting in a lower energy geometry than a fully symmetrical conjugated structure, although the energy differences are often small.[12,243] As with aromatic systems, the criteria for the description of antiaromatic molecules continues to evolve.

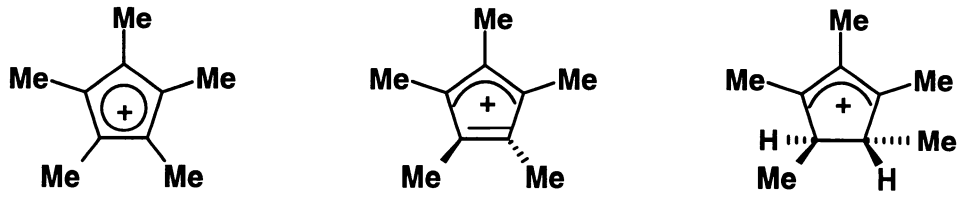

4.3 **4.4** **4.5**

*Chart 4.2: Lambert's pentamethylcyclopentadienyl cation **4.4** and the revised structure **4.5**.*

The observation of antiaromatic cations has also been the subject of considerable interest, with the initial report,[244] and the subsequent refutation,[245,246] of evidence for the formation of the pentamethylcyclopentadienyl cation, **4.3** (Chart 4.2). Lambert and co-workers have described the synthesis and X-ray crystal structure of the cation **4.3** as the tetrakis-(pentafluorophenyl)borate salt.[244] The remarkable stability of this antiaromatic species was attributed to the presence of the methyl groups as well as the choice of counteranion and solvent. The structure was distorted appreciably from planarity and the bond lengths within the ring varied from 1.39 Å to 1.51 Å. The bonding arrangement in the structure was described as "allyl-like", with an approximate single bond within the ring (**4.4**).[244] Moreover, the authors conducted ESR investigations and observed no signals, thus concluding that a triplet cation was unlikely, and that the molecule was a stable singlet. This report sparked immediate disbelief in the scientific community, and close re-examination of the structure and the properties of the species led to the reassignment of the structure as that of the pentamethylcyclopentenyl cation **4.5**.[245,246] Nonetheless, investigations into the formation and reactivity of

antiaromatic species continue, and the cyclopentadienyl cation in particular remains the subject of substantial research.

Evidence for the intermediacy of cyclopentadienyl cations, generated by protonation of cyclopentadienols,[247-250] or in solvolysis studies,[251,252] has been reported, and these ions are often the subject of computational studies.[253-258] Early reports by Ziegler and Schnell[247] of the formation and spectroscopic characterization of the pentaphenylcyclopentadienyl cation **4.7**, formed by acidification of the alcohol **4.6**, were later revised by Breslow and Chang,[248,249] as the cation reacted further to form the cyclopentadienes (**4.8**) after a few seconds

Scheme 4.1

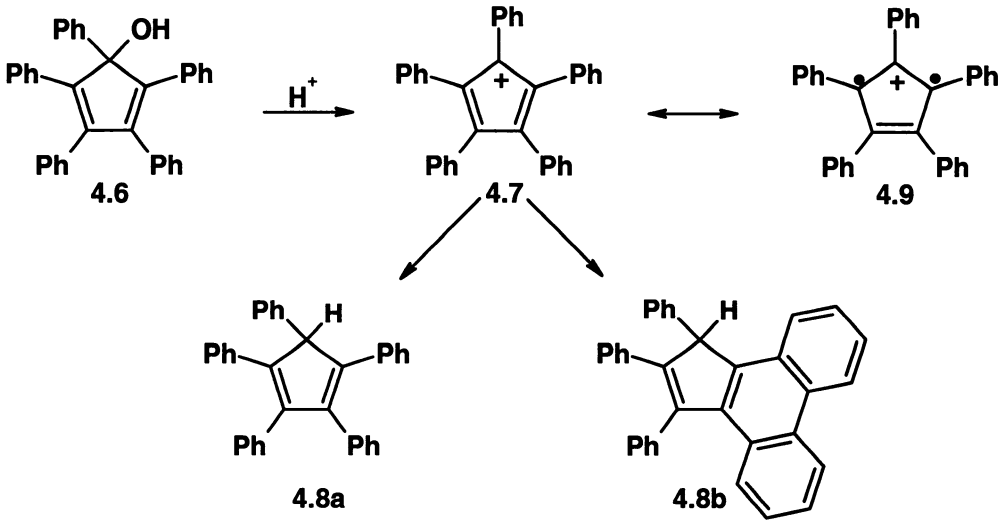

(Scheme 4.1). Moreover, Carpentier[250] protonated the alcohol, **4.10**, with sulfuric acid and used UV spectroscopy to confirm the structure of the resulting cation

(**4.11**) in which the charge was localized on the oxygen atom rather than being delocalized in the 5-membered ring (**4.12**, Scheme 4.2).

Scheme 4.2

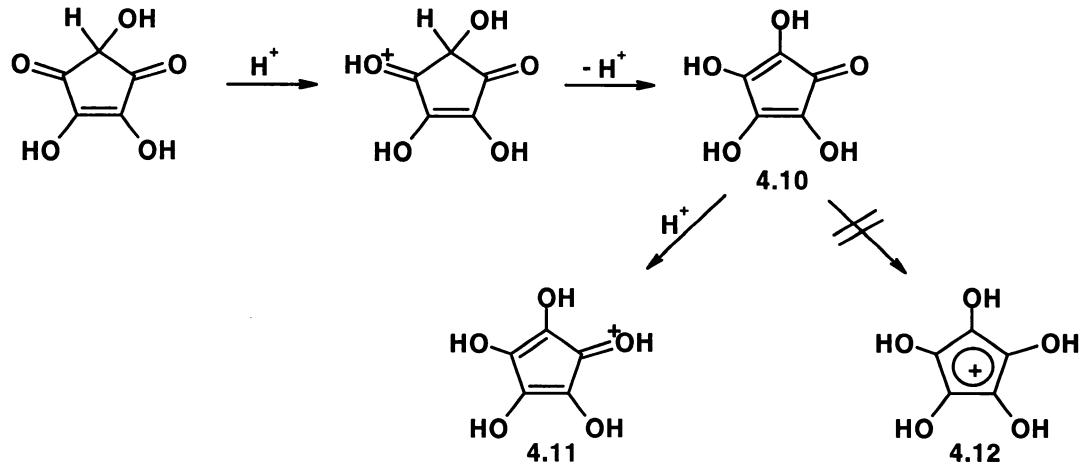

There have also been reports of reactions of cyclopentadienones and cyclopentadienols with Lewis acids. The reaction of **4.6** with BF_3 in CH_2Cl_2 at –60 °C resulted in the formation of a bright blue solution of the cation **4.7** in equilibrium with the triplet biradical **4.9** (Scheme 4.1).[248,249] Moreover, the treatment of **1.26** with aluminum trichloride was reported by Allen and VanAllen in 1943,[259] and the product was assigned as the ketone **4.13**, in which the double bonds were reduced (Scheme 4.3). This result was later refuted by Sonntag, et al.,[260] who described the product as dihydrophencyclone **4.14** after characterization with UV spectroscopy and comparison with an authentic sample. The *cis* or *trans* disposition of the phenyl groups was not determined until 2002.[261]

Scheme 4.3

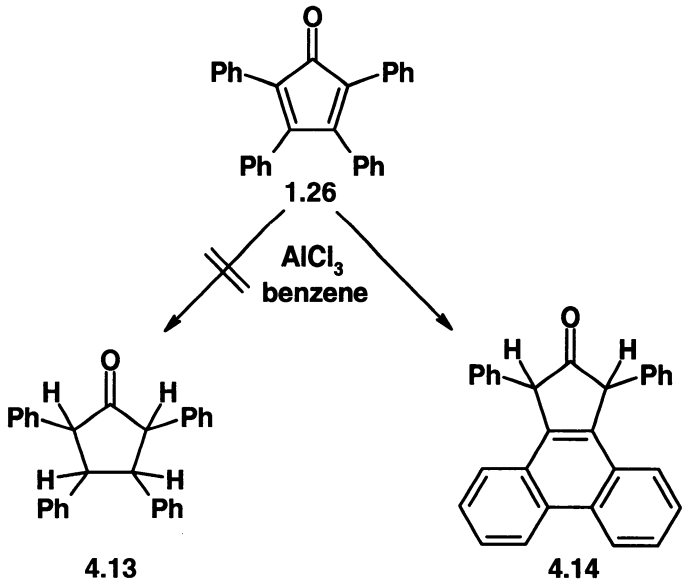

More recently, Allen and Tidwell have reported solvolysis studies of antiaromatic cations.[251,252] Placing **4.15** in a variety of solvents gave UV spectra consistent with the loss of the trifluoroacetate leaving group (Scheme 4.4). A preparative scale process gave products representing elimination and

Scheme 4.4

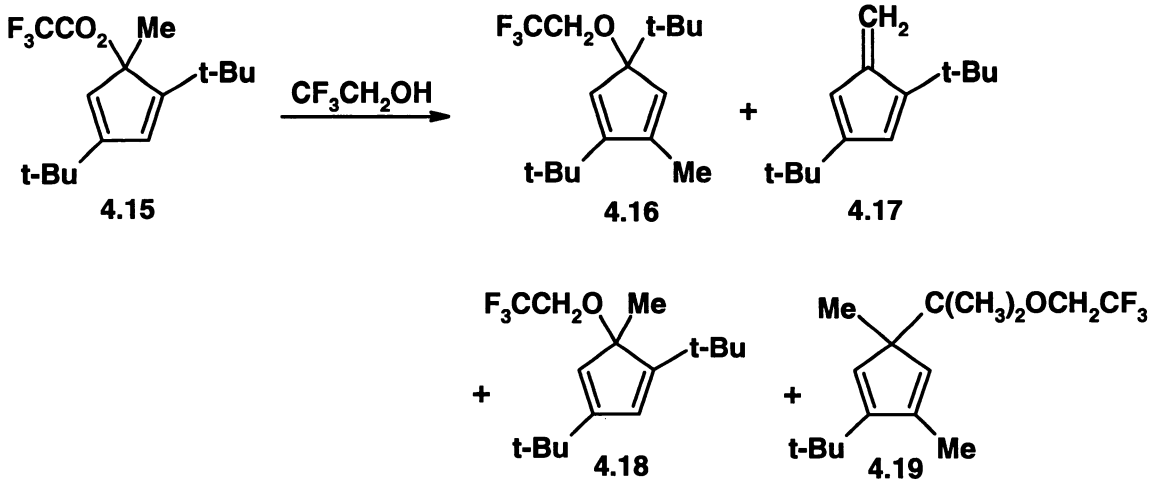

substitution with or without allylic or skeletal rearrangement (**4.16** – **4.19**); these results were consistent with the formation of a cationic intermediate. The comparison of this reactivity with the cyclopentenyl analogue, **4.20** (Chart 4.3), gave a rate depression of 10^{14}, which was attributed to the antiaromaticity of the intermediate.[251] Similar results were also obtained for the related derivative **4.21**.[252]

Numerous other investigations of cyclopentadienyl cations have been reported, including IR spectroscopic studies,[262,263] electrochemical inquiries,[264] and trapping reactions with a variety of nucleophiles.[265] Moreover, Breslow has reported the detection of the triplet state for a number of cations using ESR, and this has been found to be the ground state in most instances.[253,266,267] Overall, as described by Tidwell,[12] discussions of anti-aromaticity have been "episodic", and contentious, and this area of research will continue to be a topic of much interest and debate.

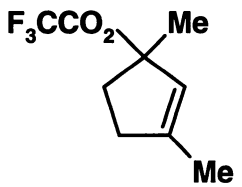

4.20

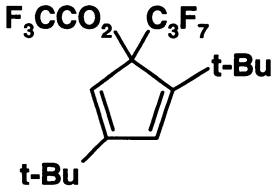

4.21

*Chart 4.3: Molecules **4.20** and **4.21** investigated by Allen and Tidwell.*

4.1.3 Ferrocenyl-Stabilized Antiaromatic Cations

The use of transition metals for the stabilization and characterization of short-lived species has been well established.[268-272] Examples include cobalt-coordinated fluorenyl, indenyl and cyclopentadienyl cations, such as molecules **4.23a** and **4.23b**, which were formed by the protonation of the corresponding alcohols, **4.22a** and **4.22b** (Scheme 4.5).[273] In these instances, the electron deficiency was relieved by the direct overlap of a vacant orbital at the cationic site with a filled metal orbital, as evidenced by the pronounced tilting of the cation towards the metal center.[274-281] This electronic stabilization imparted conformational rigidity, which had application in stereoselective nucleophilic addition reactions,[274,282] and was manifested in the restricted rotation of the exocyclic bond, as observed by NMR spectroscopy.[283-290] For instance, Müller has reported the generation of the ferrocenyl-stabilized cation **4.24**, and its subsequent reactions with a series of nucleophiles.[274] The bending of the cation towards the metal allowed for the formation of the allene products **4.27** – **4.29**,

Scheme 4.5

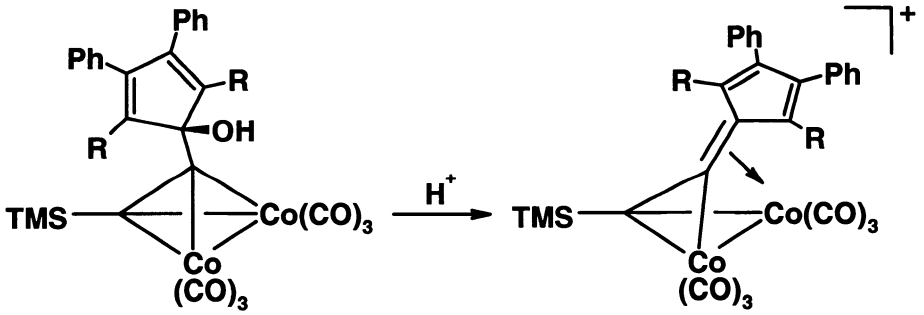

4.22a: R = Ph
4.22b: R = Et

4.23a: R = Ph
4.23b: R = Et

Scheme 4.6

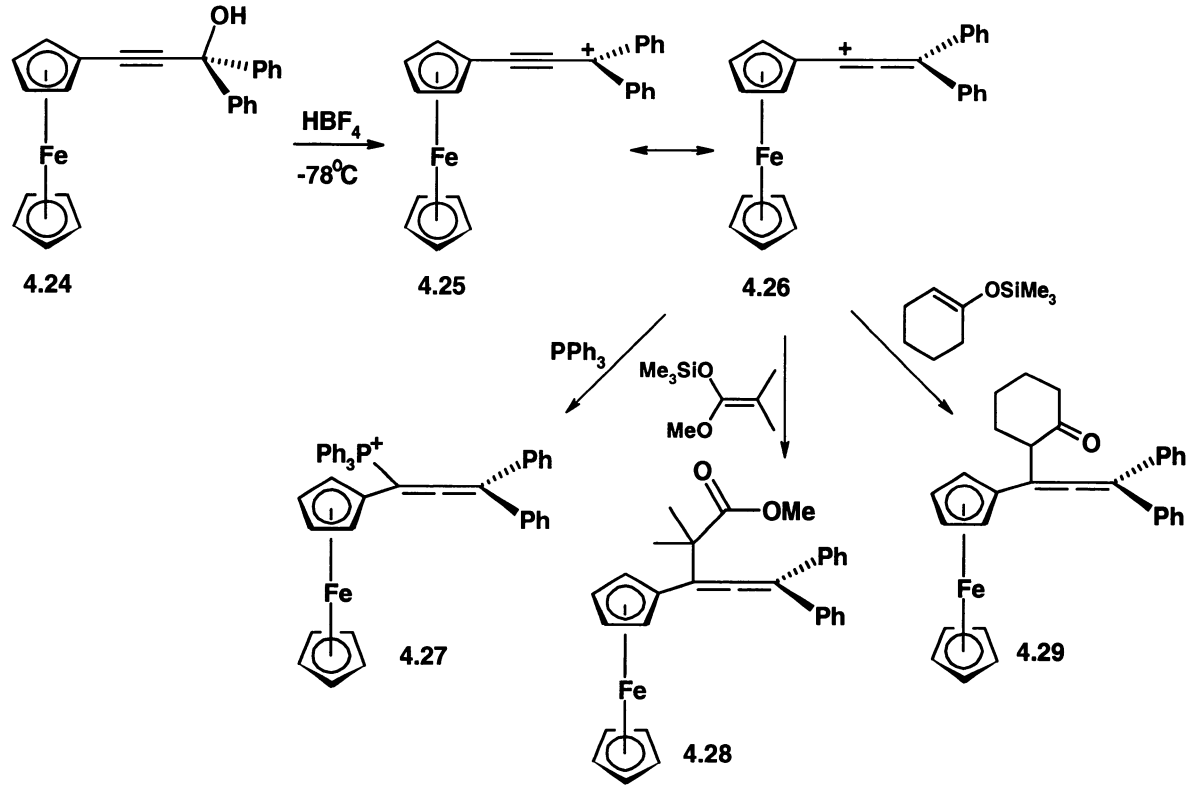

which was consistent with the contribution of the allenylium structure **4.26** to the stabilization of the cation (Scheme 4.6). Moreover, Turbitt and Watts have observed the temperature-dependent NMR spectra of the cation **4.30**, and determined the barrier to rotation around the Fc-(C^+HMe) bond to be approximately 20 kcal mol^{-1} (Scheme 4.7).[289] Thus, the stabilization of carbocations in the α-position was well established in ferrocenyl-substituted systems. There are numerous other examples in the literature that use ferrocene to offer stability to cations that are otherwise not isolable, for instance, allenyl[275,291] and allyl[292] systems, vinyl[293] and cyclopropyl[294] cations, as well as norbornan-2-yl[295] and azulenyl[296] derivatives.

Scheme 4.7

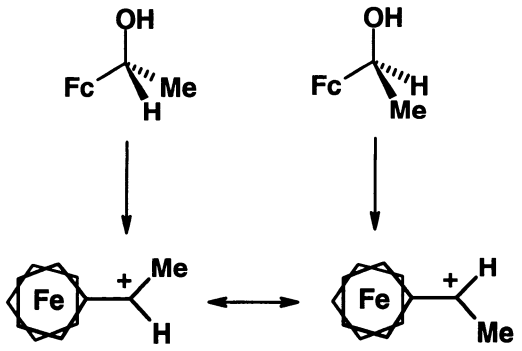

4.30

The structure and bonding of ferrocenyl carbenium ions has been the subject of discussion and debate, and several structures were described in the early literature to account for the unique properties of these complexes.[288,297,298] In 1961, Dannenberg proposed the displacement of the Fe-Cp group towards the exocyclic carbon in order to optimize metal-ligand bonding (**4.31**).[288,297] Caïs has suggested that better overlap would occur in a bent structure (**4.32**),[298] while Traylor[299] and Lillya[300] favoured structures with no interaction between the iron and the exocyclic atom (**4.33**, Chart 4.4). More recently, the combination of

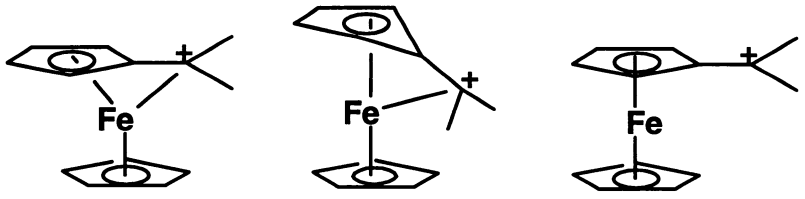

4.31 **4.32** **4.33**

Chart 4.4: Early structure and bonding proposals for ferrocenyl carbonium ions.

physical methods and calculations has affirmed the fulvenoid structure, **4.34**, in which the steric and electronic nature of the substituents R dictates the extent to which the exocyclic double bond leans toward the metal.[275,283]

Caïs has reported the X-ray crystal structure of the α,α-diferrocenylmethylium tetrafluoroborate complex, **4.35**, and asserted that the geometric flexibility of the cation allowed it to maximize metal – ligand interactions and determined the stability of the complex.[301] These observations have been manifested in other structures,[276-281] including the recent reports of the first crystal structure of a primary ferrocenylcarbocation, **4.36**,[277] and of the ruthenocenylmethylium cations, **4.37**[278] (Chart 4.5).

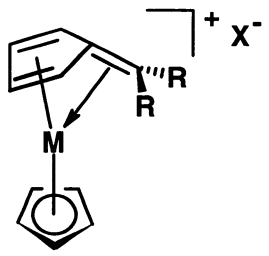

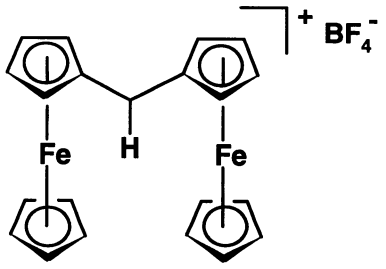

4.34: M = Fe
4.36: M = Fe; X = $B\{C_6H_3(CF_3)_2\}_4^-$; R = H
4.37a: M = Ru; X = $B\{C_6H_3(CF_3)_2\}_4^-$; R = H
4.37b: M = Ru; X = $CF_3SO_3^-$; R = H

4.35

*Chart 4.5: Ferrocenyl carbonium ions **4.34** – **4.37**.*

In an attempt to use steric crowding to stabilize transient species, the protonation reactions of tetraphenylcyclopentadienone (**1.26**, page 23) and 3-ferrocenyl-2,4,5-triphenylcyclopentadienone (**1.27**) have been performed, as these reactions might be expected to yield stabilized cyclopentadienyl cations. In

the case of the metal-stabilized system, DFT calculations have been used to rationalize the observed rotational barriers, and to evaluate the structures of the neutral molecule and the resulting cation; these results have been published.[302]

4.2 Results and Discussion

4.2.1 Protonation of Tetraphenylcyclopentadienone

The protonation study was conducted on the NMR scale by first cooling the cyclopentadienone in CD_2Cl_2 to –78 °C in an NMR tube, followed by the addition of two drops of acid to the solution. The reaction required the use of an extremely strong acid: protonation did not occur with trifluoroacetic acid, thus trifluoromethonesulfonic (triflic) acid was used. The necessity for such a strong acid offered evidence for the instability of the transient products formed. The protonation led to a complex mixture of products that was not immediately identifiable by NMR spectroscopy. The reaction was repeated on a much larger scale in an attempt to separate and identify the numerous fractions (by using flash column chromatography, followed by preparative-HPLC purification). The largest contributor (62%) proved to be tetracyclone (**1.26**). The major product (21% based on the percentage that reacted) was determined to be 5-*H* benzo[*a*]fluorene-5-one, **4.38** (Scheme 4.8), by NMR spectroscopy, mass spectrometry and X-ray crystallography. The X-ray crystal structure of **4.38** is displayed in Figure 4.1.

Scheme 4.8

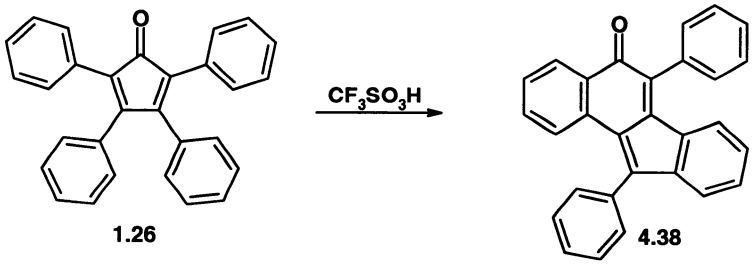

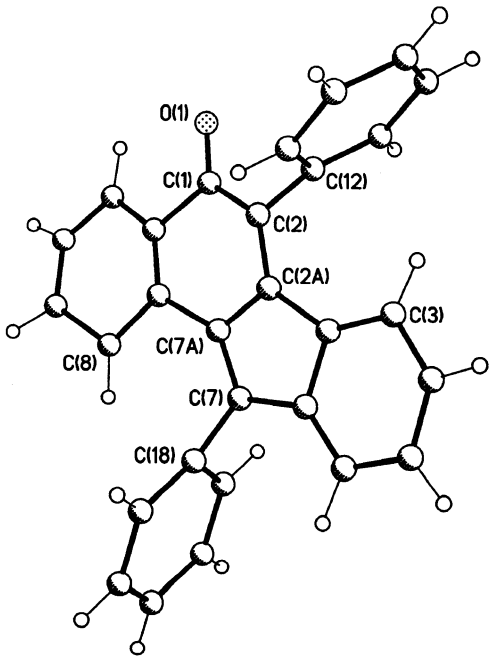

*Figure 4.1: The X-ray crystal structure of **4.38**.*

The crystals of **4.38** were extremely small, and did not diffract well enough to allow for full anisotropic refinement, thus an isotropic model is presented in Figure 4.1. Moreover, the central ring skeleton was extremely disordered, thus appeared distorted from planarity. The use of synchrotron radiation to give improved data is currently being explored. The compound crystallized in space

group Pc, and there were three (disordered) molecules in the unit cell; the outer two were arranged so that the C=O functionalities were pointing in opposite directions, and the third lay in between and was essentially perpendicular. The average C=O bond length was 1.19(2) Å, which was slightly shorter than in the parent cyclopentadienone.[242] The central ring skeleton was effectively planar (but with a slight twist), and the phenyl substituents were oriented almost perpendicular to this central plane, at 96° and 100°.

Scheme 4.9

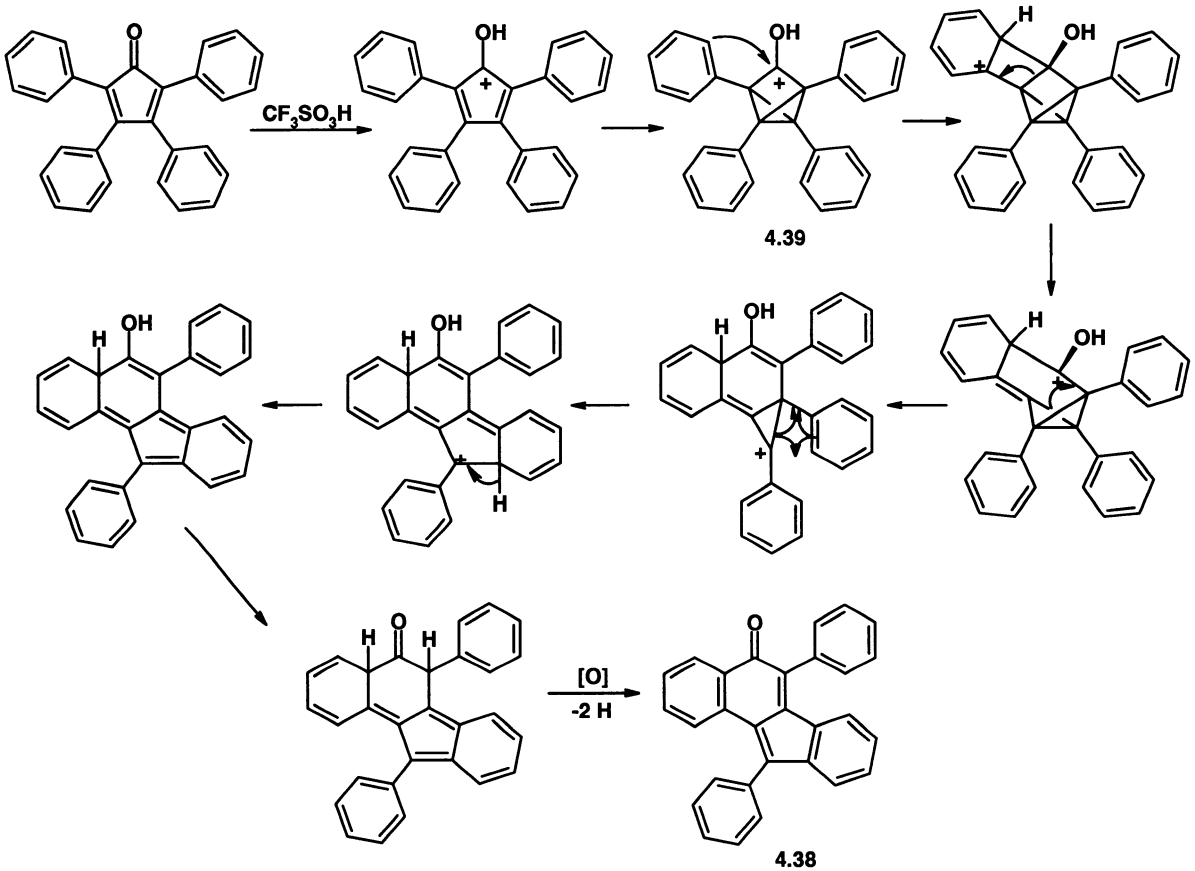

The formation of **4.38** required the generation of a cationic site at the carbonyl carbon atom, which could then be migrated through the 5-membered ring onto a peripheral phenyl substituent. The distortion from planarity required to achieve the extensive bond migrations necessary could be accomplished by the formation of the diagonally bonded intermediate, **4.39** (Scheme 4.9). There is precedent for the formation of such "cross-over" intermediates in the formation of tetrahedranes from sterically crowded cyclopentadienones.[303-306] For instance, Maier and co-workers have described the UV irradiation of tetra-*t*-butyl cyclopentadienone (**4.40**), which forms the analogous diagonally-bonded intermediate, then loses CO, yielding tetra-*t*-butyl tetrahedrane (**4.41**, Scheme 4.10).[303] In the production of **4.38**, opening of the 5-membered ring was followed by several bond migrations and the final oxidation step, leading to the observed product.

Scheme 4.10

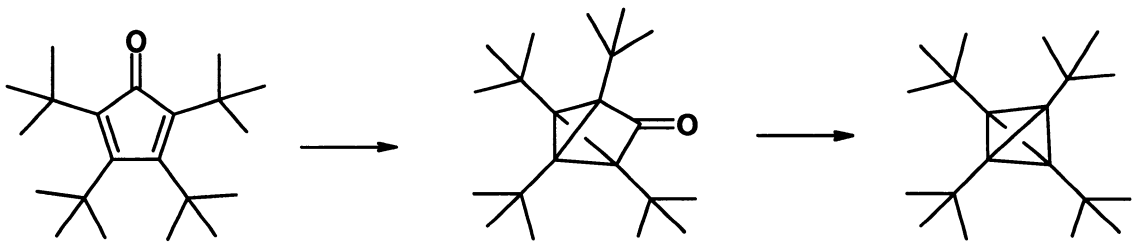

4.40 **4.41**

The sole mention of **4.38** in the literature is as a tentatively identified product of the drastic hydrolytic conditions leading to the electrophilic cyclization and elimination of hydrazine from **4.42**.[307] Unfortunately, this report did not

include any characterization of this product for comparison. An isomer of **4.38** has also been reported, as a pyrolysis product of tetracyclone.[308] The formation of **4.43** was reported to involve the cleavage of the carbonyl-olefin bond of tetracyclone, followed by bond rotation and shifts to form **4.44**, which could then be dehydrogenated by tetracyclone (Scheme 4.11).

Scheme 4.11

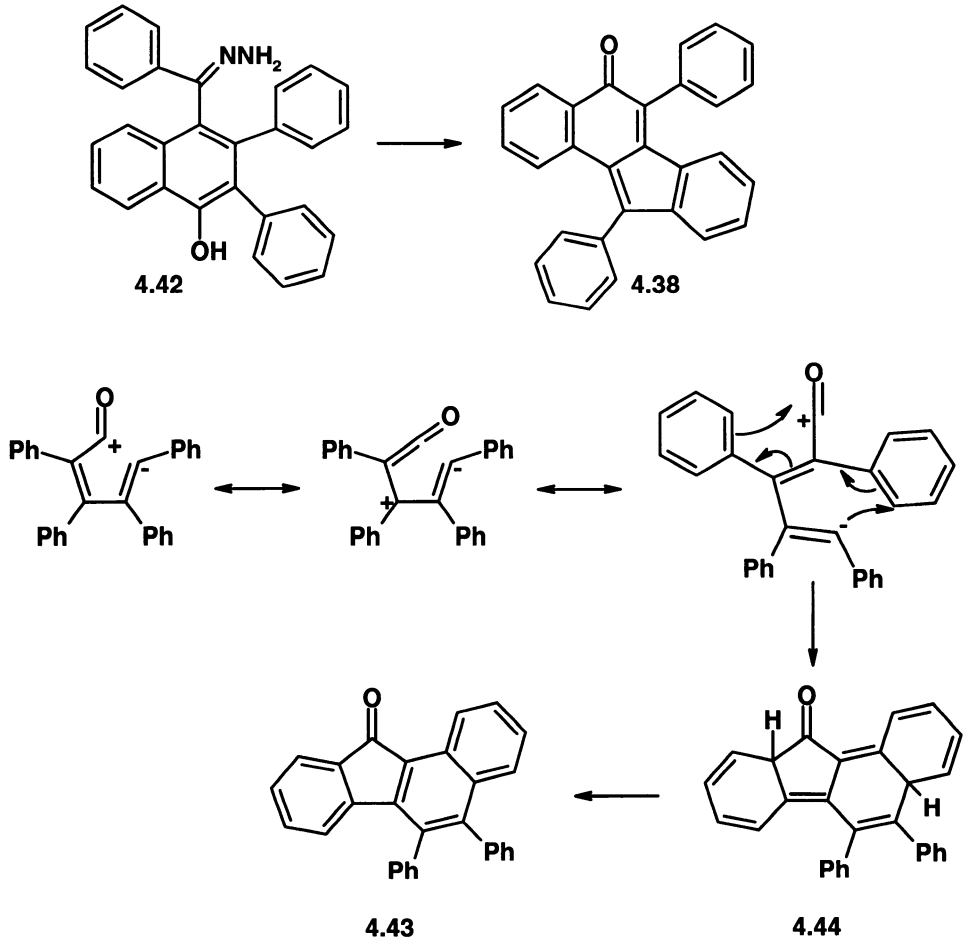

Also isolated from the reaction mixture was a product consistent with the reduction of another molecule of tetracyclone, yielding cyclopentenone **4.45**,

which comprised 8% of the product mixture. This compound was characterized by NMR spectroscopy and mass spectrometry (Figure 4.2). The crystal structure of **4.45** has already been reported,[309,310] and in this instance, the *trans* isomer of **4.45** was obtained, in accord with the literature characterization.[310]

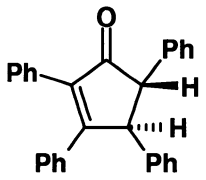

4.45

Figure 4.2: The cyclopentenone product, ***4.45****.*

Of the remaining fractions, the characterization of the three most abundant products was attempted using NMR spectroscopy and mass spectrometry. However, the complexity of the spectra obtained prevented the unambiguous identification of their structures. The data obtained for all isolated fractions is presented in the Experimental Section.

4.2.2 3-Ferrocenyl-2,4,5-triphenylcyclopentadienone

4.2.2.1 NMR Spectroscopic Results

The ^{1}H and ^{13}C NMR spectra of the neutral cyclopentadienone (**1.27**) exhibited no decoalescence behaviour and were consistent with the rapid rotation of the phenyl groups and ferrocenyl substituent, on the NMR time-scale, to temperatures as low as –80 °C. The protonation study was conducted by cooling a solution of the cyclopentadienone in CD_2Cl_2 to –78 °C in an NMR tube,

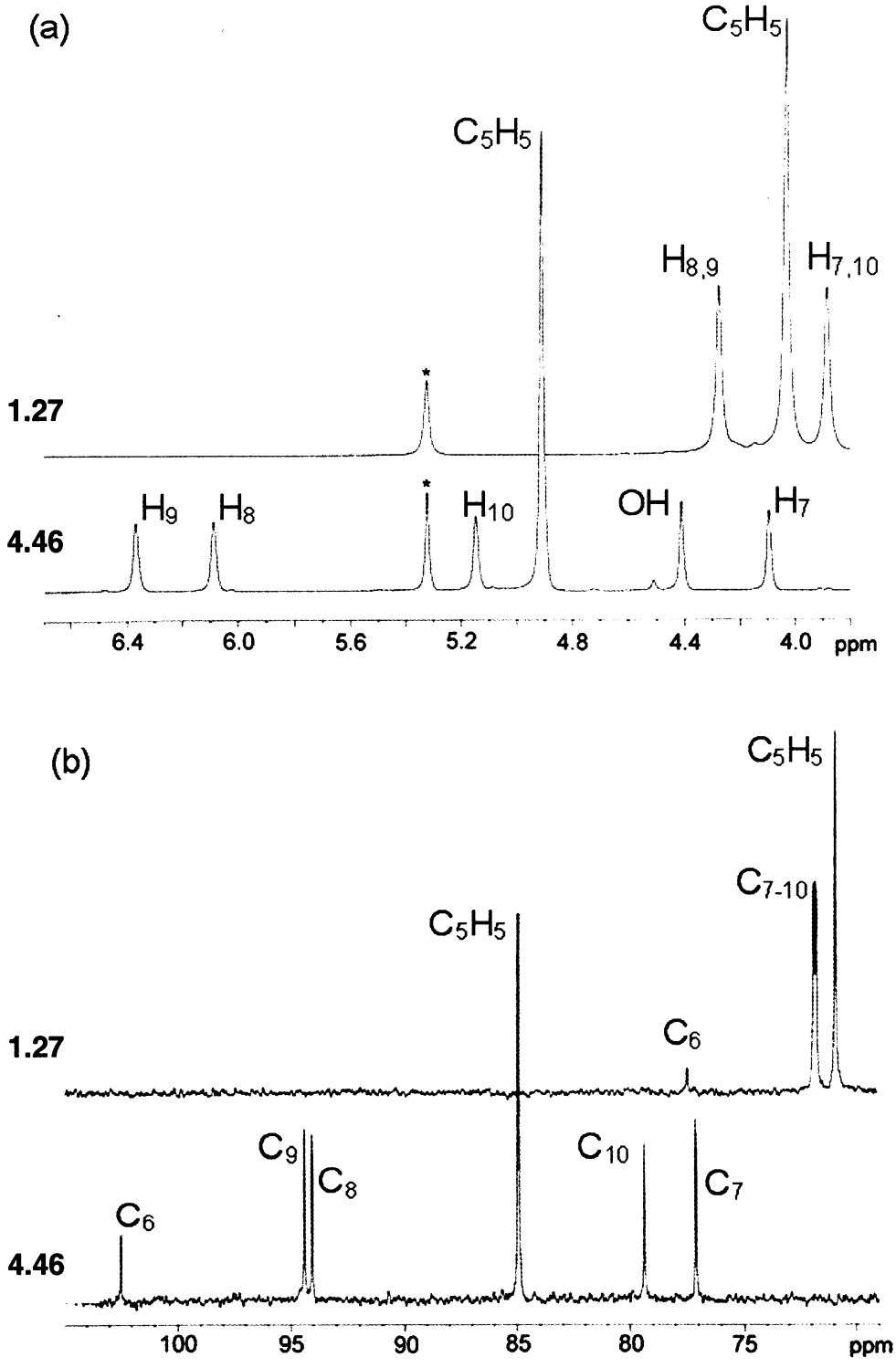

*Figure 4.3: 500 MHz ^1H (a) and 125 MHz ^{13}C (b) NMR spectra of 3-ferrocenyl-2,4,5-triphenylcyclopentadienone, **1.27** and its protonation product, **4.46** (at –20 °C); the dichloromethane solvent resonance is marked with an asterisk.*

followed by the addition of trifluoroacetic acid and acquisition of the NMR spectra at –80 °C. The appearance of a new peak in the ^{1}H NMR spectrum at 4.41 ppm was accompanied by the splitting of the ferrocenyl-C_5H_4 peaks at 3.88 and 4.27 ppm into four peaks (4.09 - 6.37 ppm), revealing their non-equivalence (Figure 4.3a). These findings were mirrored in the ^{13}C NMR spectrum (Figure 4.3b), and were attributable to the restricted rotation of the ferrocenyl group relative to the central ring in the hydroxyfulvene complex **4.46**. Figure 4.4 presents the 2-D ^{1}H-^{1}H COSY NMR spectrum obtained at –20 °C, clearly outlining the assignment of the four ferrocenyl resonances and the new hydroxy proton; the assignments were unambiguously defined based on the results of ^{1}H-^{13}C HSQC and HMBC, as well as the ^{1}H-^{1}H COSY experiments. The signal at the lowest frequency was assigned to proton 7, as it lay in the shielding region of the most hindered phenyl group on the cyclopentadienone ring (protons were numbered according to the

Scheme 4.11

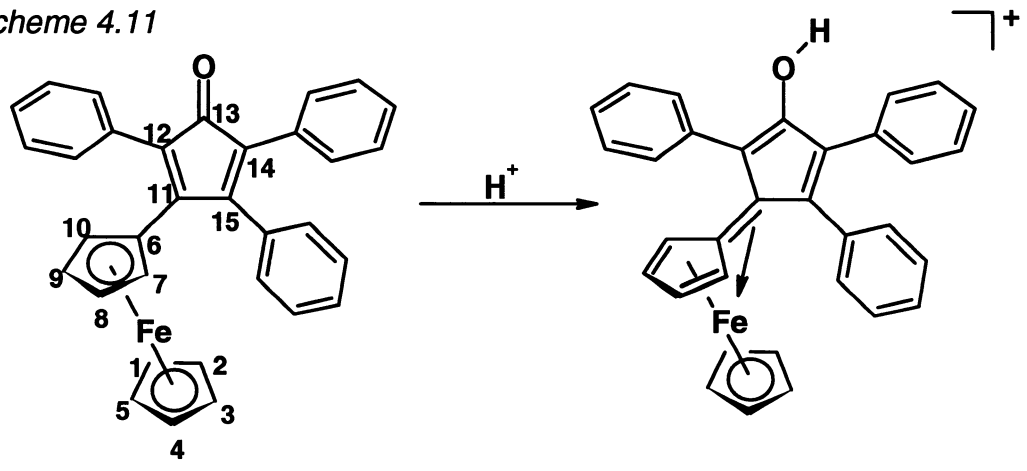

1.27 **4.46**

carbon to which they were attached; Scheme 4.11). Proton 10 was in a similar environment but the corresponding phenyl group was in a less hindered locale, thus it was not restricted to a perpendicular conformation. As a result, this proton resonated at a higher frequency (lower field); the assignment of the remaining protons followed accordingly.

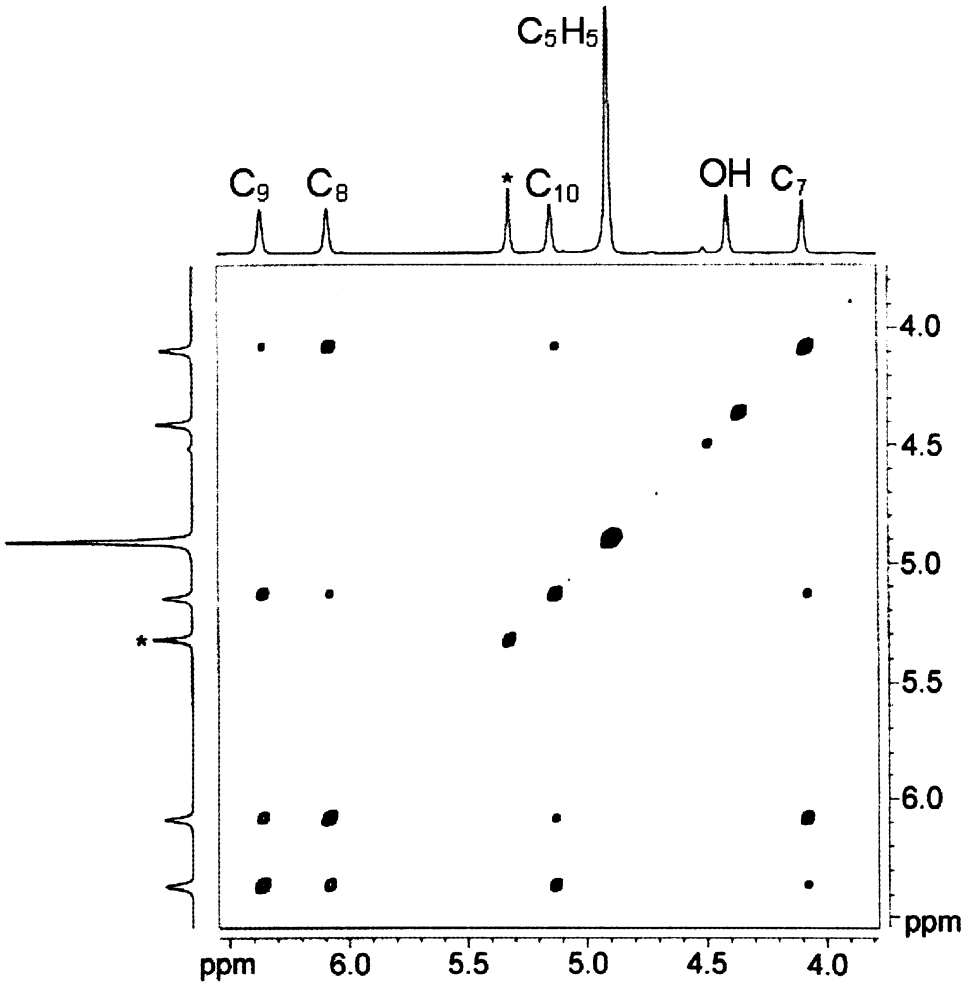

Figure 4.4: ^{1}H-^{1}H COSY NMR spectrum of the protonated molecule, ***4.46****, showing correlations between pairs of protons in the C_5H_4 ring.*

Restricted rotation of the ferrocenyl group was consistent with the formation of the cation (**4.46**), in which the Cp-Fe^+ fragment was coordinated to a fulvalenoid system (Scheme 4.11). The delocalization of the positive charge onto the ferrocenyl ring was clear from the dramatic deshielding of the proton and carbon resonances compared to the shifts observed in the neutral cyclopentadienone and related compounds (Table 4.1).

Table 4.1: NMR Spectral Data[a]

Proton	**1.27**	**1.27**·$Fe(CO)_3$[92]	**1.27**·Rh(acac)[92]	**4.46**
H_7	3.88	3.57	4.03	4.09
H_8	4.27	4.1	4.18	6.08
H_9	4.27	4.1	4.18	6.37
H_{10}	3.88	3.50	3.77	5.14
C_5H_5	4.02	3.92	3.92	4.91
Carbon				
C_6	77.44			102.47
C_7	71.72	69.25	70.42	77.09
C_8	71.83	70.74	70.66	94.05
C_9	71.83	70.74	72.60	94.39
C_{10}	71.72	69.25	71.12	79.36
C_5H_5	70.87	70.34	69.99	84.92

[a]Chemical shifts in ppm.

These findings were in agreement with an early study by Caïs on the proton NMR of a variety of ferrocenyl carbenium ions,[311] in which a "metal participation" model was invoked to explain the experimental data. It was suggested that the metal moved closer to the cationic center than in the neutral

analogue, thus increasing the electron density at protons 7 and 10 relative to protons 8 and 9, resulting in a noticeable deshielding of the latter protons. Substituting the cationic carbon with electron-donating groups minimized the geometric perturbation of the iron, thus diminishing the effect. Moreover, the induced field attributable to the magnetic anisotropy of the iron was described as a major contributor to the shielding of protons 7 and 10, as confirmed by the substitution of alkyl groups with aryl substituents. As the positive charge was delocalized onto the aryl rings, the movement of the iron was reduced and the affected protons experienced less shielding. Complementary work by Dannenberg and co-workers achieved the same result.[288] In agreement with these analyses, there have been several similar studies performed on the ^{13}C NMR spectra of ferrocenyl-stabilized cations.[287,312-317] In each case, the marked deshielding of the cationic carbon and the shielding influence of electron-donating substituents has been explained in terms of the delocalization of the positive charge throughout the ferrocenyl group and the fulvenoid structure of the substituted cyclopentadienyl ring. The trends evident in the spectra of the present study echoed these results and the analogous structural interpretations. Given these data, a complex in which the iron has moved closer to the cationic center may be anticipated, resulting in the formation of the first organometallic hydroxyfulvalene complex.

The removal of the degeneracy of the ferrocenyl-C_5H_4 protons as the cation was generated was also an important feature of the NMR spectra. There

was no evidence for decoalescence of these protons at –80 °C in the neutral species; however, it was apparent that, on the NMR timescale, the ferrocenyl group was not rotating in the cation. If the signals of the ferrocenyl protons of the cation had coalesced at 0 °C, this would have corresponded to a rotational barrier of 13 kcal mol^{-1}; the true barrier was evidently greater than this minimum value. Furthermore, if, for simplicity, the assumption is made that the chemical shift differences in the neutral molecule are the same as those displayed by the protonated species, and if the onset of decoalescence had been observed at –80 °C, the barrier to rotation would have been approximately 9 kcal mol^{-1}; clearly the actual barrier was less than this value.

Finally, the protonation of the carbonyl oxygen and formation of a hydroxyl group have also been confirmed by *in situ* IR spectroscopy, as the C=O peak at 1694 cm^{-1} gradually disappeared under the same reaction conditions described above. All attempts to obtain X-ray quality crystals were thwarted by the slow decomposition of the sample.

4.2.2.2 Computational Modeling

In order to rationalize the observed difference in energy barriers associated with rotation about the ferrocenyl-carbon bond in the neutral and protonated species (**1.27** and **4.46**), computational studies were performed using Density Functional Theory (DFT). Models **4.47** and **4.48** were built by replacing phenyl groups with hydrogen atoms to mimic compounds **1.27** and **4.46**, and

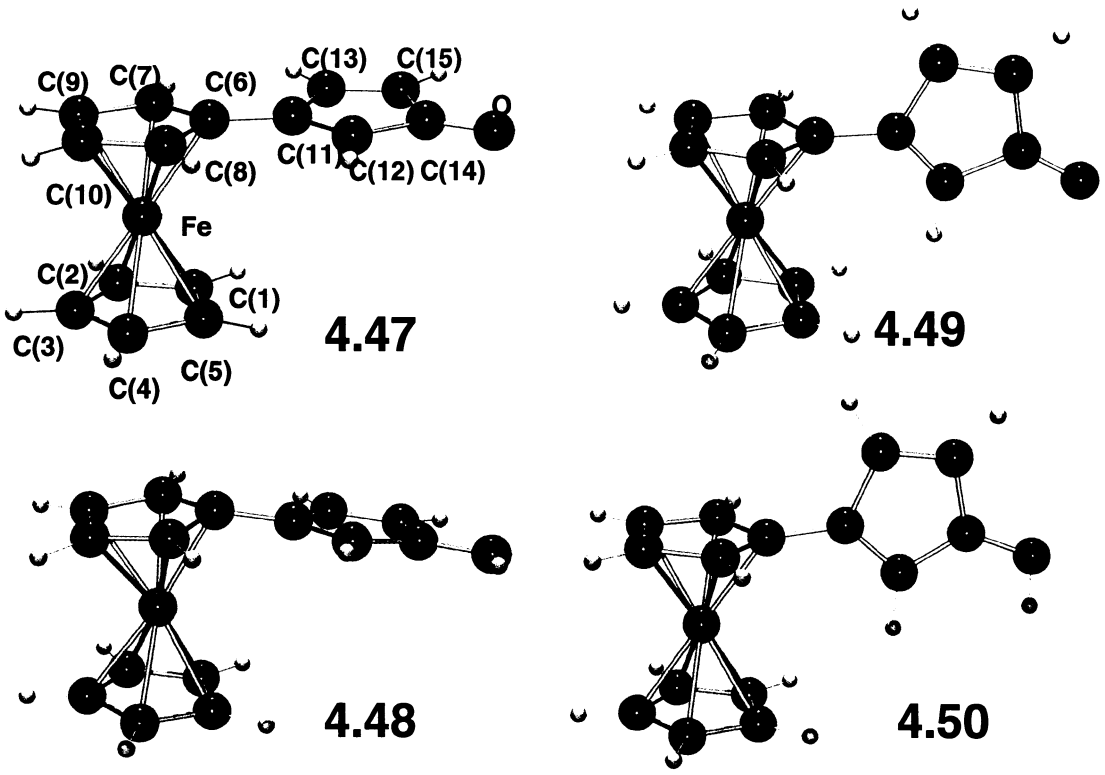

*Figure 4.5: Structural models of compounds **1.27** and **4.46**.*

their ground-state structures were fully optimized without any symmetry constraints (Figure 4.5). Selected structural features of the neutral and protonated models, as well as their rotational transition states (**4.49**, **4.50**), are summarized in Table 4.2. Each of the computed Fe-C, C-C, C-O and C-H bond lengths corresponded to literature values of related compounds, including **4.36**, **4.37a**, **4.51** and **4.52** (Chart 4.6, page 130), within 0.05 Å, and the analogous bond angles were within 0.1°.

The Fe-C distances in the C_5H_4R ring of the ground state neutral molecule 3-ferrocenylcyclopentadienone, **4.47**, ranged from 2.07 Å to 2.10 Å in the ground

Table 4.2: Computed Structural Details[a]

Bond Distance	**4.36**[b]	**4.37a**[c]	**4.47**	**4.48**	**4.49**	**4.50**	**4.51**[d]	**4.52**[e]	Literature[f]
$Fe-C_6$	1.97	2.080	2.10	2.08	2.07	2.06	2.009		2.517, 2.070
$Fe-C_7$	2.05	2.177	2.08	2.08	2.08	2.08	2.060		2.142,2.217
$Fe-C_8$	2.12	2.245	2.09	2.13	2.09	2.12	2.095		2.060, 2.243
$Fe-C_9$	2.14	2.235	2.09	2.13	2.09	2.12	2.085		2.060, 2.213
$Fe-C_{10}$	2.05	2.175	2.07	2.10	2.08	2.08	2.018		2.142, 2.162
C_6-C_7	1.45	1.458	1.45	1.46	1.44	1.45	1.438	1.476	1.477
C_6-C_{10}	1.42	1.459	1.45	1.46	1.44	1.45	1.445	1.476	1.477
C_7-C_8	1.38	1.413	1.43	1.42	1.43	1.43	1.413	1.333	1.414
C_8-C_9	1.46	1.429	1.43	1.43	1.43	1.43	1.425	1.479	1.399
C_9-C_{10}	1.42	1.412	1.43	1.42	1.43	1.43	1.402	1.333	1.414
C_6-C_{11}	1.37	1.405	1.45	1.41	1.47	1.46	1.416	1.339	1.357, 1.446
$C_{11}-C_{12}$			1.37	1.42	1.35	1.38		1.476	
$C_{11}-C_{15}$			1.51	1.50	1.52	1.51		1.476	
$C_{12}-C_{13}$			1.48	1.39	1.50	1.35		1.333	
$C_{13}-C_{14}$			1.52	1.48	1.51	1.46		1.479	
$C_{14}-C_{15}$			1.34	1.48	1.51	1.46		1.333	
$C_{13}-O$			1.23	1.33	1.23	1.32			
Angle	**4.36**[b]	**4.37a**[c]	**4.47**	**4.48**	**4.49**	**4.50**	**4.51**[d]		Literature
α	4.7°	7.1°	1.6°	7.9°	1.2°	0.6°	11.4°		4-5°,[g] 4.2°,[h] 5.7°[h]
β	23.6°	42.6°	0.4°	8.4°	3.0°[j]	5.9°[j]	20.7°		28.9°,[f] 10-20°[g]
γ			5.4°	6.3°	89.7°	83.4°			1.22°-7.57°[i]

[a]All bond lengths in Å; [b]Reference 227; [c]Reference 278; [d]Reference 276; [e]Reference 323; [f]References 281,319; [g]Reference 275; [h]Reference 302; [i]References 276, 319-322; [j]Bent away from Fe, all others are bent towards Fe.

state. Moreover, the cyclopentadienone C-C bond lengths of **4.47** were consistent with the localized structure **4.53** (Chart 4.7), with a C=O bond length of 1.23 Å (literature[92] 1.216(11) Å, 1.226(3) Å). The cyclopentadienone ring was

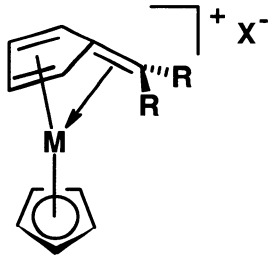

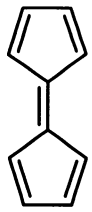

4.36: M = Fe; X = $B\{C_6H_3(CF_3)_2\}_4^-$; R = H

4.37a: M = Ru; X = $B\{C_6H_3(CF_3)_2\}_4^-$; R = H

4.51: M = Fe; X = BF_4^- ; R = Ph

4.52

Chart 4.6: Structural models for comparison of computational data.

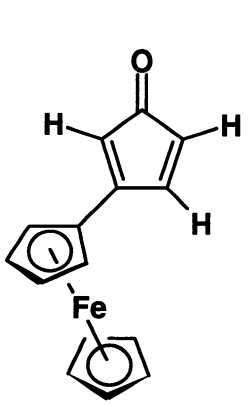

4.53

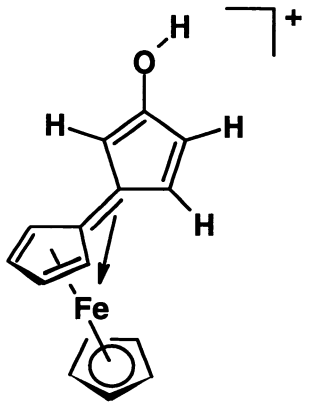

4.54

*Chart 4.7: Localized (**4.53**) and delocalized (**4.54**) bonding structures for the neutral molecule and cation.*

slightly rotated (twisted) out of the plane of the C_5H_4 ring (γ) and bent towards the metal atom (β) (Chart 4.8). The two possible twist orientations were considered as initial points in the optimization, leading to two different minima; the dihedral angle (γ) in the resulting lowest energy structure was 5.4°, which was within the range of values (1.2° to 7.6°) found in related structures in the literature.[318-323] As a consequence of the position of the cyclopentadienone group, the ferrocenyl

cyclopentadienyl rings adopted a staggered orientation to minimize steric interactions.

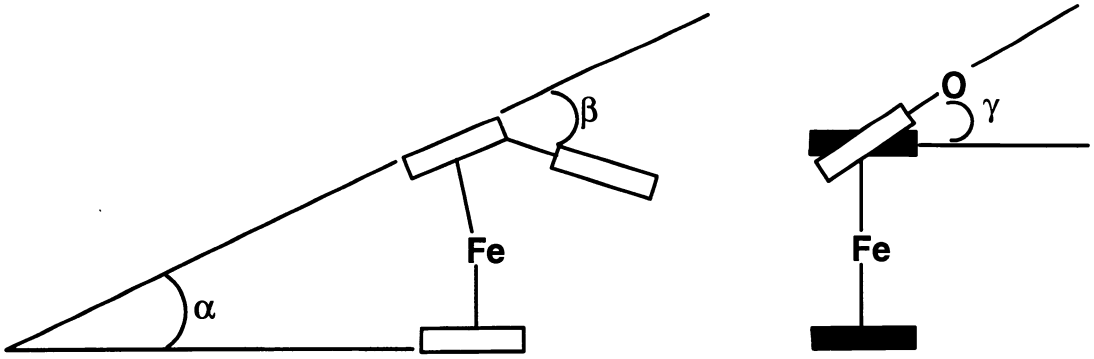

Chart 4.8: Definition of angles for structural analysis.

The protonated molecule (**4.48**) exhibited a slightly greater range of Fe-C distances than the neutral analogue, from 2.08 Å (C_6) to 2.13 Å (C_8, C_9). This elongation of bond lengths suggested a slight shift in the position of the metal from the center of the cyclopentadienyl ring towards the cationic center. Similar behaviour has been seen in the X-ray crystal structures of molecules **4.36**[277] and **4.37a**,[278] as well as the cation **4.51**.[276] This effect was also consistent with the NMR spectroscopic properties of the cation and similar compounds,[287,288,311] in which the change in the position of the metal was manifested in the deshielding of the proton and carbon atoms relative to the chemical shifts in their neutral analogues.

In the protonated molecule, the C-O bond length was increased to 1.33 Å, intermediate between the normal C=O and C-O distances (1.21 Å and 1.42 Å respectively).[324] The C-C bond lengths in these structures suggested greater

delocalization, such as in molecule **4.54** depicted in Chart 4.7. Furthermore, there was a tilt (α) of 7.8° between the cyclopentadienyl rings of the ferrocenyl group. Lukasser[275] has estimated a range of 4 to 5° for the tilt of the cyclopentadienyl rings in other protonated structures as a consequence of the participation of the iron atom in the delocalization of the positive charge. This trend was also apparent in related structures, with angles of 4.7°, 7.1° and 11.4° for cations **4.36**,[277] **4.37a**[278] and **4.51**.[276] As noted by Caïs,[311] the molecule must be sufficiently flexible to allow for favourable orbital overlap and adequate stabilization of the cation.

The cationic species also exhibited the twist (γ) and bend (β) predicted for the neutral molecule. Again, both twist directions were considered and, in this case, the optimizations converged to essentially the same geometry in which the oxygen was pointed towards the metal. A twist angle of 6.3° was found for **4.48**, which was very similar to the neutral analogue, however, an even larger β-value of 8.4° was computed. Lukasser has estimated values between 10° and 20° for the bend in protonated structures,[275] and larger angles of 20.7° (**4.51**),[276] 23.6° (**4.36**)[277] and 42.6° (**4.37a**)[278] have been observed crystallographically. As anticipated, the ring was tilted towards the metal to allow for the necessary electronic stabilization, resulting in a hydroxy-fulvalene ligand.

The initial structures of the transition states were obtained by rotating the external ring relative to the ferrocenyl group and were fully optimized without restrictions. The computed bond lengths in the transition state **4.49** of the neutral

molecule were very similar to the ground state, and no major geometric reorganization occurred upon rotation. One feature of note was the bend angle (β) of the external ring, in this case 3.0° away from the metal as a result of steric interactions with the C_5H_5 ring.

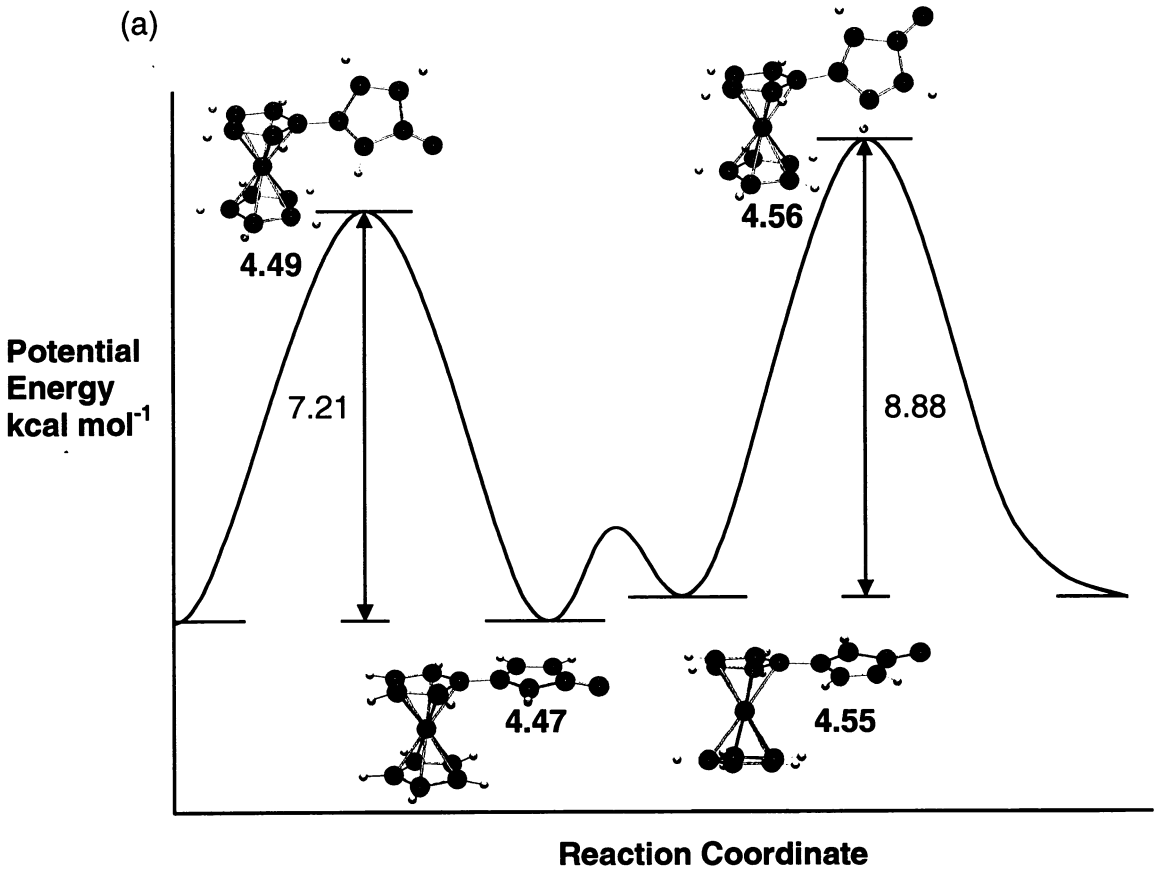

Figure 4.6a: Potential energy diagram for the neutral species.

The transition state (**4.50**) of the cation exhibited the same elongation of the Fe-C bond lengths observed in the ground state, from 2.06 Å (C_6) to 2.12 Å (C_8, C_9), confirming the same minor movement of the metal closer to the cationic center. However, in this case, the C_6-C_{11} bond distance was lengthened, and the

protonated ring experienced a structural reorganization, as evidenced by the changes in bond lengths. The tilt in the ground state of the cation was no longer present in the transition state, the angle between the cyclopentadienyl rings of the ferrocene was only 0.6°. This geometric reorganization resulted in a structure in which the ferrocenyl group did not participate in charge stabilization. The protonated ring was bent away from the metal, in this case by 5.9°, as a result of the steric interaction of the OH and the C_5H_5 ring.

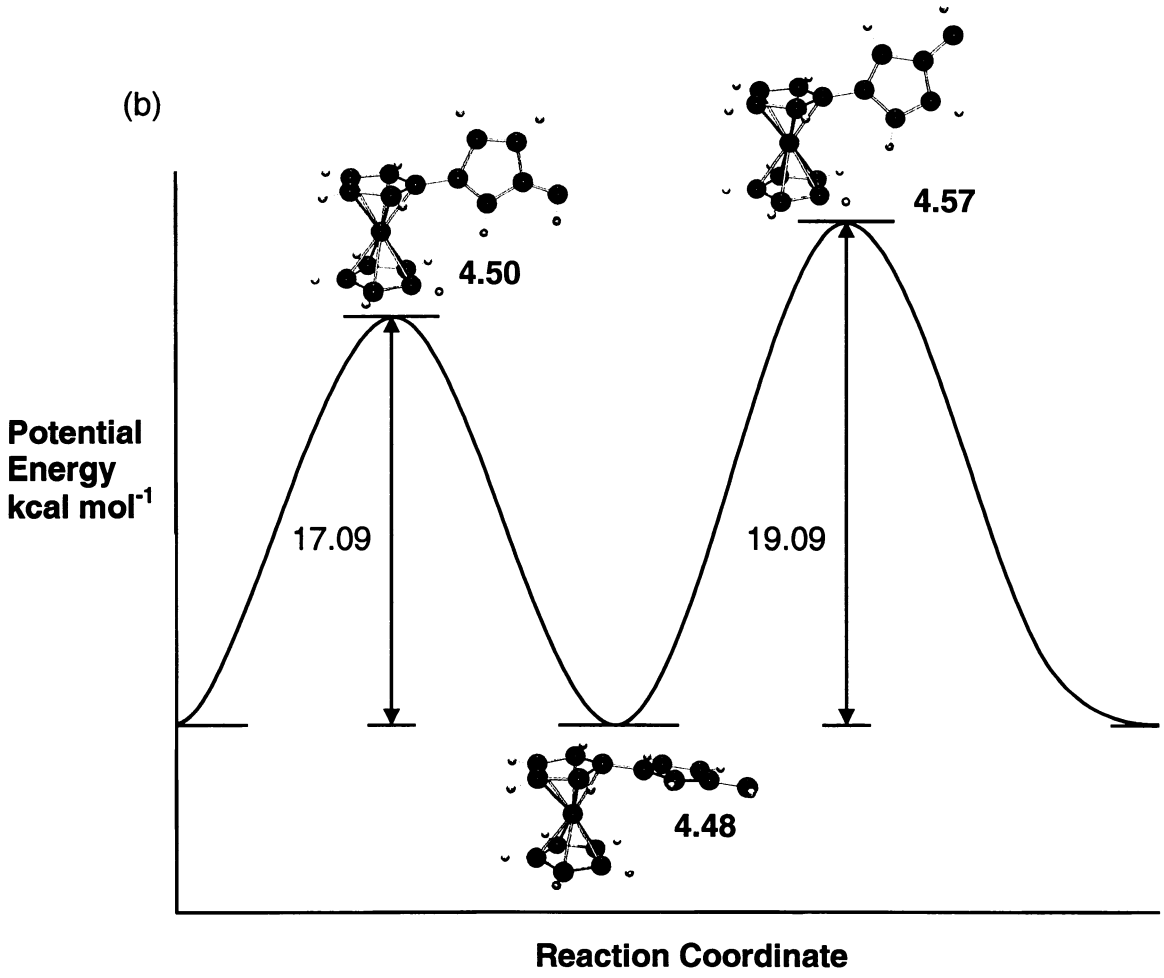

Figure 4.6b: Potential energy diagram for the cationic species.

Figures 4.6(a) and 4.6(b) portray potential energy diagrams outlining the possible rotamers, the transition states (**4.55**, **4.56**, **4.57**), and their relative energies. The minimum barrier to rotation of the ferrocenyl group, relative to the cyclopentadienone ring in the neutral species, was found to be 7.2 kcal mol^{-1}. This is in agreement with the experimental NMR data, which suggested a maximum barrier of 9 kcal mol^{-1}. Moreover, the minimum barrier to rotation in the protonated version was calculated to be 17.1 kcal mol^{-1}, again in correspondence with the NMR spectroscopic behaviour of the cation, which suggested a barrier considerably in excess of 13 kcal mol^{-1}. In examining the structural parameters of the neutral molecule, there was no significant geometrical reorganization or charge relocation upon rotation to the transition state, as would be anticipated since there was no need for charge stabilization within the ferrocenyl group. Conversely in the cation, the ground state charge distribution involved both the fulvalene rings and the remainder of the ferrocenyl group. Upon rotation, the molecule underwent structural reorganization and electron density redistribution as the ferrocenyl group could no longer stabilize the positive charge; the primary adjustment was the migration of the positive charge from C_{11} to C_{13} (Table 4.3). Overall, these changes resulted in a much higher barrier to rotation for the protonated molecule. There are several examples of the observation of restricted rotation in ferrocenyl carbenium ions,[275,283-290] however there was only one experimental estimate of the barrier (20 kcal mol^{-1}).[289]

Table 4.3: Charge Distribution

Atom	**4.47**	**4.48**	**4.49**	**4.50**
Fe	0.0558	0.0559	0.0559	0.0214
C_1-C_5(av)	0.2324	0.2691	0.2239	0.2551
C_6	0.0995	0.0549	0.0473	0.0422
C_7-C_{10}(av)	0.2207	0.2571	0.2180	0.2482
C_{11}	0.1709	0.2095	0.1135	0.1382
C_{12}	0.1003	0.0942	0.1417	0.1206
C_{13}	0.4870	0.4752	0.5003	0.5104
C_{14}	0.0957	0.1439	0.0930	0.1354
C_{15}	0.2077	0.2174	0.2185	0.2353
O	-0.5390	-0.4637	-0.5234	-0.4298

4.3 Conclusions

Treatment of 3-ferrocenyl-2,4,5-triphenylcyclopentadienone **1.27** with trifluoroacetic acid resulted in the formation of the hydroxy-fulvalene cation **4.46**. Proton and carbon NMR spectra of **4.46** displayed restricted rotation of the ferrocenyl group relative to the protonated ring. This observation may be rationalized in terms of the geometric reorganization required to stabilize the positive charge in the transition state. The deshielding of the ferrocenyl proton and carbon NMR chemical shifts in **4.46** (relative to **1.27**), confirmed the participation of the iron in the stabilization of the positive charge. The computed barriers to rotation in the neutral and protonated models were 7.2 kcal mol^{-1} and 17.1 kcal mol^{-1}, respectively.

In contrast, the protonation of tetracyclone resulted in the formation of the extensively rearranged product **4.38**, and the dihydro product **4.45**. In the

absence of a metal fragment, the lack of stabilizing features in tetracyclone forced the antiaromatic cation to immediately rearrange to a large number of complex products.

CHAPTER FIVE

Towards an Organometallic Molecular Brake: Haptotropic Shifts as Controls Over Barriers to Rotation

5.1 Introduction

5.1.1 Haptotropic Shifts

As outlined in the Introduction, the prefix η^n is used to describe the number of attachment points to a metal (hapticity); thus ferrocene is represented by $(\eta^5\text{-}C_5H_5)_2Fe$. The concept of *haptotropic shifts* was introduced in 1978 to describe the situation in which a metal center alters its hapticity to, or migrates across the surface of a ligand that offers multiple coordination sites.[325] The situation arises most often in the case of polyenes, in which there are several unsaturated rings that can coordinate to the metal, and a haptotropic rearrangement describes the migration of the metal unit across the surface of the molecule from one coordination site to another (Scheme 5.1).[326]

Scheme 5.1

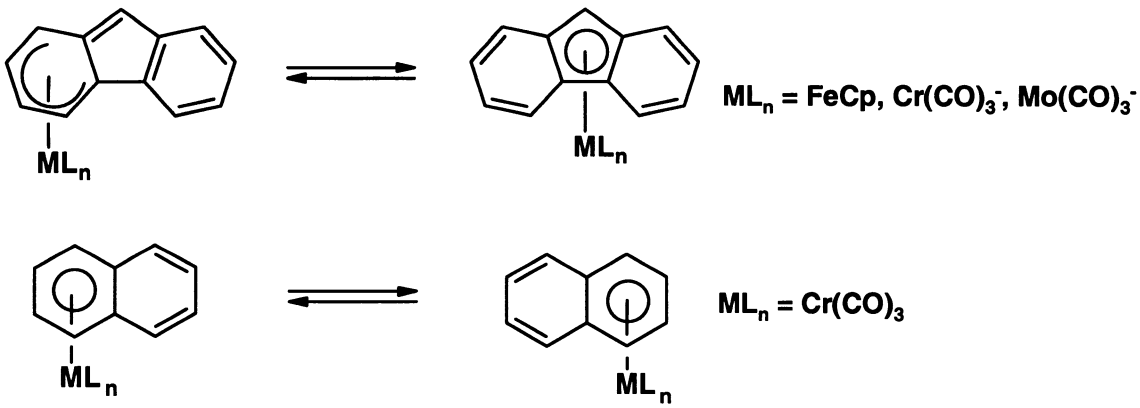

Scheme 5.2

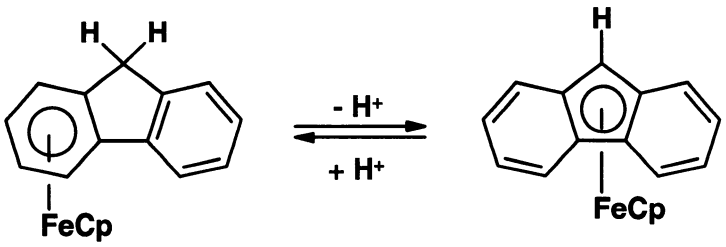

5.1

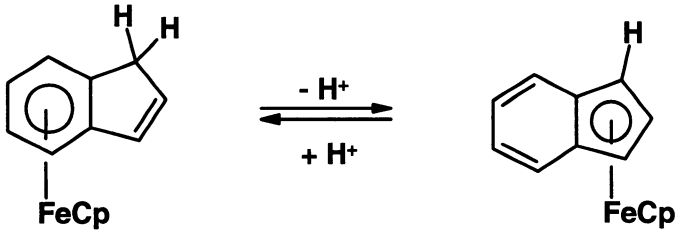

5.2

Examples of such rearrangements were found in fluorenyl- and indenyl-substituted metal complexes (**5.1**, **5.2**; Scheme 5.2).[326] In these instances, the metal migrated from the 6-membered ring to the 5-membered ring across a significant activation energy barrier. Studies have been conducted in order to determine the lowest-energy pathway of these rearrangements relative to a dissociative process in which the metal dissociated from the ligand, then became coordinated at the new site. In some cases, the circuitous path taken by the metal resulted in the loss of bonding interactions with the polyene unit; the dissociative, intermolecular pathway would compete under these circumstances. In other situations, the least-motion path retained some bonding interactions, thus this process was favoured.[326,327] For instance, the movement of the

$(C_5H_5)Fe$ fragment in the indenyl anion (**5.2**) has been calculated to occur via the exocyclic η^3 transition state (path B) rather than the least motion pathway (A) from ring center to ring center, or the dissociative pathway (C) involving an η^1 intermediate (Chart 5.1).[326,328]

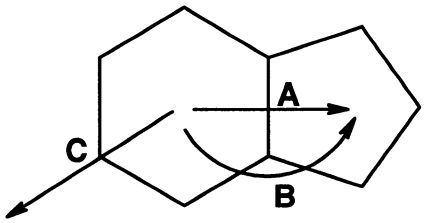

Chart 5.1: Possible pathways for metal migration in indene.

A particularly elegant example of haptotropic shifts was presented in 1993 as a study of the 4*H*-cyclopenta[*def*]phenanthrene ligand, which offered numerous possible sites for coordination.[328] The ligand formed the metal complexes **5.3** and **5.4**, and in both cases deprotonation induced migration from the 6- to the 5-membered ring (Scheme 5.3). This may be contrasted with the analogous manganese complex of the hydrogenated ligand **5.7**, which yielded a neutral complex upon deprotonation and only performed the η^6 to η^5 migration

Scheme 5.3

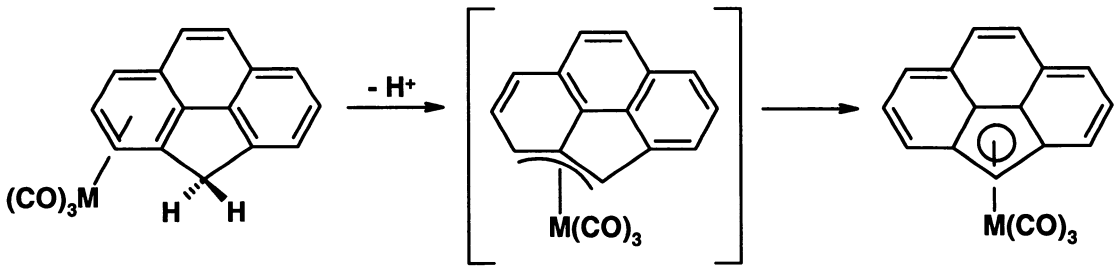

5.3: M = Cr
5.4: M = Mn+

5.5: M = Cr
5.6: M = Mn

upon heating to 60 °C (Scheme 5.4). This result was rationalized by considering an exocyclic transition state for migration in complexes **5.3** and **5.4**, in which the migrating metal fragment was η^3 bonded to the ligand, maintaining the aromatic character of the polyene. This arrangement did not maintain aromaticity in the reduced system (**5.7**) because the central 6-membered ring was not aromatic, and as a result the migration was not as energetically favourable.[328]

Scheme 5.4

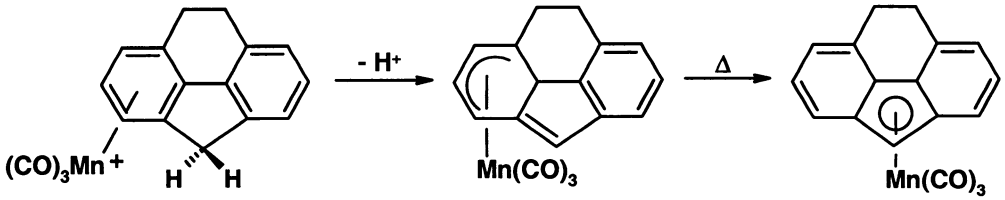

5.7 **5.8**

The potential for the use of this phenomenon as a control over barriers to rotation has been explored by using indenyl substituents as ligands in crowded molecules. The migration of the metal from the 6- to the 5-membered ring following deprotonation of the complex would influence the steric contribution of the metal fragment on the rotation of the remainder of the molecule. This effect can then be reversed by protonation, thereby offering pH control over the barrier to rotation.

5.1.2 Molecular Gears

Molecular gears are of interest as a result of their close resemblance to their macroscopic namesakes. Other microscopic analogues of common

machinery[44,329] include molecular propellers,[43,52,206,330] motors[331-333] and ratchets;[167,168,334] each functions as a result of the controlled interaction of different fragments of the molecule. As described in the Introduction, the development of gearing systems has focused on the triptycene fragment (**1.64**), since it offers three "teeth" and the capability to be functionalized at the 9 and 10 positions.

The use of the triptycenyl fragment has appeared in several reports of molecular gearing,[131-136,138,145,146,149-151,153,198,335,336] and methylene- or oxygen-linked triptycenes (**5.9**) have been found to undergo correlated rotation with barriers of only 1-2 kcal mol^{-1}.[198] In contrast, barriers to gear slippage in 2-chloro substituted derivatives (**5.10**) ranged from 20.4 to 41.0 kcal mol^{-1}, depending on the identity of the linker X.[153,337] Moreover, barriers for (1,4-dimethyl-9-triptycyl)(1-halo-9-triptycyl)ethynes (**1.70**) ranged from 11.6 (F) to 17.3 (I) kcal

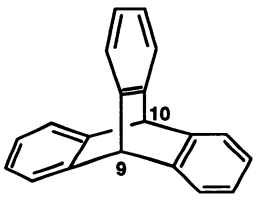

1.64

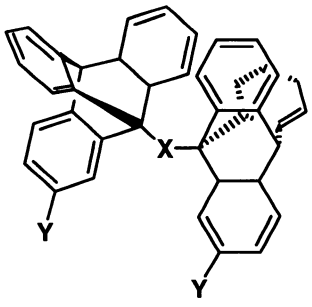

5.9: X = O, CH_2; Y = H
5.10: X = CH_2, NH, O, SiH_2, PH, S; Y = Cl

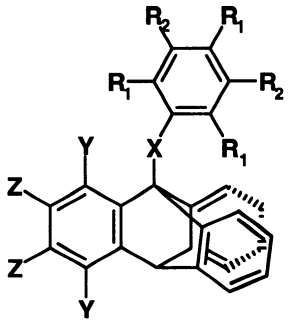

5.11: X = CH_2; R_1, R_2, Y, Z = H
5.12: X = CH_2; R_1 = CH_3; R_2 = H; Y, Z = H, CH_3, OCH_3, Br
5.13: X = O; R_1 = H; R_2 = CH_3; Y = F, Br, CH_3, OCH_3, $C(CH_3)_3$; Z = F, H, Br

Chart 5.2: Substituted triptycene derivatives.

mol^{-1},[154] and substituting the halogen for phenyl or mesityl groups increased this barrier to 15.8 – 18.8 kcal mol^{-1}.[156]

Several benzyl-,[131,135] mesityl-[131,132] and phenoxy-[135,137] substituted triptycene derivatives have also been investigated. Yamamoto and Oki have determined that peri-unsubstituted benzylic triptycenes (**5.11**) preferred isolated rotation (gear slippage, ~10 kcal mol^{-1}) over correlated rotation, whereas the barriers for the two processes were comparable in singly peri-substituted derivatives (>13 kcal mol^{-1}).[131,144] Substitution on the benzylic group and in the peri-position (**5.12**) increased the barrier to gear slippage, resulting exclusively in correlated disrotation (12–17 kcal mol^{-1}),[131] which has also been confirmed in related studies by Mislow et al.[132] In phenoxy derivatives (**5.13**), however, the lowest barrier process was dependent on the size of the peri-substituent; F and OCH_3 exhibited gear rotation (10-12 kcal mol^{-1}), whereas CH_3, Br and $C(CH_3)_3$ preferred isolated aryl rotation (15-17 kcal mol^{-1}).[134,137] In several cases, atropisomers have been isolated and identified for peri-substituted derivatives, with barriers to rotation of ~26 kcal mol^{-1} (Chart 5.2).[136,138,141,143,144]

A different approach to develop this chemistry is the use of migrating metal fragments to control the ability of the triptycene to rotate. It has been well established that the deprotonation of (η^6-indene)ML_n complexes leads to the migration of the metal onto the 5-membered ring;[116] protonation leads to the reverse process. This phenomenon can be applied to triptycene derivatives with the goal of controlling the barrier to rotation. Substituting an indenyl fragment

onto the triptycene framework offers the potential for haptotropic shifts of a coordinated metal unit.

5.2 Results and Discussion

5.2.1 Synthesis

The design of the target molecule involves indenyl substitution at the 9-position of the triptycene since this location offers the greatest interaction with all of the triptycene blades equally. Triptycene is easily produced by the action of benzyne on anthracene (Scheme 1.9), and the 9-position is more accessible in the anthracene precursor, so indenyl substitution onto the anthracene would offer the most facile route to the desired product. In order to join the anthracene and the indene, a carbon-carbon bond must be formed, so an organometallic synthesis can be used. Since 9-bromoanthracene is readily available commercially, the organometallic reagent should be located on the indenyl unit. The most facile means to accomplish this would be to deprotonate indene (which is also commercially available) and add the organometallic reagent.

Scheme 5.5 illustrates the synthetic route to the desired derivatives. Deprotonation of indene, followed by addition of (tributyl)tin chloride afforded complex **5.14**, which underwent a Stille coupling reaction with 9-bromoanthracene to give **5.15** in 42% yield. Treatment with benzyne (generated from isoamyl nitrite and anthranilic acid) then formed the triptycenyl fragment, **5.16** in 29% yield. The final stage involved coordination of the organometallic

moiety, with the ultimate goal being the use of protonation or deprotonation to induce migration (Scheme 5.5). All products were purified by column chromatography, and characterized by mass spectrometry and NMR spectroscopy.

Scheme 5.5

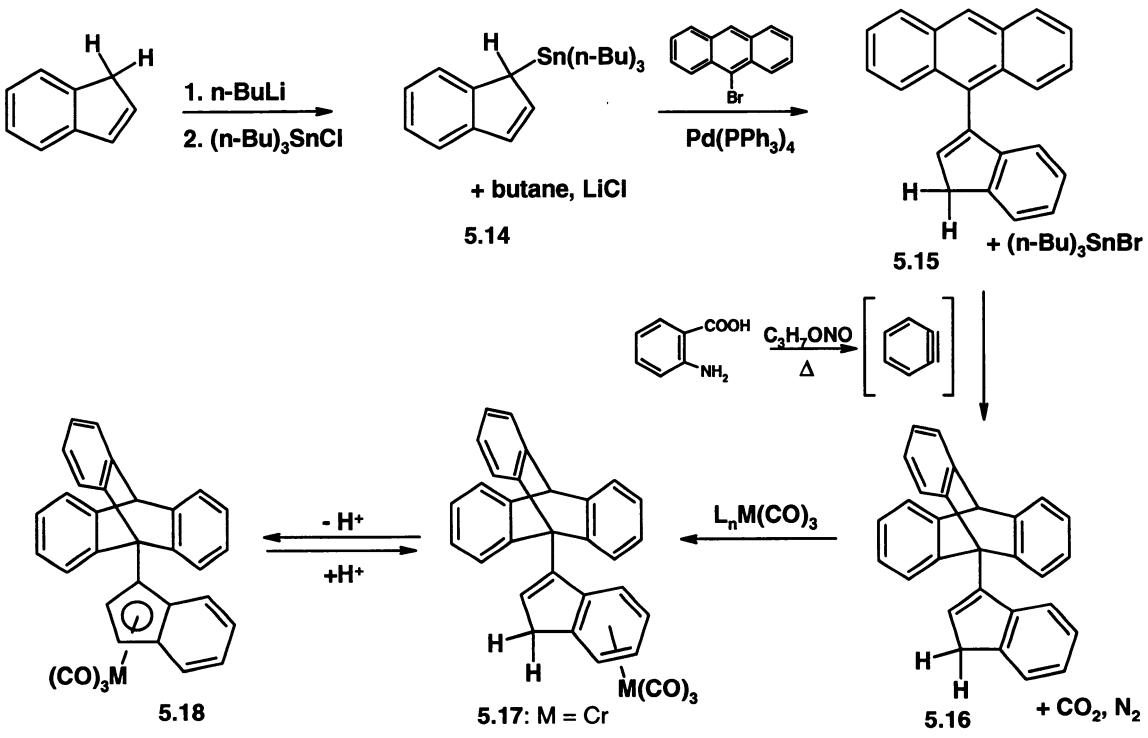

5.2.2 X-Ray Crystallographic Results

The product of the initial Stille coupling (**5.15**) has also been characterized by X-ray crystallography, and its structure is displayed as Figure 5.1. The indenyl-anthracene C(9)-C(11) bond length was 1.492(2) Å, and the indenyl substituent was twisted at an angle of 74.1° from the plane of the anthracene.

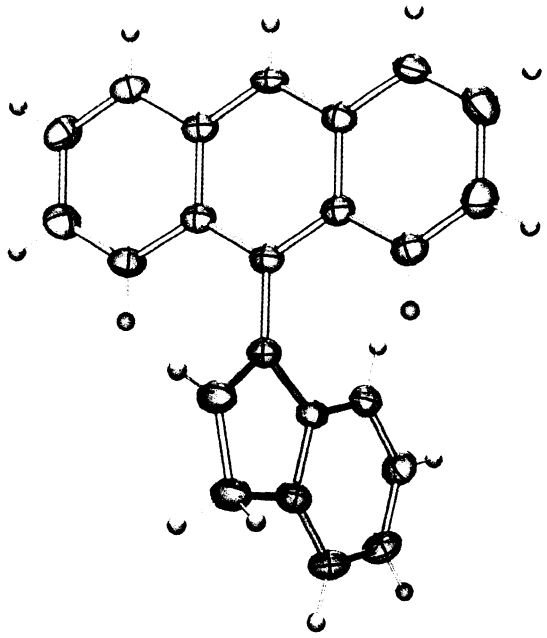

Figure 5.1: X-ray crystal structure of (9-indenyl)anthracene, ***5.15****.*

The treatment of **5.15** with benzyne resulted in the formation of the bulky ligand **5.16**, which was also characterized by NMR spectroscopy and X-ray crystallography (Figure 5.2).

There were several interesting features of the crystal structure, beginning with the slight lengthening of the C-C bond joining the indene and triptycene to 1.520(4) Å (compared to 1.492 Å in **5.15**) as a result of the added steric hindrance of the triptycene unit. The indene was almost perfectly staggered between two benzene fragments of the triptycene (55.5°), and was also slightly bent out of the plane of the central carbons (7.3°). Moreover, the interplanar angles between the blades of the triptycene have been increased to 127° for the

blades bisected by the indenyl group; the other angles were decreased to 114° and 119° from the anticipated 120°.

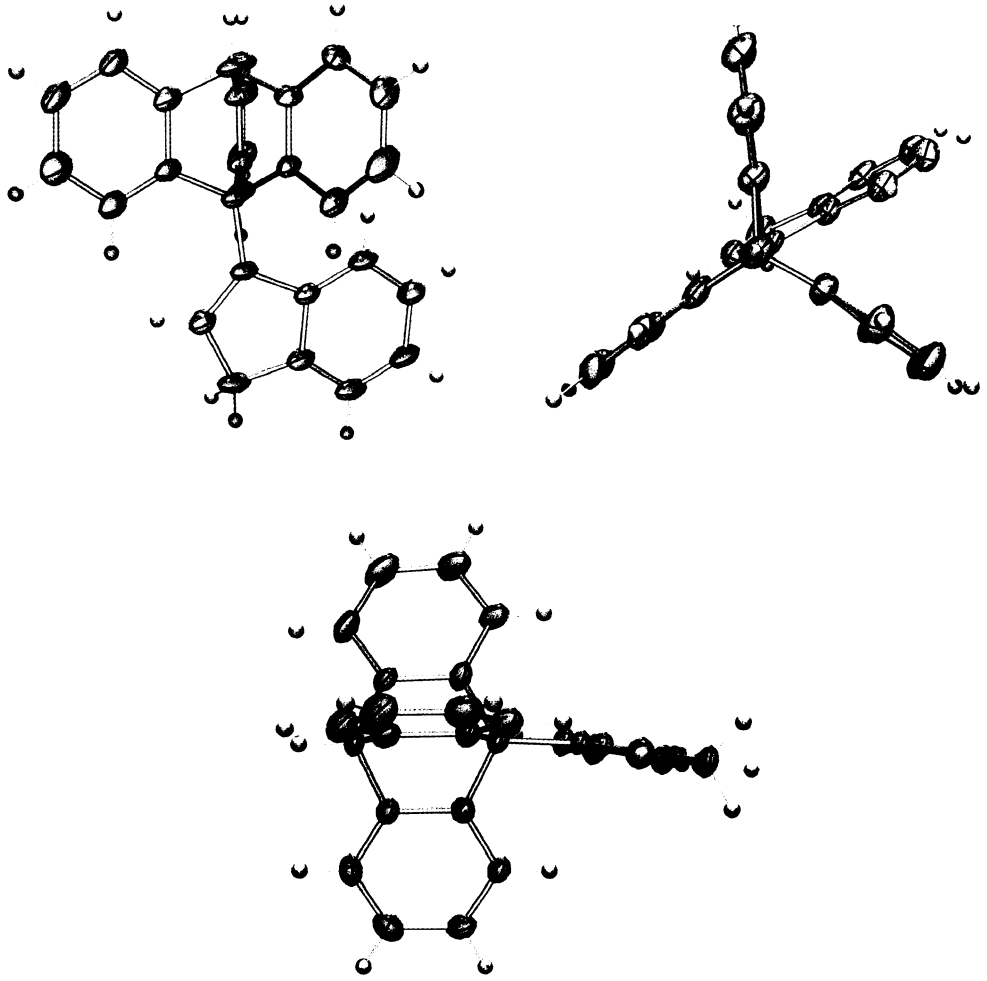

Figure 5.2: X-ray crystal structure of (9-indenyl)triptycene, ***5.16****.*

There are no X-ray crystal structures of directly related derivatives in the literature for comparison, however, the C(9)-CH_2 bond lengths in **5.18** and **1.65** were 1.533(4) Å[144] 1.541(11) Å,[143] respectively, and the analogous C(9)-C(19)

distance in **5.19** was 1.582(4) Å (Chart 5.3).[142] In each case, however, one of the blades of the triptycene was 1,4-dimethyl substituted, thus resulting in a greater interaction with the peripheral group. Nonetheless, there was clearly significant steric interaction between the indenyl substituent in **5.16** and the peri-hydrogens of the triptycene unit.

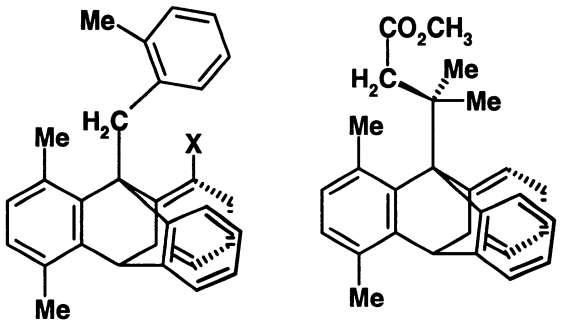

1.65: X = Br
5.18: X = Cl

5.19

*Chart 5.3: Molecules **1.65, 5.18** and **5.19**.*

The reaction of **5.16** with $Cr(CO)_6$ in di-*n*-butyl ether/THF resulted in the formation of complex **5.20** in 42% yield, in which the chromium carbonyl was coordinated to one of the blades of the triptycene unit, instead of the more crowded indenyl substituent (Scheme 5.6). There are a few reports of organometallic derivatives of unsubstituted triptycene in which a metal moiety was coordinated to one or more of the propeller blades,[157-164] however, reports of metal complexes in which there was also a substituent on the 9-position of the triptycene do not exist.

Scheme 5.6

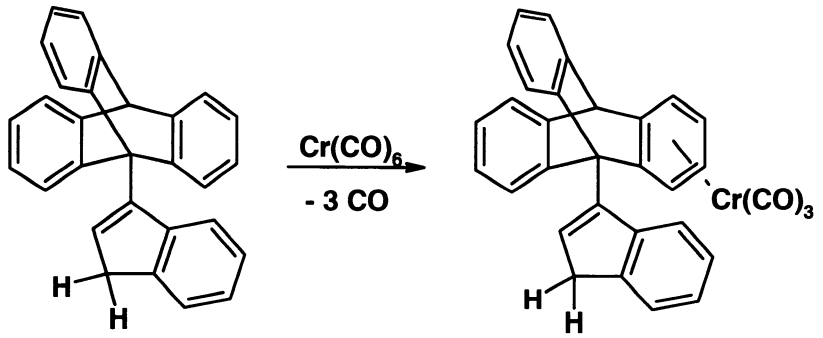

5.16 **5.20**

The crystal structure of **5.20** appears as Figure 5.3. The complex crystallized in space group P-1, and there was one benzene solvent molecule present in the structure. As would be anticipated, the carbonyl groups were almost perfectly staggered relative to the carbon atoms in the ring of the triptycene blade. The C(9)-C(17) bond length of 1.519(5) Å did not change significantly from that in **5.16**, and the bend of the indenyl substituent out of the plane was 8.4(2)°, only slightly larger than in the uncomplexed ligand (7.3°). However, there was a dramatic change in the interplanar angles of the triptycene blades. The angle between the blades bisected by the indenyl group was 126°, as was the angle containing the metal moiety. In order to accommodate the bulky groups between the other blades, the angle between blades containing no substitutents was drastically reduced to 108°. In the structures of the mono-, bis- and tris-chromium carbonyl triptycene complexes (**1.73**, **5.21**, **5.22**, Chart 5.4),[160,164] there were only small deviations from the expected 120° (~2°),

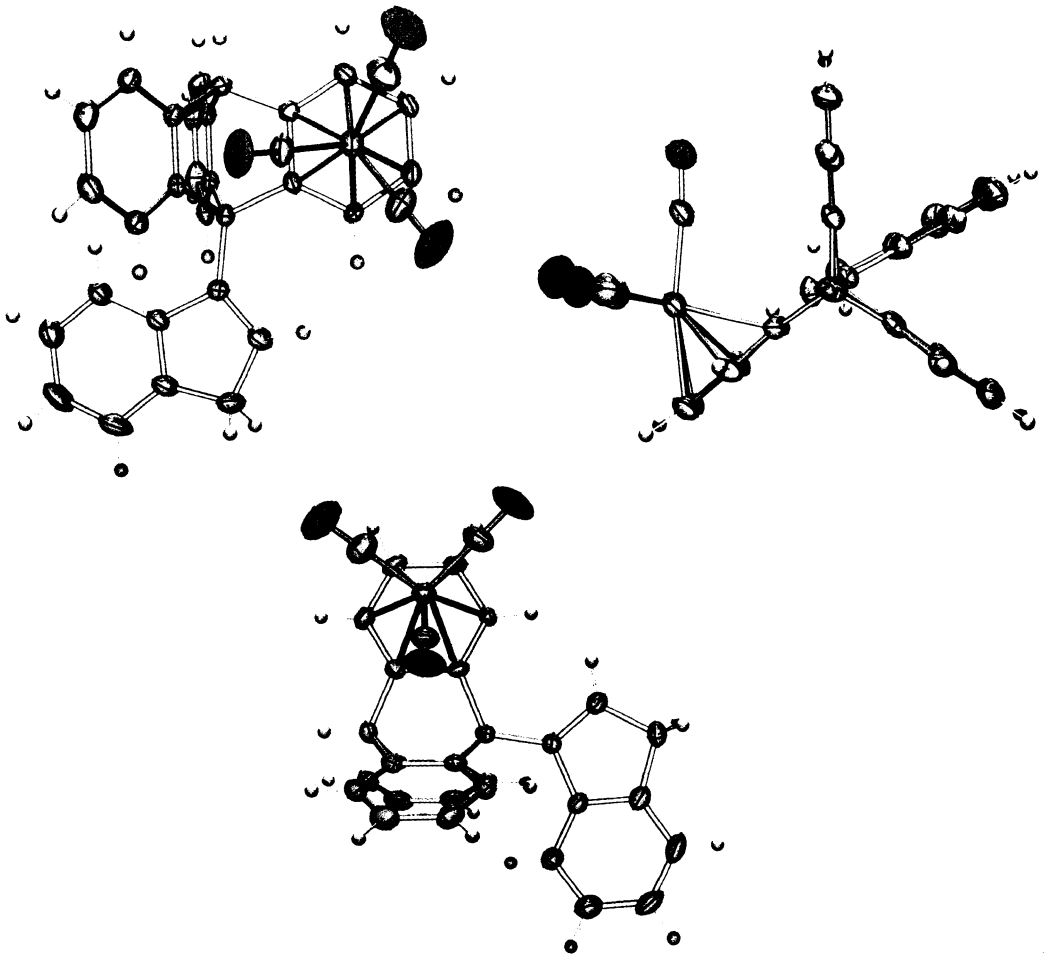

*Figure 5.3: X-ray crystal structure of chromium carbonyl complex **5.20**.*

whereas the bulkier $Co_4(CO)_9$ moiety increased the angle to 124.1° in **5.23**, and decreased the angle of the uncoordinated blades to 117.0 and 118.9°.[160] Both instances displayed less deviation than complex **5.20**, thus the presence of the indenyl substituent clearly had a significant impact on the arrangement of the ligands in order to minimize repulsion.

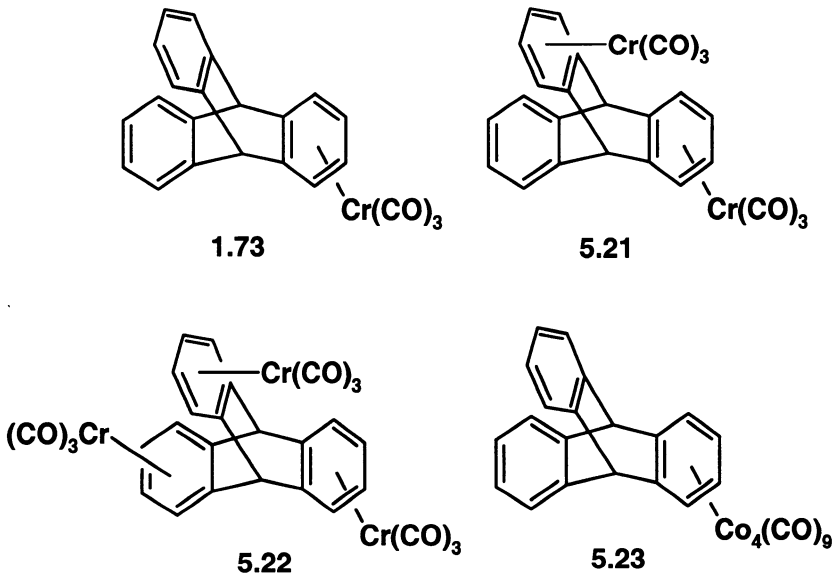

Chart 5.4: Metal complexes of triptycene.

It was clear that the incorporation of the metal fragment between two blades created less steric crowding than coordination to the 6-membered ring of the indene, which would have induced interactions between the carbonyl groups and the rotating blades of the triptycene. The ability of the molecule to increase the distance between the blades would also assist in the formation of the observed complex. As a first attempt at creating such a crowded molecule, this approach confirmed the extreme steric interactions that would result from coordination of the metal to the indenyl unit. In order to accomplish the initial goal, the steric crowding of the indene in future systems must be comparable to, or less than, that resulting from metal coordination to the triptycene blades.

5.2.3 NMR Spectroscopic Results

The room temperature ^{1}H NMR spectrum of **5.16** exhibited significant broadening, thus variable-temperature NMR spectroscopic experiments were performed in an attempt to adequately characterize the complex. It was clear from the resulting spectra that the presence of the indenyl substituent alone was enough to cause restricted rotation of the triptycene fragment. As the sample was cooled, the peaks began to sharpen and decoalesce (Figure 5.4), and at 233 K, the triptycene stopped rotating on the NMR time-scale such that the indene was located between two of the benzene units, as depicted in the solid state structure. This was evident since the peaks for the protons in the blades of the

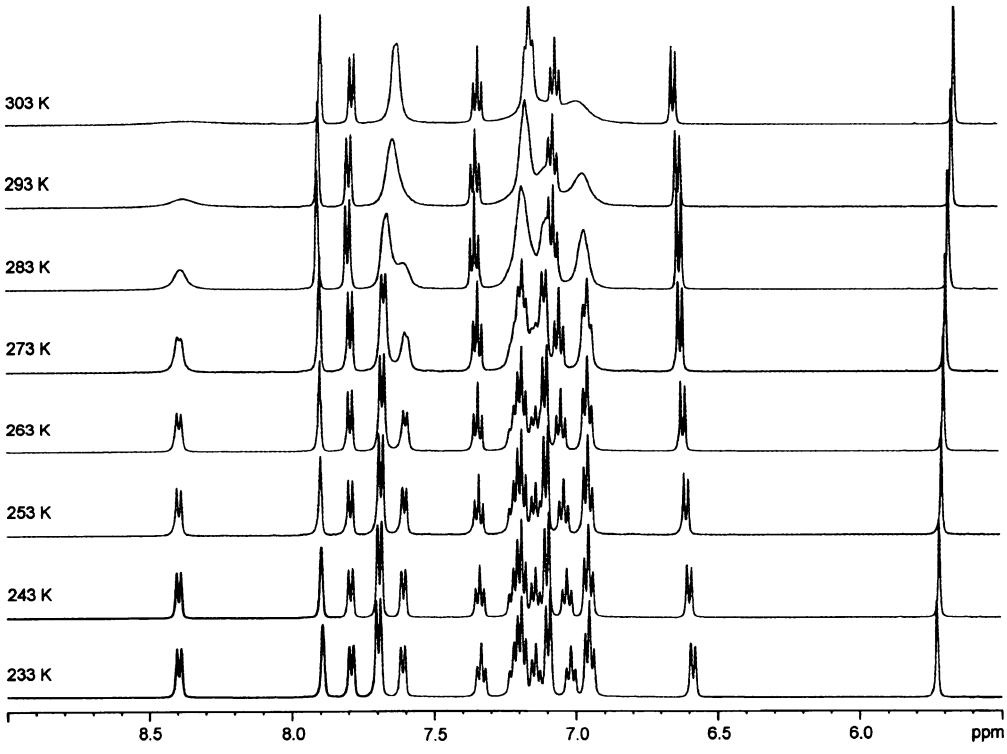

*Figure 5.4: Variable-temperature ^{1}H NMR of **5.16**.*

triptycene exhibited a 2:1 pattern (by integration), suggesting that two blades were equivalent and that one blade was in a unique environment.

The doublets at 7.6 (1H) and 7.7 ppm (2H) have been assigned using standard two-dimensional NMR techniques to the protons of the blade closest to the indene fragment; protons 1, 8 and 13, as defined by the numbering in the crystal structure and the standard labelling of triptycene molecules in the literature. At low temperature, protons 1 and 8 were equivalent since they were located on either side of the indenyl unit, and proton 13 was unique. The peaks assigned to these protons broadened and moved closer together as the temperature was raised, finally coalescing into one broad peak at 293 K when the triptycene was rotating and all 3 protons were equivalent. This fluxional behaviour yielded a barrier to rotation of approximately 12 kcal mol^{-1}, which lies within the range of singly *peri*-substituted benzylic derivatives (~12-17 kcal mol^{-1}) but is less than those for derivatives highly substituted in the *peri*-position of the triptycene and on the benzylic group (~26 kcal mol^{-1}). Moreover, this appears to be the largest barrier observed in a system that is *not* substituted on the blades of the triptycene unit.

Variable-temperature NMR spectra were also acquired for the chromium derivative **5.20**. In this case, the extremely complicated low-temperature ^1H spectra (collected in CD_2Cl_2) revealed the presence of two rotamers in a 2:1 ratio (Figure 5.5), determined by peak integration and assigned by standard two-dimensional NMR techniques. For instance, it was clear that the well-resolved

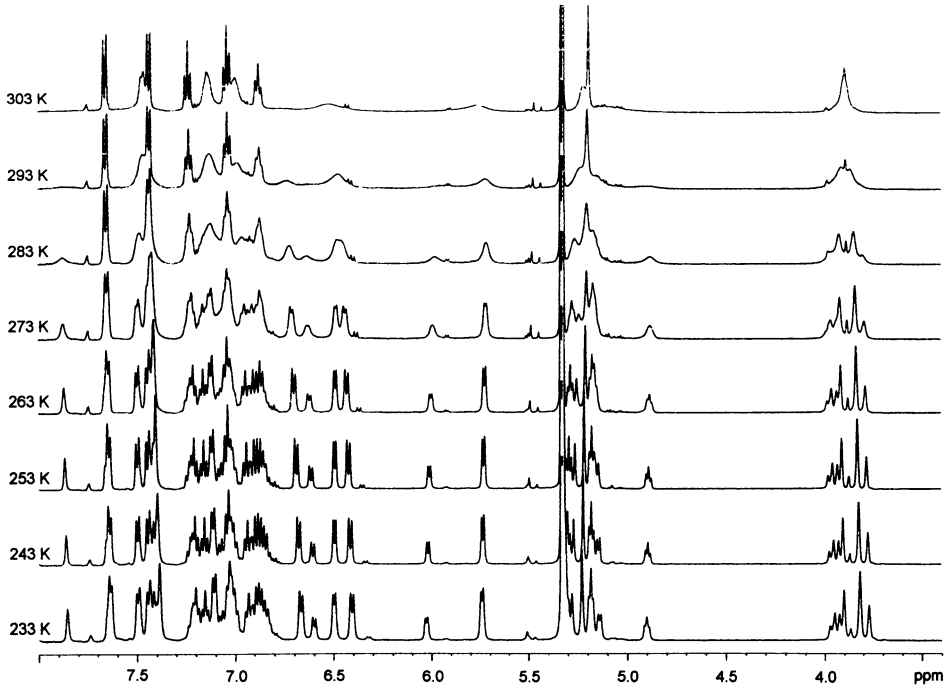

*Figure 5.5: Variable-temperature ^{1}H NMR of chromium complex **5.20**.*

doublets at 5.74 ppm (2H) and at 6.02 ppm (1H) were coalescing at 303 K. These protons have been assigned to equivalent positions on the triptycene blade coordinated to the metal, and resulted in a barrier to rotation of ~13 kcal mol^{-1} to be determined, which was very similar to the uncomplexed molecule **5.16** (~12 kcal mol^{-1}). An examination of the crystal structure revealed that there were two possible orientations for the molecule in the low-temperature limit of restricted rotation. The indenyl unit may be found between the two uncomplexed blades, as in the solid state, or it may be located between an uncomplexed blade and the $Cr(CO)_3$-coordinated triptycene blade (Chart 5.5). It is reasonable to assume that the lowest energy rotamer was that found in the solid state, thus this

isomer would be present in higher proportion than the other rotamer at low temperature, resulting in the 2:1 pattern observed in the ^{1}H NMR spectrum.

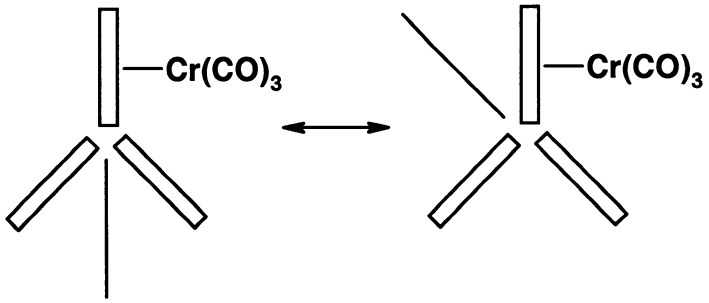

*Chart 5.5: Rotamers of **5.20**, illustrating the two possible positions of the indenyl group.*

The spectra were also complicated in the region of the indenyl CH_2 protons. The non-equivalence of each proton at low temperature as the indene rotation slowed (resulting in 2 equivalent doublets which coupled strongly with each other), as well as the presence of two rotamers in an approximately 2:1 ratio (doubling the number of expected peaks), resulted in a complex multiplet. Moreover, the singlet assigned to H_{10} at ~5.2 ppm split into two singlets as the temperature was reduced. Also contained in this crowded multiplet were the peaks for the other protons on the triptycene blade that was complexed to the chromium moiety, which subsequently became more resolved at lower temperatures. The ^{13}C spectra confirmed the observation of two rotamers by displaying two peaks for the indenyl CH_2 carbon, as well as two environments for the carbonyl carbons at low temperature.

Warming the sample to room temperature resulted in extreme broadening of the peaks, thus the spectra were also collected at high temperatures in DMSO.

Again using two-dimensional techniques to assign the peaks, the spectra at 70 °C revealed the presence of only one isomer (Figure 5.6), and the ^{13}C spectra concurred.

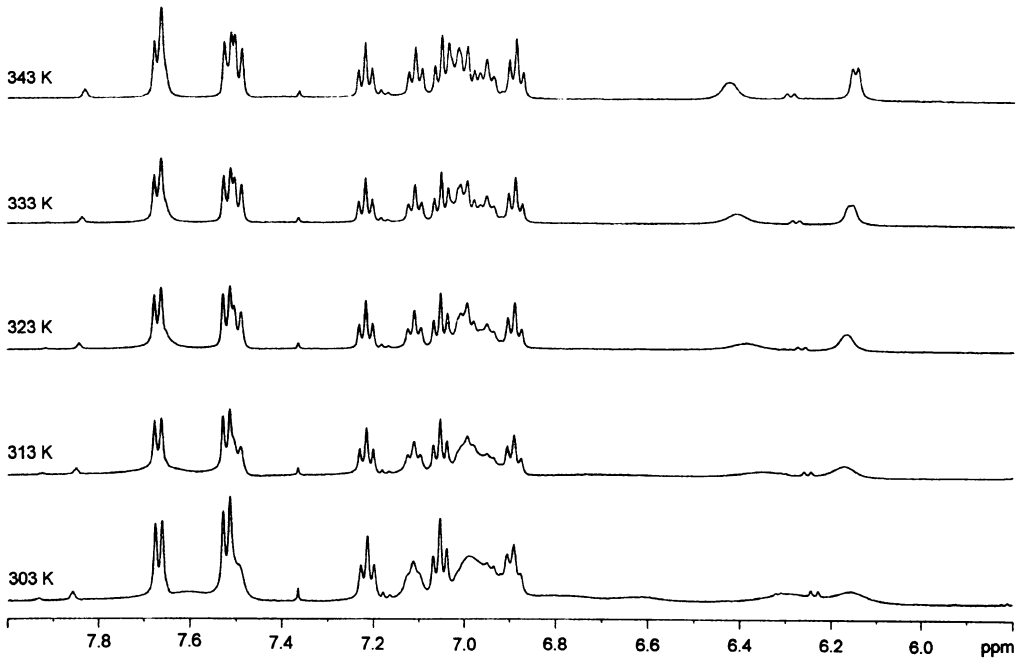

*Figure 5.6: High-temperature ^1H NMR of **5.20** in the region of the aromatic protons; there is only one isomer at elevated temperatures.*

5.2.4 Attempted Formation of Manganese Derivatives

The prospect of coordinating a metal species to the 5-membered ring of the indene was even more complicated by the increased steric hindrance at that locale relative to the 6-membered ring. Nonetheless, a metal moiety may bond to an anionic 5-membered ring to attain an 18-electron count. In this case,

complex **5.16** would be deprotonated first, followed by the addition of the metal derivative to yield **5.24** (Scheme 5.7). Protonation of the molecule would then induce migration of the metal to the indenyl 6-membered ring, which would be extremely favourable because steric hindrance would be alleviated.

Deprotonation of **5.16**, followed by the addition of $Mn(CO)_5Br$ was expected to coordinate $Mn(CO)_3$ to the 5-membered ring of the indene. Instead, a mixture of products was obtained, including the metal dimers $Mn_2(CO)_{10}$ and $Mn_2(CO)_8Br_2$. These results were consistent with electron transfer from the anion to the metal, resulting in dimerization reactions of both the metal fragments and the organic moiety (Scheme 5.7).

Scheme 5.7

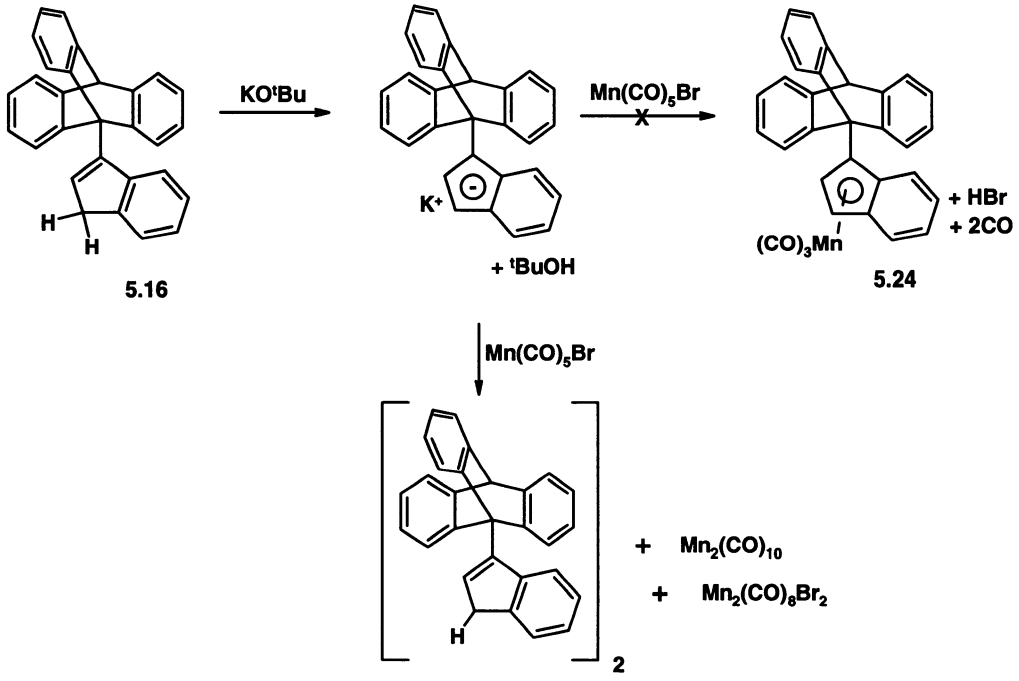

There are many other examples of electron transfer reactions involving manganese in the literature.[338-343] In particular, manganese tris(hexafluoroacetyl-acetonate), **5.25**, has been used to oxidize a number of hydrocarbons. In many cases, electron transfer from the ligand to the metal and the formation of dissociated ligand radicals was the initial step in the process.[343] For instance, the manganese complex **5.25** oxidized 2,4-di-*t*-butyl phenol (**5.26**) to the bis(phenol) (**5.27**) quantitatively in just minutes (Chart 5.7). Hydrogen atoms were abstracted from the phenol molecules by the manganese complex, which led to rearrangement and dimerization. Therefore, it was not unreasonable that similar behaviour in the indenyl-triptycene system was observed, especially if the indenyl group was too crowded to accommodate a metal moiety. A stronger base may also be used in this reaction in order to ensure that the indenyl triptycene is completely deprotonated before addition of the metal unit.

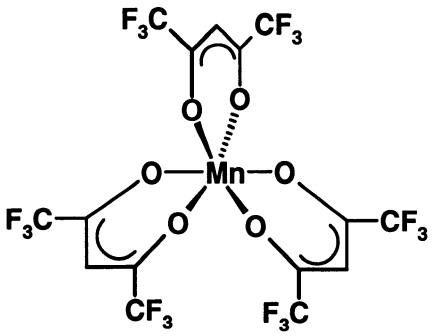

5.25

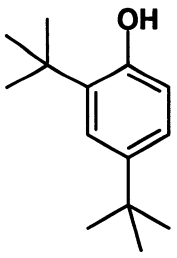

5.26

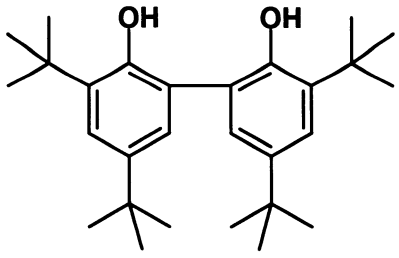

5.27

*Chart 5.7: Manganese tris(hexafluoroacetylacetonate), **5.25** and molecules **5.26** and **5.27**.*

5.3 Conclusions

The addition of an indenyl substituent to a triptycene unit dramatically increased the barrier to rotation of the blades; coordination of a chromium carbonyl moiety resulted in addition to one of the blades rather than the more crowded indenyl group. The organic and organometallic complexes have been characterized by X-ray crystallography and variable-temperature NMR spectroscopy, revealing the presence of two rotamers at low temperature in the case of the metal derivative, and yielding barriers to rotation of 14 and 15 kcal mol^{-1} for the uncomplexed and chromium carbonyl derivatives, respectively. Attempted coordination of a metal fragment to the indenyl 5-membered ring yielded instead products consistent with radical couplings of the starting materials. Overall, the indenyl group experienced substantial steric crowding, which prevented the coordination of a metal unit. Future derivatives must place the indene in a comparable steric environment to that of the triptycene blades.

CHAPTER SIX

The Unexpected Reactivity of Fluorenyl Radicals

6.1 Introduction

6.1.1 A Potential Molecular Machine

The advancement made towards observing correlated rotation by using naphthyl groups as peripheral substituents (Chapters 2 and 3), as well as the potential for control offered by haptotropic shifts (Chapter 5) prompted consideration of the bulky fluorenyl ligand (**6.1**) as an attractive target for incorporation into a sterically crowded benzene. Coordination of the ligand via the 5-membered ring (C9) would allow for the extension of the blade both above and below the plane of the central ring, thus preventing the formation of any proximal/distal rotamers to alleviate steric repulsion. Furthermore, coordination of a metal fragment to one of the 6-membered rings, followed by deprotonation and migration to the 5-membered ring would greatly increase the steric contribution of the ligand, as well as offering pH control over the process. The development of such a system is unprecedented, and offers a wealth of potential towards achieving the ultimate goal of designing a controllable molecular machine. As the first step on the road to this objective, the pentaphenylfluorenyl benzene ligand was proposed.[344,345]

6.1.2 Fluorenyl-Substituted Benzene Derivatives

There are numerous examples of phenyl-substituted fluorenes, and several crowded derivatives have been investigated as systems that exhibit restricted rotation about single bonds.[346-349] Siddall and Stewart reported studies on naphthyl- and phenyl-substituted compounds **6.2** – **6.7**, and determined a barrier to rotation of 29.8 kcal mol^{-1} for **6.7**.[350] The ground state geometry of these molecules possessed the perpendicular arrangement of the aryl group relative to the planar framework of the fluorene, and restricted rotation was observed for complexes **6.2** – **6.4**. In contrast, the *meta*-and *para*- substituted derivatives did not exhibit slowed rotation. In a related study, Bartle and co-workers reported a barrier to rotation in 1-naphthylfluorene **6.8** of ~ 18 kcal mol^{-1}.[351] Clearly, the presence of the *ortho*-substituent had a dramatic influence on the steric hindrance in the complex (Chart 6.1).

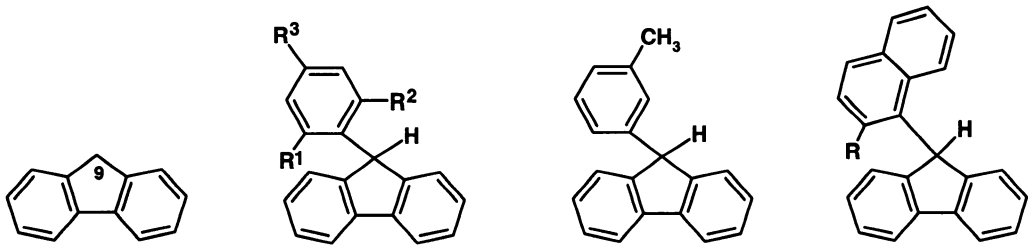

6.1

6.2: $R^1 = CH_3$; R^2, R^3 = H
6.3: R^1, $R^2 = CH_3$; R^3 = H
6.4: R^1, R^2, $R^3 = CH_3$
6.5: $R^3 = CH_3$; R^1, R^2 = H

6.6

6.7: R = CH_3
6.8: R = H

*Chart 6.1: Fluorene (**6.1**) and fluorenyl-substituted benzenes and naphthalenes.*

An interesting investigation regarding the influence of steric factors on the bond angles and ^{13}C NMR characteristics in a series of 9-*o*-alkylphenylfluorenes (**6.2**, **6.9**, **6.10**) has also been conducted.[352] In this study, Oki et al. examined the role of the geometry about a tetrahedral carbon atom in determining its ^{13}C chemical shift. At reduced temperatures, these bulky derivatives exhibited two ^{13}C signals for the fluorenyl sp^3 carbon, one for each rotamer, and bulkier alkyl groups resulted in greater chemical shift differences between the peaks. Moreover, the $^1J_{CH}$ coupling constant for the 9-carbon in rotamer (b) (in which the methyl group is above the plane of the fluorene, Scheme 6.1) decreased with increasing alkyl group size. The coupling constant is directly related to the *s*-character of the C-H bonding orbital, thus a decrease represents greater *p* character. This behaviour was attributed to the bending of the C(9)-C_{ar} bond away from the fluorene ring to relieve the steric strain caused by the interaction between the fluorenyl unit and the alkyl group.[352] In the *t*-butyl substituted derivative (**6.10**), only one isomer was observed in the NMR spectra as the *t*-butyl group did not protrude into the space occupied by the fluorene, preferring the less sterically hindered position (rotamer (a)). Similarly, 9-(*o*-isopropylphenyl)fluorene (**6.9**) existed as two isomers in solution, but evaporation of the solvent formed one isomer exclusively, as determined by X-ray crystallography (Scheme 6.1).[353]

A complementary approach used to describe the steric strain in these complexes has been the rate of reactivity, specifically substitution at C(9). The

Scheme 6.1

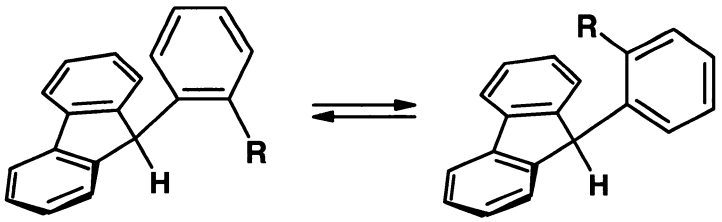

(a) **(b)**

6.2: R = CH_3
6.9: R = $CH(CH_3)_2$
6.10: R = $C(CH_3)_3$

rate of lithiation in 9-aryl fluorenes was found to be directly related to the size of the aryl substituent(s). In *ortho*- or *meta*-methylated derivatives (**6.2**, **6.6**), the rate of reaction was relatively fast, as the aryl group could rotate so that the alkyl group was located above the plane of the fluorene, thus allowing access to the hydrogen at C(9) (rotamer (b)). However, disubstituted (**6.3**, **6.4**) or *t*-butyl substituted (**6.10**) derivatives had very slow reaction rates since there was always an alkyl group blocking attack at C(9) (rotamer (a)). The *t*-butyl group did not rotate above the fluorene ring because of the resulting steric interactions. Furthermore, this study was correlated with the ^{13}C spectroscopic results described above, as the reaction rates of mono-substituted derivatives were also influenced by the bending of the aryl group away from the fluorene to reduce steric repulsion; this would also impede access to C(9).[354]

In some cases, however, the presence of peripheral substituents can decrease the barrier to rotation by increasing the congestion and energy of the

ground state. Of course, the steric interactions in the transition state are also increased, and if this change is more pronounced than in the ground state, a positive buttressing effect results, and the barrier to rotation is increased, as depicted in the examples above and others.[355] However, in some cases, there is a lowering of the barrier to rotation as a result of "negative buttressing effects", as observed in **6.11** and some triptycene derivatives.[355] The barrier to rotation was greater in **6.11** than in **6.12**. The indirect influence of the *meta*-methyl groups on the steric crowding of the *ortho*-methyl substituents increased the energy of the ground state to a greater degree than the transition state (for molecule **6.12**), thus the barrier to rotation was reduced relative to **6.11** (Chart 6.2).

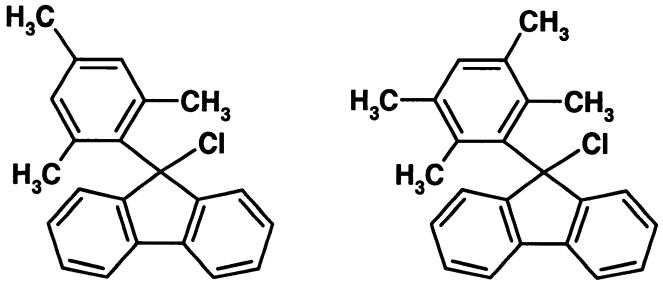

6.11 **6.12**

*Chart 6.2: Molecules **6.11** and **6.12** serve as examples of buttressing effects on barriers to rotation.*

Through these investigations of restricted aryl rotation and the resulting affects on the properties and reactivities of 9-aryl fluorenes, the steric encumbrance of this ligand has been clearly established. There have been no reports of perarylated derivatives or the correlated rotation of substituents, thus

the potential of pentaphenylfluorenyl benzene as a ligand remains to be explored.

6.2 Results and Discussion

6.2.1 Synthetic Strategy

The proposed synthetic approach towards the preparation of pentaphenylfluorenyl benzene is outlined in Scheme 6.2. The unsymmetrical alkyne **6.13** would be used in a Diels-Alder addition to tetracyclone (**1.26**), which, with concomitant loss of CO, would give the desired derivative **6.14**. The attempted route to the alkyne involved the treatment of 9-bromofluorene with phenylethynyl lithium; the reaction was performed at –78 °C in order to minimize

Scheme 6.2

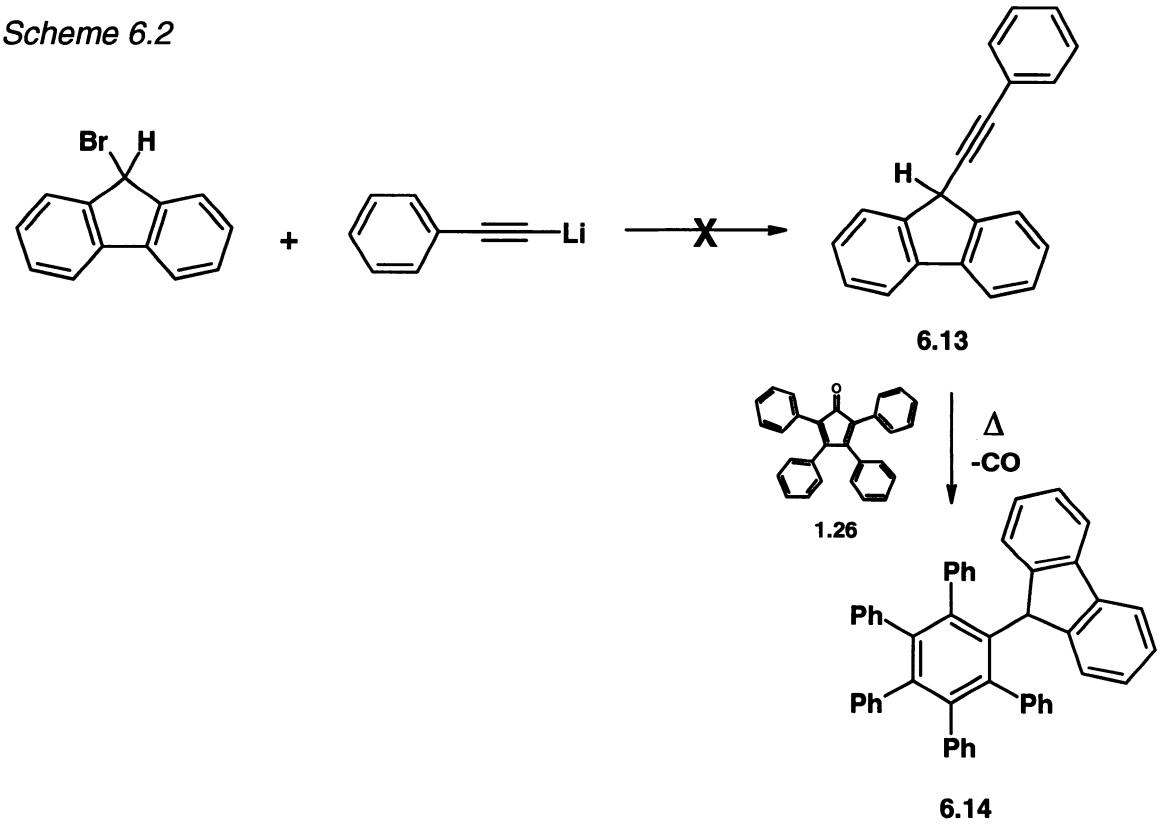

carbene formation, since the original literature synthesis reported a yield of only 10%, presumably as a result of further reactions of the fluorenyl carbene.[356]

6.2.2 Gomberg Dimerization

Treatment of 9-bromofluorene with phenylethynyl lithium resulted in the formation of numerous red, orange, and yellow products after chromatographic separation. The dimers 9,9'-bifluorenyl (**6.15**) and 9,9'-bifluorenylidene (**6.16**) were identified as products by NMR spectroscopy and X-ray crystallography (combined yield 16%); both are known molecules and their crystal structures have been reported.[357-359] A third contributor (12%) to the reaction products was the tetrameric product, **6.17**, in which a 9,9'-bifluorenyl ligand was linked to a 9,9'-bifluorenylidene moiety. This product was also identified by mass spectrometry, NMR spectroscopy and X-ray crystallography (Chart 6.3), and these results have recently been published.[344]

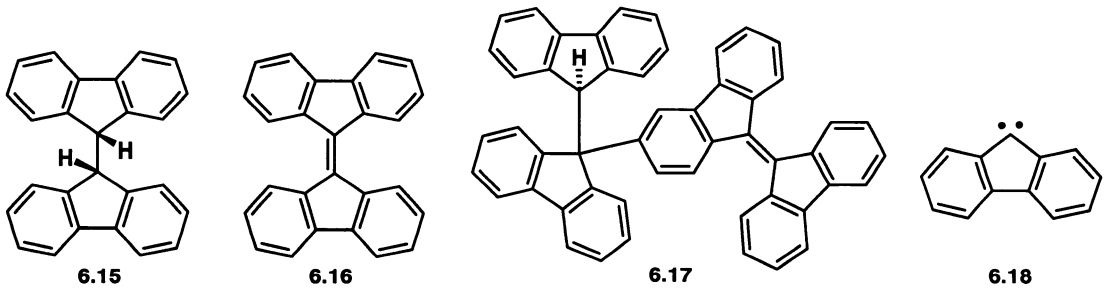

Chart 6.3: Dimeric and tetrameric products from reactions of fluorenylidene carbene, ***6.18****.*

Figure 6.1a illustrates the crystal structure of **6.17**, and reveals the linkage of the dimers from the C(9) position of the 9,9'-bifluorenyl to the C(3) site of the 9,9'-bifluorenylidene, with a C(9)-C(3) bond length of 1.545(4) Å. Figure 6.1b displays the similarity of the tetramer with the two contributing dimeric components. For instance, the two fluorenyl units adopted a gauche conformation in the 9,9'-bifluorenyl fragment, analogous to the parent dimer.[359] Moreover, the interplanar angle between the two fluorenylidene fragments was 35° as a result of steric crowding. This is comparable to the dihedral angles reported in other bifluorenylidenes, which range from 31° to 34°.[357,358]

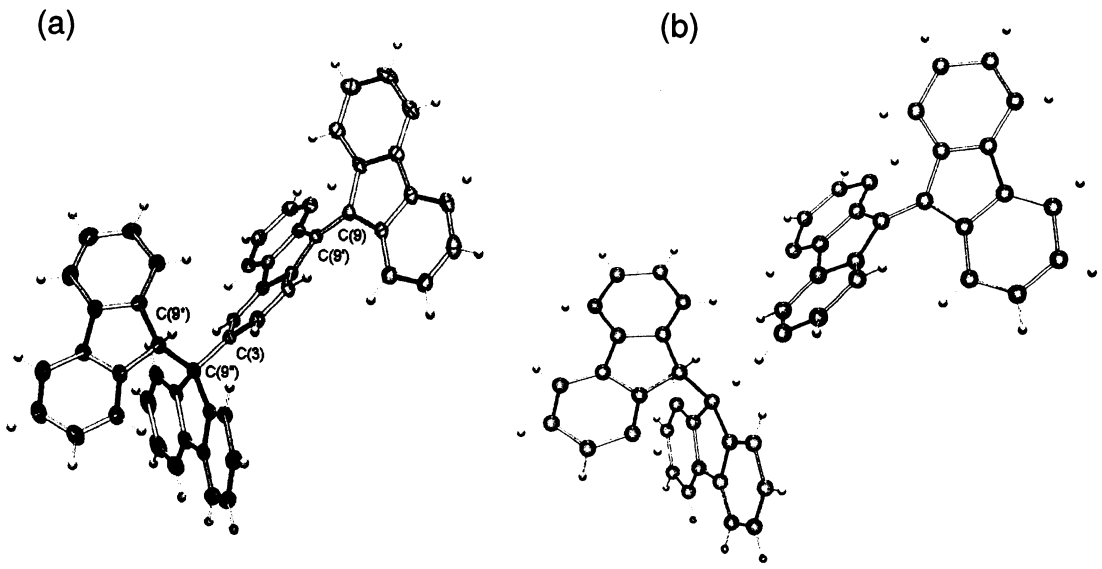

*Figure 6.1: X-ray crystal structure of the tetramer **6.17**, and comparison to the overlap of fragments **6.15** and **6.16**.*

The products identified were consistent with formation of fluorenylidene carbene (**6.18**), generated by deprotonation and subsequent elimination of bromide from C(9). The production of 9,9'-bifluorenylidene by treatment of 9-bromofluorene with bases in *t*-butyl alcohol[360] and DMSO[361] has previously been reported.[360] Handoo described the near quantitative formation of the dimer (**6.16**) upon treatment of 9-bromofluorene with KOH in DMSO.[361] Similarly, Bethell described the use of benzyltrimethylammonium hydroxide and potassium *t*-butoxide as bases in the formation of bifluorenylidene, and performed kinetic studies to show the bimolecular displacement mechanism as the favoured pathway for the reaction. Furthermore, the ground state of the carbene is known to be a triplet,[362,363] although the singlet state is also accessible,[364] thus radical abstraction and dimerization are feasible processes. Wasserman and co-workers,[362] as well as Hutchison,[363] have described the structure and properties of the ground state triplet of fluorenylidene carbene,[362] and Jones has described some reactivity consistent with the presence of the singlet.[364] Although there are numerous reports of investigations of fluorenyl or bifluorenylidene radicals[349,365-370] and carbenes,[371] reference to the tetrameric product **6.17** or any related derivatives has not been encountered.

Two potential routes to the tetramer may be proposed (Scheme 6.3).[344] Both begin with the generation of the triplet carbene **6.18** and the initial coupling product **6.19**. A resonance structure can then be proposed in which a radical

Scheme 6.3

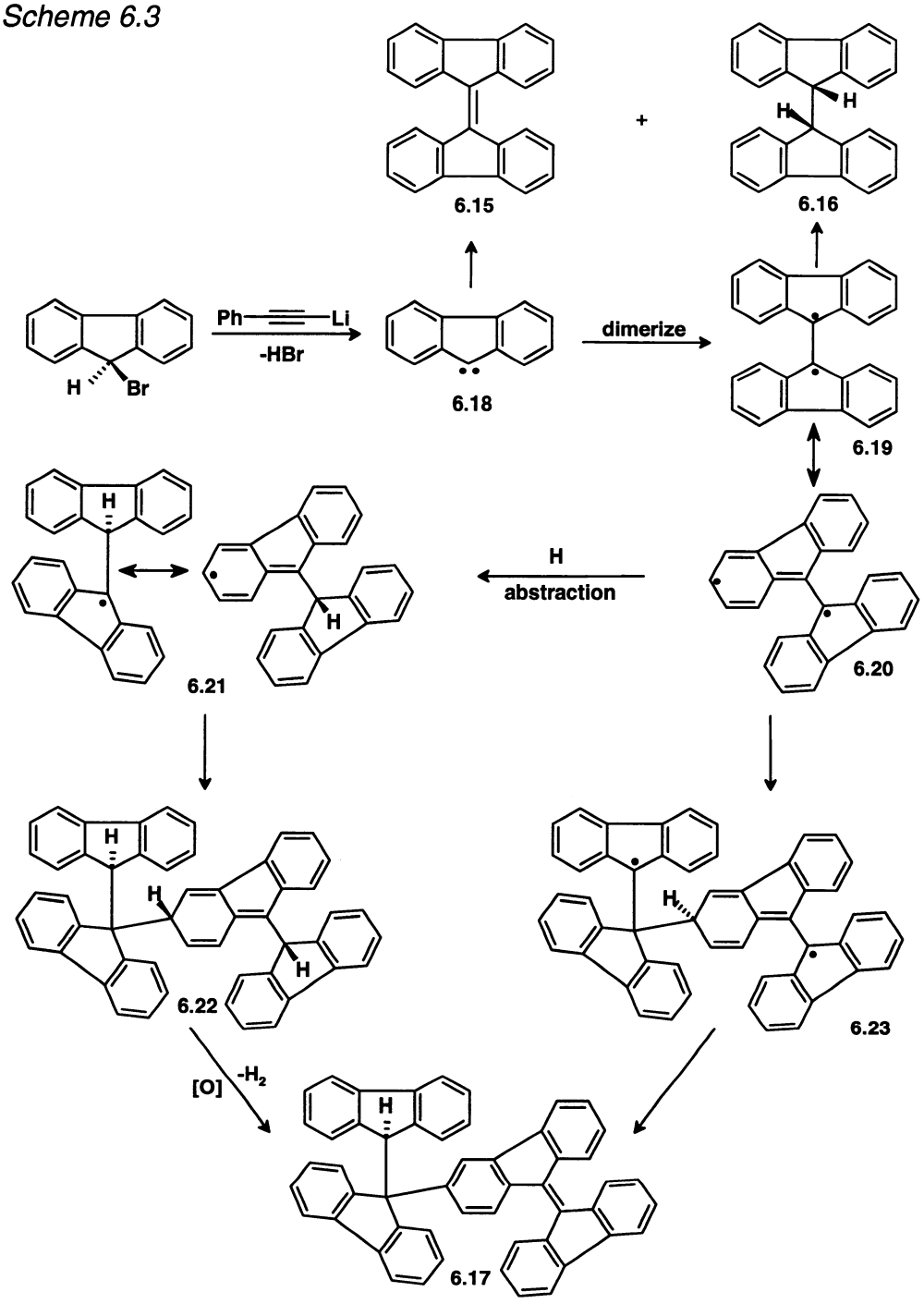
6.15
+
6.16
Ph—Li
-HBr
H
Br
6.18
dimerize
6.19
H
abstraction
6.20
H
6.21
H
H
6.22
H
H
6.23
[O]
-H2
H
6.17

site is localized onto the phenyl periphery of the fluorene (**6.20**). In one scenario, this diradical abstracts a hydrogen to form the known radical **6.21**,[369,370] followed by dimerization to give **6.22**; oxidation and loss of H_2 can yield the final product. Another possible route proceeds via the direct coupling of diradicals **6.19** and **6.20** to give the tetramer (**6.23**); subsequent migration of a single hydrogen affords the product, **6.17**.

Both potential routes involve the coupling of radicals on the 9-fluorenyl position and on the 6-membered ring. This dimerization is reminiscent of the classic Gomberg-rearrangement, in which triphenylmethyl radicals couple via transmission of the radical onto one of the phenyl groups because of steric hindrance at the central carbon (Scheme 6.4).[372-374] Gomberg's work initiated the study of free radicals, and this has been described as one of the most important discoveries of the twentieth century.[374] After the successful preparation of tetraphenylmethane, Gomberg attempted the synthesis of hexaphenylethane (**6.24**), the next member of the series. Treatment of triphenylmethylchloride with powdered metallic silver in benzene yielded a colourless compound that reacted rapidly with oxygen. Numerous experiments on this product led Gomberg to the proposal that he had synthesized the triphenylmethyl radical (**6.25**), which was in equilibrium with its dimer in solution. The structure of the dimer was later reported to be **6.26**, resulting from coupling between a radical site at the central carbon and on one of the phenyl rings.[375] Since these reports, there have been numerous investigations of the coupling of

sterically hindered radicals, and in many cases, products analogous with **6.26** were reported.[376] However, blocking the *para*-positions of the phenyl substituents did lead to coupling at the more crowded central carbons.[376]

Scheme 6.4

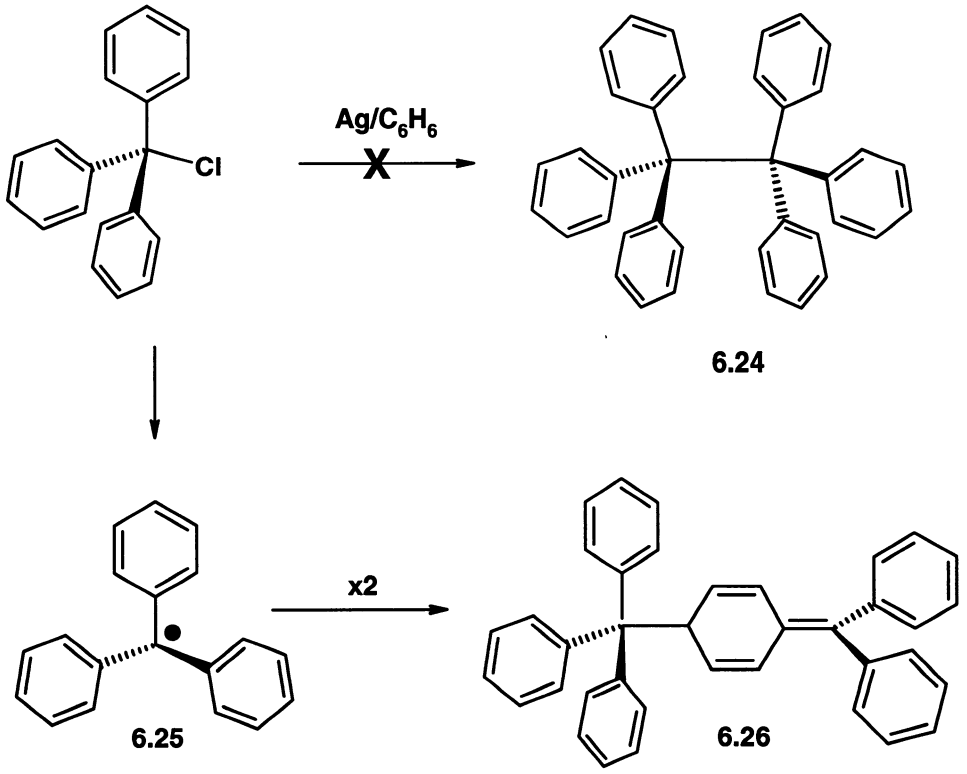

In the case of the bifluorenylidene radicals, the possibility of migration of the radical to the phenyl periphery followed by coupling suggested that the radicals were long-lived. This may have been the result of the non-planarity of the two fluorenyl fragments because of steric interactions. This would have hindered radical coupling and favoured the formation of the Gomberg-type dimerization product **6.17**. Persistent carbenes have long been of interest, and

Tomioka has led the search for long-lived triplet carbenes.[377-379] Particularly relevant to this work is Tomioka's description of the generation and characterization of triplet aryl-substituted anthryl carbenes (**6.27**), in which the anthracene provided a site for extensive delocalization of the unpaired electrons, essentially serving as a "reservoir".[378] This discussion was also extended to bis(anthryl) derivatives (**6.28**), in which the carbene was almost linear with delocalization of the electrons onto the anthryl groups, which were oriented perpendicular to each other (Scheme 6.5). The main route of decay of these

Scheme 6.5

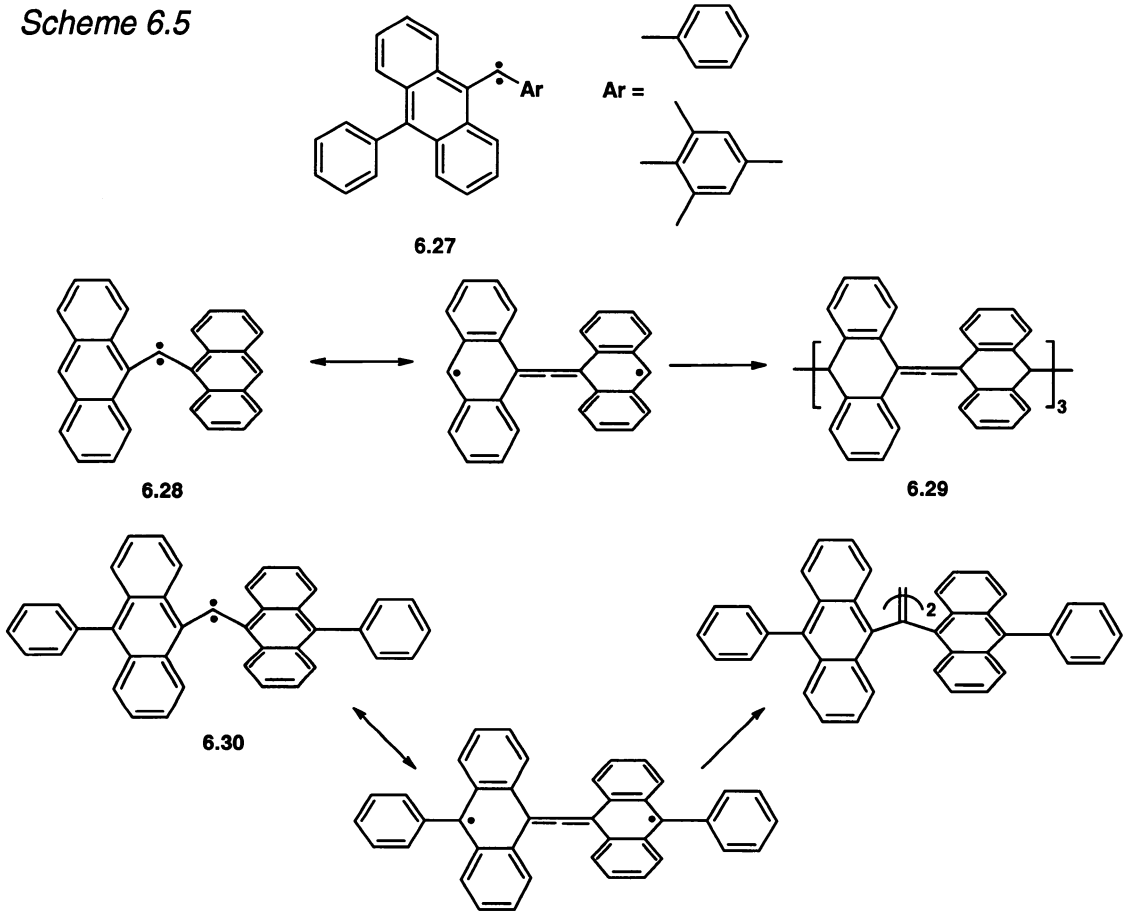

carbenes was trimerization to give the cyclic **6.29**, whereas derivatives substituted in the 10 position of the anthracene (**6.30**) did not form trimers, as the aryl groups prevented the electrons from "leaking out".[379] These results supported the feasibility of the proposed mechanism for the formation of the tetramer, **6.17**, in which the fluorenyl groups provided steric shielding to protect the carbene center and offered a site for electron delocalization, which led to further reactions resulting in the observed products.

6.2.3 An Alternative Route

As a consequence of the unexpected radical reactivity, an alternative route to the unsymmetrical alkyne was selected. Addition of phenylethynyl lithium to fluorenone[371,380] afforded the alcohol **6.31**. Treatment of **6.31** with BF_3 and triethylsilane[381] then gave the desired product (Scheme 6.6), using an

Scheme 6.6

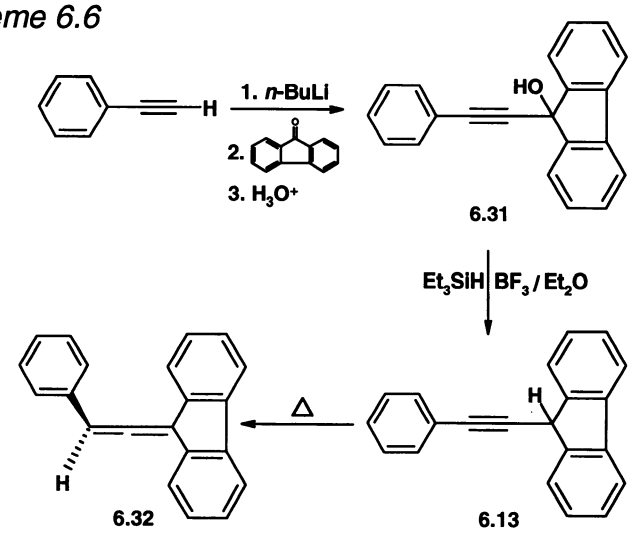

established procedure.

The alkyne **6.13** was characterized using mass spectrometry, NMR spectroscopy and X-ray crystallography; the crystal structure is presented in Figure 6.2. The C≡C bond length was 1.195(2) Å and the fluorenyl substituent was almost exactly perpendicular to the PhC≡C plane (91.2°), although it was bent away from the alkyne by 129.7°. This was an interesting contrast to dinaphthylacetylene (**3.10**) in which the naphthyl substituents were parallel to each other.

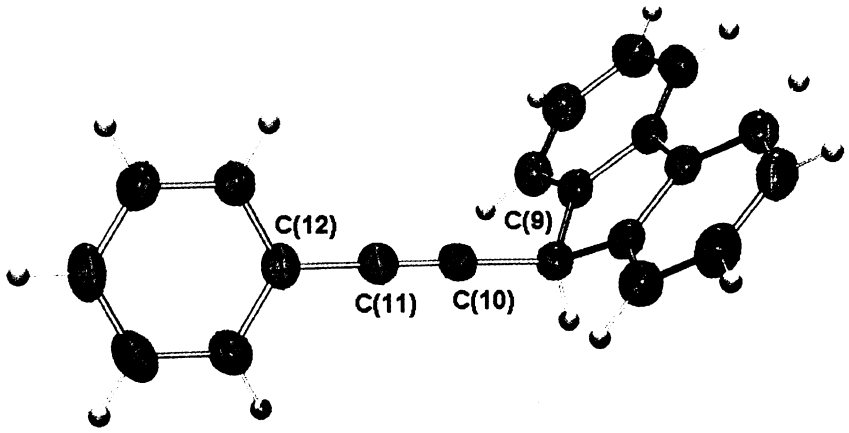

Figure 6.2: Crystal structure of phenylethynyl fluorene, ***6.13****.*

6.2.4 Attempted Diels-Alder Reaction

A Diels-Alder addition of the alkyne to tetracyclone was attempted in order to produce the desired benzene derivative (**6.14**). The reaction involved very high temperatures, and the mixture was not protected from the atmosphere since

the anticipated product was not expected to be air or moisture sensitive. As above, the reaction led to a complex mixture of products that was not easily separated or identified; these products are depicted in Chart 6.4.

After numerous attempts at chromatographic separation, a blue powder (55%) and a yellow solid (13%) were obtained, however, both exhibited complex ^{1}H NMR spectra. Fortunately, the yellow compound produced large crystals suitable for an X-ray crystallographic investigation. Upon analysis, the X-ray crystal structure revealed the presence of two molecules that had co-crystallized, each possessing a substituted naphthacene framework (Chart 6.4); the structure of the first product is illustrated in Figure 6.3.

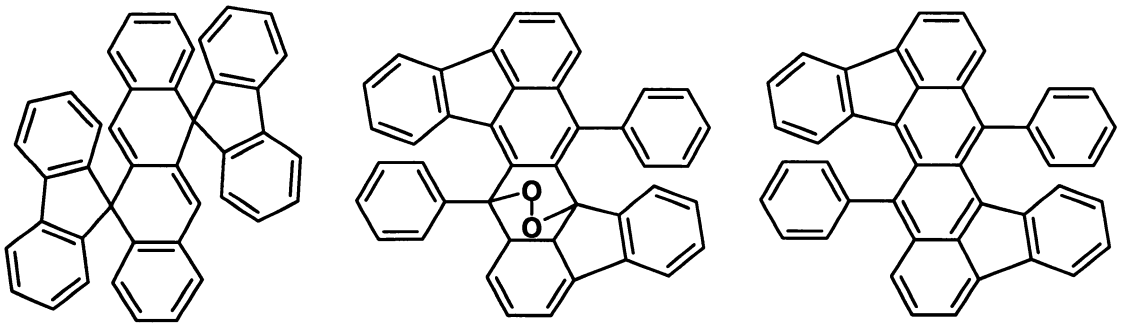

6.33 **6.34** **6.35**

Chart 6.4: Products of attempted Diels-Alder reaction.

The yellow product, molecule **6.33**, was a dihydronaphthacene in which the fluorenyl groups were spiro-bonded to the central ring framework at C(5) and C(11) and were oriented in a perpendicular arrangement relative to the ring to which they were bonded. The central ring skeleton was bent about the central bond by 22°, and there was a slight twist to the rings. The molecule exhibited

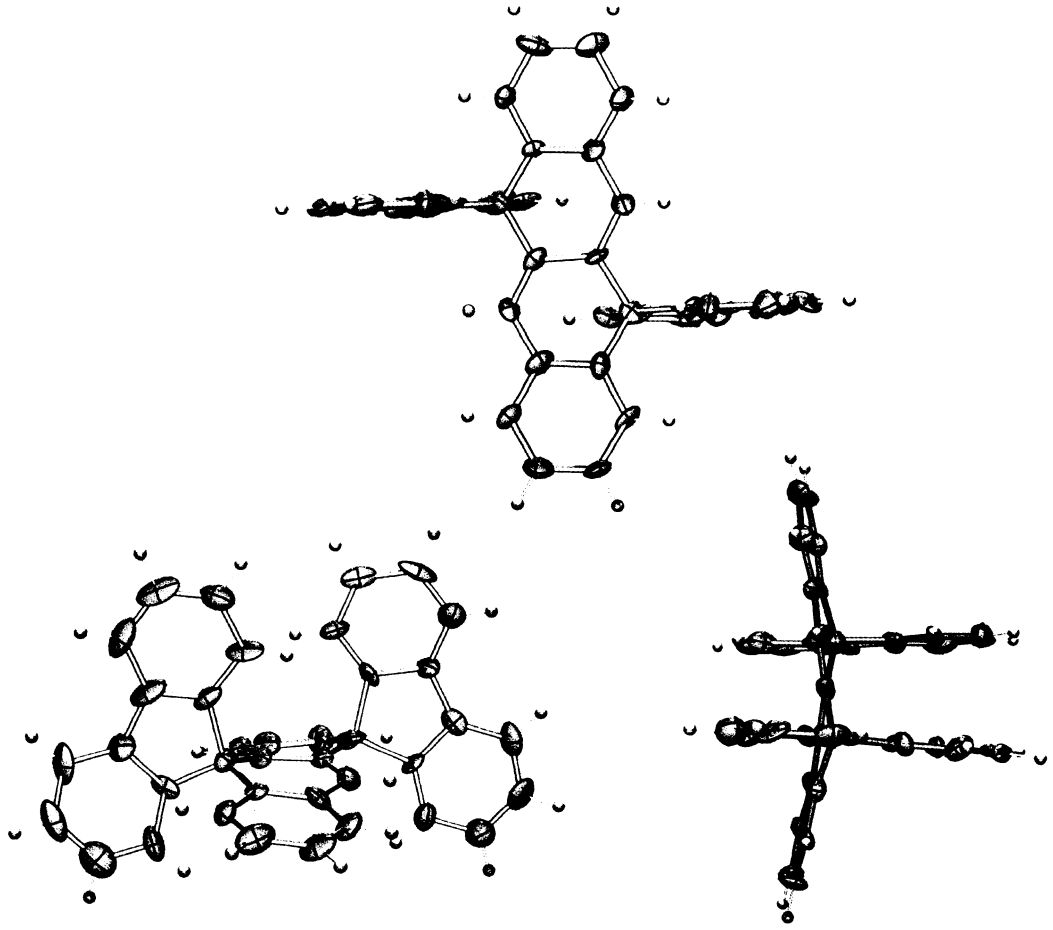

*Figure 6.3: Views of the X-ray crystal structure of the naphthacene **6.33**, illustrating the bend and twist of the central ring skeleton.*

centrosymmetric C_{2h} symmetry in solution, as the ^{1}H NMR spectrum revealed the anticipated doublet-triplet-triplet-doublet patterns for the fluorenyl substituents and terminal phenyl rings. The solid state geometry may be contrasted with the structures of tetracene (**6.36**),[382-386] pentacene (**6.37**),[384,386-389] hexacene (**6.38**),[389] and rubrene (**6.39**),[390] each of which maintained a planar ring structure. There are other examples of distorted ring structures in the literature: the Ru(C_5Me_5) substituted complex (**6.40**) displayed a dramatic helical twist of 62°

about the central rubrene core.[391] The adjacent phenyl groups rotated to avoid interactions between the bulky Ru moiety and the naphthacene unit, and the repulsion between the twisted phenyl groups resulted in the observed structure. Moreover, Pascal and co-workers have described substituted anthracenes and pentacenes that exhibited severe twisting of the central ring skeleton.[392,393] In molecules **6.41**, the incorporation of the central core as part of a terminal polycyclic ring structure forced the helical geometry. In each instance, suitable substitution was required to impose the twisted arrangement (Chart 6.5).

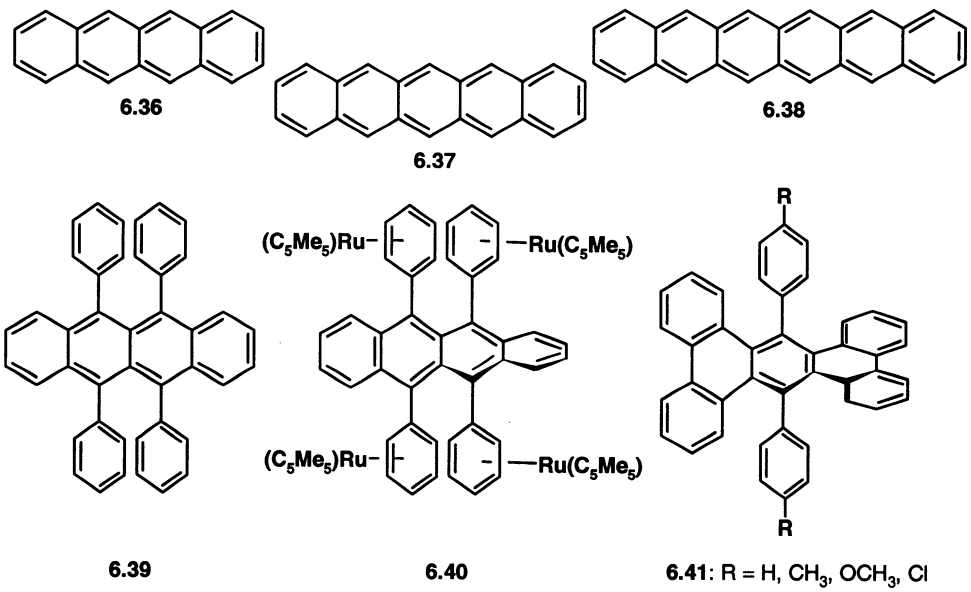

*Chart 6.5: Planar polycyclic hydrocarbons **6.36** – **6.39**, and twisted molecules **6.40** and **6.41**.*

In the second contributor to the co-crystal, the terminal rings in the naphthacene framework were derived from fluorenyl groups, and the phenyl substituents were bonded to C(8) and C(16) (**6.34**), as displayed in the X-ray

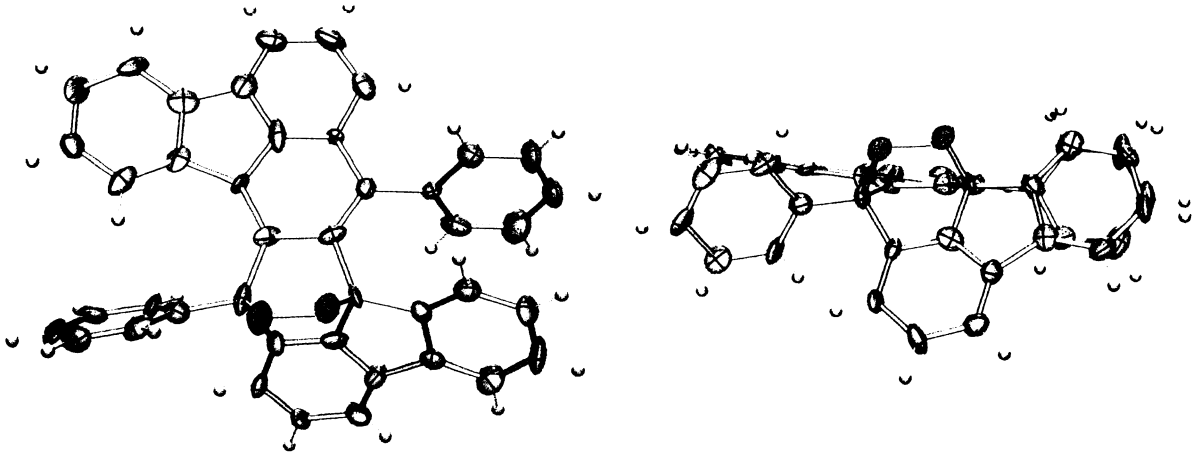

*Figure 6.4: Crystal structure of the peroxide **6.34**, again revealing the extreme bend and twist of the central naphthacene framework.*

crystal structure (Figure 6.4). There was a peroxy linkage bridging C(7b) and C(16) (O-O 1.527 Å), which created a folding of the central ring skeleton such that the dihedral angle between the terminal rings was 116°. In addition, one of the phenyl substituents was cleanly overlapped with the phenyl periphery of a fluorenyl group. The peroxide and the phenyl group bonded to C(16) were nearly coplanar (~ 5°) and were bent approximately 60° from the plane of the fluorenyl group at C(7b), whereas the other phenyl substituent displayed a dihedral angle of 69° relative to the fluorenyl group at the opposite end of the molecule.

There are no known peroxy-bridged naphthacenes in the literature for comparison, however, there has been some discussion in the literature on related species (Chart 6.6). Dufraisse and co-workers described the formation of rubrene peroxide (**6.42**), observed experimentally by the colour change of rubrene (**6.39**) in solution when exposed to light and air from red to

colourless.[394,395] Wasserman and co-workers used related peroxy-bridged polycyclic aromatic molecules to generate singlet oxygen, which could then be reacted with other substrates.[396] In general, the compounds under study were created under photolysis conditions in aerated solutions of carbon disulfide. The same peroxy derivative of rubrene, as well as 9,10-diphenylanthracene peroxide (**6.44**), have also been prepared in microemulsions containing hydrogen peroxide. Molybdate ions were used in this case to catalyze the disproportionation of H_2O_2 to give singlet oxygen.[397]

Erkoç has conducted a series of calculations in order to investigate the structural and electronic properties of rubrene and its peroxide, and to determine the favoured rubrene peroxide isomer (**6.42**, **6.43**).[398] The addition of oxygen to rubrene may occur at a terminal or internal aromatic ring, and in each case, the structure was predicted to be severely distorted from planarity. The calculations

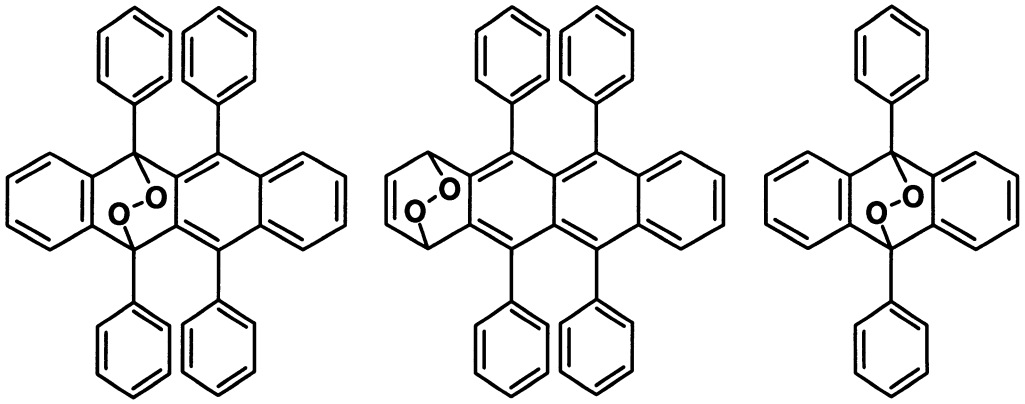

6.42 **6.43** **6.44**

Chart 6.6: Peroxides of rubrene and 9,10-diphenylanthracene.

determined that both isomers were relatively similar in energy and that positioning the peroxide on an internal ring was slightly lower in energy, which is consistent with the X-ray crystal structure of **6.34**.

Obtaining the crystal structures of **6.33** and **6.34** assisted in the determination of the structure of the major product **6.35** (45%), which decomposed readily in solution in the presence of air and light from a bright blue to a pale yellow solution. The 2-dimensional NMR spectroscopic and mass spectrometric data were consistent with the formation of the C_{2h}-symmetric naphthacene precursor to the peroxide **6.34**. A pure sample of **6.34** was later recovered from the decomposition of **6.35**, and positively identified by mass spectrometry and NMR spectroscopy.

6.2.5 Proposed Mechanism of Reaction

The formation of the products **6.33**, **6.34** and **6.35** at high temperatures was consistent with the dimerization of the allene isomer of the alkyne, **6.32** (Scheme 6.6, page 172). It is known that the alkyne is in equilibrium with the allene,[356] and dimerizations of such species have been described. Rewicki and coworkers described the thermal dimerization of **6.32**,[356] and characterized the head-to-tail dimer **6.45** by X-ray crystallography,[399] which was the major product of the reaction (84%). This yellow compound contained a central cyclobutane ring; one fluorene was attached via a double bond and the other formed a spiro-[fluorene-cyclobutane] system. One of the C-C bonds in the central ring had an

extremely long bond of 1.61 Å, and this resulted in unexpected reactivity, such as thermal rearrangement and catalytic hydrogenation, as well as fission of the weak bond. The other product of the dimerization was a red material (8%) that the authors were not able to characterize.[356]

Scheme 6.7

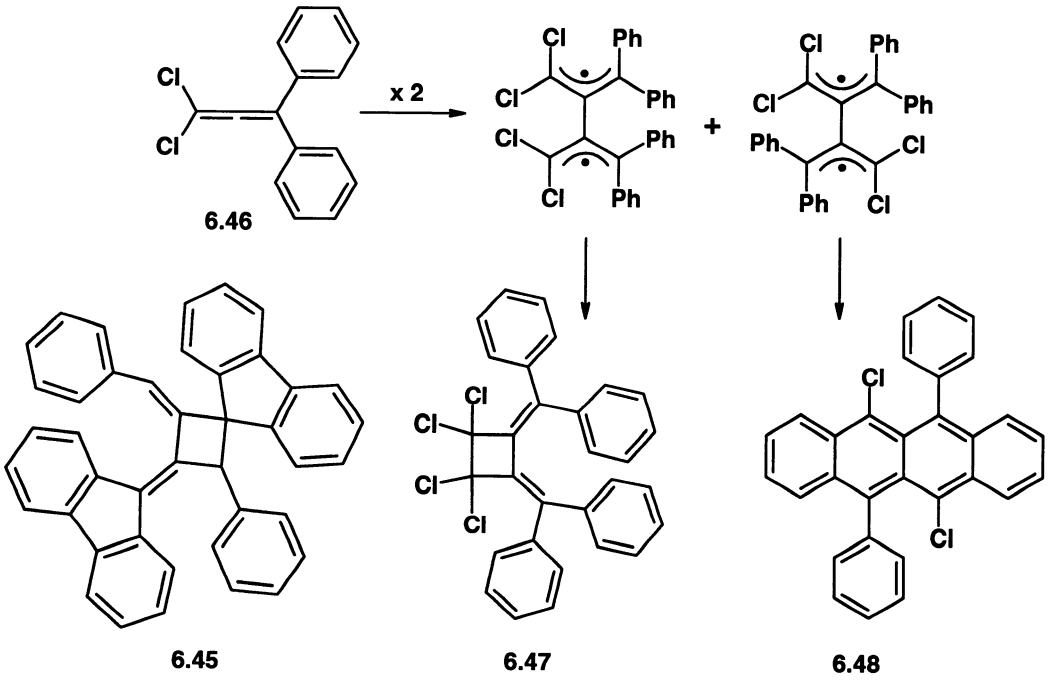

Later investigations of dichlorodiphenylallene **6.46** (and related derivatives) revealed the formation of the expected 2+2 dimer (**6.47**) resulting from the closure of the bis(allyl) radical (Scheme 6.7). A series of ring-opening and closing reactions, and loss of HCl, also led to the naphthacene **6.48** in high yield.[400-402] The authors crucially recognized the potential formation of the

intermediate 1,4-allyl-biradicals that could be delocalized onto the *ortho*-positions of the aromatic rings, thus providing a route to the six-membered ring products. In other instances, there was no evidence for a second ring-opening product, and only the cyclobutane derivatives were observed.[403-405]

The ideas presented in the literature for the formation of allene dimers can be applied to the understanding of the formation of the products **6.33**, **6.34** and **6.35** (Scheme 6.8). The initial product was the cyclobutane dimer, as determined by Rewicki *et al.*, which could then ring open to give the diradical **6.49**. The radical could then migrate onto one of the phenyl rings (**6.50**), or onto the phenyl periphery of the fluorenyl substituent (**6.51**). Coupling of the radicals then led to molecules **6.52** and **6.53** respectively, and disrotatory electrocyclization of the 6π system in each case yielded the naphthacene skeletons **6.54** and **6.55**. Oxidation in air and loss of hydrogen then generated the products **6.33** and **6.35**. Upon exposure to light and air, **6.35** decomposed to give the peroxide **6.34**, as established for the related species described above.

The fate of the tetracyclone (**1.26**) used as the diene in the attempted Diels-Alder reaction remains to be determined. Much of **1.26** was recovered unreacted (~70%), however, no products consistent with the reaction of tetracyclone with the alkyne or allene were isolated or characterized.

Scheme 6.8

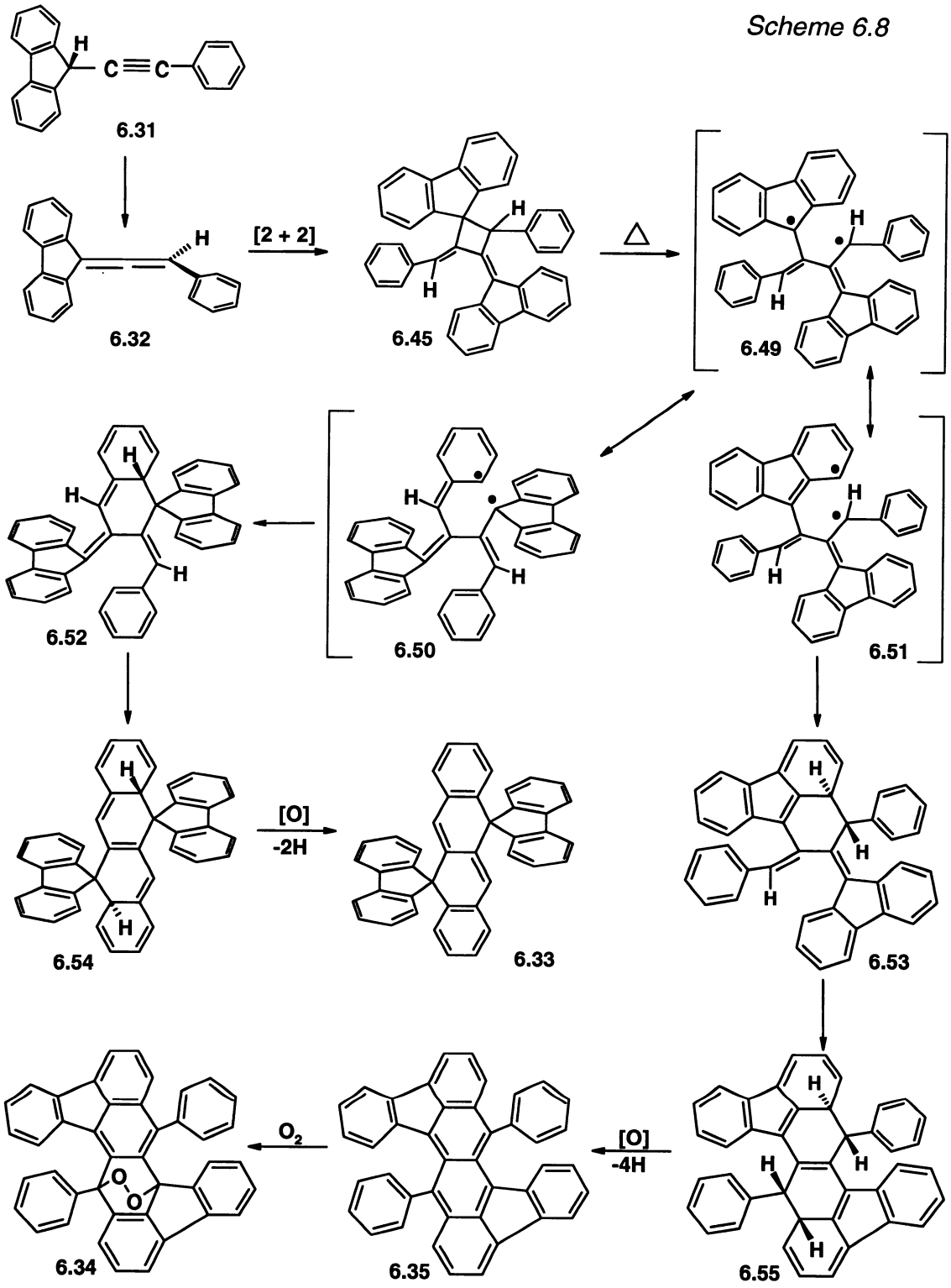

Tetracyclone has been used as a trapping agent of benzyne intermediates at 300 – 325 °C, and was described as stable at these temperatures, although decomposition occurred at 375 °C.[308] Furthermore, upon pyrolysis at 410 – 425 °C, none of the ketone was recovered. The major products of the pyrolysis were assigned as compounds **6.56** – **6.58**, and characterization was based on UV and IR spectra, as well as melting point comparison with authentic samples (Scheme 6.9). Numerous uncharacterized hydrocarbon products were also reported, with molecular weights ranging from 437 to 1060.[308] The major products obtained from the attempted Diels-Alder reaction were the allene dimer products described above, and unreacted tetracyclone (~70% of starting material recovered). There were no products isolated consistent with the formation of the compounds described by McNelis,[308] though there were numerous small

Scheme 6.9

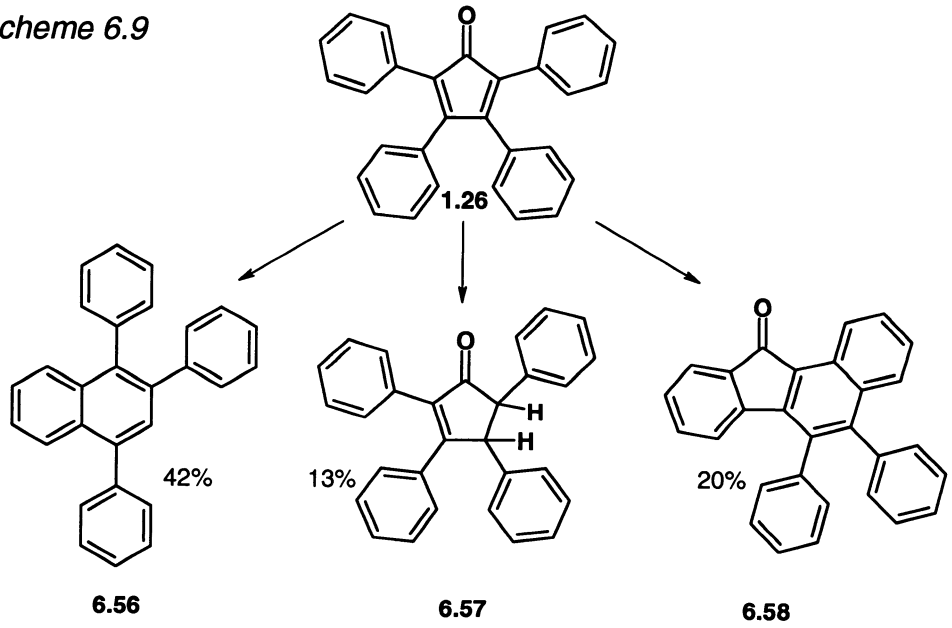

fractions that were not in sufficient abundance for satisfactory identification or characterization.

6.3 Conclusions

Treatment of 9-bromofluorene with phenylethynyl lithium resulted in the unexpected formation of the tetramer **6.17**, as well as the dimeric products **6.15** and **6.16**. The tetramer arose from the Gomberg-type dimerization of fragments **6.15** and **6.16** via linkage of the C(9) position of the 9,9'-bifluorenyl unit with the C(3) site of 9,9'-bifluorenylidene. An alternative route to phenylethynyl fluorene was successfully followed, allowing for the X-ray crystallographic characterization of **6.13**.

The attempted Diels-Alder treatment of the alkyne **6.13** with tetracyclone yielded instead the allene-dimer products **6.33** and **6.35**. Compound **6.35** was oxidized in the presence of air and light in solution to give the peroxide **6.34**, which was the first such molecule to be characterized by X-ray crystallography.

In light of the unexpected reactivity of the fluorenyl unit in carbene and radical reactions, the ligand is not an appropriate choice for incorporation into a polyaryl benzene framework. This initial investigation yielded numerous interesting results that advanced the understanding of related reactions in the literature, as well as allowing for the proposal of reaction mechanisms consistent with the formation of the unexpected dimeric and tetrameric products.

CHAPTER SEVEN

Future Work

7.1 Review of Progress

The overall objective of this research was to create a system that exhibited correlated rotation. The primary methods to accomplish this were (i) incorporating β-naphthyl groups into 5- and 6-membered organic and organometallic molecules in order to increase the steric hindrance of and interactions between the peripheral aryl substituents, (ii) integrating triptycene architectures into organometallic complexes that model molecular gears and brakes, and (iii) utilizing haptotropic shifts to control barriers to rotation in crowded molecules.

In Chapter 2 the inclusion of the bulky naphthyl groups into tetraarylcyclopentadienone molecules was described, which allowed for the distinction between distal and proximal naphthyl isomers. Rhodium acetylacetonate derivatives were prepared and characterized, and the consequent dynamic behaviour resulted in the determination of a barrier of 8.2 kcal mol^{-1} for naphthyl rotation. This barrier was comparable to a *meta*-phenyl substituted complex, and the ability of the naphthyl groups to adopt distal and proximal orientations assisted in alleviating the steric interactions between the peripheral substituents. Further advancing on this approach, the sterically crowded hexanaphthylbenzene and pentanaphthylferrocenylbenzene were also synthesized and characterized in Chapter 3. It was clear that the naphthyl

groups experienced significant steric strain in these complexes, and this research provided a model for future systems containing fully planar peripheral blades.

The incorporation of a metal fragment into a crowded cyclopentadienone has dramatically influenced the stability of its protonation product, as described in Chapter 4. The treatment of tetraphenylcyclopentadienone and 3-ferrocenyl-2,4,5-triphenylcyclopentadienone with strong acids resulted in the characterization of distinct products, consistent with metal-assisted stabilization of the cationic intermediate. This work can be applied to future systems that integrate steric crowding and metal-stabilization into a reactive complex, potentially allowing for characterization of the intermediates and resulting products.

Chapters 5 and 6 explored the use of haptotropic shifts as controls over the steric interactions between crowded substitutents. A triptycene-containing organometallic molecular brake was synthesized and characterized, and has provided the first example of such extreme crowding in a system without peri-substitution. The molecule was actually too crowded to accomplish the original goal, however, this research has provided a starting point for future derivatives, and has allowed for the description of the key components that must be incorporated into the design of potential molecular brakes.

The application of this concept to a sterically crowded benzene molecule was also explored by the attempted synthesis of pentaphenylfluorenylbenzene, in which the haptotropic shifts of the metal would potentially offer control over the

barrier to rotation. Instead, the unexpected radical reactivity of the fluorenyl ligands resulted in the formation of numerous interesting molecules. Again, the important structural and electronic features of these molecules can be derived from this research and applied to future systems.

In Chapter 7, the application of these contributions to the design of future molecules will be described. Each step along the path to achieving a research goal provides both positive and negative results, which can then be used to alter the original strategy, by incorporating new scientific conclusions and by adapting to understand unexpected results.

7.2 Sterically Crowded Cyclopentadienones and Benzenes

The use of β-naphthyl substituents in hindered cyclopentadienones and benzene derivatives has increased the barrier to rotation and provided solid-state evidence for the degree of crowding. Further amplifying the steric contribution of the peripheral substituents may broaden this chemistry by providing barriers considerably in excess of those reported in the literature, with the goal of achieving correlated rotation. Using α-naphthyl or 9-anthracenyl substituents may provide the necessary crowding to achieve this objective. These groups would offer similar steric hindrance, although the 9-anthracenyl groups would extend both above and below the plane of the central ring, thus avoiding the possibility of proximal and distal isomers.

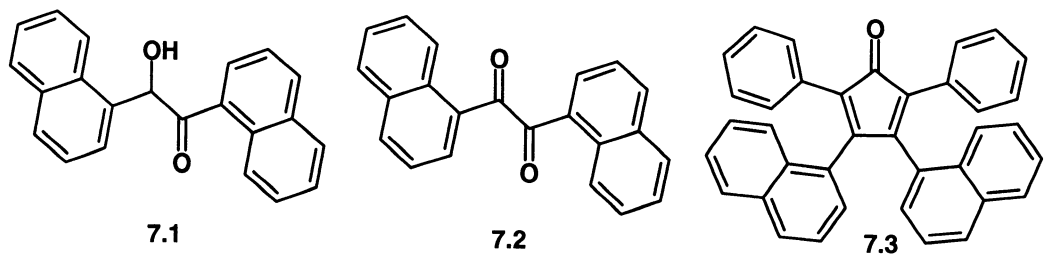

*Chart 7.1: The α-naphthyl substituted complexes **7.1** – **7.3**.*

Initial investigations of α-naphthyl substituents have illustrated the difficulty in accommodating bulky groups about a central ring. The α-naphthyl analogues of β-naphthoin (**2.13**) and β-naphthil (**2.14**), **7.1** and **7.2** have been synthesized according to literature procedures,[406,407] and **7.2** has been used in an attempt to prepare the tetraarylcyclopentadienone **7.3** (Chart 7.1). The formation of **7.3** involved two subsequent condensation reactions (Scheme 7.1), and the requirement for the diketone to achieve a "*cis*" conformation complicated the preparation in sterically bulky derivatives. The validity of this claim has been evaluated using PM3 computational studies with the Hyperchem package,[408] and the preliminary results are displayed in Table 7.1. The calculations highlight the energy difference between the *cis*- and *trans*- orientations of both naphthil compounds, and confirm that the energy barrier to rotation was significantly greater in the α-naphthyl derivative. The preferred geometry in this case involved the rotation of one of the naphthyl groups by 50°, whereas the β-analogue preferred a nearly planar arrangement; this asserted that steric factors were more prevalent in α-naphthil. Experimental evidence also supported this

result, since the aldol condensation and the formation of the cyclopentadienone occurred readily for β-naphthil, whereas the analogous reaction for the α-derivative did not occur under the non-rigorous conditions used.[409]

Table 7.1: PM3 Calculation Results for Possible Geometries of 2.14 and 7.2.

Species	Energy of "*trans*" conformation kcal mol^{-1}	Energy of "*cis*" conformation kcal mol^{-1}	Energy difference kcal mol^{-1}
α-naphthil	-78466.4	-78460.6	5.8
β-naphthil	-78582.6	-78582.0	0.6

Scheme 7.1

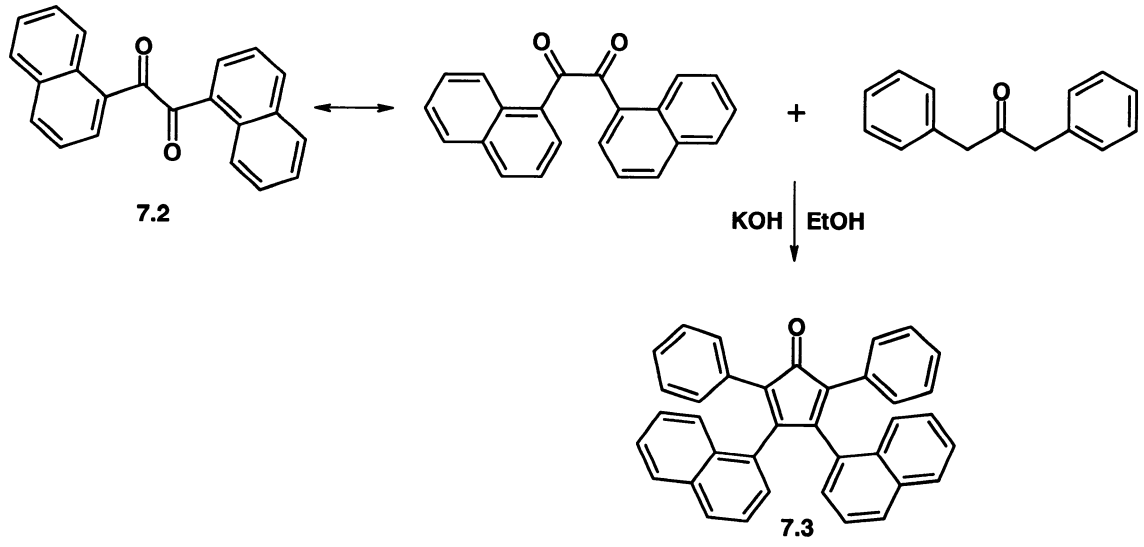

As a result of this complication, an alternative route to the crowded benzenes or cyclopentadienones may be attempted. Treatment of the prepared α-naphthil with hydrazine hydrate to give the dihydrazone **7.4** (analogous to **3.9**), followed by reduction with silver oxide, would yield the disubstituted alkyne, **7.5**.

The use of organometallic reagents as catalysts for dimerization and trimerization may then be explored. Treatment of **7.4** with $Fe_2(CO)_9$ would be expected to

Scheme 7.2

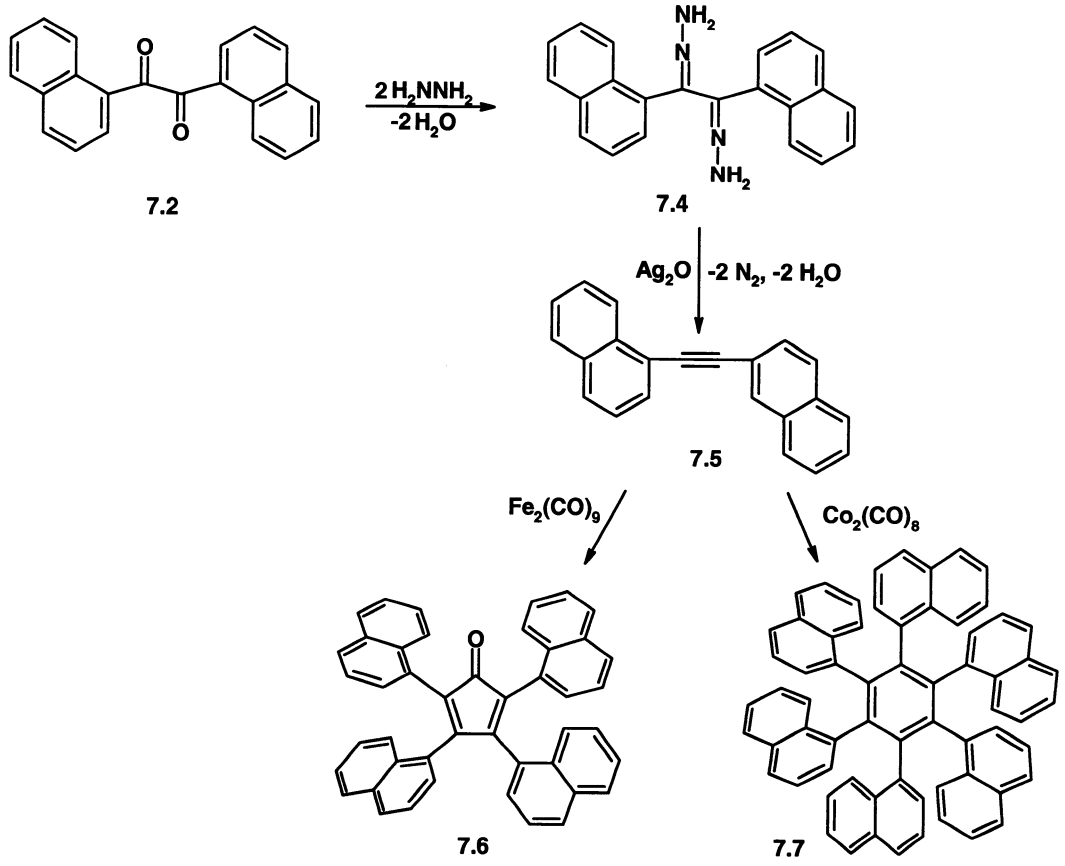

form the cyclopentadienone **7.6**.[410] In addition, cobalt carbonyl is known to induce trimerizations of alkynes,[411] this may afford the sterically crowded benzene **7.7** (Scheme 7.2). An analogous route to Schemes 7.1 and 7.2 may be explored to prepare anthracene-substituted derivatives, and these complexes may be examined with variable-temperature NMR to determine the barrier to rotation of the peripheral substituents. In the case of the α-naphthyl derivative,

the formation of proximal/distal isomers would be anticipated. The coordination of a metal fragment to the central ring may force all of the groups into the distal conformation as well as providing the unsymmetrical substitution required for observing barriers to rotation using NMR.

7.3 Organometallic Derivatives Containing Naphthyl Groups

Another key feature in the design of systems with the goal of observing correlated rotation is coordinating the motion of the organic ligand with that of the organometallic fragment. Increasing the size of the peripheral substituents in the aryl ligand can accomplish this, however, increasing the steric bulk of the other ligands on the metal moiety will also increase interactions with the organic unit. An attractive ligand with the potential to achieve this objective is the tetraphenylimidodiphosphinate molecule (**7.8**), which is known as an inorganic analogue of β-diketonates.[412] This group would be an ideal candidate to replace the acetylacetonate ligand in rhodium systems such as **2.16**. Metal complexes containing **7.8** have been reported, in particular, manganese,[413] thorium,[414] uranium,[414] and a series of lanthanide derivatives[412] have been described.

The ligand is produced by the addition of H_2O_2 to a suspension of $(PPh_2)_2NH$ in THF, followed by the deprotonation of the product (**7.9**) with sodium methoxide (Scheme 7.3).[413] The ligand (**7.8**) can then be added to rhodium chloride bis(ethylene) to give the complex **7.10**. As with **2.16**, addition of a substituted cyclopentadienone ligand would then yield **7.11**. Another advantage

to the use of **7.8** as a ligand is that it may prevent the dimerization of **7.11** and allow for the characterization of a coordinatively unsaturated rhodium complex.

Complex **7.11** should be characterized by X-ray crystallography to determine the magnitude of the interaction between all of the peripheral aryl substituents in the solid state, and variable-temperature NMR would reveal the influence of this steric interaction on the barriers to rotation of the aryl groups.

Scheme 7.3

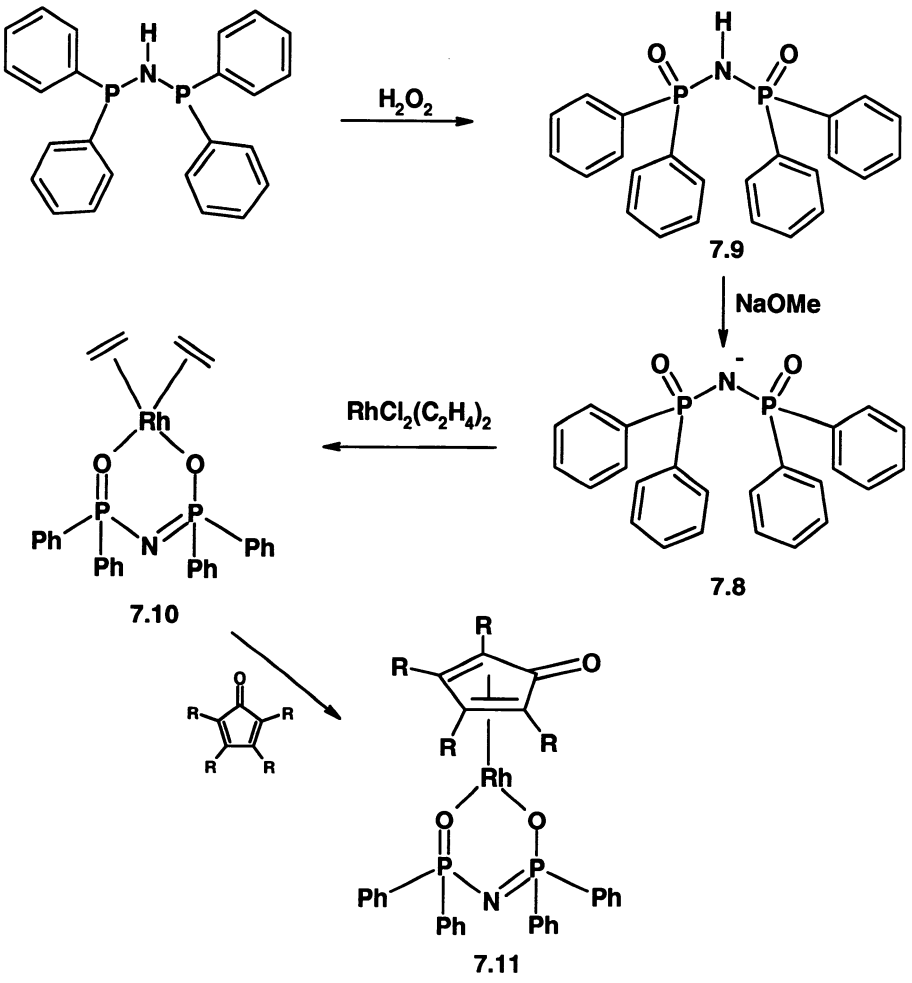

7.4 An Organometallic Molecular Brake

The first attempt at the formation of the (9-indenyl)triptycene molecular brake revealed that the steric crowding at the indenyl group must be comparable to or less than the triptycene blades in order to achieve coordination of the metal on the indene. There are a variety of potential methods to accomplish this goal.

7.4.1 Inclusion of a Spacer Atom

The incorporation of a spacer atom between the triptycene and indene may reduce the steric hindrance and allow for metal complexation. The most straightforward route to the desired complex involves the treatment of 9-hydroxyanthracene with 1-bromoindene (Scheme 7.4). There is some discussion in the literature on the stability and formation of 9-hydroxyanthracene (**7.13**), since the keto form (anthrone, **7.14**) is known to be the most stable tautomer in most solvents.[415,416] Smith and co-workers have recently conducted NMR

Scheme 7.4

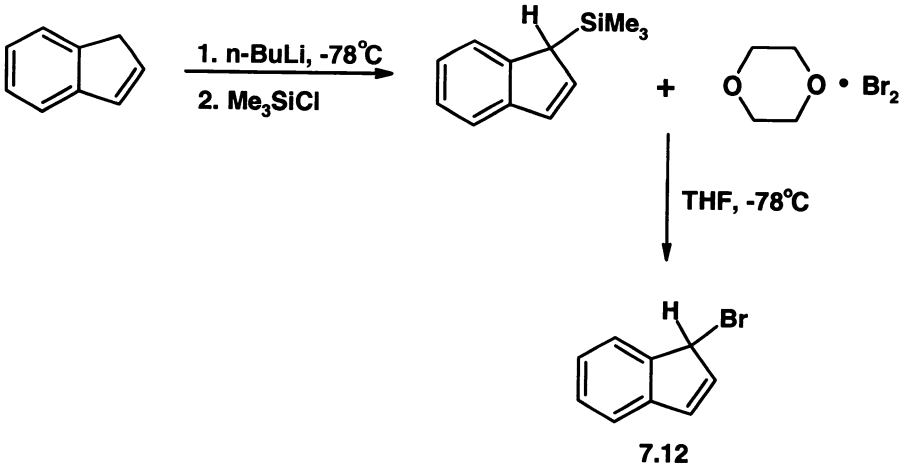

7.12

studies on this equilibrium, and have reported that the enol form is stabilized in DMSO through hydrogen bonding.[416]

The required 1-bromoindene (**7.12**) can be conveniently prepared by treatment of 1-(trimethylsilyl)indene with an excess of dioxane dibromide in THF at low temperatures.[417] The 1-(trimethylsilyl)indene can be made analogously to the tin complex **5.14**, by treatment of the indene with *n*-butyl lithium, followed by addition of trimethylsilylchloride (Scheme 7.4).

Scheme 7.5

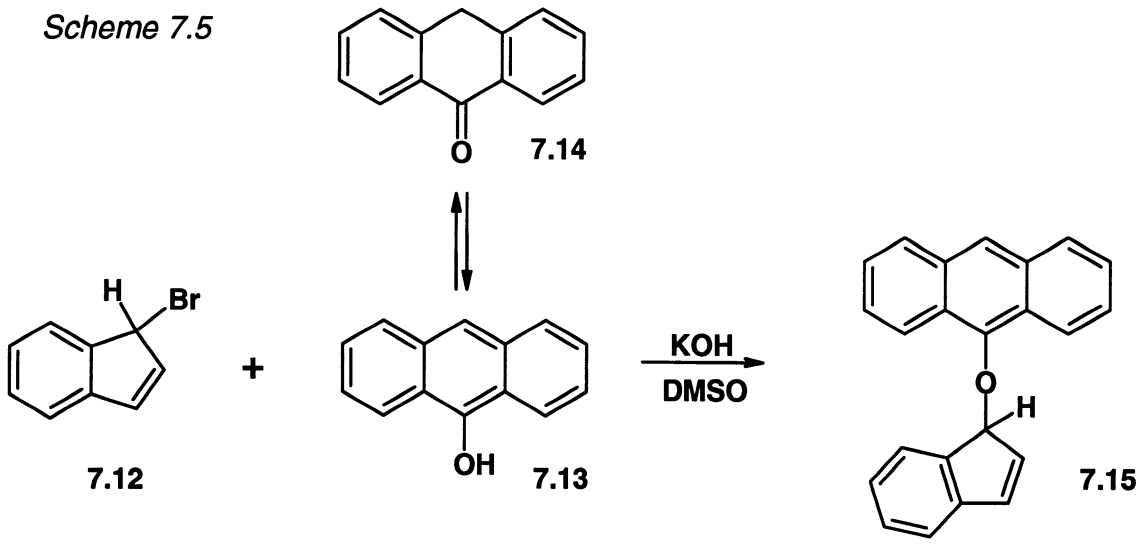

Finally, the coupling of the two fragments to form the diaryl ether complex **7.15** can be achieved by deprotonation of 9-hydroxyanthracene with KOH, followed by the addition of 1-bromoindene (Scheme 7.5).

7.4.2 Indenyl Coordination via the 6-Membered Ring

An alternative route involves the coordination of the indenyl group to the triptycene by the 6- instead of the 5-membered ring. In order to create this species, the indene must be halo-substituted on the 6-membered ring; the 5- or 6-positions would offer the most flexibility to the ligand, and the minimum steric hindrance, as well as allowing for facile deprotonation of the protons on C(1). The proposed route to 6-bromoindene is adapted from literature procedures,[418,419] and begins with the treatment of bromobenzene with chloropropionyl chloride and aluminum trichloride. The resulting *para*-disubstituted benzene (**7.16**) will then undergo ring closure upon addition to a sodium chloride/aluminum trichloride melt, resulting in the formation of 5-bromo indanone (**7.17**). Reduction with lithium aluminum chloride and dehydration by

Scheme 7.6

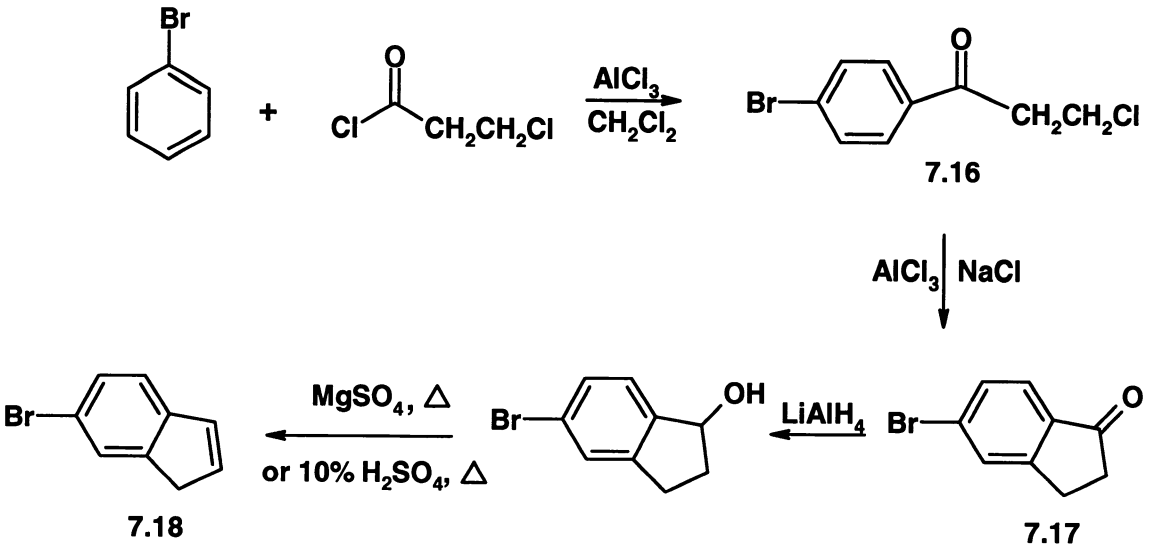

distilling over magnesium sulfate,[418] or by heating in 10% sulfuric acid,[419] would yield the final product (**7.18**, Scheme 7.6).

In order to couple the two aryl halides, a Suzuki coupling can be attempted. Formation of the required boronic acid from 6-bromoindene may be accomplished by conversion of the indene to the Grignard reagent **7.19**, followed by addition of triisopropylborate. An aqueous work-up will afford the boronic acid **7.20**.[420] The acid may then be used in a Suzuki reaction with 9-bromoanthracene, in which the palladium species catalyzes the coupling of the two aryl fragments to give **7.21** (Scheme 7.7).[420]

Scheme 7.7

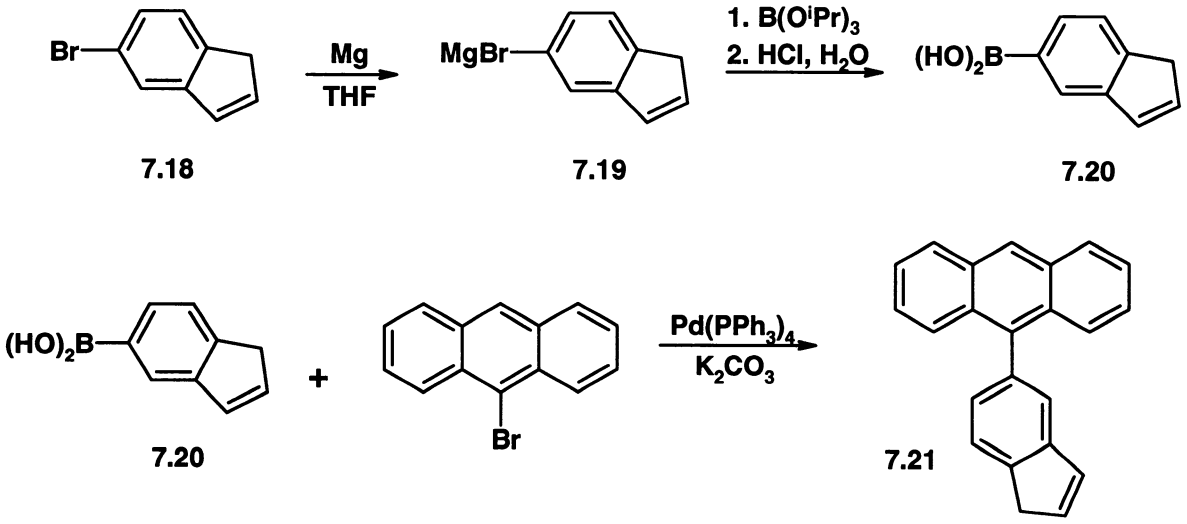

Finally, treatment of **7.15** and **7.21** with benzyne will generate the desired triptycene derivatives **7.22** and **7.23**, respectively (Scheme 7.8). These complexes can then be studied with variable-temperature NMR spectroscopy in order to determine the barrier to rotation of the triptycene blades. Coordination of

a metal fragment to the 5- or 6-membered ring of the indene, followed by protonation or deprotonation, will allow the potential use of haptotropic shifts to control the interaction of the organic and organometallic fragments to be investigated.

Scheme 7.8

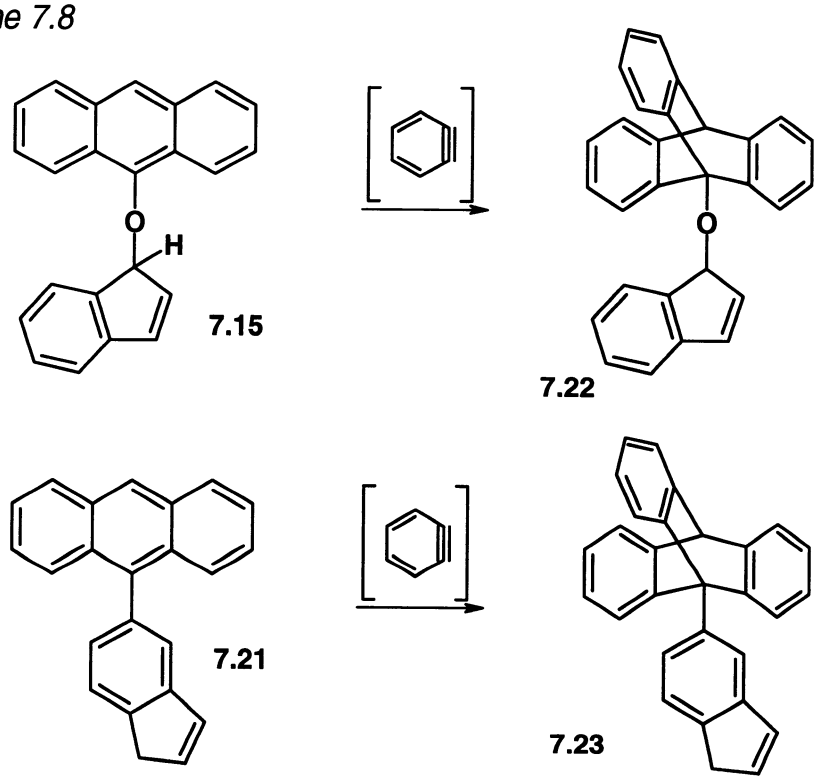

7.5 Formation of Silicon-Substituted Fluorenyl Derivatives

The complications resulting from the formation of fluorenyl carbenes and diradicals prevented the formation of the desired pentaphenylfluorenyl benzene (**6.14**). Ultimately this resulted from the equilibrium between phenylethynyl-fluorene and its allene isomer, which allowed for dimerization and further reactions. It is known that silicon-containing allenes are relatively unstable,[421-424]

therefore, a silicon-substituted derivative would not be expected to form the isomeric allene as readily, thus allowing the alkyne to continue with the desired Diels-Alder chemistry. As a result, molecule **7.24** would be an attractive target; **7.24** would maintain steric crowding and the extension of the blade above and below the plane of the central ring, as well as the possibility for haptotropic shifts and controls over the barrier to rotation. Of course, silicon is larger than carbon, which may mean the silicon-substituted fluorene would have a longer bond length to the central ring and be further removed from the propeller blades. The extent to which the size of the silicon influences the steric situation and geometry would have to be explored.

The formation of a silaallene analogous to allene **6.32** would not be a favourable process, as silaallenes are known as reactive intermediates.[421] Gordon and co-workers have performed computational investigations of the predicted geometries of silaallenes,[424] and the first stable 1-silaallene was isolated and characterized by West *et al.* in 1993.[421] The complex, **7.25**, was highly sterically crowded, and was described as the least reactive multiply-bonded silicon compound prepared to date (Chart 7.2). Other substituted silaallenes have since been investigated,[423] and more recent computational studies have been performed,[422] although much work remains to be completed to adequately understand the chemistry and reactivity of these Group 14 species containing cumulative double bonds. Overall, the formation of the 1-silaallene **7.27** is not anticipated to complicate the proposed synthesis of **7.24**.

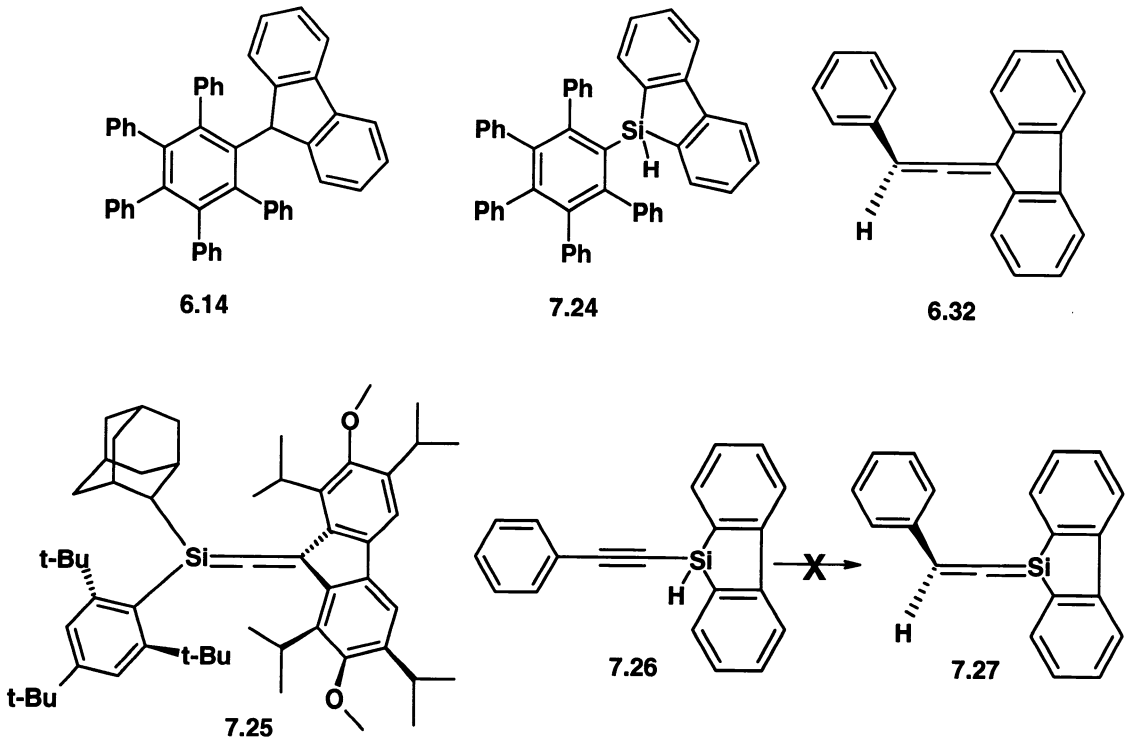

*Chart 7.2: Allenes **6.32** and **7.25**, and proposed complexes **7.24** and **7.26**.*

As with the carbon analogue, the synthesis of **7.24** begins with the production of the alkyne, **7.26**. Silafluorenes have been previously prepared and investigated,[425-429] and the most straightforward route to **7.26** involves the synthesis of chloro-silafluorene **7.29**.[430-432] The proposed preparation begins with the treatment of 1,2-dibromobenzene with *n*-butyl lithium to yield the biphenyl dimer **7.28**, followed by lithiation and finally, treatment with silicon trichloride to give the silafluorene **7.29**. Complex **7.29** can then be treated with phenylethynyl lithium, resulting in the formation of the desired alkyne, **7.26**. The

alkyne can then be used in a Diels-Alder reaction with tetracyclone (**1.26**) to afford the final product, **7.24** (Scheme 7.9).

Scheme 7.9

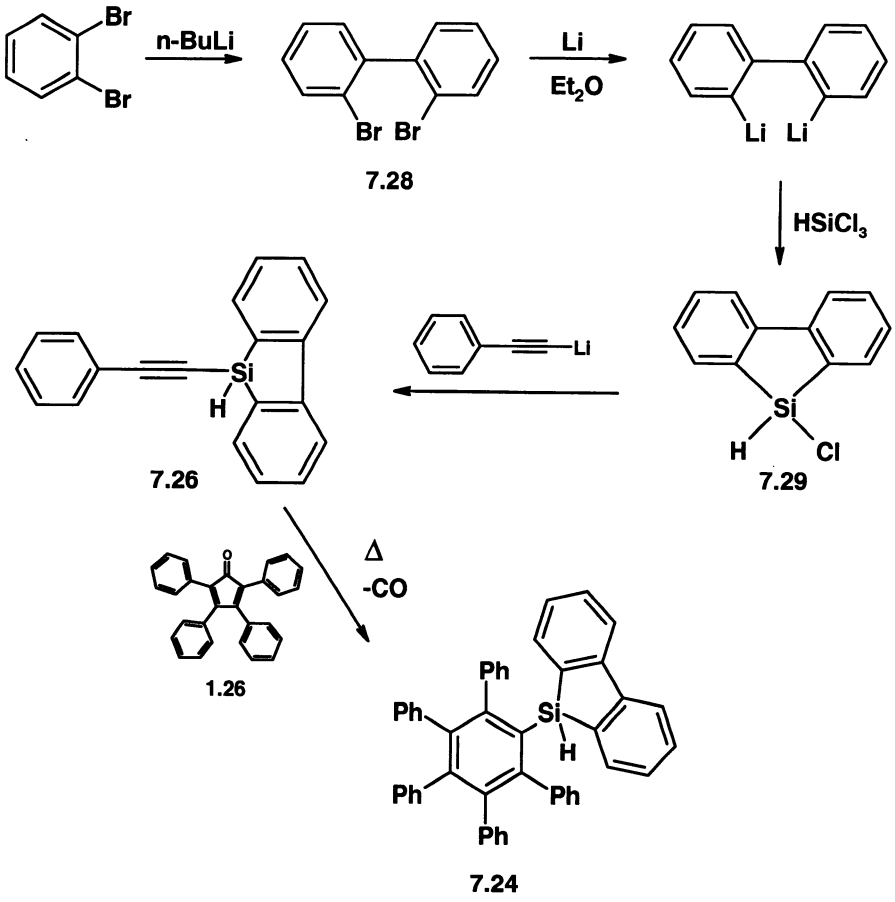

If deprotonation and elimination of chloride occurs with formation of the silylene (as in the carbon analogue), an alternative route can be chosen. For instance, initial treatment of the trichlorosilane with an excess of phenylethynyl lithium would yield the phenylethynyl silane **7.30**. Addition of the 2,2'-dilithiobiphenyl would then produce the final alkyne product, avoiding the elimination step completely (Scheme 7.10).

Scheme 7.10

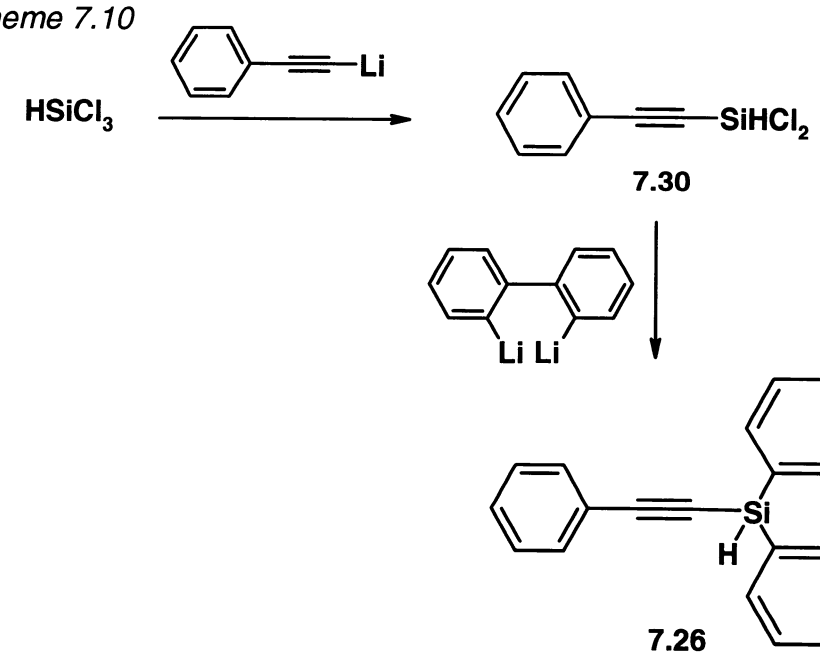

Another alternative route involves the formation of the dichloro silafluorene, which, when treated with one equivalent of phenylethynyl lithium, would afford **7.31** (Scheme 7.11). Reduction to the alkyne **7.26** can then be accomplished by treatment of **7.31** with lithium aluminum hydride, which would not be expected to reduce the triple bond since there is not a hydroxy or ether functional group near the alkyne functionality.[433]

Complex **7.24** can then be investigated using variable-temperature NMR spectroscopy in order to determine the barrier to rotation of the sila-fluorenyl and phenyl substituents. Coordination of a metal moiety to the 6-membered ring, followed by deprotonation and migration to the 5-membered ring should increase the steric hindrance in the complex and allow for pH control over the barrier to rotation. An X-ray crystallographic analysis would offer insight into the steric

crowding surrounding the sila-fluorene, and allow for the determination of possible metal coordination.

Scheme 7.11

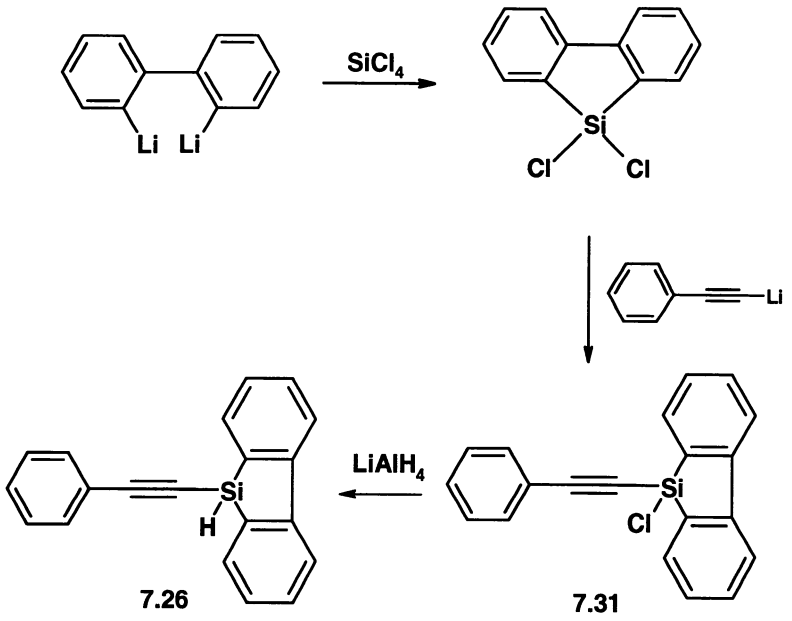

CHAPTER EIGHT

Experimental Details

8.1 General Methods

All reactions involving organometallic reagents were carried out under an atmosphere of dry nitrogen employing conventional benchtop and glovebag techniques. Tetrahydrofuran and diethyl ether solvents were dried according to standard procedures before use.[434] Silica gel (Rose Scientific; particle size 20-45 μm) was employed for flash column chromatography. ^{1}H and ^{13}C NMR spectra were obtained on a Bruker AV200 spectrometer at 200 MHz and 50 MHz, respectively, or on a Bruker Avance DRX-500 spectrometer at 500.13 MHz and 125.76 MHz, respectively, or on a Bruker AV-600 spectrometer at 600.13 MHz and 150.92 MHz, respectively, and were referenced to the residual proton signal, or ^{13}C signal, of the solvent. Spectra were collected at room temperature unless otherwise noted, and all assignments were based on standard ^{1}H-^{1}H and ^{1}H-^{13}C two-dimensional techniques (COSY, HSQC, HMBC). ^{31}P NMR spectra were acquired at 202.46 MHz and were externally referenced to the ^{31}P signal of 85% H_3PO_4 in D_2O. Mass spectra were measured on a Finnigan 4500 spectrometer by direct electron impact (DEI) or direct chemical ionization (DCI) with NH_3, or on a Micromass GCT TOF instrument, as well as electrospray (ESI). Infrared spectra were recorded on a Bio-Rad FTS-40 spectrometer, *in situ* infrared spectra were recorded on an ASI Applied Systems ReactIR 1000 with a SiComp probe. Melting points (uncorrected) were determined on a Fisher-Johns

melting point apparatus. Elemental analyses were performed by Guelph Chemical Laboratories, Guelph, Ontario, Canada.

The reagents not described below were used as received from commercial sources. (Acetylacetonato)bis(ethylene)rhodium(I),[435] (acetylacetonato)(2,3,4,5-tetraphenylcyclopentadienone) rhodium(I) (**2.9**),[92] 1,3-bis(*m*-xylyl)propanone,[209] 2,4,5-triphenyl-3-ferrocenylcyclopentadienone (**1.27**),[436] $Pd(PPh_3)_4$,[437] tributylstannylindene[438] and 9-phenylethynylfluoren-9-ol[371] were prepared as previously described.

8.2 Lineshape Analysis

NMR simulations (Chapter 2) were carried out using the program MEXICO.[28,439] The program did an iterative least-squares fit of the calculated lineshape to the experimental data, and was capable of varying all the parameters: shifts, couplings and rates. This was a standard, non-mutual (non-degenerate) exchange problem. In this analysis, the chemical shift difference and rate were varied (using a simplex algorithm) to obtain the best fit. Errors were estimated by changing the parameters and visually monitoring the fit to the experimental data; the errors quoted correspond to a clear and obvious mismatch between calculated and observed spectra.

8.3 Preparative Purifications

The separation and purification of fractions resulting from the protonation of tetraphenylcyclopentadienone (Chapter 4) were performed on an HP 1090 Series II liquid chromatograph equipped with an HP diode array detector (200 – 600 nm). Analytical injections (5 μL) were made onto a Restek PAH column (4.6 mm x 200 mm, 3μm packing, Restek, Belefonte, PA) at a flow rate of 0.80 mL min^{-1}. Preparative HPLC separations (100 μL injection volume) were performed using an Envirosap PAH column (10 mm x 250 mm, 5 μm C_{18}; Phenomenex, Torrence, CA) at a flow rate of 3.5 mL min^{-1}. The solvent gradient program used was as follows: 0 min., 85% CH_3CN, 15% H_2O; 10 min., 100% CH_3CN; 15 min., 25% CH_2Cl_2, 75 % CH_3CN. UV/Vis spectra were collected during all runs from 240 to 600 nm. Different spectral windows were used for monitoring the chromatograms in real time, depending on whether the runs were analytical or preparative. For the analytical runs, the spectral windows were (a) 250 – 390 nm and (b) 252 – 286 nm. For the preparative runs the spectral windows were shifted to accommodate the significant absorbances. Samples for preparative separations were prepared by dissolving solid products from column chromatography fractions in 50:50 CH_3CN:CH_2Cl_2 to a concentration of 50 mg mL^{-1}. These solutions were filtered through a Luer-fitted 13 μm filter into a clean glass autosampler vial (2 mL). All peaks collected in the preparative mode were analyzed directly on the analytical column to determine the purity of the collected samples.

8.4 Computational Details

Optimization of model geometries (Chapter 4) were performed using ADF 2002.01,[440] with gradient-corrected density-functional-theory (DFT) with Becke's exchange functional[441] and Perdew's correlation functional[442] (BP86). All basis functions have triple-ζ quality and are composed of uncontracted Slater-type orbitals (STOs).[443] The $(1s)^2$ core electrons of C and O and the (1s2s2p) core electrons of Fe have been treated with the frozen core approximation.[444] In each SCF cycle, an auxiliary basis set of s, p, d, f and g STOs has been used to fit the molecular densities and to represent the Coulomb and exchange potentials. The barriers to rotation have not been corrected for zero-point energies.

8.5 Crystallographic Data

X-ray crystallographic data were collected from suitable samples mounted with epoxy on the end of thin glass fibers. For **2.16a**, the rapid lattice solvent evaporation was minimized by the mounting of a suitable crystal in an atmosphere saturated with solvent, and quickly freezing it to 173 K on the diffractometer. Data were collected on a P4 Bruker diffractometer equipped with a Bruker SMART 1K CCD area detector or on a 3-circle D8 Bruker diffractometer equipped with a Bruker SMART 6000 CCD area detector (both employing the program SMART)[445] and a rotating anode utilizing graphite-monochromated Mo Kα radiation (λ = 0.710 73 Å) or a rotating anode utilizing cross-coupled parallel focusing mirrors to provide monochromated Cu Kα radiation (λ = 1.541 78 Å),

respectively. Data processing was carried out by use of the program SAINT,[446] while the program SADABS[447] was utilized for the scaling of diffraction data, the application of a decay correction and an empirical absorption correction based on redundant reflections. Structures were solved by using the direct-methods procedure in the Bruker SHELXL[448] program library and refined by full-matrix least-squares methods on F^2. All non-hydrogen atoms were refined using anisotropic thermal parameters, with the exception of **2.17b**, **3.16** and **4.38**, in which the crystals did not diffract beyond ~1 Å, creating difficulties in refining anisotropically on the carbon atoms. Hydrogen atoms were added as fixed contributors at calculated positions, with isotropic thermal parameters based on the carbon atom to which they are bonded. In the course of the refinement process for **2.17a** and **2.17b**, several dichloromethane solvent molecules were located in the asymmetric unit, and a satisfactory refinement of the solvate atomic positions was not attained, though the diffraction data allowed for complete anisotropic refinement of the target molecules. As a result, the values for the residual electron density in the region of the solvent molecules and the refinement statistics associated with the structures are high. Three disordered naphthyl groups were located in the course of the refinement process for **3.16**, which complicated the analysis; rigid naphthyl groups were imposed. For **3.13**, an *ab initio* structure solution was obtained using Accelrys Materials Studio Version 2.2.1 (2002) by Accelrys Inc.[240] Fully labelled thermal ellipsoid plots for all structures are provided in Appendix I.

8.6 Synthesis and Characterization of Prepared Compounds

1,2-Di-(β-naphthyl)-2-hydroxyethanone, β-naphthoin (2.13): In an adaptation of the literature procedure for the synthesis of benzoin,[406] β-naphthaldehyde (10.1 g, 0.06 mmol) and NaCN (1.9 g, 0.04 mmol) were dissolved in 20 mL H_2O and 40 mL ethanol, then stirred under reflux for approximately 30 minutes, resulting in the formation of a thick, yellow precipitate, which was filtered by suction and dried to give **2.13** (8.2 g, 0.03 mol; 88%) as a pale yellow powder, mp 124–126 °C (lit.[449] 125–126 °C). Further concentration of the reaction mixture gave an additional 0.8 g of product, resulting in an overall yield of 96%. ^{1}H NMR (200 MHz, CD_2Cl_2): δ 8.53 (1H, s, naphthyl-H_1), 8.03–7.44 (13H, m, naphthyl rings), 6.31 (1H, s, CH), 4.68 (1H, br, OH). ^{13}C NMR (50 MHz, CD_2Cl_2): δ 199.3 (CO), 137.2, 136.1, 133.8, 133.5, 132.6, 131.3 (naphthyl C's), 131.6, 130.0, 129.4, 128.9, 128.3, 128.0, 127.7, 127.3, 126.9, 125.2, 124.5 (naphthyl CH's), 76.7 (CH-OH). MS (DEI; *m/z* (%)): 312 (M^+, 2%), 155 ($C_{10}H_7CO$, 99), 127 ($C_{10}H_7$, 100), 101 (C_8H_5, 13), 77 (C_6H_5, 24). MS (DCI (NH_3); *m/z* (%)): 330 (M+H+NH_3, 1%), 313 (M+H, 37), 312 (M^+, 22), 295 (M-OH, 100), 267 ($C_{21}H_{15}$, 4), 201 ($C_{16}H_9$, 15), 155 ($C_{10}H_7CO$, 26), 128 ($C_{10}H_8$, 4), 77 (C_6H_5, 1). HRMS (EI): Calculated for $C_{22}H_{16}O_2$: 312.1150. Found: 312.1135.

1,2-Di-(β-naphthyl)ethan-1,2-dione, β-naphthil (2.14): The literature procedure for the synthesis of benzil[407] was modified for the preparation of **2.14**. Thus,

$CuSO_4$ (8.8 g, 0.05 mol) was added to 13 mL pyridine and 25 mL H_2O in a 250 mL round-bottom flask. When all the $CuSO_4$ was dissolved, 1,2-di-(β-naphthyl)-2-hydroxyethanone (**2.13**) (8.2 g, 0.03 mol) was added and the reaction mixture was stirred under reflux for approximately 2 hours, then left to cool overnight. The blue aqueous layer was decanted, leaving a yellow solid that was washed with water, then with hot HCl (10%). The product was filtered, then dissolved in CH_2Cl_2, dried over $MgSO_4$, filtered and the solvent was removed under vacuum to give **2.14** (7.5 g, 0.02 mol; 93%) as a yellow powder, mp 157–160 °C (lit.[449] 158–159 °C). ^1H NMR (200 MHz, CD_2Cl_2): [assignments are quoted with respect to the normal labeling for a β-naphthyl substituent] δ 8.47 (1H, s, naphthyl-H_1), 8.15 (1H, dd, $^3J_{H4-H3}$ = 8.6 Hz, $^3J_{H4-H5}$ = 1.5 Hz, naphthyl-H_4), 8.04-7.92 (3H, m, naphthyl-$H_{3,5,8}$), 7.67 (1H, ddd, $^3J_{H6-H5,H6-H7}$ = 5.9 Hz, $^4J_{H6-H8}$ = 1.2 Hz, naphthyl-H_6), 7.58 (1H, ddd, $^3J_{H7-H6,H7-H8}$ = 7.6 Hz, $^4J_{H7-H5}$ = 1.2 Hz, naphthyl-H_7); (assignments for naphthyl-H_6 and H_7 may be interchanged). ^{13}C NMR (50 MHz, CD_2Cl_2): δ 195.2 (CO), 136.8, 132.7, 130.8 (naphthyl C's), 133.9, 130.2, 129.9, 129.5, 128.3, 127.6, 123.9 (naphthyl CH's). MS (DEI; *m/z* (%)): 310 (M^+, 6%), 155 ($C_{10}H_7CO$, 100), 127 ($C_{10}H_7$, 97), 101 (C_8H_5, 10), 77 (C_6H_5, 19). MS (DCI (NH_3); *m/z* (%)): 328 (M+NH_3+H, 37%), 311 (M+H, 69), 310 (M^+, 15), 190 (17), 172 ($C_{11}H_8O_2$, 52), 155 ($C_{10}H_7CO$, 100), 144 ($C_{10}H_8O$, 19), 80 (40). HRMS (EI): Calculated for $C_{22}H_{14}O_2$: 310.0994. Found: 310.0977.

3,4-Di-(β-naphthyl)-2,5-diphenylcyclopentadienone (**2.15a**): Analogous to the synthesis of tetracyclone,[450] β-naphthil (**2.14**) (4.7 g, 0.02 mol) and 1,3-diphenyl-propanone (3.5 g, 0.02 mol) were dissolved in 125 mL of hot ethanol with stirring. Once the reaction mixture began to reflux, KOH (0.9 g, 0.02 mol) dissolved in approximately 10 mL hot ethanol, was added dropwise through the top of the condenser. The solution darkened immediately from yellow to deep red, eventually turning very dark red/purple. The solution was stirred for approximately 30 minutes, then cooled and the solvent was removed under vacuum to leave **2.15a** (4.4 g, 9.13 mmol; 61%) as a dark purple powder, mp 227–230 °C (lit.[451] 227–229 °C). Calc. for $C_{37}H_{24}O \cdot H_2O$: C, 88.41; H, 5.22%. Found: C, 88.21; H, 4.68%. IR (CH_2Cl_2): ν_{max}/cm^{-1} at 1710 (CO). ^1H NMR (500 MHz, CD_2Cl_2): δ 7.76 (2H, d, $^3J_{H5\text{-}H6}$ = 7.9 Hz, naphthyl-H_5), 7.62 (2H, d, $^3J_{H4\text{-}H3}$ = 8.3 Hz, naphthyl-H_4), 7.49 (2H, d, $^3J_{H8\text{-}H7}$ = 8.8 Hz, naphthyl-H_8), 7.48 (2H, s, naphthyl-H_1), 7.46 (2H, dd, $^3J_{H6\text{-}H5}$ = 7.5 Hz, $^3J_{H6\text{-}H7}$ = 7.5 Hz, naphthyl-H_6), 7.37 (2H, dd, $^3J_{H7\text{-}H6}$ = 7.2 Hz, $^3J_{H7\text{-}H8}$ = 7.2 Hz, naphthyl-H_7), 7.30 (6H, s, phenyl-$H_{2,4,6}$), 7.25 (4H, s, phenyl-$H_{3,5}$), 7.11 (2H, d, $^3J_{H3\text{-}H4}$ = 8.2 Hz, naphthyl-H_3). ^{13}C NMR (125 MHz, CD_2Cl_2): δ 200.9 (CO), 155.2 (naphthyl-C_2, cyclopentadienone-C_3), 133.6 (naphthyl-C_{4a}), 133.4 (naphthyl-C_{8a}), 131.7 (phenyl-C_1), 131.5 (cyclopentadienone-C_2), 130.9 (phenyl-$C_{2,6}$), 129.7 (naphthyl-C_1), 128.8 (naphthyl-C_8), 128.6 (phenyl-$C_{3,4,5}$), 128.3 (naphthyl-C_5), 128.1 (naphthyl-C_4), 127.4 (naphthyl-$C_{6,3}$), 126.9 (naphthyl-C_7); (assignments for naphthyl-H,C_5 and H,C_8, naphthyl-H,C_6 and H,C_7 and naphthyl-C_{4a} and C_{8a} may be interchanged).

MS (DEI; *m/z* (%)): 484 (M^+, 2%), 280 ($C_{10}H_7CHCHC_{10}H_7$, 10), 228 ($C_{10}H_7C{\equiv}CC_6H_5$, 4), 140 ($C_{10}H_7CH$, 12), 125 (15), 85 (62), 84 (100). MS (DCI (NH_3); *m/z* (%)): 485 (M+H, 17%), 228 ($C_{10}H_7C{\equiv}CC_6H_5$, 2), 136 (14), 125 (100). HRMS (EI): Calculated for $C_{37}H_{24}O$: 484.1827. Found: 484.1808.

3,4-Di-(β-naphthyl)-2,5-di(*m*-xylyl)cyclopentadienone (**2.15b**): As with **2.15a**, β-naphthil (**2.14**) (0.8 g, 2.0 mmol) and 1,3-bis(3,5-dimethylphenyl)propanone[209] (1.0 g, 3.8 mmol) were dissolved in 125 mL of hot ethanol with stirring. While the mixture was refluxing, KOH (0.3 g, 5.4 mmol) dissolved in 10 mL hot ethanol was added dropwise through the top of the condenser, and the solution darkened to a red/purple colour. The solution was stirred for approximately 30 minutes, then cooled, resulting in the formation of a dark purple solid which was collected by vacuum filtration to give **2.15b** (0.9 g, 1.6 mmol; 82%), mp 285–288°C. Calc for $C_{42}H_{32}O$: C, 91.08; H, 5.97%. Found: C, 90.65; H, 6.09%. IR (CH_2Cl_2): ν_{max}/cm^{-1} at 1708 (CO). ^1H NMR (500 MHz, CD_2Cl_2): δ 7.75 (2H, dd, $^3J_{H5\text{-}H6}$ = 8.1 Hz, $^4J_{H5\text{-}H7}$ = 1.2 Hz, naphthyl-H_5), 7.60 (2H, d, $^3J_{H4\text{-}H3}$ = 8.4 Hz, naphthyl-H_4), 7.48 (2H, d, $^3J_{H8\text{-}H7}$ = 8.1 Hz, naphthyl-H_8), 7.44 (2H, s, naphthyl-H_1), 7.43 (2H, ddd, $^3J_{H6\text{-}H7}$ = 7.5 Hz, $^3J_{H6\text{-}H5}$ = 6.9 Hz, $^4J_{H6\text{-}H8}$ = 1.3 Hz, naphthyl-H_6), 7.35 (2H, ddd, $^3J_{H7\text{-}H6}$ = 8.1 Hz, $^3J_{H7\text{-}H8}$ = 6.9 Hz, $^4J_{H7\text{-}H5}$ = 1.2 Hz, naphthyl-H_7), 7.10 (2H, dd, $^3J_{H3\text{-}H4}$ = 8.5 Hz, $^4J_{H3\text{-}H1}$ = 1.7 Hz, naphthyl-H_3), 6.88 (6H, s, xylyl-$H_{2,4,6}$), 2.16 (12H, s, xylyl-CH_3). ^{13}C NMR (50 MHz, CD_2Cl_2): δ 201.2 (C=O), 154.8 (naphthyl-C_2), 138.1 (xylyl-$C_{3,5}$), 133.6 (naphthyl-C_{4a}), 133.3 (naphthyl-C_{8a}), 131.7

(cyclopentadienone-C_2), 131.5 (cyclopentadienone-C_3), 129.9 (xylyl-C_4), 129.6 (naphthyl-C_1), 128.7 (naphthyl-C_8), 128.5 (xylyl-$C_{2,6}$), 128.2 (naphthyl-C_5), 127.9 (naphthyl-C_4), 127.5 (naphthyl-C_3), 127.2 (naphthyl-C_6), 127.0 (xylyl-C_1), 126.7 (naphthyl-C_7), 21.6 (xylyl-CH_3); (assignments for naphthyl-H,C_5 and H,C_8, naphthyl-H,C_6 and H,C_7 and naphthyl-C_{4a} and C_{8a} may be interchanged). MS (DEI; *m/z* (%)): 540 (M^+, 27%), 512 (M-CO, 4), 278 ($C_{10}H_7C{\equiv}CC_{10}H_7$, 11), 256 ($C_{10}H_7C{\equiv}CC_6(CH_3)_2H_3$, 25), 239 (6), 128 ($C_{10}H_8$, 4), 84 (100). MS (DCI (NH_3); *m/z* (%)): 557 (M+NH_3, 8%), 541 (M+H, 100), 279 ($C_{10}H_7C{\equiv}CC_{10}H_7$+H, 8), 396 (M-$C_{10}H_7$-OH, 8), 256 ($C_{10}H_7C{\equiv}CC_6(CH_3)_2H_3$, 17), 86 (24). HRMS (EI): Calculated for $C_{41}H_{32}O$: 540.2453. Found: 540.2438.

(Acetylacetonato)(3,4-di-(β-naphthyl)-2,5-diphenylcyclopentadienone)-rhodium(I), (2.16a): (Acetylacetonato)bis(ethylene)rhodium(I) (0.2 g, 0.9 mmol) and **2.15a** (0.3 g, 0.5 mmol) were dissolved in 30 mL dry THF and stirred under gentle reflux for approximately 2 hours under an atmosphere of dry nitrogen. The volume of the solution was reduced to half under vacuum, and 10 mL of hexanes was added, resulting in the formation of a red precipitate, which was collected by vacuum filtration to give **2.16a** (0.3 g, 0.4 mmol; 78%) as a red powder, mp 267 °C (dec). Crystals of **2.16a** were grown by recrystallization and slow evaporation from CH_2Cl_2. Calc for $C_{42}H_{31}O_3Rh$: C, 73.47; H, 4.55%. Found: C, 73.95; H, 4.34%. IR (CH_2Cl_2): ν_{max}/cm^{-1} at 1640 (CO). ^1H NMR (500 MHz, CD_2Cl_2): δ 7.95 (2H, s, naphthyl-H_1), 7.83 (4H, dd, $^3J_{H2\text{-}H3}$ = 7.2 Hz, $^4J_{H2\text{-}H4}$ = 1.3

Hz, phenyl-$H_{2,6}$), 7.73 (2H, dd, $^3J_{H5-H6}$ = 8.1 Hz, $^4J_{H5-H7}$ = 1.3 Hz, naphthyl-H_5), 7.59 (2H, d, $^3J_{H4-H3}$ = 8.5 Hz, naphthyl-H_4), 7.56 (2H, d, $^3J_{H8-H7}$ = 8.2 Hz, naphthyl-H_8), 7.50 (2H, dd, $^3J_{H3-H4}$ = 8.5 Hz, $^4J_{H3-H1}$ = 1.2 Hz, naphthyl-H_3), 7.45 (2H, ddd, $^3J_{H6-H7}$ = 8.1 Hz, $^3J_{H6-H5}$ = 6.9 Hz, $^4J_{H6-H8}$ = 1.3 Hz, naphthyl-H_6), 7.38 (2H, ddd, $^3J_{H7-H6}$ = 8.1 Hz, $^3J_{H7-H8}$ = 6.9 Hz, $^4J_{H7-H5}$ = 1.3 Hz, naphthyl-H_7), 7.33 (2H, tt, $^3J_{H4-H(3+5)}$ = 7.2 Hz, $^4J_{H4-H(2+6)}$ = 1.3 Hz, phenyl-H_4), 7.26 (4H, dd, $^3J_{H3-H2}$ = 7.8 Hz, $^3J_{H3-H4}$ = 7.2 Hz, phenyl-$H_{3,5}$), 5.50 (1H, s, acac-γH), 2.13 (6H, s, acac-CH_3). ^{13}C NMR (125 MHz, CD_2Cl_2): δ 188.1 (acac-CO), 163.6 (C=O), 133.5 (naphthyl-C_{4a}), 133.3 (naphthyl-C_{8a}), 131.3 (phenyl-$C_{2,6}$, naphthyl-C_1), 128.5 (naphthyl-$C_{8,3}$), 128.4 (phenyl-$C_{3,4,5}$), 128.3 (naphthyl-C_5), 128.1 (naphthyl-C_4), 127.3 (naphthyl-C_6), 127.0 (naphthyl-C_7), 99.5 (acac-γC), 95.5 (cyclopentadienone-C_3), 95.4 (naphthyl-C_2), 76.1 (cyclopentadienone-C_2), 76.1 (phenyl-C_1), 27.7 (acac-CH_3); (assignments for naphthyl-H,C_5 and H,C_8, naphthyl-H,C_6 and H,C_7 and naphthyl-C_{4a} and C_{8a} may be interchanged). MS (ESI; *m/z* (%)) 687 (M+H, 4%), 669 (M-H_2O, 100). HRMS (EI): Calculated for $C_{42}H_{31}O_3Rh$: 686.1328. Found: 686.1240.

(Acetylacetonato)[3,4-di-(β-naphthyl)-2,5-di(*m*-xylyl)cyclopentadienone]-rhodium(I), (2.16b): As with **2.16a**, (acetylacetonato)bis(ethylene)rhodium(I) (0.4 g, 1.6 mmol) and **2.15b** (0.8 g, 1.5 mmol) were dissolved in 30 mL dry THF and stirred under gentle reflux for approximately 2 hours under an atmosphere of dry nitrogen. The volume of the solution was reduced under vacuum to

approximately 15 mL, then 10 mL of hexanes was added dropwise, resulting in the formation of a precipitate of **2.16b** (1.0 g, 1.4 mmol; 90%) as a red powder which was collected by vacuum filtration, mp 244–247 °C. Crystals of **2.16b** were grown by recrystallization and slow evaporation from CH_2Cl_2. Calc for $C_{46}H_{39}O_3Rh$: C, 74.39; H, 5.29%. Found: C, 73.85; H, 5.70%. IR (CH_2Cl_2): ν_{max}/cm^{-1} at 1638 (CO). ^1H NMR (500 MHz, CD_2Cl_2): δ 7.99 (2H, s, naphthyl-H_3), 7.73 (2H, d, $^3J_{H8-H7}$ = 8.1 Hz, naphthyl-H_8), 7.58 (2H, s, naphthyl-H_1), 7.58 (2H, d, $^3J_{H5-H6}$ = 7.8 Hz, naphthyl-H_5), 7.54 (2H, s, naphthyl-H_4), 7.52 (4H, s, xylyl-$H_{2,6}$), 7.44 (2H, dd, $^3J_{H7-H6}$ = 7.0 Hz, $^4J_{H7-H5}$ = 7.0 Hz, naphthyl-H_7), 7.37 (2H, dd, $^3J_{H6-H7}$ = 7.2 Hz, $^3J_{H6-H5}$ = 7.2 Hz, naphthyl-H_6), 6.97 (2H, s, xylyl-H_4), 5.53 (1H, s, acac-γH), 2.24 (12H, s, xylyl-CH_3), 2.16 (6H, s, acac-CH_3). ^{13}C NMR (125 MHz, CD_2Cl_2): δ 188.0 (acac-CO), 164.0 (C=O), 133.4 (naphthyl-C_{4a}), 133.3 (naphthyl-C_{8a}), 131.2 (naphthyl-C_3), 130.0 (xylyl-C_4), 129.6 (xylyl-$C_{3,5}$), 129.1 (xylyl-$C_{2,6}$), 128.5 (naphthyl-C_4), 128.5 (naphthyl-C_1), 128.3 (naphthyl-C_8), 127.9 (naphthyl-C_5), 127.2 (naphthyl-C_7), 126.9 (naphthyl-C_6), 99.5 (acac-γC), 95.6 (cyclopentadienone-C_3), 95.5 (naphthyl-C_2), 76.8 (cyclopentadienone-C_2), 76.7 (xylyl-C_1), 27.7 (acac-CH_3), 21.5 (xylyl-CH_3); (assignments for naphthyl-H,C_5 and H,C_8, naphthyl-H,C_6 and H,C_7 and naphthyl-C_{4a} and C_{8a} may be interchanged). MS (ESI; *m/z* (%)) 743 (M+H, 2%), 725 (M-H_2O, 100), 684 (M-CO-2CH_3-H, 11). HRMS (EI): Calculated for $C_{46}H_{39}O_3Rh$: 742.1954. Found: 742.1894.

(Acetylacetonato)(3,4-di-(β-naphthyl)-2,5-diphenylcyclopentadienone)(triphenylphosphine) rhodium(I), (**2.17a**): Triphenylphosphine (0.1 g, 0.2 mmol) was dissolved in 10 mL dry THF and added by syringe to a stirring solution of **2.16a** (0.1 g, 0.2 mmol) in 30 mL dry THF under an atmosphere of dry nitrogen. The mixture was stirred under reflux for 1 hour, and the solvent was reduced to half under vacuum. Hexanes (10 mL) was added, resulting in the formation of a yellow precipitate, which was collected by vacuum filtration to give **2.17a** (0.2 g, 0.2 mmol; 98%) as a yellow powder, mp 185-188 °C. Crystals of **2.17a** were grown by recrystallization and slow evaporation from CH_2Cl_2. Calc for $C_{60}H_{46}O_3PRh{\cdot}CH_2Cl_2$: C, 70.92; H, 4.69%. Found: C, 70.60; H, 4.15%. IR (CH_2Cl_2): ν_{max}/cm^{-1} at 1635 (CO). ^1H NMR (500 MHz, CD_2Cl_2): δ 8.03 (2H, s, naphthyl-H_1), 7.70 (4H, d, $^3J_{H2\text{-}H3}$ = 7.5 Hz, phenyl-$H_{2,6}$), 7.64 (2H, dd, $^3J_{H5\text{-}H6}$ = 7.0 Hz, $^4J_{H5\text{-}H7}$ = 1.6 Hz, naphthyl-H_5), 7.62 (2H, dd, $^3J_{H8\text{-}H7}$ = 7.1 Hz, $^4J_{H8\text{-}H6}$ = 1.8 Hz, naphthyl-H_8), 7.45 (2H, d, $^3J_{H4\text{-}H3}$ = 8.6 Hz, naphthyl-H_4), 7.37 (2H, dd, $^3J_{H6\text{-}H7}$ = 7.9 Hz, $^3J_{H6\text{-}H5}$ = 6.9 Hz, naphthyl-H_6), 7.36 (2H, dd, $^3J_{H7\text{-}H6}$ = 7.9 Hz, $^3J_{H7\text{-}H8}$ = 6.8 Hz, naphthyl-H_7), 7.27 (2H, d, $^3J_{H3\text{-}H4}$ = 8.5 Hz, naphthyl-H_3), 7.21 (6H, d, $^3J_{H2\text{-}H3}$ = 8 Hz, PPh_3-phenyl-$H_{2,6}$), 7.21 (3H, t, $^3J_{H4\text{-}H3}$ = 8 Hz, PPh_3-phenyl-H_4), 7.17 (2H, t, $^3J_{H4\text{-}H3}$ = 7.4 Hz, phenyl-H_4), 7.02 (4H, dd, $^3J_{H3\text{-}H4}$ = 7.7 Hz, $^3J_{H3\text{-}H2}$ = 7.7 Hz, phenyl-$H_{3,5}$), 6.97 (6H, dd, $^3J_{H3\text{-}H4}$ = 6.5 Hz, $^3J_{H3\text{-}H2}$ = 6.9 Hz, PPh_3-phenyl-$H_{3,5}$), 5.13 (1H, s, acac-γH), 1.80 (6H, s, acac-CH_3). ^{13}C NMR (125 MHz, CD_2Cl_2): δ 188.4 (acac-CO), 170.2 (C=O), 134.6 (d, $^2J_{CP}$ = 10.6 Hz, PPh_3-phenyl-$C_{2,6}$), 133.2 (naphthyl-C_{4a}), 133.0 (naphthyl-C_{8a}), 131.6 (naphthyl-C_1), 131.3 (d,

$^1J_{CP}$ = 50.7 Hz, PPh_3-phenyl-C_1), 131.0 (phenyl-$C_{2,6}$), 129.8 (PPh_3-phenyl-C_4), 128.8 (naphthyl-C_3), 128.5 (naphthyl-C_5), 128.1 (naphthyl-C_8), 128.0 (d, $^3J_{CP}$ = 12.9 Hz, PPh_3-phenyl-$C_{3,5}$), 127.9 (phenyl-$C_{3,5}$), 127.8 (naphthyl-C_6), 127.1 (naphthyl-C_4), 126.8 (naphthyl-C_7), 126.6 (phenyl-C_4), 104.7 (naphthyl-C_2, cyclopentadienone-C_3), 101.7 (acac-γC), 64.2 (phenyl-C_1, cyclopentadienone-C_2), 28.7 (acac-CH_3); (assignments for naphthyl-H,C_5 and H,C_8, naphthyl-H,C_6 and H,C_7 and naphthyl-C_{4a} and C_{8a} may be interchanged). ^{31}P NMR (202 MHz, CD_2Cl_2, 243 K): δ 22.5 (d, $^1J_{RhP}$ = 165.6 Hz, Rh-PPh_3); (202 MHz, CD_2Cl_2, 163 K): δ 23.5 (d, $^1J_{RhP}$ = 159.8 Hz, Rh-PPh_3), 22.9 (d, $^1J_{RhP}$ = 156.8 Hz, Rh-PPh_3). MS (ESI; *m/z* (%)): 949 (M+H, 3%), 890 (M-CO-2CH_3-H, 7), 849 (M+H-acac, 83), 557 ($C_4(C_6H_5)_2(C_{10}H_7)_2$Rh-H, 9), 277 ($C_{10}H_7C{\equiv}CC_{10}H_6$, 100).

(Acetylacetonato)(3,4-di-(β-naphthyl)-2,5-di-*m*-xylylcyclopentadienone)(triphenylphosphine) rhodium(I), (2.17b): Triphenylphosphine (0.3 g, 1.1 mmol) was dissolved in 10 mL dry THF and added by syringe to a stirring solution of **2.16b** (0.8 g, 1.1 mmol) in 30 mL dry THF under an atmosphere of dry nitrogen. The mixture was stirred under reflux for 1 hour, and the solvent was reduced to half under vacuum. Approximately 10 mL of hexanes was added, creating a yellow/orange precipitate of **2.17b**, (0.9 g, 0.9 mmol; 84%), which was collected by vacuum filtration, mp 188-191 °C. Crystals of **2.17b** were grown by recrystallization and slow evaporation from CH_2Cl_2. Calc for $C_{64}H_{54}O_3PRh{\cdot}2H_2O$: C, 73.84; H, 5.62%. Found: C, 73.44; H 6.45%. IR (CH_2Cl_2): ν_{max}/cm^{-1} at 1626

(CO). ^{1}H NMR (500 MHz, CD_2Cl_2): δ 8.14 (2H, s, naphthyl-H_1), 7.68 (4H, d, $^{3}J_{H5\text{-}H6}$ = ~7 Hz, naphthyl-$H_{5,8}$), 7.51 (2H, d, $^{3}J_{H4\text{-}H3}$ = 8.5 Hz, naphthyl-H_4), 7.41 (4H, s, xylyl-$H_{2,6}$), 7.39 (2H, d, $^{3}J_{H6\text{-}H5}$ = 6.8 Hz, naphthyl-H_6), 7.38 (2H, d, $^{3}J_{H7\text{-}H8}$ = ~7 Hz, naphthyl-H_7), 7.37 (2H, d, $^{3}J_{H3\text{-}H4}$ = 8.9 Hz, naphthyl-H_3), 7.31 (6H, d, $^{3}J_{H2\text{-}H3}$ = 8.6 Hz, PPh_3-phenyl-$H_{2,6}$), 7.27 (3H, t, $^{3}J_{H4\text{-}H3}$ = 7.3 Hz, PPh_3-phenyl-H_4), 7.05 (6H, dd, $^{3}J_{H3\text{-}H4}$ = 6.7 Hz, $^{3}J_{H3\text{-}H2}$ = 6.9 Hz, PPh_3-phenyl-$H_{3,5}$), 6.87 (2H, s, xylyl-H_4), 5.20 (1H, s, acac-γH), 2.15 (12H, s, xylyl-CH_3), 1.85 (6H, s, acac-CH_3), (couplings for naphthyl-$H_{5,7,8}$ were not well resolved as a result of overlap). ^{13}C NMR (125 MHz, CD_2Cl_2): δ 188.1 (acac-CO), 170.2 (C=O), 137.1 (xylyl-$C_{3,5}$), 134.7 (d, $^{2}J_{CP}$ = 17.6 Hz, PPh_3-phenyl-$C_{2,6}$), 133.2 (naphthyl-C_{4a}), 133.0 (naphthyl-C_{8a}), 131.6 (naphthyl-C_1), 131.5 (d, $^{1}J_{CP}$ = 43.2 Hz, PPh_3-phenyl-C_1), 130.0 (naphthyl-C_7), 129.7 (PPh_3-phenyl-C_4), 129.2 (xylyl-C_2), 128.3 (xylyl-C_4), 128.2 (naphthyl-C_5), 128.1 (naphthyl-C_8), 127.9 (d, $^{3}J_{CP}$ = 9.2 Hz, PPh_3-phenyl-$C_{3,5}$), 127.0 (naphthyl-C_4), 126.7 (naphthyl-C_3), 126.5 (naphthyl-C_6), 104.4 (naphthyl-C_2, cyclopentadienone-C_3), 101.4 (acac-γC), 64.3 (xylyl-C_1, cyclopentadienone-C_2), 28.8 (acac-CH_3), 21.5 (xylyl-CH_3); (assignments for naphthyl-H,C_5 and H,C_8, naphthyl-H,C_6 and H,C_7 and naphthyl-C_{4a} and C_{8a} may be interchanged). ^{31}P NMR (202 MHz, CD_2Cl_2, 243 K): δ 23.4 (d, $^{1}J_{RhP}$ = 167.3 Hz, Rh-PPh_3); (202 MHz, CD_2Cl_2, 163 K): δ 23.5 (d, $^{1}J_{RhP}$ = 164.2 Hz, Rh-PPh_3), 23.2 (d, $^{1}J_{RhP}$ = 158.4 Hz, Rh-PPh_3). MS (ESI; *m/z* (%)): 1005 (M+H, 7), 946 (M-CO-2CH_3-H, 38), 905 (M-Hacac, 18), 743 (M-PPh_3, 11), 725 (M-PPh_3-H_2O, 100), 684 (M-PPh_3-CO-2CH_3, 9), 631 (13).

(Acetylacetonato)(2,3,4,5-tetraphenylcyclopentadienone)(triphenyl-phosphine) rhodium(I), (**2.17c**): As with **2.17a**, triphenylphosphine (0.2 g, 0.8 mmol) was dissolved in 10 mL dry THF and added dropwise by syringe to a stirring solution of **2.9** (0.3 g, 0.4 mmol) in 30 mL dry THF under an atmosphere of dry nitrogen. After heating to reflux for 1 hour, the solvent was removed under vacuum to give **2.17c** (0.1 g, 0.2 mmol, 36%) as a yellow/orange powder, mp 136 °C (dec). Calc for $C_{52}H_{42}O_3PRh{\cdot}CH_2Cl_2$: C, 68.23; H, 4.76%. Found: C, 68.10; H, 5.06%. IR (CH_2Cl_2): ν_{max}/cm^{-1} at 1627 (CO). ^1H NMR (500 MHz, CD_2Cl_2): δ 7.65, 7.29 (8H, d, $^3J_{H2\text{-}H3}$ = 7.6 Hz, phenyl-$H_{2,6}$), 5.94 (9H, m, PPh_3), 7.14 (4H, t, $^3J_{H4\text{-}H3}$ = 7.0 Hz, phenyl-H_4), 7.08, 7.05 (8H, dd, $^3J_{H3\text{-}H4}$ = 7.4 Hz, $^3J_{H3\text{-}H2}$ = 8.5 Hz, phenyl-$H_{3,5}$), 6.97 (6H, s, PPh_3), 4.98 (1H, s, acac-γH), 1.75 (6H, s, acac-CH_3). ^{13}C NMR (125 MHz, CD_2Cl_2): δ 188.1 (acac-CO), 170.0 (C=O), 135.5, 134.6, 134.5, 132.7, 131.6, 131.0, 129.7, 128.0, 127.9, 127.8, 126.5 (aromatic rings), 101.6 (acac-γC), 28.8 (acac-CH_3). ^{31}P NMR (81 MHz, CD_2Cl_2): δ 21.1 (d, $^1J_{RhP}$ = 162.5 Hz, Rh-PPh_3). MS (ESI; *m/z* (%)): 849 (M+H, 0.7%), 790 (M-CO-2CH_3-H, 9), 749 (M-Hacac, 100), 279 ($C_4(C_6H_5)_3$, 6).

Di-(β-naphthil)dihydrazone (**3.9**): Compound **3.9** was prepared according to the procedure for the synthesis of (dibenzil)dihydrazone.[452] β-naphthil (**2.14**, 4.5 g, 15 mmol) was dissolved in 50 mL *n*-propanol by heating and stirring, then hydrazine hydrate (1.9 mL, 40 mmol) was added dropwise, and the solution was stirred under reflux for 50 hours. The reaction mixture was cooled to room

temperature, then in ice, and the resulting white precipitate was filtered by suction and dried to give **3.9** (2.2 g, 6.4 mmol, 43%), as a white powder, mp 183-184 °C. Crystals of **3.9** were grown in an NMR tube by slow evaporation from CD_2Cl_2. ^1H NMR (600 MHz, CD_2Cl_2): δ 8.09 (1H, dd, $^3J_{H3-H4}$ = 9.0 Hz, 1.8 Hz, naphthyl-H_3), 7.86 (1H, d, $^3J_{H4-H3}$ = 8.4 Hz, naphthyl-H_4), 7.81 (1H, d, $^3J_{H8-H7}$ = 7.8 Hz, naphthyl-H_8), 7.74 (1H, s, naphthyl-H_1), 7.70 (1H, d, $^3J_{H5-H6}$ = 7.8 Hz, naphthyl-H_5), 7.44 (1H, dd, $^3J_{H6-H5}$ = 7.8 Hz, $^3J_{H6-H7}$ = 7.2 Hz, naphthyl-H_6), 7.40 (1H, dd, $^3J_{H7-H8}$ = 7.8 Hz, $^3J_{H7-H6}$ = 7.2 Hz, naphthyl-H_7), 5.92 (2H, s, NH_2). ^{13}C NMR (150 MHz, CD_2Cl_2): δ 142.3 (C=N), 134.1, 134.0 (naphthyl-$C_{4a,8a}$), 133.0 (naphthyl-C_2), 129.1 (naphthyl-C_5), 128.8 (naphthyl-C_4), 128.5 (naphthyl-C_8), 126.9 (naphthyl-C_6, C_7), 125.9 (naphthyl-C_1), 123.3 (naphthyl-C_3). MS (DEI; *m/z* (%)): 338 $[M]^+$ (49), 321 $[M\text{-}NH_3]^+$ (12), 294 $[(C_{10}H_7C)_2NH_2]$ (15), 278 $[C_{10}H_7C{\equiv}CC_{10}H_7]^+$ (10), 169 $[C_{10}H_7CNNH_2]^+$ (37), 153 $[C_{10}H_7CN]^+$ (46), 139 $[C_{10}H_7C]^+$ (26), 127 $[C_{10}H_7]^+$ (100), 115 $[C_9H_7]^+$ (21), 101 $[C_8H_5]^+$ (9), 84 $[(CNNH_2)_2]^+$ (28), 77 $[C_6H_5]^+$ (17), 59 (15). MS (DCI; *m/z* (%)): 340 $[M+2H]^+$ (100), 339 $[M+H]^+$ (38), 338 $[M]^+$ (14), 323 $[M\text{-}NH]^+$ (4), 312 $[M+2H\text{-}2N]^+$ (10). HRMS (EI): Calculated for $C_{22}H_{18}N_4$: 338.1531. Found: 338.1509.

Di-β-naphthylacetylene (**3.10**): The synthesis of **3.10** was adapted from a literature preparation.[453] Silver (I) oxide (2.0 g, 8.7 mmol) was added to a solution of **3.9** (0.8 g, 2.2 mmol) in 125 mL benzene. The mixture was stirred at room temperature for 3.5 hours, then filtered to remove any Ag_2O, leaving a bright

yellow solution. The solvent was removed under vacuum to give **3.10** (0.6 g, 2.1 mmol, 95%), mp 224 – 225 °C. Crystals of **3.10** were grown by recrystallization and slow evaporation from CH_2Cl_2. ^1H NMR (600 MHz, CD_2Cl_2): δ 8.12 (1H, s, br, naphthyl-H_1), 7.88 (1H, s, br, naphthyl-H_4), 7.86 (2H, s, br, naphthyl-$H_{5,8}$), 7.64 (1H, d, $^3J_{H3\text{-}H4}$ = 9.0 Hz, naphthyl-H_3), 7.55 – 7.53 (2H, m, naphthyl-$H_{6,7}$). ^{13}C NMR (150 MHz, CD_2Cl_2): δ 133.7, 133.5 (naphthyl-$C_{4a,8a}$), 132.0 (naphthyl-C_1), 128.9 (naphthyl-C_4), 128.7 (naphthyl-C_3), 128.3 (naphthyl-$C_{5,8}$), 127.4, 127.3 (naphthyl-$C_{6,7}$), 121.1 (naphthyl-C_2), 90.1 (C≡C). MS (DEI; *m/z* (%)): 278 $[M]^+$ (100), 139 $[C_{10}H_7C]^+$ (35), 138 $[C_{10}H_6C]^+$ (36). MS (DCI; *m/z* (%)): 296 $[M+H+NH_3]^+$ (100), 279 $[M+H]^+$ (93). HRMS (EI): Calculated for $C_{22}H_{14}$: 278.1096. Found: 278.1092.

Di-β-naphthylmethylketone (3.11): Bromomethylnaphthalene (5.2 g, 0.02 mol) was added to a solution of tetrabutylammonium bromide (0.9 g, 2.9 mmol) in 80 mL of benzene and 60 mL of 33% NaOH in water. The flask was protected from the light and iron pentacarbonyl was added dropwise (3.2 mL, 0.02 mol). The mixture was stirred under nitrogen for 3 hours, then poured into a beaker containing 50 mL of benzene and a few crystals of iodine. This solution was stirred for 30 minutes, then washed successively with aqueous sodium thiosulfate, 10% HCl and water. The organic fraction was dried over magnesium sulfate, filtered under suction and the solvent was removed using a rotary evaporator to give the desired product as a yellow powder (2.9 g, 9.4 mmol,

79%). The product was purified by column chromatography (50:50 hexanes, CH_2Cl_2) to give a white powder, mp 125 – 128 °C. ^{1}H NMR (500 MHz, CD_2Cl_2): δ 7.85 (2H, m, naphthyl-H_6), 7.83 (2H, d, $^3J_{H4-H3}$ = 8.7 Hz, naphthyl-H_4), 7.80 (2H, m, naphthyl-H_7), 7.65 (2H, s, naphthyl-H_1), 7.49 (4H, m, naphthyl-$H_{5,8}$), 7.30 (2H, d, $^3J_{H3-H4}$ = 8.3 Hz, naphthyl-H_3), 3.96 (4H, s, CH_2). ^{13}C NMR (125 MHz, CD_2Cl_2): δ 205.9 (CO), 134.2 (naphthyl-C_{4a}), 133.1 (naphthyl-C_2), 132.5 (naphthyl-C_{8a}), 128.9 (naphthyl-C_1), 128.8 (naphthyl-C_4), 128.3 (naphthyl-C_6), 128.2 (naphthyl-C_3), 128.1 (naphthyl-C_7), 126.8 (naphthyl-C_5), 126.3 (naphthyl-C_8), 49.9 (CH_2). MS (DEI; *m/z* (%)): 310 (M^+, 1), 256 (19), 186 (57), 160 (24), 141 ($C_{10}H_7$-CH_2, 100), 127 ($C_{10}H_7$, 33), 115 (34), 86 (51). MS (DCI; *m/z* (%)): 311 (M+H, 5), 310 (M^+, 7), 282 (6), 168 (5), 141 ($C_{10}H_7$-CH_2, 100), 115 (27), 84 (14). HRMS (EI): Calculated for $C_{22}H_{18}O$: 310.1358. Found: 310.1352.

Tetra-β-naphthylcyclopentadienone (3.12): Dinaphthylmethyl ketone (**3.11**, 1.1 g, 3.6 mmol) was dissolved in 25 mL of ethanol and added dropwise to a stirring solution of β-naphthil (**2.14**, 1.3 g, 4.3 mmol) and KOH (0.2 g, 3.6 mmol) in 100 mL ethanol. The solution was heated to reflux for 2 hours, gradually darkening from yellow to dark red/purple. The mixture was cooled to room temperature and filtered with suction to give a dark purple solid of **3.12** (1.3 g, 2.2 mmol, 61%), mp 264-267 °C. Crystals of **3.12** were grown by recrystallization and slow evaporation from CH_2Cl_2 and hexanes. ^{1}H NMR (500 MHz, CD_2Cl_2): δ 7.99 (2H, d, $^4J_{H1-H3}$ = 1.0 Hz, naphthyl-H_1), 7.77 (4H, d, $^3J_{H5-H6}$ = 9.5 Hz, naphthyl-

$H_{5,8}$), 7.76 (2H, d, $^3J_{H5\text{-}H6}$ = 8.2 Hz, naphthyl-H_5), 7.62 (2H, d, $^3J_{H4\text{-}H3}$ = 8.9 Hz, naphthyl-H_4), 7.61 (2H, d, $^3J_{H3\text{-}H4}$ = 9.4 Hz, naphthyl-H_3), 7.53 (2H, d, $^4J_{H1\text{-}H3}$ = ~1 Hz, naphthyl-H_1), 7.36 (2H, ddd, $^3J_{H6\text{-}H5}$ = 8.1 Hz, $^3J_{H6\text{-}H7}$ = 6.9 Hz, $^4J_{H6\text{-}H8}$ = 1.2 Hz, naphthyl-H_6), 7.22 (2H, dd, $^3J_{H4\text{-}H3}$ = 8.6 Hz, $^4J_{H4\text{-}H5}$ = 1.7 Hz, naphthyl-H_4), 7.14 (2H, dd, $^3J_{H3\text{-}H4}$ = 8.5 Hz, 1.7 Hz, naphthyl-H_3), 7.49 – 7.43 (8H, m, naphthyl-$H_{6,7,7,8}$). ^{13}C NMR (125 MHz, CD_2Cl_2): δ 200.9 (CO), 155.5 (naphthyl-C_2), 133.9, 133.7 (naphthyl-$C_{9,10}$), 133.4, 133.2 (naphthyl-$C_{9,10}$), 131.5 (cyclopentadienone-C), 130.6 (naphthyl-C_1), 129.9 (naphthyl-C_1), 129.2 (cyclopentadienone-C), 128.9 (naphthyl-$C_{5,8}$), 128.8, 127.4, 126.9, 126.7 (naphthyl-$C_{6,7,7,8}$), 128.3 (naphthyl-C_5), 128.2 (naphthyl-C_4), 128.1 (naphthyl-C_4), 127.9 (naphthyl-C_3), 127.5 (naphthyl-C_3), 126.9 (naphthyl-C_6), 126.5 (naphthyl-C_2). MS (DEI; *m/z*, (%)): 584 (M^+, 21), 278 ($C_{10}H_7$≡$C_{10}H_7$, 95), 247 (29), 155 ($C_{10}H_7$-CO, 100), 127 ($C_{10}H_7$, 69). MS (DCI; *m/z*, (%)): 585 (M+H, 25), 246 (21), 204 (100), 125 (38), 94 (26), 76 (35). HRMS (EI): Calculated for $C_{45}H_{28}O$: 584.2140. Found: 584.2139.

Hexa-β-naphthylbenzene (3.13): Benzophenone (5 g) was melted over a free flame in a 100 mL round-bottom flask fitted with an air condenser. Dinaphthylacetylene (**3.10**, 0.2 g, 0.8 mmol) and tetranaphthylcyclopentadienone (**3.12**, 0.6 g, 1.0 mmol) were added to the flask, which was heated over a free flame for 30-35 minutes. The solution was cooled almost to room temperature and 10 mL of benzene was added to prevent the solidification of the benzophenone. After cooling, 10 mL of hexanes was added, resulting in the

precipitation of a white powder of hexanaphthylbenzene (0.4 g, 0.5 mmol, 60%), collected by vacuum filtration, mp ~ 400 °C. ^{1}H NMR (500 MHz, d^{6}-DMSO, 363 K): δ 7.61 (1H, s), 7.44 (1H, s, br), 7.41 (1H, d, J_{HH} = 6.0 Hz), 7.24 (2H, s), 7.16 (2H, m). ^{1}H NMR (500 MHz, CD_2Cl_2, 303 K): δ 8.12 (1H, s, br), 7.87 (3H, s, br), 7.64 (1H, s, br), 7.53 (2H, s, br). ^{13}C NMR (125 MHz, CD_2Cl_2): δ 133.7 (naphthyl-C), 133.5 (naphthyl-C) 132.0 (naphthyl-CH), 129.0 (naphthyl-CH), 128.7 (naphthyl-CH), 128.4 (naphthyl-CH), 128.4 (naphthyl-CH), 127.4 (naphthyl-CH), 127.3 (naphthyl-CH), 121.2 (naphthyl-C), 90.6 (C_6). MS (ESI): 835.6 (M+H). HRMS (EI): Calculated for $C_{66}H_{42}$: 834.3287. Found: 834.3163.

2-Ferrocenyl-2-hydroxy-1-(β-naphthyl)ethanone: Ferrocene carboxaldehyde (7.1 g, 0.03 mol), β-naphthaldehyde (5.8 g, 0.04 mol) and NaCN (1.2 g, 0.02 mol) were dissolved in 20 mL H_2O and 40 mL ethanol, then heated to reflux for 1 hour. The solution was cooled, resulting in the formation of a red precipitate, which was collected by suction filtration to give the desired product (9.1 g, 0.02 mol, 73%), m.p. 142-145 °C (dec). The solid was purified by column chromatography under nitrogen (50:50 hexanes/CH_2Cl_2). ^{1}H NMR (500 MHz, CD_2Cl_2): δ 7.90 (1H, s, naphthyl-H_1), 7.88 (1H, d, $^{3}J_{H8-H7}$ = 8.9 Hz, naphthyl-H_8), 7.86 (1H, d, $^{3}J_{H4-H3}$ = 8.5 Hz, naphthyl-H_4), 7.84 (1H, dd, $^{3}J_{H5-H6}$ = 7.9 Hz, 1.7 Hz, naphthyl-H_5), 7.52 (1H, m, naphthyl-H_6), 7.50 (1H, m, naphthyl-H_7), 7.43 (1H, dd, $^{3}J_{H3-H4}$ = 8.5 Hz, $^{4}J_{H3-H1}$ = 1.6 Hz, naphthyl-H_3), 5.67 (1H, d, $^{3}J_{H-OH}$ = = 6.0 Hz, CH), 4.89 (1H, dd, $^{3}J_{H2-H3}$ = 1.3 Hz, $^{4}J_{H2-H4}$ = 1.3 Hz, ferrocenyl-H_2), 4.69 (1H, dd, $^{3}J_{H5-H4}$ = 1.3 Hz, $^{4}J_{H5-H2}$ =

1.3 Hz, ferrocenyl-H_5), 4.65 (1H, d, $^3J_{H\text{-}OH}$ = 6.0 Hz, OH), 4.56 (1H, ddd, $^3J_{H3\text{-}H2}$ = 2.4 Hz, $^3J_{H3\text{-}H2}$ = 2.4 Hz, $^4J_{H3\text{-}H5}$ = 1.2 Hz, ferrocenyl-H_3), 4.47 (1H, ddd, $^3J_{H4\text{-}H3}$ = 2.4 Hz, $^3J_{H4\text{-}H5}$ = 2.2 Hz, $^4J_{H4\text{-}H2}$ = 1.3 Hz, ferrocenyl-H_4), 4.08 (5H, s, ferrocenyl-C_5H_5). ^{13}C NMR (125 MHz, CD_2Cl_2): δ 203.6 (CO), 133.8 (naphthyl-C_{4a}), 133.7 (naphthyl-C_{8a}), 129.3 (naphthyl-C_4), 128.5 (naphthyl-C_8), 128.2 (naphthyl-C_2), 128.2 (naphthyl-C_5), 127.8 (naphthyl-C_1), 127.0 (naphthyl-C_6), 127.0 (naphthyl-C_7), 125.4 (naphthyl-C_3), 77.5 (ferrocenyl-*ipso*-C), 75.4 (C-OH), 73.6 (ferrocenyl-C_3), 73.6 (ferrocenyl-C_4), 70.8 (ferrocenyl-C_5), 70.7 (ferrocenyl-C_5H_5), 70.4 (ferrocenyl-C_2). IR (KBr): 3364 cm^{-1} (OH), 1656 cm^{-1} (CO). MS (DEI; *m/z* (%)): 370 (M^+, 96), 353 (M-OH, 17), 213 (C_5H_5-Fe-C_5H_4-CO, 100), 185 (C_5H_5-Fe-C_5H_4, 39), 129 (74), 121 (35), 81 (17). MS (DCI; *m/z* (%)): 372 (M+2H, 30), 371 (M+H, 100), 370 (M^+, 30), 353 (M-OH, 30), 213 (C_5H_5-Fe-C_5H_4-CO, 30), 129 (18). HRMS (EI): Calculated for $C_{22}H_{18}O_2Fe$: 370.0656. Found: 370.0647.

1-Ferrocenyl-2-(β-naphthyl)ethanedione (3.14): 2-Ferrocenyl-2-hydroxy-1-(β-naphthyl)ethanone (6.5 g, 0.02 mol) was dissolved in 150 mL $CHCl_3$ and heated to reflux. In small portions, freshly prepared MnO_2 was added (2.3 g, 0.02 mol) and the mixture was stirred under reflux for 24 hours. After cooling to room temperature, the solution was filtered and the solvent was removed by rotary evaporation to give **3.14** (5.7 g, 0.02 mol, 88%) as a red solid, m.p. 98-100 °C (dec). Pure **3.14** was obtained by column chromatography under nitrogen (50:50 CH_2Cl_2 : hexanes). ^1H NMR (500 MHz, CD_2Cl_2): δ 8.60 (1H, s, naphthyl-H_1),

8.12 (1H, dd, $^3J_{H3-H4}$ = 8.6 Hz, $^4J_{H3-H1}$ = 1.7 Hz, naphthyl-H_3), 8.00 (1H, d, $^3J_{H4-H3}$ = 8.6 Hz, naphthyl-H_4), 8.00 (1H, d, naphthyl-H_8), 7.93 (1H, dd, naphthyl-H_5), 7.66 (1H, ddd, $^3J_{H6-H7}$ = 7.5 Hz, $^3J_{H6-H5}$ = 6.9 Hz, $^4J_{H6-H8}$ = 1.2 Hz, naphthyl-H_6), 7.59 (1H, ddd, $^3J_{H7-H8}$ = 8.2 Hz, $^3J_{H7-H6}$ = 7.5 Hz, $^4J_{H7-H5}$ = 1.1 Hz, naphthyl-H_7), 4.90 (2H, dd, $^3J_{H2-H3}$ = 2.0 Hz, $^4J_{H2-H4}$ = 1.9 Hz, ferrocenyl-$H_{2,5}$), 4.71 (2H, dd, $^3J_{H3-H2}$ = 2.0 Hz, $^4J_{H3-H5}$ = 2.0 Hz, ferrocenyl-$H_{3,4}$), 4.28 (5H, s, ferrocenyl-C_5H_5). ^{13}C NMR (125 MHz, CD_2Cl_2): δ 199.3 (naphthyl-C=O), 193.5 (ferrocenyl-C=O), 136.8 (naphthyl-C_2), 133.6 (naphthyl-C_1), 133.1 (naphthyl-C_{4a}), 131.0 (naphthyl-C_{8a}), 130.5 (naphthyl-C_8), 129.9 (naphthyl-C_6), 129.5 (naphthyl-C_4), 128.5 (naphthyl-C_5), 127.7 (naphthyl-C_7), 124.7 (naphthyl-C_3), 75.4 (ferrocenyl-*ipso*-C), 74.6 (ferrocenyl-$C_{3,4}$), 71.1 (ferrocenyl-$C_{2,5}$), 71.1 (ferrocenyl-C_5H_5). IR (KBr): 1669 cm^{-1} (CO), 1650 cm^{-1} (CO). MS (DEI; *m/z* (%)): 368 (M^+, 100), 213 (C_5H_5-Fe-C_5H_4-CO, 75), 185 (C_5H_5-Fe-C_5H_4, 15), 155 ($C_{10}H_7$-CH_2O, 10), 129 (40), 127 ($C_{10}H_7$, 20), 84 (25). MS (DCI; *m/z* (%)): 369 (M+H, 100), 213 (C_5H_5-Fe-C_5H_4-CO, 29), 155 ($C_{10}H_7$-CH_2O, 14), 129 (14). HRMS (EI): Calculated for $C_{22}H_{16}O_2Fe$: 368.0465. Found: 368.0500.

2,4,5-Tri-β-naphthyl-3-ferrocenylcyclopentadienone (3.15): 1-Ferrocenyl-2-naphthylethanedione (**3.14**, 0.8 g, 2.1 mmol) and KOH (0.2 g, 3.6 mmol) were dissolved in 50 mL ethanol and heated to reflux. A solution of di-(β-naphthylmethyl)ketone (**3.11**, 0.7 g, 2.2 mmol) dissolved in 50 mL ethanol was added dropwise, the mixture was then stirred under reflux for 2 hours. The

solution was cooled to room temperature, then in ice, and filtered with suction to give **3.15** as a dark blue powder (0.7 g, 1.1 mmol, 49%), m.p. 247-250 °C (dec). The powder was purified by column chromatography under nitrogen (50:50 CH_2Cl_2 : hexanes) before further use. The sample is indefinitely stable as a solid, however, it decomposes in a wide variety of solvents over time. ^1H NMR (500 MHz, CD_2Cl_2): δ 7.94 (9H, m, naphthyl-H), 7.61 (9H, m, naphthyl-H), 7.39 (2H, m, naphthyl-H), 7.18 (1H, m, naphthyl-H), 4.25 (2H, s, ferrocenyl-$H_{2,5}$), 4.05 (5H, s, ferrocenyl-C_5H_5), 3.98 (2H, s, ferrocenyl-$H_{3,4}$). ^{13}C NMR (125 MHz, CD_2Cl_2): δ 200.27 (CO), 157.6, 154.0 (cyclopentadienone-C), 134.2, 134.0, 133.8, 133.7, 133.6, 133.4, 133.0, 132.2 (naphthyl-C's), 130.5, 129.9 (naphthyl-CH's), 129.3 (naphthyl-C), 128.9, 128.8, 128.7, 128.6, 128.5, 128.3, 128.0, 127.8, 127.6, 127.3, 126.8, 126.5 (naphthyl-CH's), 123.8 (cyclopentadienone-C), 77.7 (ferrocenyl-*ipso*-C), 72.1 (ferrocenyl-$C_{2,5}$), 72.0 (ferrocenyl-$C_{3,4}$), 71.0 (C_5H_5). IR (KBr): 1689 cm^{-1} (CO). HRMS (EI): Calculated for $C_{45}H_{30}OFe$: 642.1646. Found: 642.1635.

Ferrocenyl-penta-(β-naphthyl)benzene (3.16): Benzophenone (5g) was melted by heating to 120 °C in a 100 mL round bottom flask. The temperature of the oil bath was increased to 150°C, then di(β-naphthyl)acetylene (**3.10**, 0.4 g, 1.5 mmol) and 2,4,5-tri(β-naphthyl)-3-ferrocenylcyclopentadienone (**3.15**, 1.0 g, 1.5 mmol) were added. The mixture was stirred and heated at 180-190 °C for 52 hours with a reflux condenser (to prevent loss of benzophenone). The flask was

cooled almost to room temperature and benzene (5 mL) was added to prevent solidification of the benzophenone. The resulting mixture was purified by column chromatography under nitrogen (75:25 CH_2Cl_2 : hexanes) to give **3.16** as a yellow-orange powder (0.3 g, 0.3 mmol, 22%), m.p. 260 °C (dec). Crystals of **3.16** were grown by numerous recrystallizations and slow evaporation from CH_2Cl_2 in the dark at 0°C. ^{1}H NMR (500 MHz, CD_2Cl_2): δ 7.81 – 7.00 (35H, m, naphthyl-H), 3.75 (2H, s, ferrocenyl-$H_{2,5}$), 3.69 (2H, s, ferrocenyl-$H_{3,4}$), 3.59 (5H, s, C_5H_5). ^{13}C NMR (125 MHz, CD_2Cl_2): δ 142.6 – 125.7 (naphthyl-CH, C, cyclopentadienone-C), 87.5 (C_5H_4-C), 73.6 (ferrocenyl-$C_{2,5}$), 69.6 (C_5H_5), 67.5 (ferrocenyl-$C_{3,4}$). MS (ESI): 892.4 (M^+, 100). HRMS (EI): Calculated for $C_{66}H_{44}Fe$: 892.2792. Found: 892.2721.

Protonation of Tetracyclone (1.26): 2,3,4,5-Tetraphenylcyclopentadienone (~ 50 mg) was dissolved in CD_2Cl_2 in an NMR tube and cooled to –78 °C; 2 drops of trifluoromethylsulfonic (triflic) acid were added and the tube was shaken. The NMR spectra were immediately recorded at –80 °C. ^{1}H NMR (500 MHz, CD_2Cl_2): δ 7.99 (1H), 7.84 (2H), 7.70 (4H), 7.61 (2H), 7.50 (3H), 7.43 (10H), 7.30 (31H), 7.17 (41H), 6.85 (22H), 5.63 (1H). ^{13}C NMR (125 MHz, CD_2Cl_2): δ 204.7, 194.2, 170.3, 161.4, 157.0, 148.3, 140.5, 135.4, 135.1, 133.6 – 127.4, 121.9, 119.4, 116.9, 114.4, 59.8.

Characterization of 4.38: Pure **4.38** was obtained by preparative HPLC purification, as outlined above. Crystals of **4.38** were grown by slow evaporation from a mixture of CH_2Cl_2 and hexanes, from a sample collected as HPLC eluent, as described above. (Numbering is in accord with the crystal structure): ^{1}H NMR (500 MHz, CD_2Cl_2): δ 8.07 (1H, d, $^3J_{H11\text{-}H10}$ = 7.8 Hz, H_{11}), 7.61 (2H, dd, $^3J_{Hm\text{-}Ho}$ = 7.2 Hz, $^3J_{Hm\text{-}Hp}$ = 6.9 Hz, phenyl-*m* H), 7.58 (1H, m, phenyl-*p* H), 7.55 (1H, m, phenyl-*p* H), 7.53 (2H, m, phenyl-*m* H), 7.51 (2H, dd, $^3J_{Ho\text{-}Hm}$ = 7.5 Hz, $^4J_{Ho\text{-}Hp}$ = 1.5 Hz, phenyl-*o* H), 7.38 (2H, dd, $^3J_{Ho\text{-}Hm}$ = 7.5 Hz, $^4J_{Ho\text{-}Hp}$ = 2.1 Hz, phenyl-*o* H), 7.29 (1H, dd, $^3J_{H10\text{-}H11}$ = 7.7 Hz, $^3J_{H10\text{-}H9}$ = 7.0 Hz, H_{10}), 7.27 (1H, d, $^3J_{H8\text{-}H9}$ = 7.2 Hz, H_8), 7.22 (1H, dd, $^3J_{H9\text{-}H8}$ = 7.6 Hz, $^3J_{H9\text{-}H10}$ = 7.0 Hz, H_9), 7.05 (1H, dd, $^3J_{H5\text{-}H6}$ = 7.6 Hz, $^3J_{H5\text{-}H4}$ = 7.5 Hz, H_5), 6.82 (1H, d, $^3J_{H6\text{-}H5}$ = 7.4 Hz, H_6), 6.81 (1H, dd, $^3J_{H4\text{-}H5}$ = 7.5 Hz, $^3J_{H4\text{-}H3}$ = 7.1 Hz, H_4), 6.39 (1H, d, $^3J_{H3\text{-}H4}$ = 7.9 Hz, H_3). ^{13}C NMR (125 MHz, CD_2Cl_2): δ 186.0 (C=O), 149.0, 148.6, 147.0, 137.1, 136.5, 134.1, 130.8, 130.6 ($C_{2,2a,2b,6a,7,7a,7b,11a}$), 135.4, 135.2 ($C_{12,18}$), 132.8 ($C_9$), 130.7 ($C_5$), 130.2, 129.1 (phenyl-*o* C), 130.0, 128.9 (phenyl-*m* C), 129.6, 129.0 (phenyl-*p* C), 128.3 (C_4, C_{10}), 128.2 (C_{11}), 125.9 (C_3, C_8), 122.8 (C_6). HRMS (EI): Calculated for $C_{29}H_{18}O$: 382.1671. Found: 382.1666.

Characterization of 4.45: ^{1}H NMR (600 MHz, CD_2Cl_2): δ 7.34 – 7.38 (5H, m), 7.30 – 7.33 (3H, m), 7.23 – 7.26 (2H, m), 7.18 – 7.23 (5H, m), 7.14 – 7.18 (5H, m), 4.61 (1H, s, br, cyclopentenone H), 3.73 (1H, d, J_{HH} = 2.0 Hz, cyclopentenone H). ^{13}C NMR (150 MHz, CD_2Cl_2): δ 205.7 (C=O), 169.7, 142.0,

139.9, 135.2, 132.7 (phenyl-*ipso* C and cyclopentenone C=C), 130.4, 129.6, 129.5, 129.4, 128.9, 128.8, 128.6, 128.3 (phenyl-*o*, *m* carbons), 130.0, 128.6, 127.8, 127.6 (phenyl-*p* carbons), 63.9 (cyclopentenone CH), 58.0 (cyclopentenone CH). HRMS (EI): Calculated for $C_{29}H_{22}O$: 386.1671. Found: 386.1666.

Characterization of 3 other unidentified fractions in protonation of 1.26:

Fraction 1: ^{1}H NMR (600 MHz, CD_2Cl_2): δ 8.06 (2H, dd, J_{HH} = 7.8 Hz, 1.8 Hz), 7.49 – 7.56 (12H, m), 7.43 – 7.45 (4H, m), 7.40 (4H, tt, J_{HH} = 7.2 Hz, 1.2 Hz), 7.33 – 7.36 (12H, m), 7.27 – 7.31 (15H, m), 7.21 – 7.24 (6H, m), 6.78 (2H, d, J_{HH} = 1.2 Hz), 6.75 (2H, dd, J_{HH} = 6.5 Hz, 1.8 Hz), 6.34 (2H, d, J_{HH} = 7.8 Hz). The recovered sample concentration was not sufficient to obtain satisfactory ^{13}C data. HRMS (EI): Calculated for $C_{35}H_{61}O_4$: 545.4570. Found: 545.4568.

Fraction 2: ^{1}H NMR (600 MHz, CD_2Cl_2): δ 7.97 (1H, dd, J_{HH} = 0.6 Hz, 2.4 Hz), 7.56 – 7.59 (2H, m), 7.50 – 7.55 (4H, m), 7.47 – 7.48 (2H, m), 7.31 – 7.43 (17H, m), 7.22 (1H, dd, J_{HH} = 8.4 Hz, 0.6 Hz), 7.11 (1H, dd, J_{HH} = 9.0 Hz, 2.4 Hz), 7.05 (1H, ddd, J_{HH} = 7.6 Hz, 7.2 Hz, 0.6 Hz), 6.82 (2H, ddd, J_{HH} = 7.0 Hz, 6.6 Hz, 1.2 Hz), 6.38 (1H, dd, J_{HH} = 7.8 Hz, 1.2 Hz). ^{13}C NMR (150 MHz, CD_2Cl_2): δ 201.1, 185.6, 152.7, 149.7, 148.6, 146.9, 138.4, 138.0, 137.1, 136.5, 135.4, 135.1, 133.5, 133.3, 131.7, 130.8, 130.7, 130.1, 130.0, 129.6, 129.5, 129.4, 129.2, 129.1, 129.0, 128.8, 128.7, 128.5, 128.2, 128.0, 126.5, 126.2, 122.9. HRMS (EI): Calculated for $C_{45}H_{31}O_2$: 603.2324. Found: 603.2315.

Fraction 3: ^{1}H NMR (600 MHz, CD_2Cl_2): δ 8.44 (2H, d, J_{HH} = 2.4 Hz), 7.53 – 7.55 (10H, m), 7.47 – 7.49 (2H, m), 7.44 – 7.45 (4H, m), 7.38 (4H, s, br), 7.31 – 7.33 (10H, m), 7.23 – 7.25 (4H, m), 7.19 (4H, dd, J_{HH} = 7.8 Hz, 7.5 Hz), 7.15 (2H, d, J_{HH} = 3.0 Hz), 7.11 (2H, dd, J_{HH} = 8.4 Hz, 1.8 Hz), 7.04 (2H, dd, J_{HH} = 7.5 Hz, 7.2 Hz), 6.91 – 6.99 (20H, m), 6.79 – 6.83 (4H, m), 6.37 (2H, d, J_{HH} = 7.8 Hz), 5.41 (2H, s). ^{13}C NMR (150 MHz, CD_2Cl_2): δ 204.9, 185.5, 167.7, 149.6, 148.6, 147.0, 143.5, 142.0, 139.5, 139.1, 138.8, 137.1, 136.5, 135.4, 135.2, 135.1, 134.5, 133.3, 132.9, 132.7, 130.8, 130.3, 130.2, 130.1, 129.9, 129.6, 129.4, 129.1, 129.0, 128.9, 128.8, 128.7, 128.6, 128.4, 128.3, 127.9, 127.2, 126.5, 126.1, 125.9. HRMS (EI): Calculated for $C_{38}H_{74}O_2$: 578.5638. Found: 578.5683.

Protonation of 1.27: 3-Ferrocenyl-2,4,5-triphenylcyclopentadienone[436] (**1.27**, 30 mg) was dissolved in CD_2Cl_2 in an NMR tube and cooled to –78 °C; 2 drops of trifluoroacetic acid were added and the tube was shaken. The NMR spectra were subsequently recorded over the range –80 °C to –20 °C. The improved resolution at –20 °C assisted in the interpretation of the spectra, thus peak assignments refer to this temperature. ^{1}H NMR (500 MHz, CD_2Cl_2): δ 7.69 (1H, s, phenyl *para*-H), 7.61 (1H, s, phenyl *para*-H), 7.55 - 7.40 (8H, m, phenyl *ortho*-H, *meta*-H), 7.29 (2H, d, $^{3}J_{Ho\text{-}Hm}$ = 6.6 Hz, phenyl *ortho/meta*-H), 7.21 (2H, d, $^{3}J_{Hm\text{-}Ho}$ = 6.2 Hz, phenyl *ortho/meta*-H), 7.04 (1H, d, $^{3}J_{Hp\text{-}Hm}$ = 5.4 Hz, phenyl *para*-H), 6.37 (1H, s, H_9), 6.08 (1H, s, H_8), 5.14 (1H, s, H_{10}), 4.91 (5H, s, C_5H_5), 4.41 (1H, s, OH), 4.09 (1H, s, H_7). ^{13}C NMR (125 MHz, CD_2Cl_2): δ 166.7, 148.3,

147.2, 135.2 ($C_{11,12,14,15}$), 131.8 (phenyl-CH), 131.6 (phenyl-CH), 131.3 (phenyl-C), 130.6 (phenyl-C), 130.4 (phenyl-CH), 130.3 (phenyl-CH), 130.0 (phenyl-CH), 129.7 (phenyl-C), 129.6, 129.4, 127.9, 127.3 (phenyl-CH), 102.5 (C_6), 94.9 (C_9), 94.1 (C_8), 84.9 (C_5H_5), 79.4 (C_{10}), 77.1 (C_7), 60.2 (C_{13}).

(9-Indenyl)anthracene (5.15): In a 100 mL round bottom flask, 6.2 g (24 mmol) of 9-bromoanthracene and 0.9 g (0.8 mmol) of freshly prepared $Pd(PPh_3)_4$[437] were stirred in 35 mL DMF under nitrogen. Tributylstannylindene[438] (7.5 g, 19 mmol) was added with a syringe, and the orange solution was stirred at 110 °C for 2 hours. The mixture was cooled to room temperature and 20 mL of water was added, followed by extraction with diethyl ether. The combined organic extracts were washed with saturated NaCl solution and water, dried over $MgSO_4$, filtered and the solvent was removed under vacuum. The crude beige solid was purified by using flash column chromatography (100% hexanes to 50:50 hexanes: CH_2Cl_2) to give **5.15** as a pale yellow solid (2.2 g, 7.5 mmol, 42%). Mp 142-145 °C. Crystals of **5.15** were easily grown by crystallization from CH_2Cl_2. ^1H NMR (500 MHz, CD_2Cl_2): (numbering is in accord with the crystal structure) δ 8.57 (1H, s, H_{10}), 8.10 (2H, d, $^3J_{H1\text{-}H2}$ = 8.5 Hz, $H_{1,8}$), 7.96 (2H, dd, $^3J_{H4\text{-}H3}$ = 8.8 Hz, 0.7 Hz, $H_{4,5}$), 7.70 (1H, d, $^3J_{H17\text{-}H16}$ = 7.5 Hz, H_{17}), 7.51 (2H, ddd, $^3J_{H2\text{-}H1}$ = 7.6 Hz, $^3J_{H2\text{-}H3}$ = 7.5 Hz, $^4J_{H2\text{-}H4}$ = 1.0 Hz, $H_{2,7}$), 7.38 (2H, ddd, $^3J_{H3\text{-}H4}$ = 7.8 Hz, $^3J_{H3\text{-}H2}$ = 7.7 Hz, $^4J_{H3\text{-}H1}$ = 1.1 Hz, $H_{3,6}$), 7.30 (1H, dd, $^3J_{H16\text{-}H17}$ = 8.0 Hz, $^3J_{H16\text{-}H15}$ = 7.7 Hz, H_{16}), 7.15 (1H, dd, $^3J_{H15\text{-}H16}$ = 7.4 Hz, $^3J_{H15\text{-}H14}$ = 7.4 Hz, H_{15}), 6.77 (1H, t,

$^3J_{H12\text{-}H13}$ = 1.9 Hz, H_{12}), 6.71 (1H, d, $^3J_{H14\text{-}H15}$ = 7.6 Hz, H_{14}), 3.88 (2H, d, $^3J_{H13\text{-}H12}$ = 1.8 Hz, H_{13}). ^{13}C NMR (125 MHz, CD_2Cl_2): δ 147.3 (C_{17a}), 144.6 (C_{13a}), 142.5 (C_{11}), 135.8 (C_{12}), 132.2 ($C_{8a,9a}$), 131.6 (C_9), 130.9 ($C_{4a,10a}$), 129.1 ($C_{1,8}$), 127.3 (C_{10}), 127.2 ($C_{4,5}$), 126.9 (C_{15}), 126.0 ($C_{3,6}$), 125.9 ($C_{2,7}$), 125.6 (C_{16}), 124.5 (C_{17}), 121.2 (C_{14}), 39.6 (C_{13}). HRMS (EI): Calculated for $C_{23}H_{16}$: 292.1252. Found: 292.1233.

(9-Indenyl)triptycene (5.16): In a 100 mL 3-neck round bottom flask with a reflux condenser, **5.15** (2.5 g, 8.6 mmol) was dissolved in 20 mL DME, and heated to 100 °C. Anthranilic acid (5.5 g, 40 mmol) and isoamyl nirite (8.7 mL, 64 mmol) were added cautiously dropwise from separate syringes over 3-4 hours. The mixture was heated overnight, cooled to room temperature, and the solvent was removed under vacuum. The residue was subjected to flash column chromatography (100% hexanes to 50:50 hexanes: CH_2Cl_2), to give **5.16** as a white solid (0.9 g, 2.5 mmol, 29%). Mp 247 – 249 °C. Crystals of **5.16** were grown by recrystallization and slow evaporation from CH_2Cl_2. ^1H NMR (500 MHz, CD_2Cl_2): (numbering is in accord with the crystal structure) δ 8.34 (1H, d, $^3J_{H16\text{-}H15}$ = 7.7 Hz, H_{16}), 7.85 (1H, s, H_{18}), 7.75 (1H, d, $^3J_{H20\text{-}H21}$ = 7.4 Hz, H_{20}), 7.64 (2H, d, $^3J_{H1\text{-}H2}$ = 7.3 Hz, $H_{1,8}$), 7.56 (1H, d, $^3J_{H13\text{-}H14}$ = 7.1 Hz, H_{13}), 7.17 (1H, m, H_{15}), 7.29 (1H, dd, $^3J_{H21\text{-}H20}$ = 7.3 Hz, $^3J_{H21\text{-}H22}$ = 7.3 Hz, H_{21}), 7.15 (2H, m, $H_{2,7}$), 7.10 (1H, dd, $^3J_{H14\text{-}H13}$ = 7.3 Hz, $^3J_{H14\text{-}H15}$ = 7.3 Hz, H_{14}), 7.03 (2H, d, $^3J_{H4\text{-}H3}$ = 7.6 Hz, $H_{4,5}$), 6.98 (1H, dd, $^3J_{H22\text{-}H21}$ = 7.5 Hz, $^3J_{H22\text{-}H23}$ = 7.5 Hz, H_{22}), 6.91 (2H,

dd, $^3J_{H3-H4}$ = 7.5 Hz, $^3J_{H3-H2}$ = 7.5 Hz, $H_{3,6}$), 6.51 (1H, d, $^3J_{H23-H22}$ = 7.8 Hz, H_{23}), 5.67 (1H, s, H_{10}), 3.94 (2H, s, H_{19}). ^{13}C NMR (125 MHz, CD_2Cl_2): δ 148.4 (C_{11}), 146.7 (C_{12}), 145.4 ($C_{4a,10a,19a}$), 144.5 ($C_{8a,9a}$), 143.8 (C_{23a}), 140.1 (C_{17}), 134.8 (C_{18}), 125.9 ($C_{4,5}$), 125.5 ($C_{2,7,23}$), 124.9 ($C_{15,22}$), 124.8 (C_{14}), 124.5 (C_{21}), 124.4 ($C_{3,6}$), 124.1 (C_{13}), 123.8 (C_{20}), 123.5 ($C_{1,8}$), 123.3 (C_{16}), 56.4 (C_9), 54.3 (C_{10}), 39.4 (C_{19}). HRMS (EI): Calculated for $C_{29}H_{20}$: 368.1565. Found: 368.1531.

(9-Indenyl)triptycene chromium carbonyl (5.17): Chromium hexacarbonyl (130 mg, 0.6 mmol) and **5.16** (200 mg, 0.5 mmol) were dissolved in 5 mL dry THF and 30 mL *n*-Bu_2O in a 100 mL round bottom flask, in an atmosphere of dry nitrogen and protected from light. The mixture was stirred under reflux for 4 days, during which time the solution changed from colourless to deep yellow. The reaction mixture was cooled to room temperature and the solvent was removed under vacuum; the residue was then subjected to flash column chromatography (100% hexanes to 50:50 hexanes: CH_2Cl_2), to give **5.17** as a yellow solid (120 mg, 0.3 mmol, 45%). Mp 129-131 °C. Crystals of **5.17** were grown by recrystallization and slow evaporation from CH_2Cl_2 in the dark at 0°C. IR (solid): 1978, 1907 cm^{-1} (CO's); (lit. for triptycene chromium carbonyl[160] 1975, 1910 cm^{-1}). ^1H NMR (500 MHz, CD_2Cl_2, 243 K): (numbering is in accord with the crystal structure; peaks for the minor rotamer are marked with an asterisk) δ 8.14, 7.40, 7.11, 6.85 (4H, $H_{5,6,7,8}$*), 7.86 (1H, s, H_{18}*), 7.64 (2H, d, $^3J_{H8-H7}$ = 6.8 Hz, H_8), 7.50 (2H, d, $^3J_{H13-H14}$ = 7.2 Hz, H_{13}), 7.49, 7.45-7.40, 7.23-7.11, 7.07-

7.01, 6.95-6.83 (12H, H_{23}, H_{23}*, H_{22}, H_{22}*, H_{21}, H_{21}*, H_{20}, H_{20}*), 7.40 (2H, s, H_{18}), 7.40, 7.11, 6.85 (3H, $H_{5,6,7}$*), 7.40, 7.01, 6.93, 6.60 (4H, $H_{13,14,15,16}$*), 7.19 (2H, m, H_7), 7.14, 6.93 (4H, $H_{14,15}$), 6.94 (2H, m, H_6), 6.68 (2H, d, $^3J_{H16\text{-}H15}$ = 7.7 Hz, H_{16}), 6.49 (2H, d, $^3J_{H4\text{-}H3}$ = 6.6 Hz, H_4), 6.41 (2H, d, $^3J_{H5\text{-}H6}$ = 7.0 Hz, H_5), 6.02 (1H, d, $^3J_{H4\text{-}H3}$ = 6.2 Hz, H_4*), 5.74 (2H, d, $^3J_{H1\text{-}H2}$ = 6.14 Hz, H_1), 5.30 (2H, m, H_2), 5.27 (1H, s, H_{10}*), 5.22 (2H, s, H_{10}), 5.18 (3H, dd, $^3J_{H3\text{-}H4}$ = 6.2 Hz, $^3J_{H3\text{-}H2}$ = 6.2 Hz, H_3* and H_3), 5.14 (1H, d, $^3J_{H1\text{-}H2}$ = 6.5 Hz, H_1*), 4.90 (1H, dd, $^3J_{H2\text{-}H3}$ = 6.1 Hz, $^3J_{H2\text{-}H1}$ = 6.1 Hz, H_2*), 3.78 – 3.99 (6H, m, H_{19} and H_{19}*). ^{13}C NMR (125 MHz, CD_2Cl_2, 243 K): δ 233.2 (CO*), 233.0 (CO), 147.0, 146.4, 145.1, 144.6, 144.0, 142.5 ($C_{8a,10a,11,12,19a,23a}$, $C_{8a,10a,11,12,19a,23a}$*), 138.7, 138.5 (C_{17}, C_{17}*), 137.5 (C_{18}*), 135.1 (C_{18}), 135.1, 126.1, 125.1, 124.9 ($C_{20,21,22,23}$), 126.7, 125.8, 124.0, 122.4 ($C_{20,21,22,23}$*), 126.6 (C_5*), 126.4, 125.5, 123.5 ($C_{13,14,15}$*), 125.4, 125.1 ($C_{14,15}$), 125.2 (C_5, C_{16}), 125.1 (C_{16}*), 124.9 ($C_{6,7}$, $C_{6,7}$*), 123.9 (C_8), 123.1 (C_{13}), 122.2 (C_8*), 119.5, 117.9, 117.5 ($C_{4a,9a}$, $C_{4a,9a}$*), 93.3 (C_1*), 92.1 (C_4*), 91.9 (C_1 + C_4), 90.9 (C_3), 90.0 (C_3*), 89.7 (C_2 + C_2*), 55.5 (C_9), 55.1 (C_9*), 51.9 (C_{10}, C_{10}*), 39.6 (C_{19}*), 39.4 (C_{19}). ^{1}H NMR (500 MHz, CD_2Cl_2, 343 K): δ 7.67 (1H, d, J_{HH} = 7.3 Hz), 7.66 (1H, br s, H_{18}), 7.52 (1H, d, J_{HH} = 7.3 Hz), 7.50 (1H, d, J_{HH} = 7.7 Hz), 7.22 (1H, dd, J_{HH} = 7.5 Hz, 7.4 Hz), 7.11 (1H, dd, J_{HH} = 7.5 Hz, 7.4 Hz), 7.07 – 6.98 (5H, m), 6.95 (1H, dd, J_{HH} = 7.7 Hz, 7.5 Hz), 6.89 (1H, dd, J_{HH} = 7.5 Hz, 7.4 Hz), 6.43 (1H, br s), 6.15 (1H, d, J_{HH} = 6.0 Hz), 5.51 (1H, dd, J_{HH} = 6.2 Hz, 6.2 Hz), 5.55 (1H, s, H_{10}), 5.33 (1H, dd, J_{HH} = 6.3 Hz, 6.0 Hz), 3.92 (2H, br s, H_{19}). ^{13}C NMR (125 MHz, CD_2Cl_2, 343 K): δ 212.8 (CO), 143.9, 143.7, 143.2, 137.4,

135.2, 134.2, 123.3, 122.6 ($C_{4a,8a,9a,10a,11,12,19a,23a}$), 128.8, 125.5, 124.6, 124.4, 124.2, 123.6, 123.5, 123.1 ($C_{5,6,7,8,13,14,15,16,18,20,21,22,23}$), 92.4, 92.2, 90.8, 90.2 ($C_{1,2,3,4}$), 53.3 (C_9), 50.7 (C_{10}), 38.6 (C_{19}). HRMS (EI): Calculated for $C_{32}H_{20}O_3Cr$: 504.0818. Found: 504.1776. Also isolated from the reaction mixture as a yellow solid was the bis-chromium carbonyl complex (30 mg, 0.05 mmol, 9%). HRMS (EI): Calculated for $C_{35}H_{20}O_6Cr_2$: 640.0070. Found: 640.0079.

Attempted synthesis of (9-indenyl)triptycene manganese carbonyl (5.24): (9-Indenyl)triptycene (**5.16**, 0.5 g, 1.3 mmol) was dissolved in dry CH_2Cl_2 (20 mL). Potassium *tert*-butoxide (0.1 g, 1.3 mmol) was added in portions to the stirring solution, which was then allowed to reflux under nitrogen for 30 minutes. During this time, the solution changed in colour from pale yellow to green to red/brown. A solution of $Mn(CO)_5Br$ (0.4 g, 1.6 mmol) in 10 mL dry CH_2Cl_2 was added dropwise, and the mixture was allowed to reflux overnight. The solvent was removed under vacuum, and the residue was subjected to column chromatography (100% hexanes to 100% CH_2Cl_2), resulting in the separation of three major fractions. Upon mass spectrometric identification, the product mixture was found to contain $Mn_2(CO)_{10}$ (m/z 390 g mol^{-1}, 0.1 g, 12 %), $Mn_2(CO)_8Br_2$ (m/z 494 g mol^{-1}, 0.2 g, 36 %) and a mixture of hydrocarbon products consisting of a dimer of (9-indenyl)triptycene after loss of 2 hydrogen atoms (m/z 732 g mol^{-1}, 0.1 g, 9 %), as well as unreacted **5.16** and fragments

derived from **5.16** [m/z 368 g mol^{-1} (**5.16**), 292 g mol^{-1} (**5.15**), 252 g mol^{-1} (**5.16** – indene)].

Tetramer 6.17: To a solution of phenyl acetylene (4.7 g, 0.04 mol) in 50 mL dry THF cooled to –78 °C was added *n*-butyl lithium (18mL, 2.5 mol/L in hexanes). The solution was stirred at –78 °C for 2 hours, then 9-bromofluorene (11.1 g, 0.04 mol) in 30 mL dry THF was added dropwise. The solution was allowed to warm to room temperature, and it deepened in color from yellow to deep orange-red. The reaction mixture was treated with acidified water (40mL), stirred for 20 minutes, and extracted with diethyl ether. The combined organic extracts were dried over $MgSO_4$ and the solvent was removed on a rotary evaporator to give an orange solid (5.4 g); thin layer chromatography revealed the presence of numerous fractions. The residue was subjected to column chromatography (100% hexanes to 100% CH_2Cl_2), resulting in the isolation of a mixture of **6.15** and **6.16** (1.2 g, 16%) and a pure sample of **6.17** (0.9 g, 12%), mp 287 – 289 °C. Crystals of **6.17** were grown by crystallization of an NMR sample in CD_2Cl_2. ^1H NMR (500 MHz, CD_2Cl_2, 363 K): δ 8.49 (1H, br, s), 8.34 (2H, d, J_{HH} = 7.5 Hz), 8.29 (1H, d, J_{HH} = 7.6 Hz), 8.23 (1H, d, J_{HH} = 8.5 Hz), 7.93 (1H, br, s), 7.85 (2H, br, t), 7.69 (2H, d, J_{HH} = 7.2 Hz), 7.65 (2H, d, J_{HH} = 7.3 Hz), 7.34 (3H, m), 7.30 (6H, m), 7.21 (3H, m), 7.15 (3H, br, s), 6.90 (2H, br, t), 6.45 (2H, br, s), 5.88 (1H, s, H_9). ^{13}C NMR (125 MHz, CD_2Cl_2, 363 K): δ 145.4, 143.4, 141.2, 140.8, 140.4, 140.0, 139.8, 139.4, 137.5, 136.9, 135.9 (aromatic C's), 129.2 (2 x CH), 129.1

127.3 (2 x CH), 126.9 (2 x CH), 126.8, 126.7, 126.4, 125.9, 125.8, 125.7, 125.6 (2 x CH), 124.6 (2 x CH), 124.4, 120.2, 119.9, 119.8, 119.5 (2 x CH), 119.2, 119.0 (2 x CH) (aromatic CH's), 62.0 ($HC_{9'}$), 52.7 (C_9). HRMS (EI): Calculated for $C_{52}H_{32}$: 656.2504. Found: 656.2518.

9-Phenylethynylfluorene (6.13): 9-Phenylethynylfluoren-9-ol[371] was used to prepare 6.13, following a literature procedure.[381] Crystals of **6.13** were grown from an NMR sample in CD_2Cl_2. ^1H NMR (600 MHz, CD_2Cl_2): δ 7.84 (4H, m, fluorenyl-H), 7.50 (2H, dd, $^3J_{Hm\text{-}Ho}$ = 7.6 Hz, $^3J_{Hm\text{-}Hp}$ = 7.1 Hz, phenyl *m*-H), 7.46 (4H, m, fluorenyl-H), 7.36 (3H, br s, phenyl *o*, *p*-H), 5.13 (1H, s, fluorenyl-H). ^{13}C NMR (150 MHz, CD_2Cl_2): δ 144.5, 140.9 (fluorenyl-C), 132.3 (phenyl *m*-C), 127.3 (phenyl *ipso*-C), 128.8, 128.2, 125.7, 120.7 (fluorenyl-CH's), 128.6 (phenyl *p*-C), 128.5 (phenyl *o*-C), 88.5 (fluorenyl-*C*≡), 82.5 (C_6H_5-*C*≡), 40.4 (fluorenyl-C_9). HRMS (EI): Calculated for $C_{21}H_{14}$: 266.1096. Found: 266.1068.

Attempted Diels-Alder Preparation of 6.14: Benzophenone (~5g) was dissolved by heating over a free flame in a 100 mL round bottom flask. 9-Phenylethynylfluorene (**6.13**, 990 mg, 3.7 mmol) and tetracyclone (**1.26**, 1.5 g, 4.0 mmol) were added, and the mixture was heated over a free flame with an air condenser attached for 30 minutes. The solution was cooled, and 5 mL of benzene was added to prevent solidification of the benzophenone. The mixture was subjected to column chromatography (100% hexanes to 100% CH_2Cl_2)

resulting in the isolation of two major fractions – the first fraction was identified as **6.35**, followed closely by **6.33**. Repeated purifications led to the isolation of pure **6.35** and **6.33**, which were subsequently identified by NMR spectroscopy and mass spectrometry. Upon exposure to light and air in solution, **6.35** decomposed to give a white solid, which was purified by column chromatography (50:50 hexanes: CH_2Cl_2) to give **6.34**, which was then characterized by NMR spectroscopy and mass spectrometry.

Characterization of 6.35: Yield: 570 mg, 1.0 mmol, 55%, mp 167 – 170 °C (dec). ^{1}H NMR (500 MHz, CD_2Cl_2): δ 7.96 (4H, d, $^3J_{H3\text{-}H2}$ = 8.0 Hz, $^3J_{H1\text{-}H2}$ = 6.3 Hz, $H_{1,3}$), 7.86 (2H, d, $^3J_{H4\text{-}H5}$ = 7.4 Hz, H_4), 7.67 (4H, br s, phenyl-H), 7.61 (2H, dd, $^3J_{H2\text{-}H3}$ = 7.6 Hz, $^3J_{H2\text{-}H1}$ = 6.8 Hz, H_2), 7.46 (6H, br s, phenyl-H), 7.10 (2H, dd, $^3J_{H5\text{-}H4}$ = 7.2 Hz, $^3J_{H5\text{-}H6}$ = 7.2 Hz, H_5), 6.77 (2H, dd, $^3J_{H6\text{-}H7}$ = 7.6 Hz, $^3J_{H6\text{-}H5}$ = 7.5 Hz, H_6), 6.57 (2H, d, $^3J_{H7\text{-}H6}$ = 8.0 Hz, H_7). ^{13}C NMR (125 MHz, CD_2Cl_2): δ 141.3, 140.9, 138.4, 138.2, 130.5, 128.2 (C), 134.5, 128.7 (phenyl-CH), 128.6 (C_2), 127.4 (C_1), 127.3 (C_6), 126.5 (C_7), 125.8 (C_5), 120.9 (C_4), 120.0 (C_3). HRMS (EI): Calculated for $C_{42}H_{24}$: 528.1878. Found: 528.1873.

Characterization of 6.33: Yield: 160 mg, 0.3 mmol, 17%, mp 250 – 253 °C. Co-crystals of **6.33** and **6.34** were grown by crystallization and slow evaporation from an NMR sample of **6.33** in CD_2Cl_2. ^{1}H NMR (500 MHz, CD_2Cl_2); numbering is in accord with the crystal structure: δ 7.87 (4H, d, $^3J_{H16\text{-}H15}$ = 7.5 Hz, H_{16}), 7.43 (4H,

dd, $^3J_{H15-H16}$ = 7.4 Hz, $^3J_{H15-H14}$ = 7.4 Hz, H_{15}), 7.20 (4H, dd, $^3J_{H14-H15}$ = 7.5 Hz, $^3J_{H14-H13}$ = 7.4 Hz, H_{14}), 7.16 (4H, d, $^3J_{H13-H14}$ = 7.4 Hz, H_{13}), 6.97 (2H, dd, $^3J_{H2-H1}$ = 7.5 Hz, $^3J_{H2-H3}$ = 7.6 Hz, H_2), 6.86 (2H, d, $^3J_{H1-H2}$ = 8.2 Hz, H_1), 6.76 (2H, dd, $^3J_{H3-H2}$ = 7.5 Hz, $^3J_{H3-H4}$ = 7.5 Hz, H_3), 6.28 (2H, d, $^3J_{H4-H3}$ = 7.7 Hz, H_4), 5.95 (2H, H_6). ^{13}C NMR (125 MHz, CD_2Cl_2): δ 153.5, 142.6, 140.6, 128.1, 127.9 ($C_{4a,5a,5b,6a,16a}$), 128.7 (C_{14}), 128.4 (C_{15}), 128.1 (C_1), 127.8 (C_3), 127.6 (C_2), 126.5 (C_4), 125.9 (C_{13}), 124.9 (C_6), 120.8 (C_{16}), 69.0 (C_5). HRMS (EI): Calculated for $C_{42}H_{26}$: 530.2035. Found: 530.2010.

Characterization of 6.34: Recovered from the decomposition of **6.35** in solution exposed to light, mp 261 – 264 °C. ^1H NMR (600 MHz, CD_2Cl_2); numbering is in accord with the crystal structure: δ 8.42 (1H, d, $^3J_{Hp-Hm}$ = 8.4 Hz, phenyl-*p*-H), 8.20 (1H, d, $^3J_{H1-H2}$ = 7.7 Hz, H_1), 8.15 (1H, d, $^3J_{H4-H5}$ = 7.8 Hz, H_4), 8.06 (1H, d, $^3J_{H12-H13}$ = 7.8 Hz, H_{12}), 7.96 (2H, d, $^3J_{Ho-Hm}$ = 7.0 Hz, phenyl-*o*-H), 7.89 (1H, d, $^3J_{H9-H10}$ = 7.7 Hz, H_9), 7.67 (1H, d, $^3J_{H11-H10}$ = 7.0 Hz, H_{11}), 7.64 (2H, dd, $^3J_{Hm-Ho}$ = 7.1 Hz, $^3J_{Hm-Hp}$ = 7.6 Hz, phenyl-*m*-H), 7.62 (1H, dd, $^3J_{H5-H4}$ = 7.6 Hz, $^3J_{H5-H6}$ = 7.6 Hz, H_5), 7.51 (1H, dd, $^3J_{H13-H12}$ = 7.9 Hz, $^3J_{H13-H14}$ = 7.6 Hz, H_{13}), 7.40 (1H, dd, $^3J_{H2-H1}$ = 7.9 Hz, $^3J_{H2-H3}$ = 7.5 Hz, H_2), 7.29 – 7.27 (2H, m, $H_{6,10}$), 7.21 (1H, dd, $^3J_{H14-H13}$ = 7.6 Hz, $^3J_{H14-H12}$ = 7.6 Hz, H_{14}), 7.13 – 7.10 (2H, m, $H_{3,7}$), 6.96 (2H, d, $^3J_{Ho-Hm}$ = 7.1 Hz, phenyl-*o*-H), 6.82 (1H, d, $^3J_{H15-H14}$ = 7.5 Hz, H_{15}), 6.69 (1H, d, $^3J_{Hp-Hm}$ = 8.0 Hz, phenyl-*p*-H), 6.58 (2H, dd, $^3J_{Hm-Hp}$ = 7.8 Hz, $^3J_{Hm-Ho}$ = 7.7 Hz, phenyl-*m*-H). The numbering for protons 1,2,3 and 9,10,11, as well as 4,5,6,7

and 12,13,14,15 may be interchanged. ^{13}C NMR (150 MHz, CD_2Cl_2): δ 144.3, 142.5, 141.0, 138.7, 136.6, 134.6, 133.6, 132.1 (C), 132.5, 129.7, 129.4, 129.3, 128.8, 128.0, 127.9, 127.3, 124.4, 123.8, 123.6, 122.9, 122.4, 121.6, 121.0 (CH), 128.9, 127.5, 126.5, 123.9 (2CH). HRMS (EI): Calculated for $C_{42}H_{24}O_2$: 560.1776. Found: 560.1776.

References

(1) M. Faraday, *Phil. Trans. R. Soc. (London)* **1825**, 440.

(2) E. D. Bergmann; B. Pullman, *Proceedings of the International Symposium* **1971**.

(3) A. Kekulé, *Bull. Soc. Chim. Fr.* **1865**, *3*, 98.

(4) E. Erlenmeyer, *Liebigs Ann. Chem.* **1866**, *137*, 327.

(5) A. Kekulé, *Liebigs Ann. Chem.* **1972**, *168*, 72.

(6) L. Pauling; G. W. Wheland, *J. Chem. Phys.* **1933**, *1*, 362.

(7) E. Hückel, *Z. Phys.* **1931**, *70*, 204.

(8) R. S. Mulliken, *Phys. Rev.* **1932**, *41*, 49.

(9) K. B. Wiberg, *Chem. Rev.* **2001**, *101*, 1317.

(10) W. von E. Doering; L. H. Knox, *J. Am. Chem. Soc.* **1954**, *76*, 3203.

(11) R. Breslow, *J. Am. Chem. Soc.* **1957**, *79*, 5318.

(12) A. D. Allen; T. T. Tidwell, *Chem. Rev.* **2001**, *101*, 1333.

(13) F. Bloch; W. W. Hansen; M. Packard, *Phys. Rev.* **1946**, *69*, 127.

(14) E. M. Purcell; H. C. Torrey; R. V. Pound, *Phys. Rev.* **1946**, *69*, 37.

(15) J. W. Armit; R. Robinson, *J. Chem. Soc.* **1925**, *127*, 1604.

(16) M. B. Smith; J. March, *Advanced Organic Chemistry, 5th Edition*, **2001**, John Wiley & Sons, Toronto.

(17) M. Bochmann, *Organometallics I: Complexes with Transition Metal – Carbon σ-Bonds*, **1994**, Oxford University Press, Toronto.

(18) D. F. Shriver; P. Atkins; C. H. Langford, *Inorganic Chemistry*, **1994**, W. H. Freeman & Company, New York.

(19) R. H. Crabtree, *The Organometallic Chemistry of the Transition Metals, 2nd Edition*, **1994**, John Wiley & Sons, Toronto.

(20) T. J. Kealy; P. L. Pauson, *Nature* **1951**, *168*, 1039.

(21) F. A. Cotton, *Inorg. Chem.* **2002**, *41*, 643.

(22) J. W. Faller, *Adv. Organomet. Chem.* **1977**, *16*, 211.

(23) W. von E. Doering; W. Roth, *Tetrahedron* **1963**, *19*, 715.

(24) R. S. Berry, *J. Chem. Phys.* **1960**, *32*, 933.

(25) T. S. Piper; G. Wilkinson, *J. Inorg. Nucl. Chem.* **1956**, *3*, 104.

(26) M. J. Bennett; F. A. Cotton; A. Davison; J. W. Faller; S. J. Lippard; S. M. Morehouse, *J. Am. Chem. Soc.* **1966**, *88*, 4371.

(27) R. B. Woodward; R. Hoffmann, *Angew. Chem. Int. Ed. Engl.* **1969**, *8*, 781.

(28) A. D. Bain; D. M. Rex; R. N.Smith, *Magn. Reson. Chem.* **2001**, *39*, 122.

(29) J. Sandström, *Dynamic NMR Spectroscopy*, **1982**, Academic Press, Toronto.

(30) J. H. Van't Hoff, *The Foundations of Stereochemistry* **1901**, 66.

(31) J. A. Le Bel, *The Foundations of Stereochemistry* **1901**, 47.

(32) R. B. Grossman, *J. Chem. Ed.* **1989**, *66*, 30.

(33) D. A. Long, *J. Mol. Struc.* **1985**, *126*, 9.

(34) C. A. Bischoff, *Chem. Ber.* **1890**, *23*, 620.

(35) G. H. Christie; J. Kenner, *J. Chem. Soc.* **1922**, *LXXI*, 614.

(36) H. Eyring; D. M. Grant; H. Hecht, *J. Chem. Ed.* **1962**, *39*, 466.

(37) H. Eyring, *J. Am. Chem. Soc.* **1932**, *54*, 3191.

(38) K. S. Pitzer; J. D. Kemp, *J. Am. Chem. Soc.* **1938**, *60*, 1515.

(39) J. D. Kemp; K. S. Pitzer, *J. Am. Chem. Soc.* **1937**, *59*, 276.

(40) J. D. Kemp; K. S. Pitzer, *J. Chem. Phys.* **1936**, *4*, 749.

(41) S. Brydges; L. E. Harrington; M. J. McGlinchey, *Coord. Chem. Rev.* **2002**, *233-234*, 75.

(42) D. Gust; K. Mislow, *J. Am. Chem. Soc.* **1973**, *95*, 1535.

(43) K. Mislow, *Acc. Chem. Res.* **1976**, *9*, 26.

(44) K. Mislow, *Chemtracts - Org. Chem.* **1989**, *2*, 151.

(45) M. J. Sabacky; S. M. Johnson; J. C. Martin; I. C. Paul, *J. Am. Chem. Soc.* **1969**, *91*, 7542.

(46) A. Rieker; H. Kessler, *Tet. Lett.* **1969**, 1227.

(47) H. Kessler; A. Moosmayer; A. Rieker, *Tetrahedron* **1969**, *25*, 287.

(48) R. J. Kurland; I. I. Schuster; A. K. Colter, *J. Am. Chem. Soc.* **1965**, *87*, 2278.

(49) E. E. Wille; D. S. Stephenson; P. Capriel; G. Binsch, *J. Am. Chem. Soc.* **1982**, *104*, 405.

(50) P. Finocchiaro; D. Gust; K. Mislow, *J. Am. Chem. Soc.* **1974**, *96*, 3198.

(51) R. Glaser; J. F. Blount; K. Mislow, *J. Am. Chem. Soc.* **1980**, *102*, 2777.

(52) K. Mislow; D. Gust; R. J. Finnocchiaro; R. J. Boettcher, *Top. Curr. Chem.* **1985**, *127*, 3.

(53) J. C. J. Bart, *Acta Cryst.* **1968**, *B24*, 1277.

(54) E. M. Larson; R. B. von Dreele; P. Hanson; J. D. Gust, *Acta Cryst.* **1990**, *C46*, 784.

(55) A. Almenningen; O. Bastiansen; P. N. Skancke, *Acta Chem. Scand.* **1958**, *12*, 1215.

(56) D. Gust, *J. Am. Chem. Soc.* **1977**, *99*, 6980.

(57) D. Gust; A. Patton, *J. Am. Chem. Soc.* **1978**, *100*, 8175.

(58) A. Patton; J. Wang Dirks; D. Gust, *J. Org. Chem.* **1979**, *44*, 4749.

(59) J. Haywood-Farmer; M. A. Battiste, *Chem. Ind.* **1971**, 1232.

(60) R. Willem; H. Pepermans; C. Hoogzand; K. Hallenga; M. Gielen, *J. Am. Chem. Soc.* **1981**, *103*, 2297.

(61) R. Willem; A. Jans; C. Hoogzand; M. Gielen; G. van Binst; H. Pepermans, *J. Am. Chem. Soc.* **1985**, *107*, 28.

(62) M. W. Fagan; D. Gust, *J. Org. Chem.* **1981**, *46*, 1499.

(63) H. K. Gupta; M. Stradiotto; D. W. Hughes; M. J. McGlinchey, *J. Org. Chem.* **2000**, *65*, 3652.

(64) S. Brydges; M. J. McGlinchey, *J. Org. Chem.* **2002**, *67*, 7688.

(65) J. J. Bergman; W. D. Chandler, *Can. J. Chem.* **1972**, *50*, 353.

(66) H. Kwart; S. Alekman, *J. Am. Chem. Soc.* **1968**, *90*, 4482.

(67) E. Maverick; K. N. Trueblood; D. A. Bekoe, *Acta Cryst.* **1978**, *B34*, 2777.

(68) V. Melissas; K. Faegri; J. Almlöf, *J. Am. Chem. Soc.* **1985**, *107*, 4640.

(69) D. J. Iverson; G. Hunter; J. F. Blount; J. R. Damewood; K. Mislow, *J. Am. Chem. Soc.* **1981**, *103*, 6073.

(70) D. J. Iverson; G. Hunter; J. F. Blount; J. R. Damewood Jr.; K. Mislow, *J. Am. Chem. Soc.* **1982**, *103*, 6073.

(71) I. Bar; J. Bernstein; A. Christensen, *Tetrahedron* **1977**, *33*, 3177.

(72) H. E. Gottlieb; C. Ben-Ari; A. Hassner; V. Marks, *Tetrahedron* **1999**, *55*, 4003.

(73) K. V. Kilway; J. S. Siegel, *Tetrahedron* **2001**, *57*, 3615.

(74) J. Siegel; K. Mislow, *J. Am. Chem. Soc.* **1983**, *105*, 7763.

(75) J. Siegel; A. Gutiérrez; W. B. Schweizer; O. Ermer; K. Mislow, *J. Am. Chem. Soc.* **1986**, *108*, 1569.

(76) W. Weissensteiner; A. Gutiérrez; M. D. Radcliffe; J. Siegel; M. D. Singh; P. J. Tuohey; K. Mislow, *J. Org. Chem.* **1985**, *50*, 5822.

(77) W. D. Hounshell; L. D. Iroff; D. J. Iverson; R. J. Wroczynski; K. Mislow, *Isreal J. Chem.* **1980**, *20*, 65.

(78) K. V. Kilway; J. S. Siegel, *J. Am. Chem. Soc.* **1992**, *114*, 255.

(79) G. Hunter; J. F. Blount; J. R. Damewood Jr.; D. J. Iverson; K. Mislow, *Organometallics* **1982**, *1*, 448.

(80) J. F. Blount; G. Hunter; K. Mislow, *J. Chem. Soc. Chem. Commun.* **1984**, 170.

(81) M. J. McGlinchey; J. L. Fletcher; B. G. Sayer; P. Bougeard; R. Faggiani; C. J. L. Lock; A. D. Bain; C. Rodger; E. P. Kundig; D. Astruc; J. -R. Hamon; P. L. Maux; S. Top; G. Jaouen, *J. Chem. Soc. Chem. Commun.* **1983**, 634.

(82) G. Hunter; K. Mislow, *J. Chem. Soc. Chem. Commun.* **1984**, 172.

(83) G. Hunter; T. J. R. Weakley; K. Mislow; M. G. Wong, *J. Chem. Soc. Dalton Trans.* **1986**, 577.

(84) J. A. Chudek; G. Hunter; R. L. MacKay; P. Kremminger; K. Schlogl; W. Weissensteiner, *J. Chem. Soc. Dalton Trans.* **1990**, 2001.

(85) J. A. Chudek; G. Hunter; R. L. MacKay; G. Farber; W. Weissensteiner, *J. Organomet. Chem.* **1989**, *377*, C69.

(86) P. A. Downton; B. Mailvaganam; C. S. Frampton; B. G. Sayer; M. J. McGlinchey, *J. Am. Chem. Soc.* **1990**, *112*, 27.

(87) B. Mailvaganam; C. S. Frampton; S. Top; B. G. Sayer; M. J. McGlinchey, *J. Am. Chem. Soc.* **1991**, *113*, 1177.

(88) K. V. Kilway; J. S. Siegel, *Organometallics* **1992**, *11*, 1426.

(89) B. Mailvaganam; B. E. McCarry; B. G. Sayer; R. E. Perrier; R. Faggiani; M. J. McGlinchey, *J. Organomet. Chem.* **1987**, *335*, 213.

(90) B. Mailvaganam; B. G. Sayer; M. J. McGlinchey, *J. Organomet. Chem.* **1990**, *395*, 177.

(91) A. Siegel; M. D. Rausch, *Synth. React. Inorg. Met. - Org. Chem.* **1978**, *8*, 209.

(92) H. K. Gupta; N. Rampersad; M. Stradiotto; M. J. McGlinchey, *Organometallics* **2000**, *19*, 184.

(93) H. K. Gupta; S. Brydges; M. J. McGlinchey, *Organometallics* **1999**, *18*, 115.

(94) W. -Y. Yeh; C. -L. Ho; M. Y. Chiang; I. -T. Chen, *Organometallics* **1997**, *16*, 2698.

(95) L. D. Field; T. W. Hambley; P. A. Humphrey; A. F. Masters; P. Turner, *Inorg. Chem.* **2002**, *41*, 4618.

(96) L. D. Field; K. M. Ho; C. M. Lindall; A. F. Masters; A. G. Webb, *Aust. J. Chem.* **1990**, *43*, 281.

(97) H. Adams; N. A. Bailey; A. F. Browning; J. A. Ramsden; C. White, *J. Organomet. Chem.* **1990**, *387*, 305.

(98) L. D. Field; T. W. Hambley; P. A. Humphrey; A. F. Masters; P. Turner, *Polyhedron* **1998**, *17*, 2587.

(99) H. Schumann; A. Lentz; R. Weimann; J. Pickardt, *Angew. Chem. Int. Ed. Engl.* **1994**, *33*, 1731.

(100) P. Brégaint; J. -R. Hamon; C. Lapinte, *Organometallics* **1992**, *11*, 1417.

(101) L. D. Field; A. F. Masters; M. Gibson; D. R. Latimer; T. W. Hambley; I. E. Buys, *Inorg. Chem.* **1993**, *32*, 211.

(102) F. Mao; C. E. Philbin; T. J. R. Weakley; D. R. Tyler, *Organometallics* **1990**, *9*, 1510.

(103) J. W. Chambers; A. J. Baskar; S. G. Bott; J. L. Atwood; M. D. Rausch, *Organometallics* **1986**, *5*, 1635.

(104) C. Janiak; H. Schumann, *Adv. Organomet. Chem.* **1991**, *33*, 291.

(105) M. P. Castellani; S. J. Geib; A. L. Rheingold; W. C. Trogler, *Organometallics* **1987**, *6*, 1703.

(106) M. P. Thornberry; C. Slebodnick; P. A. Deck; F. R. Fronczek, *Organometallics* **2001**, *20*, 920.

(107) M. P. Castellani; S. J. Geib; A. L. Rheingold; W. C. Trogler, *Organometallics* **1987**, *6*, 2524.

(108) M. P. Castellani; J. M. Wright; S. J. Geib; A. L. Rheingold; W. C. Trogler, *Organometallics* **1986**, *5*, 1116.

(109) P. Legzdins; R. Reina; M. J. Shaw; R. J. Batchelor; F. W. B. Einstein, *Organometallics* **1993**, *12*, 1029.

(110) H. Adams; N. A. Bailey; P. D. Hempstead; M. J. Morris; S. Riley; R. L. Beddoes; E. S. Cook, *J. Chem. Soc. Dalton Trans.* **1993**, 91.

(111) F. Mao; S. K. Sur; D. R. Tyler, *J. Am. Chem. Soc.* **1989**, *111*, 7628.

(112) R. J. Hoobler; J. V. Adams; M. A. Hutton; T. W. Francisco; B. S. Haggerty; A. L. Rheingold; M. P. Castellani, *J. Organomet. Chem.* **1991**, *412*, 157.

(113) W. M. Harrison; C. Saadeh; S. B. Colbran; D. C. Craig, *J. Chem. Soc. Dalton Trans.* **1997**, 3785.

(114) N. A. Bailey; V. S. Jassal; R. Vefghi; C. White, *J. Chem. Soc. Dalton Trans.* **1987**, 2815.

(115) M. P. Thornberry; C. Slebodnick; P. A. Deck; F. R. Fronczek, *Organometallics* **2000**, *19*, 5352.

(116) M. J. McGlinchey, *Can. J. Chem.* **2001**, *79*, 1295.

(117) L. Li; A. Decken; B. G. Sayer; M. J. McGlinchey; P. Brégaint; J. -Y. Thépot; L. Toupet; J. -R. Hamon; C. Lapinte, *Organometallics* **1994**, *13*, 682.

(118) L. C. F. Chao; H. K. Gupta; D. W. Hughes; J. F. Britten; S. S. Rigby; A. D. Bain; M. J. McGlinchey, *Organometallics* **1995**, *14*, 1139.

(119) S. Brydges; J. F. Britten; L. C. F. Chao; H. K. Gupta; M. J. McGlinchey; D. L. Pole, *Chem. Eur. J.* **1998**, *4*, 1201.

(120) B. Hankinson; H. Heaney; R. P. Sharma, *J. Chem. Soc. Perkin Trans. I* **1972**, 2372.

(121) K. Bowden; J. G. Irving; M. J. Price, *Can. J. Chem.* **1968**, *46*, 3903.

(122) B. H. Klanderman; T. R. Criswell, *J. Org. Chem.* **1969**, *34*, 3426.

(123) M. Oki, *Angew,.Chem. Int. Ed. Engl.* **1976**, *15*, 87.

(124) J. Lu; J. Zhang; X. Shen; D. M. Ho; R. A. Pascal, *J. Am. Chem. Soc.* **2002**, *124*, 8035.

(125) V. Marks; M. Nahmany; H. E. Gottlieb; S. E. Biali, *J. Org. Chem.* **2002**, *67*, 7898.

(126) S. Spyroudis; N. Xanthopoulou, *J. Org. Chem.* **2002**, *67*, 4612.

(127) M. Nakamura; M. Oki; H. Nakanishi, *Bull. Chem. Soc. Jpn.* **1974**, *47*, 2415.

(128) F. Suzuki; M. Oki; H. Nakanishi, *Bull. Chem. Soc. Jpn.* **1974**, *47*, 3114.

(129) F. Imashiro; K. Takegoshi; T. Terao; A. Saika, *J. Am. Chem. Soc.* **1982**, *104*, 2247.

(130) G. Yamamoto; M. Oki, *J. Org. Chem.* **1984**, *49*, 1913.

(131) G. Yamamoto; M. Oki, *J. Org. Chem.* **1983**, *48*, 1233.

(132) R. B. Nachbar; W. D. Hounshell; V. A. Naman; O. Wennerström; A. Guenzi; K. Mislow, *J. Org. Chem.* **1983**, *48*, 1227.

(133) G. Yamamoto, *J. Mol. Struc.* **1985**, *126*, 413.

(134) G. Yamamoto, *Bull. Chem. Soc. Jpn.* **1989**, *62*, 4058.

(135) G. Yamamoto, *Pure & Appl. Chem.* **1990**, *62*, 569.

(136) G. Yamamoto; M. Oki, *Chem. Lett.* **1984**, 97.

(137) G. Yamamoto; M. Oki, *Bull. Chem. Soc. Jpn.* **1986**, *59*, 3597.

(138) G. Yamamoto, *Chem. Lett.* **1990**, 1373.

(139) G. Yamamoto, *Chem. Lett.* **1991**, 1161.

(140) G. Yamamoto, *Bull. Chem. Soc. Jpn.* **1992**, *65*, 1967.

(141) G. Yamamoto; T. Nemoto; Y. Ohashi, *Bull. Chem. Soc. Jpn.* **1992**, *65*, 1957.

(142) R. Isaksson; M. Oki; J. Sandström; M. R. Suissa; S. Toyota, *Acta Chem. Scand.* **1993**, *47*, 570.

(143) T. Nemoto; T. Ono; A. Uchida; Y. Ohashi; G. Yamamoto, *Acta Cryst.* **1994**, *C50*, 297.

(144) T. Nemoto; Y. Ohashi; G. Yamamoto, *Acta Cryst.* **1996**, *C52*, 716.

(145) Y. Kawada; H. Iwamura, *J. Org. Chem.* **1980**, *45*, 2547.

(146) W. D. Hounshell; C. A. Johnson; A. Guenzi; F. Cozzi; K. Mislow, *Proc. Natl. Acad. Sci.USA* **1980**, *77*, 6961.

(147) H. Iwamura; K. Mislow, *Acc. Chem. Res.* **1988**, *21*, 175.

(148) F. Cozzi; A. Guenzi; C. A. Johnson; K. Mislow, *J. Am. Chem. Soc.* **1981**, *103*, 957.

(149) Y. Kawada; H. Iwamura, *J. Am. Chem. Soc.* **1981**, *103*, 958.

(150) Y. Kawada; H. Iwamura, *J. Am. Chem. Soc.* **1983**, *105*, 1449.

(151) H. Iwamura; T. Ito; K. Toriumi; Y. Kawada; E. Osawa; T. Fujiyoshi; C. Jaime, *J. Am. Chem. Soc.* **1984**, *106*, 4712.

(152) Y. Kawada; H. Sakai; M. Oguri; G. Koga, *Tet. Lett.* **1994**, *35*, 139.

(153) Y. Kawada; Y. Kimura; H. Yamazaki; J. Ishikawa; H. Sakai; M. Oguri; G. Koga, *Chem. Lett.* **1994**, 1311.

(154) S. Toyota; T. Yamamori; T. Makino; M. Oki, *Bull. Chem. Soc. Jpn.* **2000**, *73*, 2591.

(155) S. Toyota; T. Yamamori; M. Asakura; M. Oki, *Bull. Chem. Soc. Jpn.* **2000**, *73*, 205.

(156) S. Toyota; T. Yamamori; T. Makino, *Tetrahedron* **2001**, *57*, 3521.

(157) R. L. Pohl; B. R. Willeford, *J. Organomet. Chem.* **1970**, *23*, C45.

(158) G. A. Moser; M. D. Rausch, *Synth. React. Inorg. Met. - Org. Chem.* **1974**, *4*, 37.

(159) C. W. Fung; M. Khorramdel-Vahed; R. J. Ranson; R. M. G. Roberts, *J. Chem. Soc. Perkin Trans. II* **1980** , 267.

(160) R. A. Gancarz; J. F. Blount; K. Mislow, *Organometallics* **1985**, *4*, 2028.

(161) R. A. Gancarz; M. W. Baum; G. Hunter; K. Mislow, *Organometallics* **1986**, *5*, 2327.

(162) P. J. Fagan; M. D. Ward; J. C. Calabrese, *J. Am. Chem. Soc.* **1989**, *111*, 1698.

(163) H. Schmidbaur; T. Probst; O. Steigelmann, *Organometallics* **1991**, *10*, 3176.

(164) S. Toyota; H. Okuhara; M. Oki, *Organometallics* **1997**, *16*, 4012.

(165) A. M. Stevens; C. J. Richards, *Tet. Lett.* **1997**, *38*, 7805.

(166) T. R. Kelly; M. C. Bowyer; K. V. Bhaskar; D. Bebbington; A. Garcia; F. Lang; M. H. Kim; M. P. Jette, *J. Am. Chem. Soc.* **1994**, *116*, 3657.

(167) T. R. Kelly; I. Tellitu; J. P. Sestelo, *Angew. Chem. Int. Ed. Engl.* **1997**, *36*, 1866.

(168) T. R. Kelly; J. P. Sestelo; I. Tellitu, *J. Org. Chem.* **1998**, *63*, 3655.

(169) T. R. Kelly; H. De Silva; R. A. Silva, *Nature* **1999**, *401*, 150.

(170) R. Ballardini; V. Balzani; A. Credi; M. T. Gandolfi; M. Venturi, *Acc. Chem. Res.* **2001**, *34*, 445.

(171) M. Schultz, *Nature* **1999**, *399*, 729.

(172) J. F. Stoddart, *Acc. Chem. Res.* **2001**, *34*, 410.

(173) V. Balzani; A. Credi; F. M. Raymo; J. F. Stoddart, *Angew. Chem. Int. Ed.* **2000**, *39*, 3348.

(174) R. Coontz; P. Szuromi, *Science* **2000**, *290*, 1520.

(175) P. Boyer, *Biochim. Biophys. Acta* **1993**, *1140*, 215.

(176) R. K. Soong; G. D. Bachand; H. P. Neves; A. G. Olkhovets; H. G. Craighead; C. D. Montemagno, *Science* **2000**, *290*, 1555.

(177) L. Kouwenhoven, *Nature* **2000**, *407*, 35.

(178) M. C. Jiminez-Molero; C. Dietrich-Buchecker; J. -P. Sauvage, *Chem. Comm.* **2003**, 1613.

(179) Z. Dominguez; H. Dang; M. J. Strouse; M. A. Garcia-Garibay, *J. Am. Chem. Soc.* **2002**, *124*, 7719.

(180) L. Raehm; J. -M. Kern; J. -P. Sauvage, *Chem. Eur. J.* **1999**, *5*, 3310.

(181) J. K. Gimzewski; C. Joachim; R. R. Schlittler; V. Langlais; H. Tang; I. Johannsen, *Science* **1998**, *281*, 531.

(182) H. F. Bettinger; P. von R. Schleyer; H. F. Schaefer III, *J. Am. Chem. Soc.* **1998**, *120*, 1074.

(183) B. A. Kowert; W. I. Mariencheck, *J. Phys. Chem.* **1993**, *97*, 11639.

(184) T. C. Bedard; J. S. Moore, *J. Am. Chem. Soc.* **1995**, *117*, 10662.

(185) G. Jiminez-Bueno; G. Rapenne, *Tet. Lett.* **2003**, *44*, 6261.

(186) C. Joachim; H. Tang; F. Moresco; G. Rapenne; G. Meyer, *Nanotech.* **2002**, *13*, 330.

(187) P. R. Ashton; R. Ballardini; V. Balzani; A. Credi; K. R. Dress; E. Ishow; C. J. Kleverlaan; O. Kocian; J. A. Preece; N. Spencer; J. F. Stoddart; M. Venturi; S. Wenger, *Chem. Eur. J.* **2000**, *6*, 3558.

(188) T. R. Kelly, *Acc. Chem. Res.* **2001**, *34*, 514.

(189) B. X. Colasson; C. Dietrich-Buchecker; M. C. Jiminez-Molero; J. -P. Sauvage, *J. Phys. Org. Chem.* **2002**, *15*, 476.

(190) J. -P. Sauvage, *Acc. Chem. Res.* **1998**, *31*, 611.

(191) C. A. Schalley; K. Beizai; F. Vögtle, *Acc. Chem. Res.* **2001**, *34*, 465.

(192) M. -J. Blanco; M. C. Jiminez; J. -C. Chambron; V. Heitz; M. Linke; J. -P. Sauvage, *Chem. Soc. Rev.* **1999**, *28*, 293.

(193) L. Fabbrizzi; M. Licchelli; P. Pallavicini, *Acc. Chem. Res.* **1999**, *32*, 846.

(194) B. L. Feringa, *Acc. Chem. Res.* **2001**, *34*, 504.

(195) R. A. Bissell; E. Córdova; A. E. Kaifer; J. F. Stoddart, *Nature* **1994**, *369*, 133.

(196) A. B. Lindner; F. Grynszpan; S. E. Biali, *J. Org. Chem.* **1993**, *58*, 6662.

(197) N. Koga; Y. Kawada; H. Iwamura, *J. Am. Chem. Soc.* **1983**, *105*, 5498.

(198) N. Koga; Y. Kawada; H. Iwamura, *Tetrahedron* **1986**, *42*, 1679.

(199) L. E. Harrington; J. F. Britten; D. W. Hughes; A. D. Bain; J. -Y. Thépot; M. J. McGlinchey, *J. Organomet. Chem.* **2002**, *656*, 243.

(200) C. F. H. Allen, *Chem. Rev.* **1962**, *62*, 653.

(201) M. A. Ogliaruso; M. G. Romanelli; E. I. Becker, *Chem. Rev.* **1965**, *65*, 261.

(202) M. D. Rausch; E. F. Tokas; E. A. Mintz; A. Clearfield; M. Mangion; I. Bernal, *J. Organomet. Chem.* **1979**, *172*, 109.

(203) M. D. Rausch; G. F. Westover; E. Mintz; G. M. Reisner; I. Bernal; A. Clearfield; J. M. Troup, *Inorg. Chem.* **1979**, *18*, 2605.

(204) W. Clegg; J. C. Lockhart; M. B. McDonnell, *J. Chem. Soc. Perkin Trans. I* **1985**, 1019.

(205) J. C. Lockhart; M. B. McDonnell; W. Clegg; M. N. S. Hill, *J. Chem. Soc. Perkin Trans. II* **1987**, 639.

(206) S. Ito; M. Fujita; N. Morita; T. Asao, *Chem. Lett.* **1995**, 475.

(207) S. Ito; M. Fujita; N. Morita; T. Asao, *Bull. Chem. Soc. Jpn.* **1995**, *68*, 3611.

(208) R. W. Baker; M. A. Foulkes; J. A. Taylor, *J. Chem. Soc. Perkin Trans. I* **1998**, 1047.

(209) J. -Y. Thépot; C. Lapinte, *J. Organomet. Chem.* **2001**, *627*, 179.

(210) U. Kolle; J. Kossakowski; G. Raabe, *Angew. Chem. Int. Ed. Engl.* **1990**, *29*, 773.

(211) U. Kolle; C. Reitmann; G. Raabe, *Organometallics* **1997**, *16*, 3273.

(212) M. E. Smith; F. J. Hollander; R. Anderson, *Angew. Chem. Int. Ed. Engl.* **1993**, *32*, 1294.

(213) R. N. Hargreaves; M. R. Truter, *J. Chem. Soc. A* **1969**, 2282.

(214) K. Kite; A. F. Psaila, *J. Organomet. Chem.* **1992**, *441*, 159.

(215) W. Rigby; H. -B. Lee; P. M. Bailey; J. A. McCleverty; P. M. Maitlis, *J. Chem. Soc. Dalton Trans.* **1979**, 387.

(216) A. R. Siedle, *Comprehensive Coordination Chemistry* **1987**, 365.

(217) C. Saadeh; S. B. Colbran; D. C. Craig; A. D. Rae, *Organometallics* **1993**, *12*, 133.

(218) C. P. Brock; J. A. Ibers, *Acta Cryst.* **1973**, *B29*, 2426.

(219) K. Mislow, *Pure & Appl. Chem.* **1971**, *25*, 549.

(220) S. G. Davies; A. E. Derome; J. P. McNally, *J. Am. Chem. Soc.* **1991**, *113*, 2854.

(221) G. Hunter; R. L. MacKay; P. Kremminger; W. Weissensteiner, *J. Chem. Soc. Dalton Trans.* **1991**, 3349.

(222) J. A. S. Howell; M. G. Palin; P. McArdle; D. Cunningham; Z. Goldschmidt; H. E. Gottlieb; D. Hezroni-Langerman, *Organometallics* **1993**, *12*, 1694.

(223) G. Hunter; T. J. R. Weakley; W. Weissensteiner, *J. Chem. Soc. Dalton Trans.* **1987**, 1545.

(224) J. W. Faller; B. V. Johnson, *J. Organomet. Chem.* **1975**, *96*, 99.

(225) L. D. Field; B. A. Messerle; L. Soler; I. E. Buys; T. W. Hambley, *J. Chem. Soc. Dalton Trans.* **2001**, 1959.

(226) J. A. Chudek; G. Hunter; R. L. MacKay; P. Kremminger; W. Weissensteiner, *J. Chem. Soc. Dalton Trans.* **1991**, 3337.

(227) H. Shimizu, *J. Chem. Phys.* **1964**, *40*, 3357.

(228) E. L. Mackor; C. MacLean, *Prog. Nucl. Magn. Reson. Spectrosc.* **1967**, *3*, 129.

(229) K. Peruvshin; R. Reik; G. Wider; K. Wüthrich, *Proc. Natl. Acad. Sci. USA* **1997**, *94*, 12366.

(230) J. M. Chance; J. H. Geiger; K. Mislow, *J. Am. Chem. Soc.* **1989**, *111*, 2326.

(231) A. M. Rouhi, *Chem. Eng. News* **1998**, *76*, 57.

(232) D. Gust; A. Patton, *J. Am. Chem. Soc.* **1978**, *100*, 8175.

(233) J. H. Magill; A. R. Ubbelohde, *Trans. Faraday Soc.* **1958**, *54*, 1811.

(234) D. J. Plazek; J. H. Magill, *J. Chem. Phys.* **1966**, *45*, 3038.

(235) M. V. Alfimov; Yu. B. Scheck; N. P. Kovalenko, *Chem. Phys. Lett.* **1976**, *43*, 154.

(236) Y. B. Scheck; N. P. Kovalenko; M. V. Alfimov, *J. Lumin.* **1977**, *15*, 157.

(237) C. M. Whitaker; R. J. McMahon, *J. Phys. Chem.* **1996**, *100*, 1081.

(238) H. E. Katz, *J. Org. Chem.* **1987**, *52*, 3932.

(239) (a) S. R. Samanta; A. K. Mukherjee; A. J. Bhattacharyya, *Curr. Sci.* **1988**, *57*, 926. (b) Z. Marcinow; P. W. Rabideau, *J. Org. Chem.* **1990**, *55*, 3812. (c) P. N. Riley; M. G. Thorn; J. S. Vilardo; M. A. Lockwood; P. E. Fanwick; I. P. Rothwell, *Organometallics* **1999**, *18*, 3016.

(240) Accelrys Materials Studio Version 2.2.1 (2002), Accelrys Inc., Modules X-Cell and Reflex were used.

(241) L. E. Harrington; James F. Britten; M. J. McGlinchey, *Can. J. Chem.* **2003**, *81*, 1180.

(242) J. C. Barnes; W. M. Horspool; F. I. Mackie, *Acta Cryst.* **1991**, *C47*, 164.

(243) S. Zilberg; Y. Haas, *J. Am. Chem. Soc.* **2002**, *124*, 10683.

(244) J. B. Lambert; L. Lin; V. Rassolov, *Angew. Chem. Int. Ed.* **2002**, *41*, 1429.

(245) M. Otto; D. Scheschkewitz; T. Kato; M. M. Midland; J. B. Lambert; G. Bertrand, *Angew. Chem. Int. Ed.* **2002**, *41*, 2275.

(246) J. N. Jones; A. H. Cowley; C. L. B. Macdonald, *Chem. Comm.* **2002**, 1520.

(247) K. Ziegler; B. Schnell, *Ann.* **1925**, *445*, 266.

(248) R. Breslow; H. W. Chang; W. A. Yager, *J. Am. Chem. Soc.* **1963**, *85*, 2033.

(249) R. Breslow; H. W. Chang, *J. Am. Chem. Soc.* **1961**, *83*, 3727.

(250) J. -M. Carpentier, *Bull. Soc. Chim. Fr.* **1973**, 2209.

(251) A. D. Allen; M. Sumonja; T. T. Tidwell, *J. Am. Chem. Soc.* **1997**, *119*, 2371.

(252) A. D. Allen; T. T. Tidwell, *J. Org. Chem.* **2001**, *66*, 7696.

(253) E. P. F. Lee; T. G. Wright, *Phys. Chem. Chem. Phys.* **1999**, *1*, 219.

(254) Y. Shiota; M. Kondo; K. Yoshizawa, *J. Chem. Phys.* **2001**, *115*, 9243.

(255) B. S. Jursic, *J. Mol. Struc. (Theochem)* **1999**, *468*, 171.

(256) M. N. Glukhovtsev; R. D. Bach; S. Laiter, *J. Phys. Chem.* **1996**, *100*, 10952.

(257) B. Reindl; P. von R. Schleyer, *J. Comput. Chem.* **1998**, *19*, 1402.

(258) H. Jiao; P. von R. Schleyer; Y. Mo; M. A. McAllister; T. T. Tidwell, *J. Am. Chem. Soc.* **1997**, *119*, 7075.

(259) C. F. H. Allen; J. A. Van Allan, *J. Am. Chem. Soc.* **1943**, *65*, 1384.

(260) N. O. V. Sonntag; S. Linder; E. I. Becker; P. E. Spoerri, *J. Am. Chem. Soc.* **1953**, *75*, 2283.

(261) I. I. Schuster; L. Craciun; D. M. Ho; R. A. Pascal, *Tetrahedron* **2002**, *58*, 8875.

(262) H. Vancik; I. Novak; D. Kidemet, *J. Phys. Chem. A* **1998**, *102*, 8437.

(263) H. Vancik; I. Novak; D. Kidemet, *J. Phys. Chem. A* **1997**, *101*, 1523.

(264) R. Breslow; S. Mazur, *J. Am. Chem. Soc.* **1973**, *95*, 584.

(265) P. Jutzi; A. Mix, *Chem. Ber.* **1992**, *125*, 951.

(266) R. Breslow; H. W. Chang; R. Hill; E. Wasserman, *J. Am. Chem. Soc.* **1967**, *89*, 1112.

(267) M. Saunders; R. Berger; A. Jaffe; J. M. McBride; J. O'Neill; R. Breslow; J. M. Hoffman; C. Perchonock; E. Wasserman; R. S. Hutton; V. J. Kuck, *J. Am. Chem. Soc.* **1973**, *95*, 3017.

(268) M. J. McGlinchey; L. Girard; R. Ruffolo, *Coord. Chem. Rev.* **1995**, *143*, 331.

(269) P. A. Downton; B. G. Sayer; M. J. McGlinchey, *Organometallics* **1992**, *11*, 3281.

(270) L. Girard; A. Decken; A. Blecking; M. J. McGlinchey, *J. Am. Chem. Soc.* **1994**, *116*, 6427.

(271) M. Gruselle; H. El Hafa; M. Nikolski; G. Jaouen; J. Vaissermann; L. Li; M. J. McGlinchey, *Organometallics* **1993**, *12*, 4917.

(272) J. A. Dunn; J. F. Britten; J. -C. Daran; M. J. McGlinchey, *Organometallics* **2001**, *20*, 4690.

(273) J. A. Dunn; W. J. Hunks; R. Ruffolo; S. S. Rigby; M. A. Brook; M. J. McGlinchey, *Organometallics* **1999**, *18*, 3372.

(274) M. Ansorge; K. Polborn; T. J. J. Müller, *Eur. J. Inorg. Chem.* **2000**, 2003.

(275) J. Lukasser; H. Angleitner; H. Schottenberger; H. Kopacka; M. Schweiger; B. Bildstein; K. -H. Ongania; K. Wurst, *Organometallics* **1995**, *14*, 5566.

(276) U. Behrens, *J. Organomet. Chem.* **1979**, *182*, 89.

(277) A. Z. Kreindlin; F. M. Dolgushin; A. I. Yanovsky; Z. A. Kerzina; P. V. Petrovskii; M. I. Rybinskaya, *J. Organomet. Chem.* **2000**, *616*, 106.

(278) S. Barlow; A. Cowley; J. C. Green; T. J. Brunker; T. Hascall, *Organometallics* **2001**, *20*, 5351.

(279) T. A. Albright; R. Hoffmann; P. Hofmann, *Chem. Ber.* **1978**, *111*, 1591.

(280) V. G. Andrianov; Y. T. Struchkov, *J. Struc. Chem.* **1977**, *18*, 251.

(281) V. G. Andrianov; Y. T. Struchkov; V. N. Setkina; V. I. Zdanovich; A. Zh. Zhakaeva; D. N. Kursanov, *J. Chem. Soc. Chem. Commun.* **1975**, 117.

(282) S. Top; G. Jaouen; M. J. McGlinchey, *Chem.Comm.* **1980**, 1110.

(283) W. E. Watts, *J. Organomet. Chem.* **1981**, *220*, 165.

(284) T. P. E. Kenny; A. C. Knipe; W. E. Watts, *J. Organomet. Chem.* **1991**, *413*, 257.

(285) M. J. A. Habib; J. Park; W. E. Watts, *J. Chem. Soc. C* **1970**, 2556.

(286) T. S. Abram; W. E. Watts, *J. Chem. Soc. Perkin Trans. I* **1977**, 1522.

(287) E. -W. Koch; H. -U. Siehl; M. Hanack, *Tet. Lett.* **1985**, *26*, 1493.

(288) J. J. Dannenberg; M. K. Levenberg; J. H. Richards, *Tetrahedron* **1973**, *29*, 1575.

(289) T. D. Turbitt; W. E. Watts, *J. Chem. Soc. Perkin Trans. II* **1974**, 177.

(290) G. Cerichelli; B. Floris; G. Ortaggi, *J. Organomet. Chem.* **1974**, *78*, 241.

(291) T. S. Abram; W. E. Watts, *J. Chem. Soc. Perkin Trans. I* **1977**, 1532.

(292) H. Schottenberger; M. R. Buchmeiser; H. Angleitner; K. Wurst; R. H. Herber, *J. Organomet. Chem.* **2000**, *605*, 174.

(293) T. S. Abram; W. E. Watts, *J. Chem. Soc. Perkin Trans. I* **1977**, 1527.

(294) G. K. S. Prakash; H. Buchholz; V. P. Reddy; A. de Meijere; G. A. Olah, *J. Am. Chem. Soc.* **1992**, *114*, 1097.

(295) M. J. A. Habib; W. E. Watts, *J. Chem. Soc. C* **1970**, 2552.

(296) S. Ito; N. Morita; T. Asao, *J. Org. Chem.* **1996**, *61*, 5077.

(297) E. A. Hill, *J. Organomet. Chem.* **1970**, *24*, 457.

(298) M. Caïs, *Organomet. Chem. Rev.* **1966**, 435.

(299) (a) T. G. Traylor; J. C. Ware, *J. Am. Chem. Soc.* **1967**, *89*, 2304. (b) T. G. Traylor; W. Hanstein; H. J. Berwin; N. A. Clinton; R. S. Brown, *J. Am. Chem. Soc.* **1971**, *93*, 5715.

(300) C. P. Lillya; R. A. Sahatjian, *J. Organomet. Chem.* **1971**, *32*, 371.

(301) M. Caïs; S. Dani; F. H. Herbstein; M. Kapon, *J. Am. Chem. Soc.* **1978**, 1*00*, 5554.

(302) L. E. Harrington; I. Vargas-Baca; N. Reginato; M. J. McGlinchey, *Organometallics* **2003**, *22*, 663.

(303) G. Maier; S. Pfriem; U. Schäfer; K. -D. Malsch; R. Matusch, *Chem. Ber.* **1981**, *114*, 3965.

(304) G. Maier; L. H. Franz, *Liebigs Ann. Chem.* **1995**, 139.

(305) G. Maier; L.H. Franz; R. Boese, *Liebigs Ann. Chem.* **1995**, 147.

(306) G. Maier; H. Rang; R. Emrich, *Liebigs Ann. Chem.* **1995**, 153.

(307) L. Hoesch, *Chimia* **1975**, *29*, 531.

(308) E. McNelis, *J. Org. Chem.* **1965**, *30*, 4324.

(309) R. L. Harlow; S. H. Simonsen, *Cryst. Struc. Commun.* **1977**, *6*, 695.

(310) T. Takahashi; S. Huo; R. Hara; Y. Noguchi; K. Nakajima; W. -H. Sun, *J. Am. Chem. Soc.* **1999**, *121*, 1094.

(311) M. Caïs; J. J. Dannenberg; A. Eisenstadt; M. I. Levenberg; J. H. Richards, *Tet. Lett.* **1966**, *15*, 1695.

(312) A. Houlton; J. R. Miller; R. M. G. Roberts; J. Silver, *J. Chem. Soc. Dalton Trans.* **1991**, 467.

(313) A. A. Koridze; N. M. Astakhova; P. V. Petrovskii, *J. Organomet. Chem.* **1983**, *254*, 345.

(314) G. H. Williams; D. D. Traficante; D. Seyferth, *J. Organomet. Chem.* **1973**, *60*, C53.

(315) S. Braun; T. S. Abram; W. E. Watts, *J. Organomet. Chem.* **1975**, *97*, 429.

(316) G. A. Olah; G. Liang, *J. Org. Chem.* **1975**, *40*, 1849.

(317) M. Hisatome; K. Yamakawa, *Tetrahedron* **1971**, *27*, 2101.

(318) W. -Y. Wong; W. -T. Wong; K. -K. Cheung, *J. Chem. Soc. Dalton Trans.* **1995**, 1379.

(319) F. Edelmann; B. Lubke; U. Behrens, *Chem. Ber.* **1982**, *115*, 1325.

(320) H. Wadepohl; F. -J.Paffen; H. Pritzkow, *J. Organomet. Chem.* **1999**, *579*, 391.

(321) M. Tamm; A. Grzegorzewski; T. Steiner, *Chem. Ber.* **1997**, *130*, 225.

(322) H. Wadepohl; H. Pritzkow, *Acta Cryst.* **1991**, *C47*, 2061.

(323) A. P. Scott; I. Agranat; P. U. Biedermann; N. V. Riggs; L. Radom, *J. Org. Chem.* **1997**, *62*, 2026.

(324) D. R. Lide (Ed.), *CRC Handbook of Chemistry and Physics*, **2002**, CRC Press, New York.

(325) N. T. Anh; M. Elian; R. Hoffmann, *J. Am. Chem. Soc.* **1978**, *100*, 110.

(326) T. A. Albright; P. Hofmann; R. Hoffmann; C. P. Lillya; P. A. Dobosh, *J. Am. Chem. Soc.* **1983**, *105*, 3396.

(327) Y. F. Oprunenko; S. G. Malugina; Y. A. Ustynyuk; N. A. Ustynyuk; D. N. Kravtsov, *J. Organomet. Chem.* **1988**, *338*, 357.

(328) A. Decken; J. F. Britten; M. J. McGlinchey, *J. Am. Chem. Soc.* **1993**, *115*, 7275.

(329) V. Balzani; M. Gomez-Lopez; J. F. Stoddart, *Acc. Chem. Res.* **1998**, *31*, 405.

(330) D. M. Ho; R. A. Pascal, *Chem. Mater.* **1993**, *5*, 1358.

(331) J. Howard, *Nature* **1997**, *389*, 561.

(332) A. Huxley, *Nature* **1998**, *391*, 239.

(333) J. -P. Sauvage, *Acc. Chem. Res.* **1998**, *31*, 611.

(334) T. R. Kelly; R. A. Silva; H. De Silva; S. Jasmin; Y. Zhao, *J. Am. Chem. Soc.* **2000**, *122*, 6935.

(335) Y. Kawada; H. Sakai; M. Oguri; G. Koga, *Tet. Lett.* **1994**, *35*, 139.

(336) J. C. Bryan; R. A. Sachleben; A. A. Gakh; G. J. Bunick, *J. Chem. Cryst.* **1999**, *29*, 513.

(337) A. A. Gakh; R. A. Sachleben; J. C. Bryan, *Chemtech* **1997**, *27*, 26.

(338) G. Akibo-Betts; P. E. Barran; A. J. Stace, *Chem. Phys. Lett.* **2000**, *329*, 431.

(339) D. K. Rittenberg; K. Sugiura; A. M. Arif; Y. Sakata; C. D. Incarvito; A. L. Rheingold; J. S. Miller, *Chem. Eur. J.* **2000**, *6*, 1811.

(340) A. Panja; N. Shaikh; S. Gupta; R. J. Butcher; P. Banerjee, *Eur. J. Inorg. Chem.* **2003**, 1540.

(341) E. Gallo; E. Solari; N. Re; C. Floriani; A. Chiesi-Villa; C. Rizzoli, *J. Am. Chem. Soc.* **1997**, *119*, 5144.

(342) N. G. Connelly; G. R. Lewis; M. T. Moreno; A. G. Orpen, *J. Chem. Soc. Dalton Trans.* **1998**, 1905.

(343) J. R. Bryant; J. E. Taves; J. M. Mayer, *Inorg. Chem.* **2002**, *41*, 2769.

(344) L. E. Harrington; J. F. Britten; M. J. McGlinchey, *Tet. Lett.* **2003**, *44*, 8057.

(345) L. E. Harrington; M. J. McGlinchey, *Org. Lett.* **2004**, in press.

(346) S. Murata; T. Mori; M. Oki, *Chem. Lett.* **1982**, 271.

(347) S. Murata; T. Mori; M. Oki, *Bull. Chem. Soc. Jpn.* **1984**, *57*, 1970.

(348) R. A. McClelland; F. L. Cozens; J. Li; S. Steenken, *J. Chem. Soc. Perkin Trans. II* **1996**, 1531.

(349) R. C. Gostowski; T. Bailey; S. D. Bonner; E. E. Emrich; S. L. Steelman, *J.Phys.Org.Chem.* **2000**, *13*, 735.

(350) T. H. Siddall; W. E. Stewart, *J. Org. Chem.* **1969**, *34*, 233.

(351) K. D. Bartle; P. M. G. Bavin; D. W. Jones; R. L'amie, *Tetrahedron* **1970**, *26*, 911.

(352) M. Nakamura; N. Nakamura; M. Oki, *Chem. Lett.* **1977**, 17.

(353) C. Y. Meyers; Y. Hou; D. Scott; P. D. Robinson, *Acta Cryst.* **1997**, *C53*, 1149.

(354) M. Nakamura; N. Nakamura; M. Oki, *Bull. Chem. Soc. Jpn.* **1977**, *50*, 1097.

(355) G. Yamamoto; M. Suzuki; M. Oki, *Bull. Chem. Soc. Jpn.* **1983**, *56*, 809.

(356) R. Kuhn; D. Rewicki, *Chem. Ber.* **1965**, *98*, 2611.

(357) N. A. Bailey; S. E. Hull, *Acta Cryst.* **1978**, *B34*, 3289.

(358) J. -S. Lee; S. C. Nyburg, *Acta Cryst.* **1985**, *C41*, 560.

(359) D. A. Dougherty; F. M. Llort; K. Mislow, *Tetrahedron* **1978**, *34*, 1301.

(360) D. Bethell, *J. Chem. Soc.* **1963**, 666.

(361) K. L. Handoo; K. Gadru, *Indian J. Chem.* **1983**, *B22*, 909.

(362) E. Wasserman; A. M. Trozzolo; W. A. Yager; R. W. Murray, *J. Chem. Phys.* **1964**, *40*, 2408.

(363) C. A. Hutchison; G. A. Pearson, *J. Chem. Phys.* **1965**, *43*, 2545.

(364) M. Jones; K. R. Rettig, *J. Am. Chem. Soc.* **1965**, *87*, 4015.

(365) E. Font-Sanchis; C. Aliaga; E. V. Bejan; R. Cornejo; J. C. Sciano, *J. Org. Chem.* **2003**, *68*, 3199.

(366) K. Suzuki; M. Minabe; S. Kubota; T. Isobe, *Bull. Chem. Soc. Jpn.* **1970**, *43*, 2217.

(367) K. Suzuki; M. Fujimoto, *Bull. Chem. Soc. Jpn.* **1964**, *37*, 1833.

(368) K. Rakus; S. P. Verevkin; J. Schätzer; H. -D. Beckhaus; C. Rüchardt, *Chem. Ber.* **1994**, *127*, 1095.

(369) A. Van Sinoy; E. Vander Donckt, *J. Chem. Soc. Faraday Trans. I* **1976**, *72*, 2312.

(370) F. A. Neugebauer; W. R. Groh, *Tet. Lett.* **1973**, *12*, 1005.

(371) M. S. Lee; J. E. Jackson, *Res. Chem. Intermed.* **1994**, *20*, 223.

(372) M. Gomberg; D. Nishida, *J. Am. Chem. Soc.* **1923**, *45*, 190.

(373) M. Gomberg, *J. Chem. Ed.* **1932**, *9*, 439.

(374) G. B. Kauffman, *Chem. & Ind.* **2000**, *24*, 813.

(375) H. Lankamp; W. T. Nauta; C. McLean, *Tet. Lett.* **1968**, 249.

(376) C. Harnack; W. Krull; M. Lehnig; W. P. Neumann; A. K. Zarkadis, *J. Chem. Soc. Perkin Trans. II* **1994** , 1247.

(377) H. Tomioka, *Acc. Chem. Res.* **1997**, *30*, 315.

(378) H. Itakura; H. Tomioka, *Org. Lett.* **2000**, *2*, 2995.

(379) H. Tomioka; E. Iwamoto; H. Itakura; K. Hirai, *Nature* **2001**, *412*, 626.

(380) P. I. Dem'yanov; I. M. Styrkov; D. P. Krut'ko; M. V. Vener; V. S. Petrosyan, *J. Organomet. Chem.* **1992**, *438*, 265.

(381) M. G. Adlington; M. Orfanopoulos; J. L. Fry, *Tet. Lett.* **1976**, *34*, 2955.

(382) I. V. Bulgarovskaya; V. E. Zavodnik; V. M. Vozzhennikov, *Acta Cryst.* **1987**, *C43*, 764.

(383) P. J. Cox; G. A. Sim, *Acta Cryst.* **1979**, *B35*, 404.

(384) T. Takahashi; M. Kitamura; B. Shen; K. Nakajima, *J. Am. Chem. Soc.* **2000**, *122*, 12876.

(385) A. Bennett; A. W. Hanson, *Acta Cryst.* **1953**, *6*, 736.

(386) D. Holmes; S. Kumaraswamy; A. J. Matzger; K. P. C. Vollhardt, *Chem. Eur. J.* **1999**, *5*, 3399.

(387) J. E. Anthony; D. L. Eaton; S. R. Parkin, *Org. Lett.* **2002**, *4*, 15.

(388) J. E. Anthony; J. S. Brooks; D. L. Eaton; S. R. Parkin, *J. Am. Chem. Soc.* **2001**, *123*, 9482.

(389) R. B. Campbell; J. M. Robertson, *Acta Cryst.* **1962**, *15*, 289.

(390) M. Kameya; T. Naito; T. Inabe, *Bull. Chem. Soc. Jpn.* **2000**, *73*, 61.

(391) P. J. Fagan; M. D. Ward; J. V. Caspar; J. C. Calabrese; P. J. Krusic, *J. Am. Chem. Soc.* **1988**, *110*, 2981.

(392) R. A. Pascal; W. D. McMillan; D. Van Engen; R. G. Eason, *J. Am. Chem. Soc.* **1987**, *109*, 4660.

(393) R. A. Pascal; W. D. McMillan; D. Van Engen, *J. Am. Chem. Soc.* **1986**, *108*, 5652.

(394) C. Moureu; C. Dufraisse; P. M. Dean, *Compt. Rend.* **1926**, *182*, 1584.

(395) C. Moureu; C. Dufraisse; C. -L. Butler, *Compt. Rend.* **1926**, *182*, 1440.

(396) H. H. Wasserman; J. R. Scheffer; J. L. Cooper, *J. Am. Chem. Soc.* **1972**, *94*, 4991.

(397) J. -M. Aubry; S. Bouttemy, *J. Am. Chem. Soc.* **1997**, *119*, 5286.

(398) S. Erkoç, *J. Mol. Struc.* **2002**, *578*, 99.

(399) W. Dreissig; P. Luger; D. Rewicki, *Acta Cryst.* **1974**, *B30*, 2037.

(400) J. Rigaudy; P. Capdevielle, *Tetrahedron* **1977**, *33*, 767.

(401) P. Capdevielle; J. Rigaudy, *Tetrahedron* **1979**, *35*, 2093.

(402) P. Capdevielle; J. Rigaudy, *Tetrahedron* **1979**, *35*, 2101.

(403) D. J. Pesto, *J. Am. Chem. Soc.* **1979**, *101*, 37.

(404) A. J. Brattesani; E. Maverick; O. J. Muscio; T. L. Jacobs, *J. Org. Chem.* **1992**, *57*, 7346.

(405) M. Minabe; M. Yoshida; S. Saito; K. Tobita; T. Toda, *Bull. Chem. Soc. Jpn.* **1988**, *61*, 2067.

(406) R. Adams; C. S. Marvel, *Org. Synth. Coll. Vol. I* **1932**, 94.

(407) H. T. Clarke; E. E. Dreger, *Org. Synth. Coll. Vol. I* **1932**, 87.

(408) Hyperchem Pro 5.1 **1997**, Hypercube Inc.

(409) L. E. Harrington; M. J. McGlinchey, unpublished results.

(410) H. J. Knoelker; J. Heber; C. H. Mahler, *Synlett* **1992**, *12*, 1002.

(411) F. Mao; D. M. Schut; D. R. Tyler, *Organometallics* **1996**, *15*, 4770.

(412) S. W. Magennis; S. Parsons; Z. Pikramenou, *Chem. Eur. J.* **2002**, *8*, 5761.

(413) N. Zuniga-Villareal; M. R. Lezama; S. Hernandez-Ortega; C. Silvestru, *Polyhedron* **1998**, *17*, 2679.

(414) A. Carvalho; V. Garcia-Montalvo; A. Domingos; R. Cea-Olivares; N. Marques; A. Pires de Matos, *Polyhedron* **2000**, *19*, 1699.

(415) G. M. McCann; C. M. McDonnell; L. Magris; R. A. More O'Farrall, *J. Chem. Soc. Perkin Trans. II* **2002** , 784.

(416) R. J. Abraham; M. Mobli; R. J. Smith, *Magn. Reson. Chem.* **2003**, *41*, 26.

(417) J. B. Woell; P. Boudjouk, *J. Org. Chem.* **1980**, *45*, 5213.

(418) J. -P. Quere; E. Maréchal, *Bull. Soc. Chim. Fr.* **1971**, *8*, 2983.

(419) R. B. Miller; J. M. Frincke, *J. Org. Chem.* **1980**, *45*, 5312.

(420) E. G. Ijpeij; F. H. Beijer; H. J. Arts; C. Newton; J. G. de Vries; G. -J. M. Gruter, *J. Org. Chem.* **2002**, *67*, 169.

(421) G. E. Miracle; J. L. Ball; D. R. Powell; R. West, *J. Am. Chem. Soc.* **1993**, *115*, 11598.

(422) N. Sigal; Y. Apeloig, *Organometallics* **2002**, *21*, 5486.

(423) M. Trommer; G. E. Miracle; B. E. Eichler; D. R. Powell; R. West, *Organometallics* **1997**, *16*, 5737.

(424) M. S. Gordon; M. W. Schmidt; S. Koseki, *Inorg. Chem.* **1989**, *28*, 2161.

(425) J. Dubac; A. Laporterie; G. Manuel, *Chem. Rev.* **1990**, *90*, 215.

(426) Y. Liu; D. Ballweg; R. West, *Organometallics* **2001**, *20*, 5769.

(427) Y. Liu; D. Ballweg; T. Müller; I. A. Guzei; R. W. Clark; R. West, *J. Am. Chem. Soc.* **2002**, *124*, 12174.

(428) L. S. Cheng; J. Y. Corey, *Organometallics* **1989**, *8*, 1885.

(429) J. Y. Corey; C. S. John; M. C. Ohmsted; L. S. Chang, *J. Organomet. Chem.* **1986**, *304*, 93.

(430) H. Gilman; R. D. Gorsich, *J. Am. Chem. Soc.* **1958**, *80*, 3243.

(431) D. Wittenberg; H. Gilman, *J. Am. Chem. Soc.* **1958**, *80*, 2677.

(432) H. Gilman; R. D. Gorsich, *J. Am. Chem. Soc.* **1958**, *80*, 1883.

(433) J. Clayden; N. Greeves; S. Warren; P. Wothers, *Organic Chemistry*, **2001**, Oxford University Press, New York.

(434) D. D. Perrin; W. L. F. Armarego; D. L. Perrin, *Purification of Laboratory Chemicals*, **1980**, Pergamon Press, New York.

(435) R. Cramer, *Inorg. Synth.* **1974**, *15*, 14.

(436) M. D. Rausch; A. Siegel, *J. Org. Chem.* **1968**, *33*, 4545.

(437) D. R. Coulson, *Inorg. Synth.* **1972**, *13*, 121.

(438) L. H. Sommer; N. S. Marans, *J. Am. Chem. Soc.* **1951**, *73*, 5135.

(439) A. D. Bain; G. J. Duns, *Can. J. Chem.* **1996**, *74*, 819.

(440) G. Te Velde; F. M. Bickelhaupt; E. J. Baerends; C. Fonseca Guerra; S. J. A. Van Gisbergen; J. G. Snijders; T. Ziegler, *J. Comput. Chem.* **2001**, *22*, 931.

(441) A. D. Becke, *Phys. Rev. A* **1988**, *38*, 3098.

(442) J. P. Perdew, *Phys. Rev. B* **1986**, *33*, 8822.

(443) J. G. Snijders; E. G. Baerends; P. Vernooijs, *At. Data Nucl. Tables* **1982**, *26*, 483.

(444) E. G. Baerends; D. E. Ellis; P. Ros, *Chem. Phys.* **1973**, *2*, 41.

(445) G. M. Sheldrick, *SMART, Release 4.05, Siemens Energy and Automation, Inc., Madison, WI, 53719* **2002**.

(446) G. M. Sheldrick, *SAINT, Release 4.05, Siemens Energy and Automation, Inc., Madison, WI, 53719* **1996**.

(447) G. M. Sheldrick, *SADABS (Siemens Area Detector Absorption Correction), Siemens Energy and Automation, Inc., Madison, WI, 53719* **1996**.

(448) G. M. Sheldrick, *SHELXTL, Version 5.03, Siemens Crystallographic Research Systems, Madison, WI* **1994**.

(449) J. D. Fulton; R. Robinson, *J. Chem. Soc.* **1939**, 200.

(450) J. R. Johnson; O. Grummitt, *Org. Synth. Coll. Vol. III* **1955**, 806.

(451) B. A. Arbusov; J. A. Akmed-Zade, *Zh. Obshch. Khim.* **1942**, *12*, 1928.

(452) A. Yasuhara; S. Akiyama; M. Nakagawa, *Bull. Chem. Soc. Jpn.* **1972**, *45*, 3638.

(453) B. Ortiz; P. Villanueva; F. Walls, *J. Org. Chem.* **1972**, *37*, 2748.

APPENDIX I

Fully Labelled Thermal Ellipsoid Plots

Molecule 2.16a

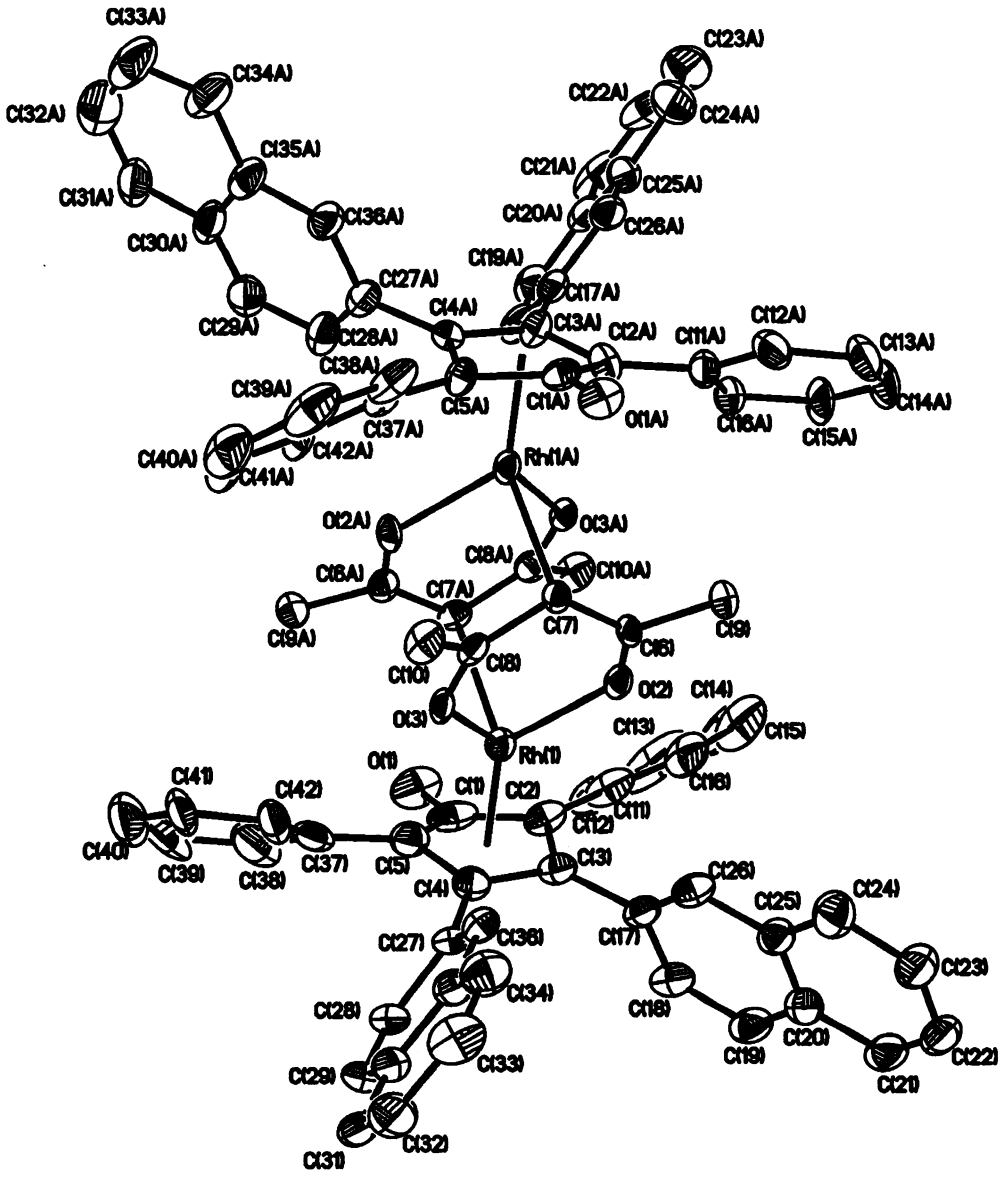

Molecule 2.16b

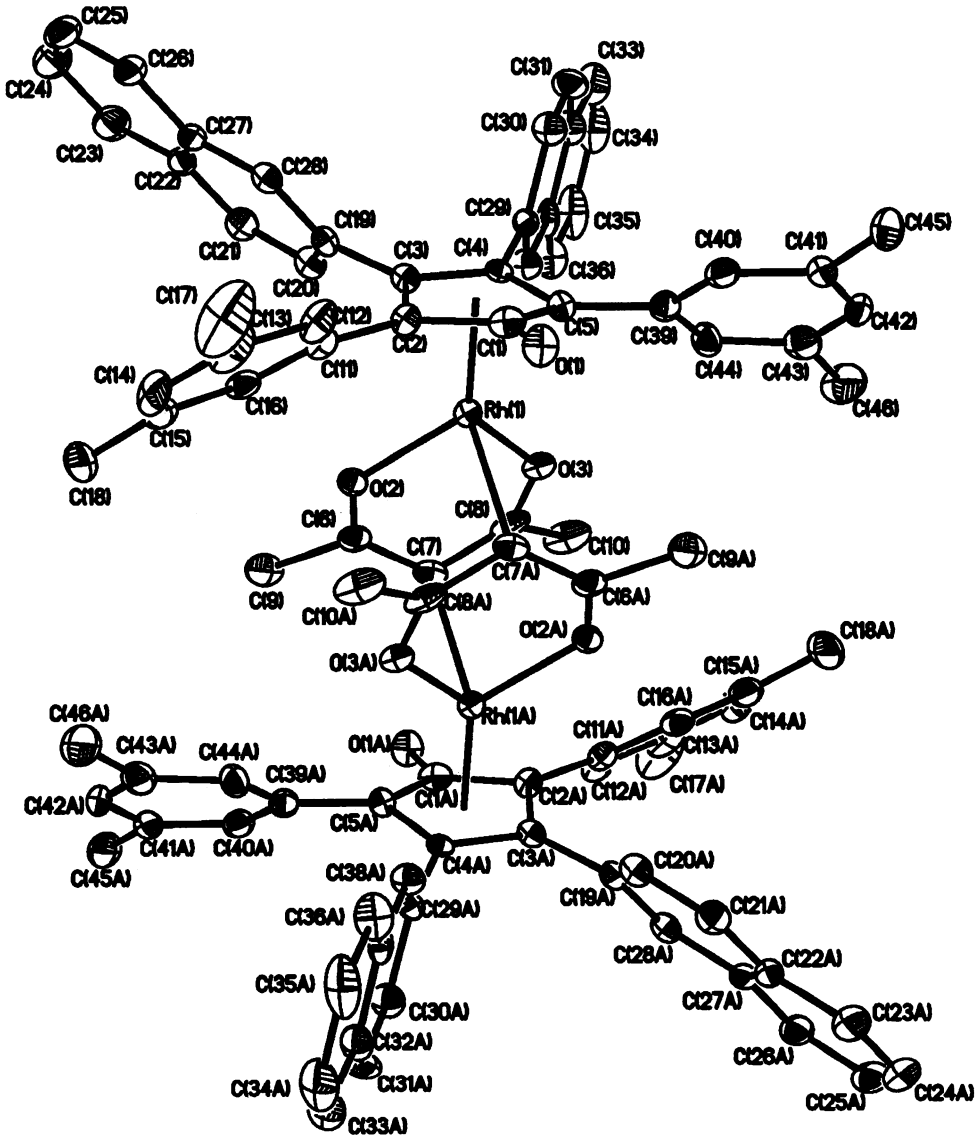

Molecule 2.17a

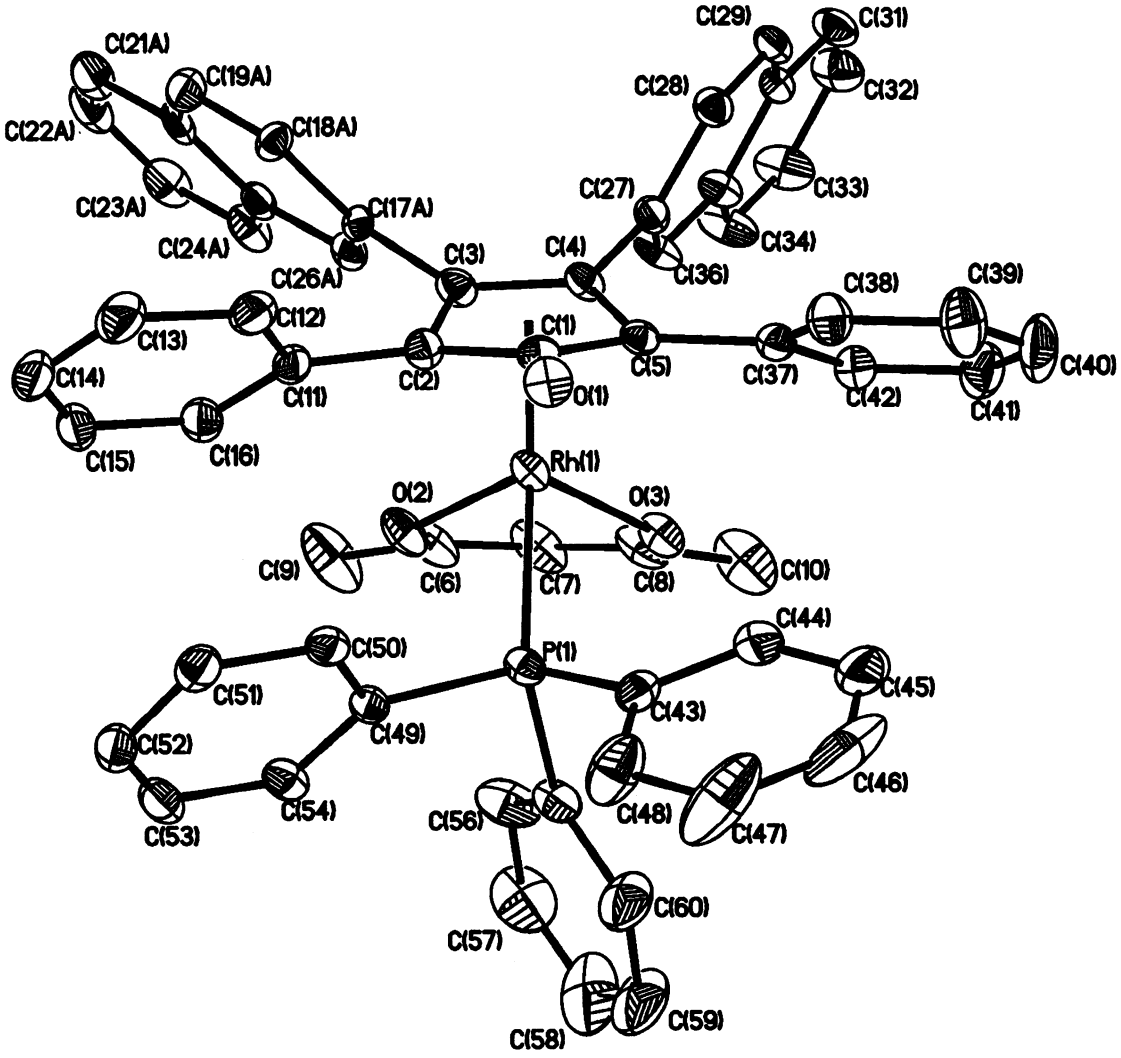

Molecule 2.17b

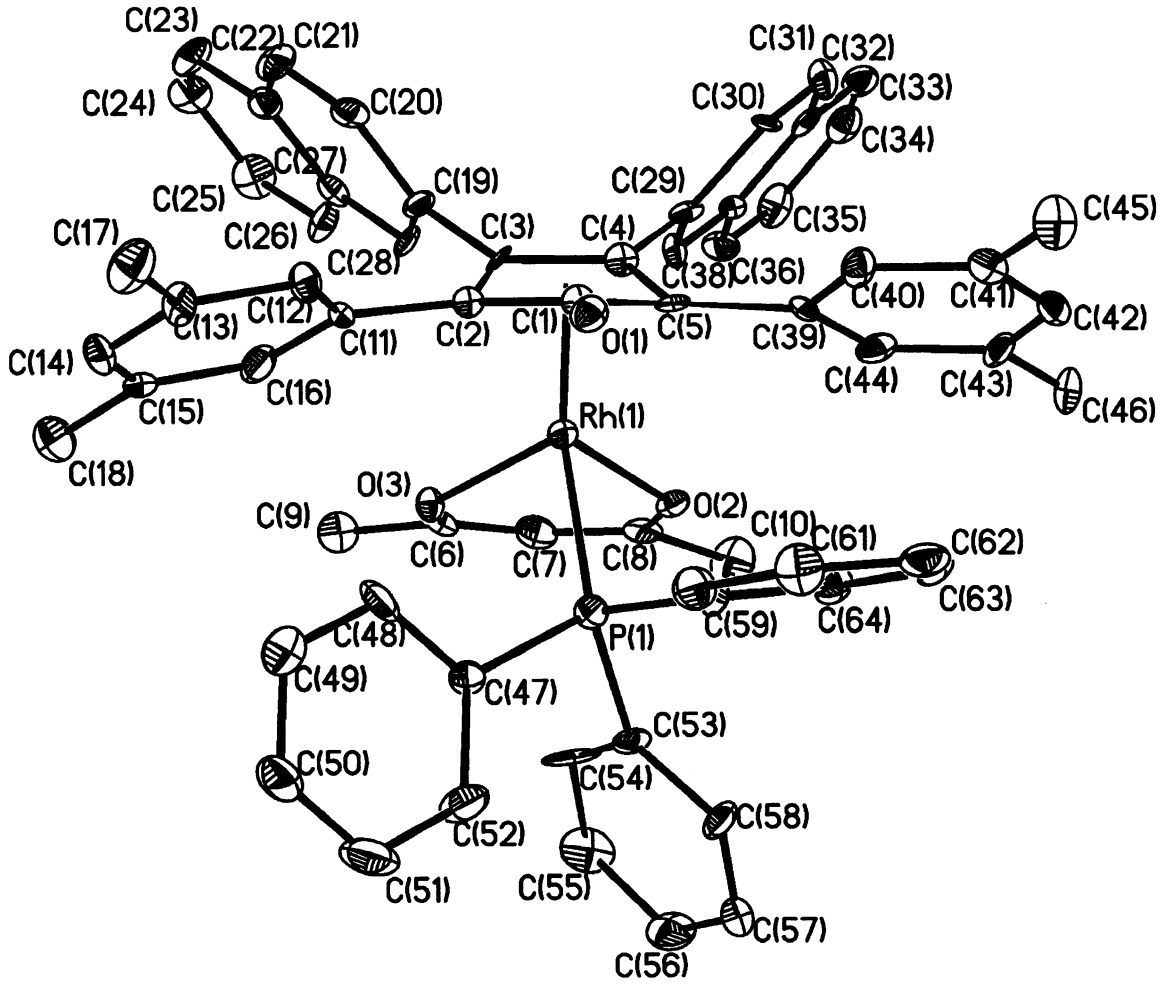

Molecule 3.9

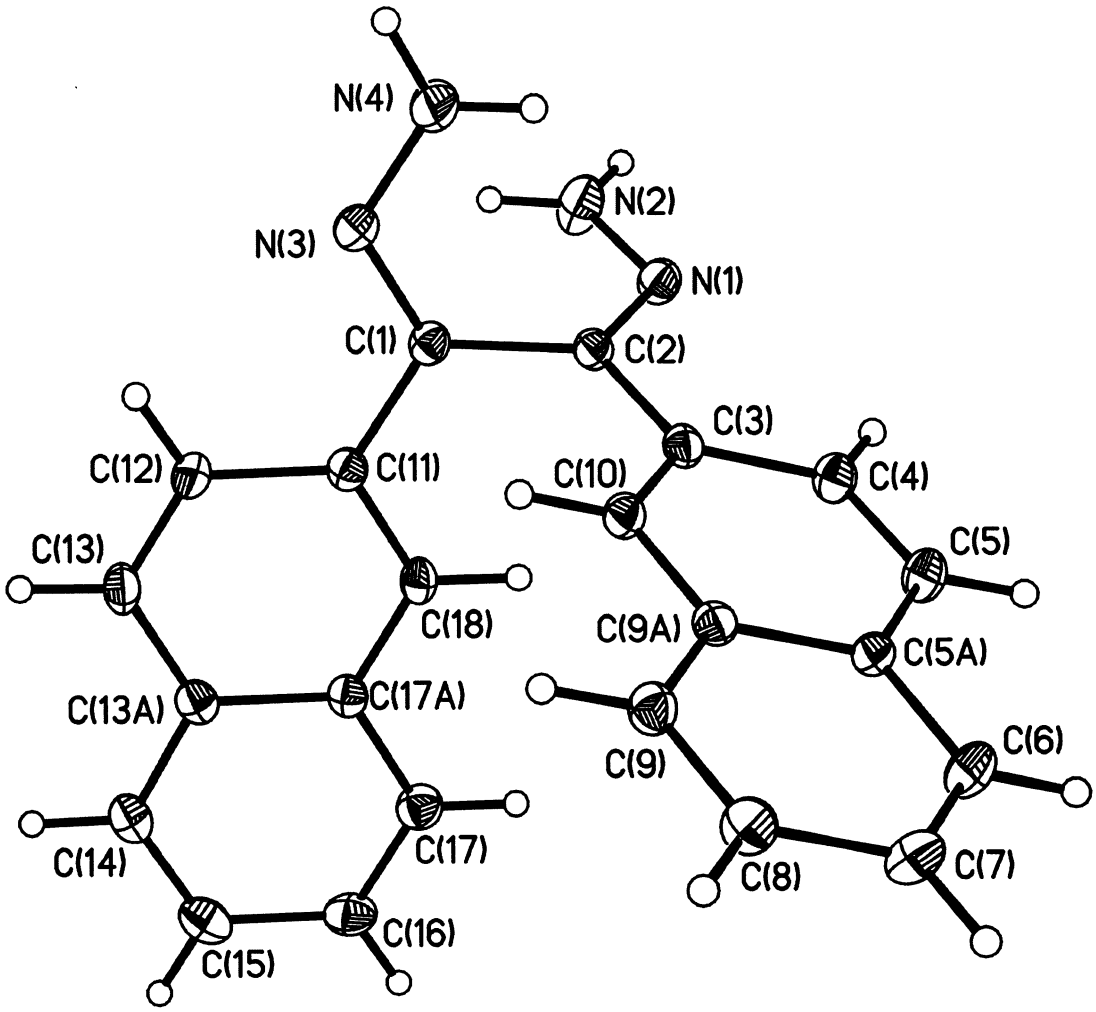
N(4)
N(2)
N(3)
N(1)
C(1)
C(2)
C(3)
C(12)
C(11)
C(10)
C(4)
C(13)
C(5)
C(18)
C(9A)
C(5A)
C(13A)
C(17A)
C(6)
C(9)
C(14)
C(17)
C(8)
C(7)
C(16)
C(15)

Molecule 3.10

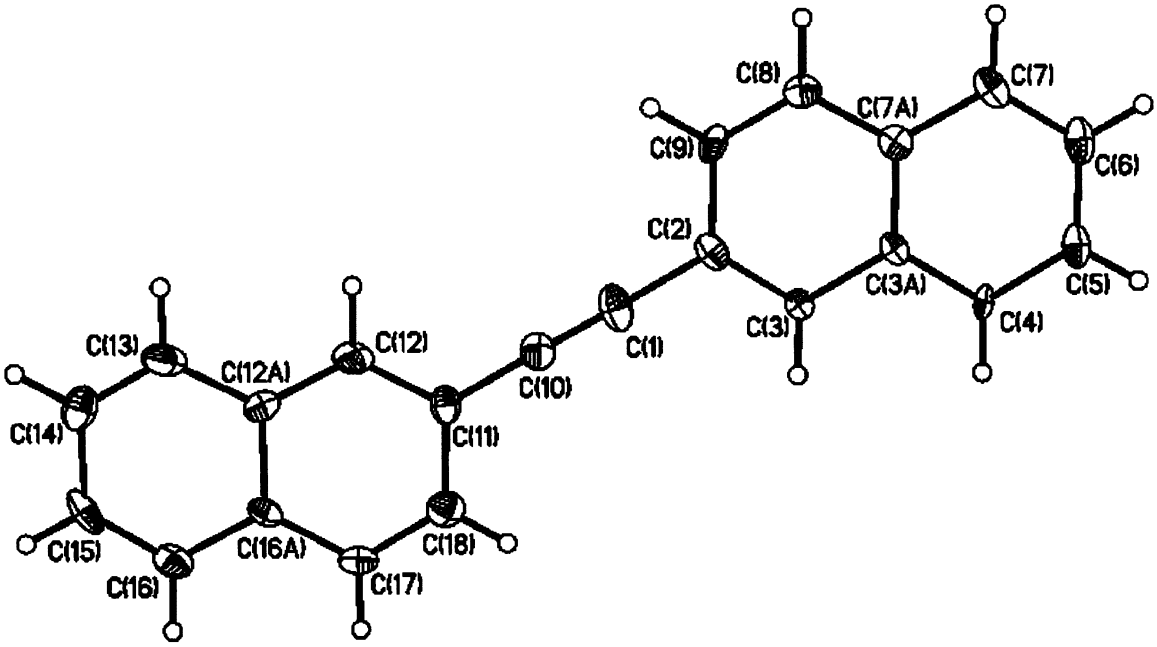

Molecule 3.12

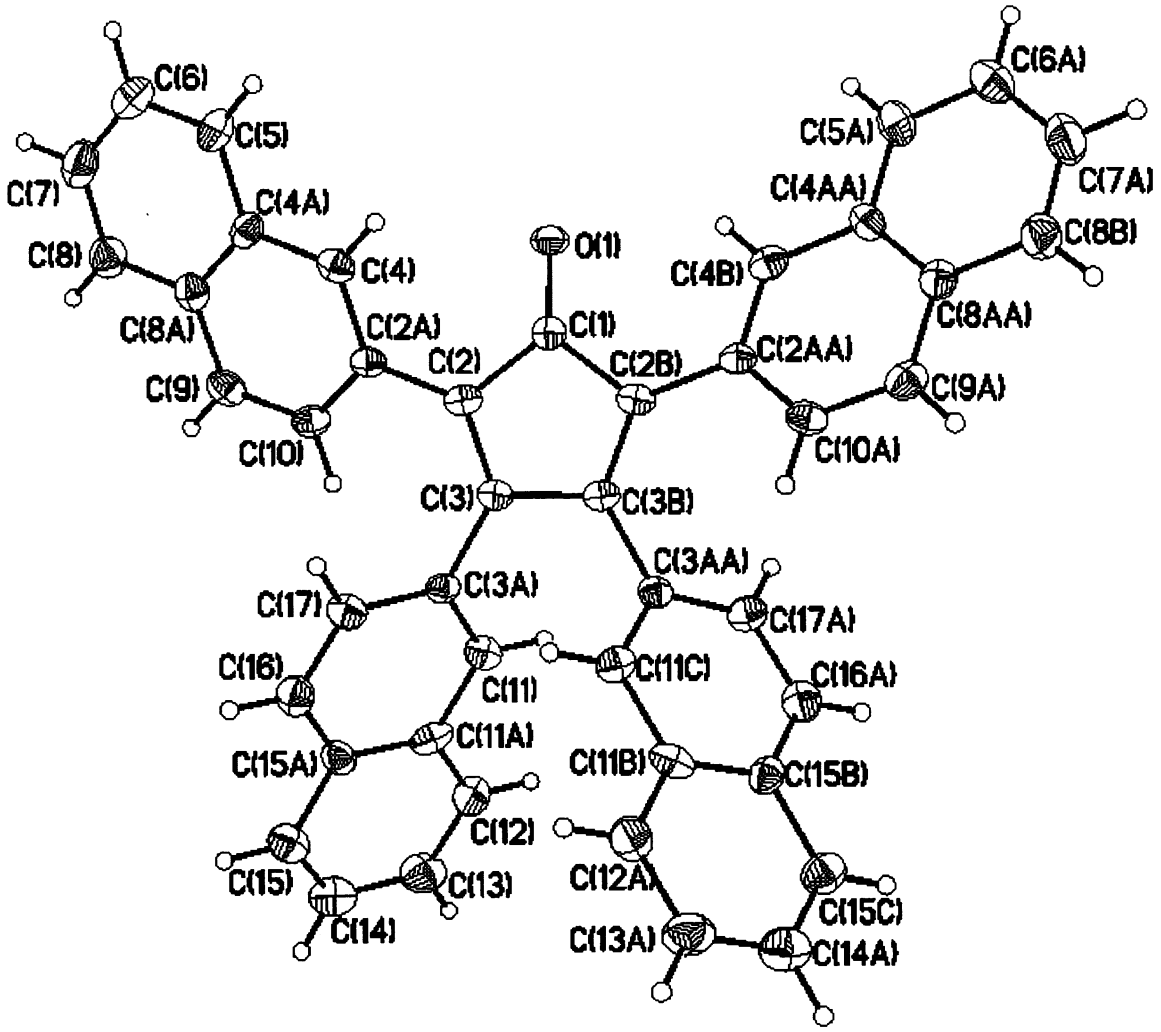

Molecule 3.16

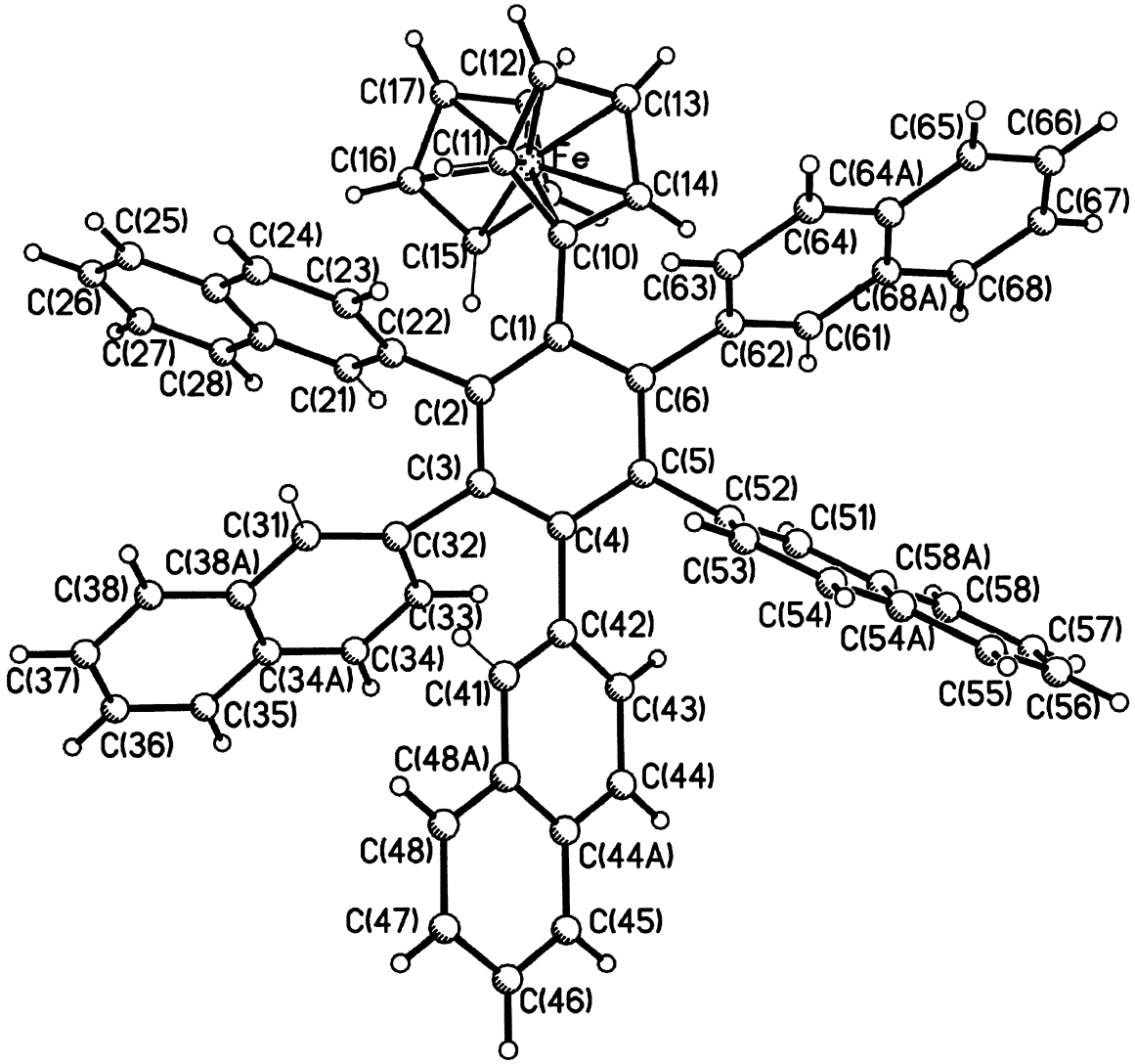

Molecule 5.15

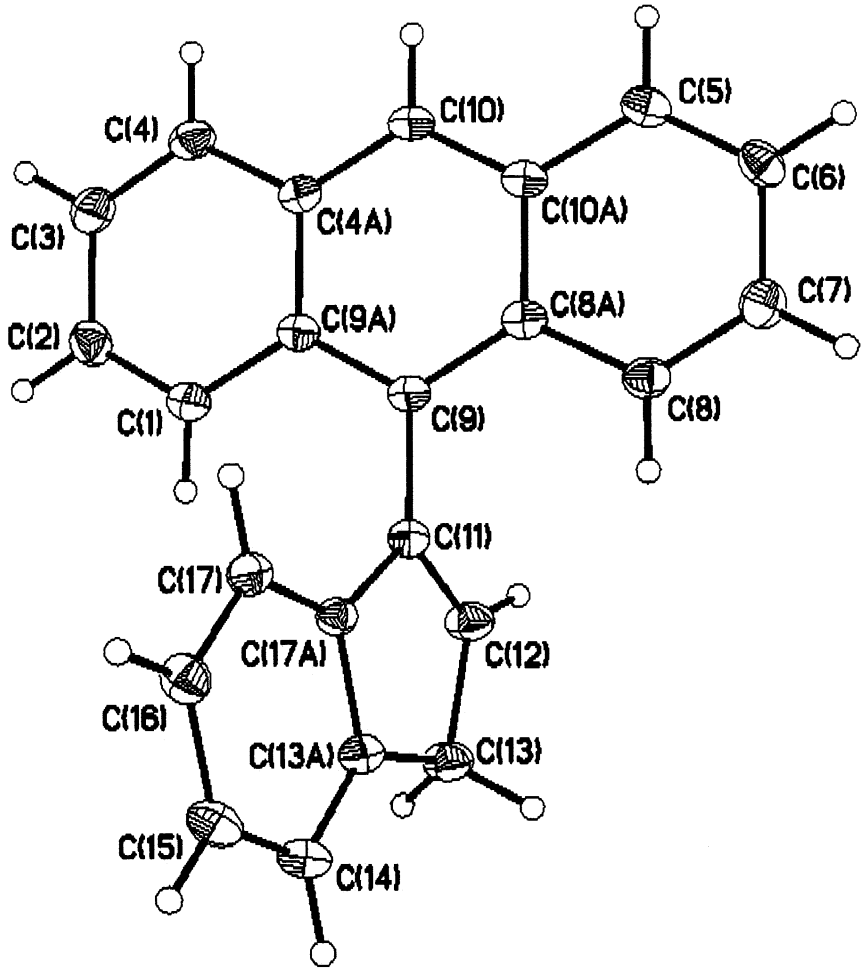

Molecule 5.16

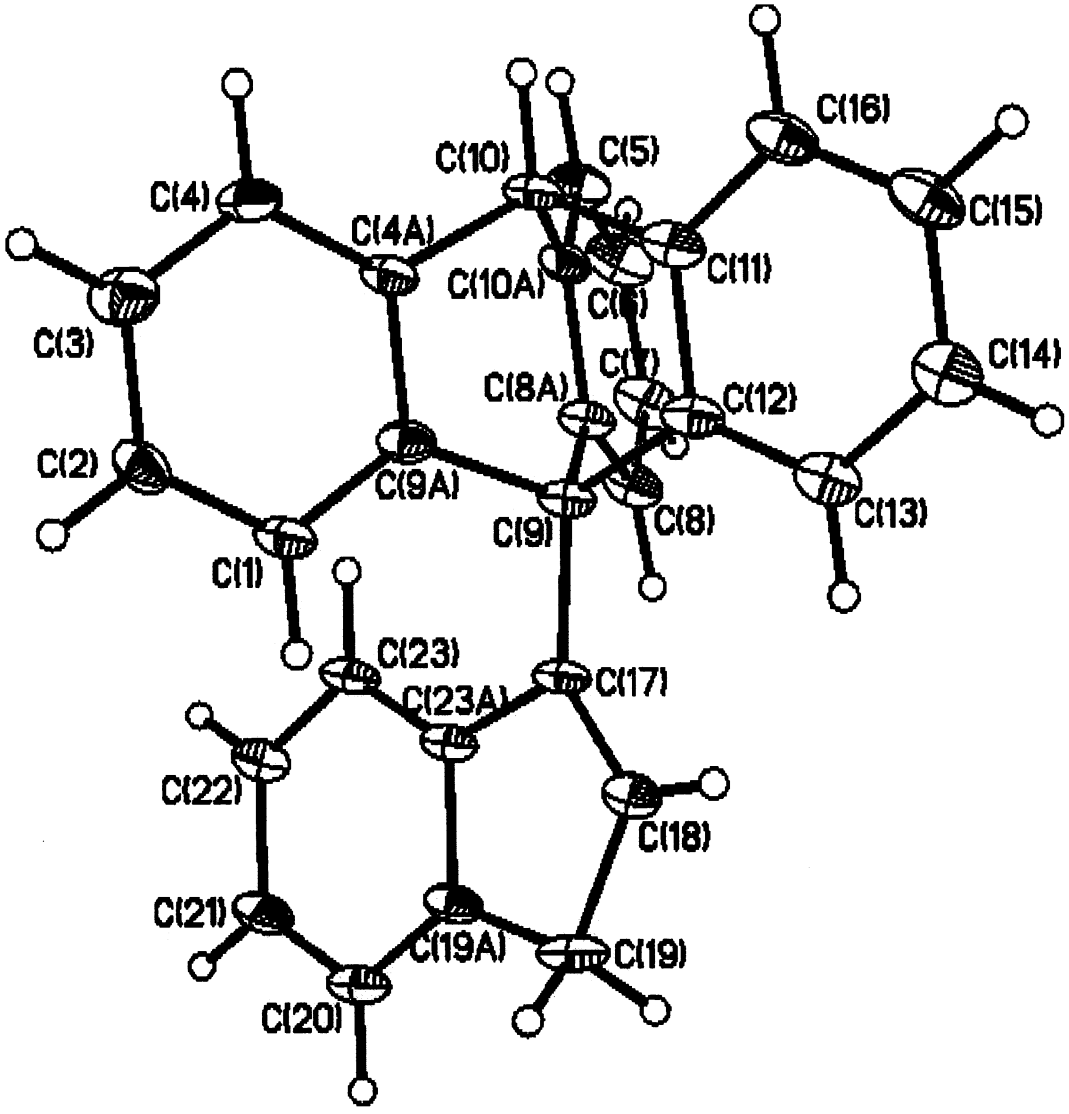

Molecule 5.20

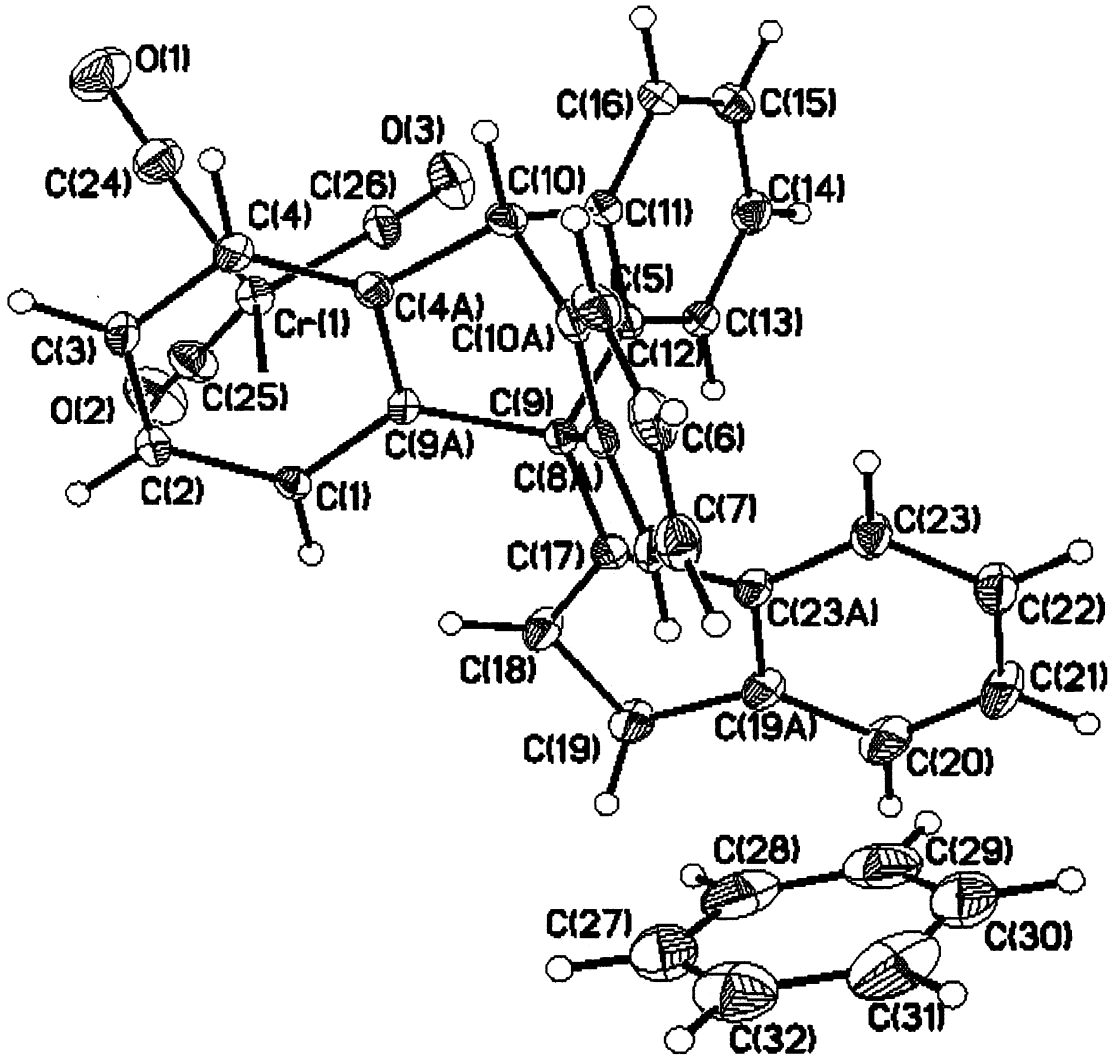

Molecule 6.13

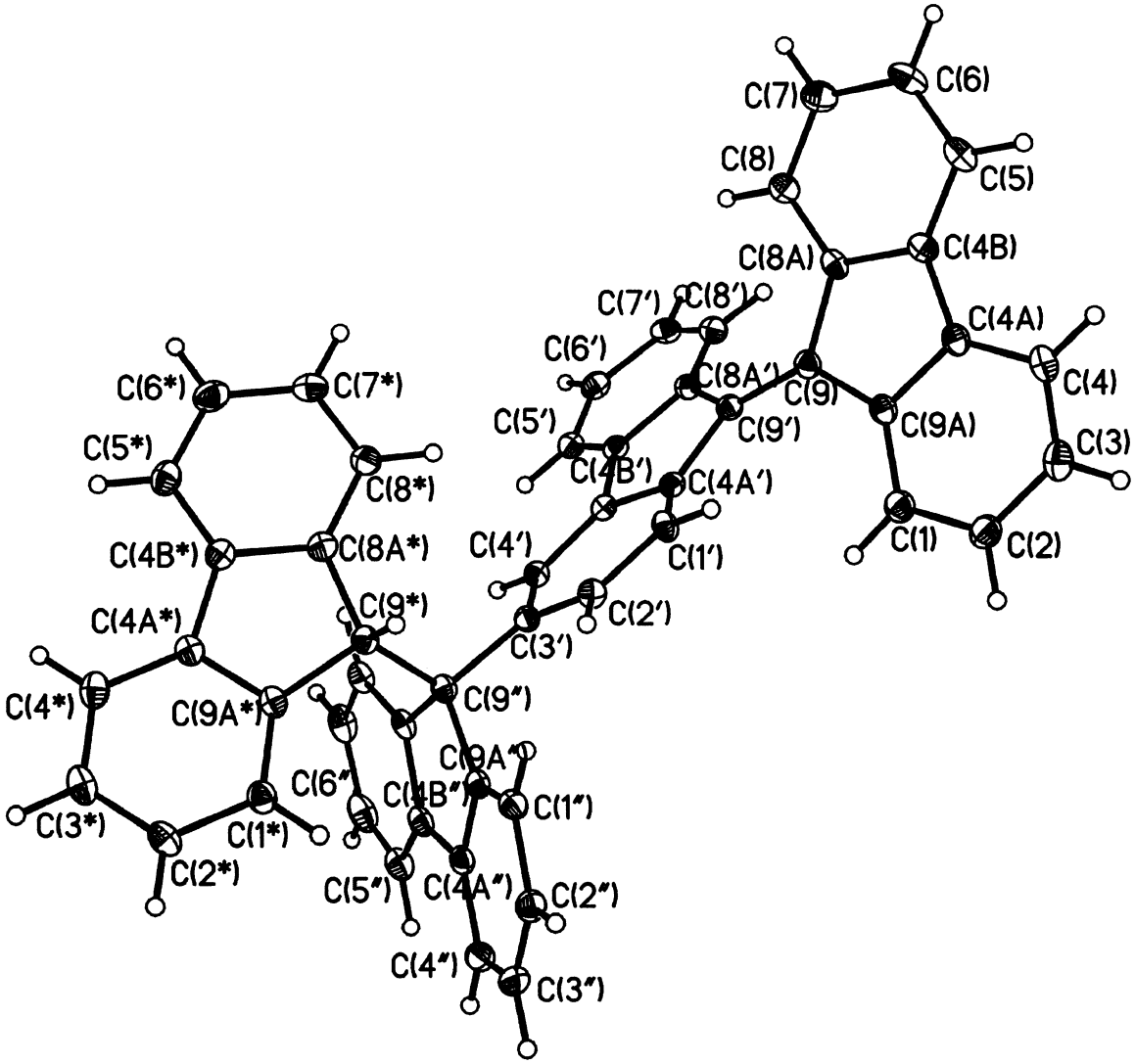

Molecule 6.17

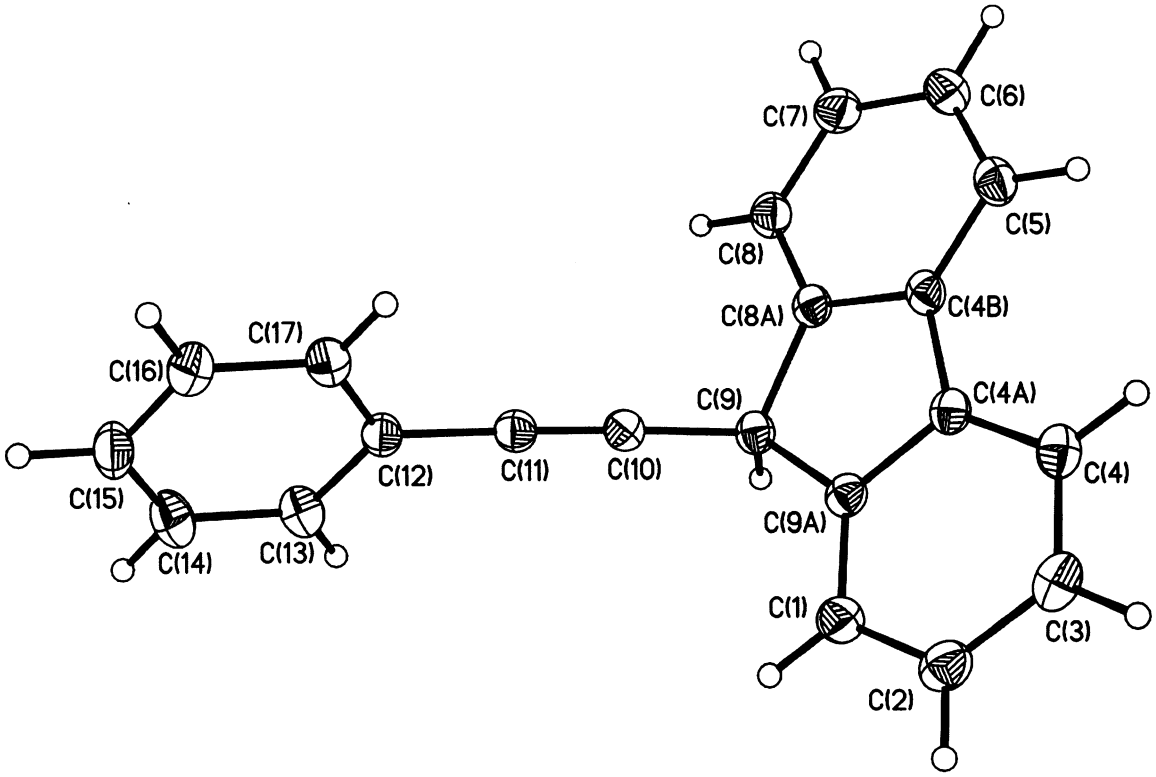

Molecule 6.33

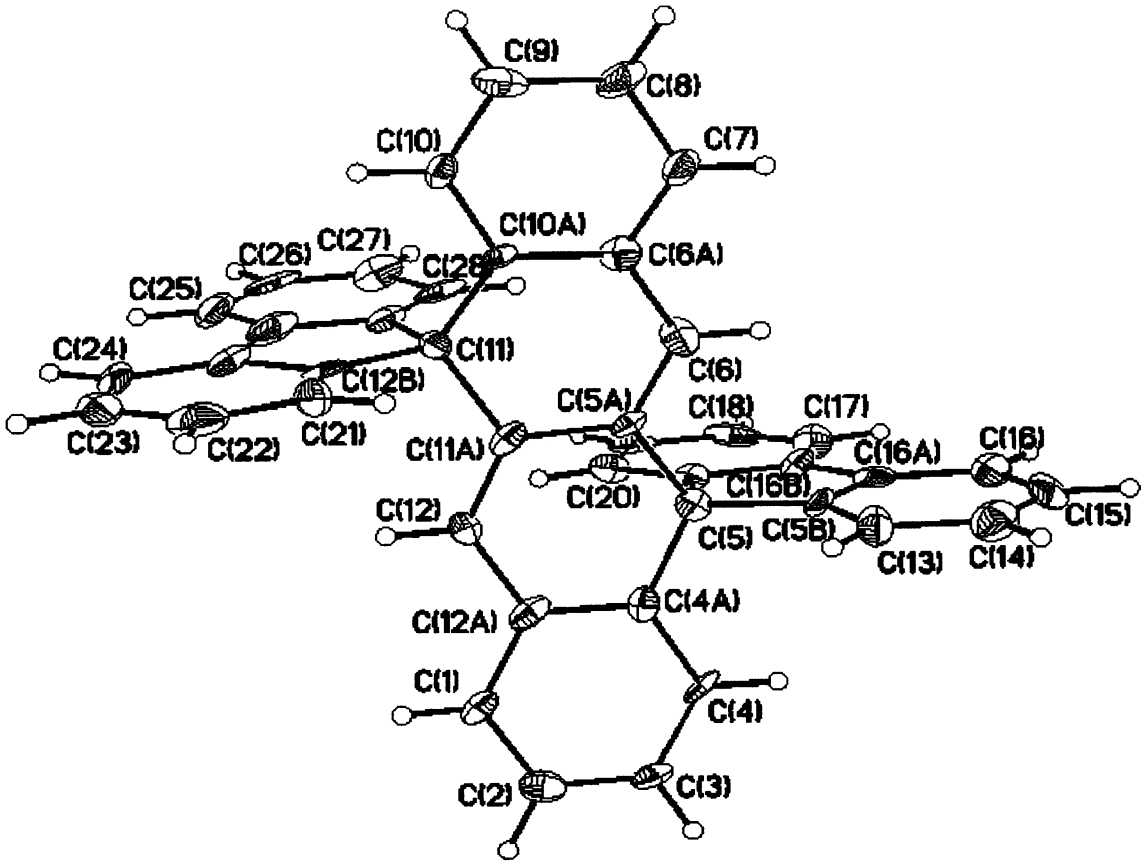

Molecule 6.34